European Journal of Taxonomy 990: 1–145
https://doi.org/10.5852/ejt.2025.990.2903
ISSN 2118-9773
www.europeanjournaloftaxonomy.eu
2025 · von Groll E.

Monograph

urn:lsid:zoobank.org:pub:EBB48E32-AFE7-45DE-8985-665968426DB0

Twenty new species of Scaphidiinae (Coleoptera: Staphylinidae) from Minas Gerais, Southeast Brazil

Elisa VON GROLL

Programa de Pós-Graduação em Biologia Animal, Universidade Federal de Viçosa, Av. Peter Henry Rolfs, s/n, 36570-900, Viçosa, MG, Brazil.
Email: elisavgroll@gmail.com

urn:lsid:zoobank.org:author:DC564233-82A9-4939-8B7A-F02C994BBA29

Abstract. Scaphidiinae (shining fungus beetles) is a subfamily of Staphylinidae generally associated with fungi and slime moulds. They are distributed worldwide, but the Brazilian fauna is poorly known. In this manuscript, twenty new species assigned to five genera are described: *Cyparium fugitivum* sp. nov., *Alexidia convivalis* sp. nov., *A. solitaria* sp. nov., *Baeocera ardua* sp. nov., *B. bottine* sp. nov., *B. colibri* sp. nov., *B. facilis* sp. nov., *B. inusitata* sp. nov., *B. pulga* sp. nov., *Scaphisoma hilarum* sp. nov., *S. infinitum* sp. nov., *S. mutabile* sp. nov., *S. peculiare* sp. nov., *Toxidium brigadeirense* sp. nov., *T. distortum* sp. nov., *T. fleche* sp. nov., *T. inusitatum* sp. nov., *T. scalenum* sp. nov., *T. speratum* sp. nov. and *T. ultimum* sp. nov. The specimens were collected in remnants of Atlantic Forest, in Minas Gerais, Southeast Brazil, directly from the host (fungi and/or slime moulds). Descriptions include host associations, illustrations of the external and internal morphology of adult males and females, whenever it is possible. Also, an illustrated key to the Brazilian genera and their respective diagnoses is provided.

Keywords. Shining rove beetles, fungus, morphology, diversity, Neotropical Region.

Von Groll E. 2025. Twenty new species of Scaphidiinae (Coleoptera: Staphylinidae) from Minas Gerais, Southeast Brazil. *European Journal of Taxonomy* 990: 1–145. https://doi.org/10.5852/ejt.2025.990.2903

Introduction

Scaphidiinae Latreille, 1806 is a clade within the family Staphylinidae comprising over 2000 described species (Löbl 2018). These beetles are distributed worldwide, with highest diversity in tropical and subtropical forests (Leschen & Löbl 1995). They are typically collected from fungi and slime moulds, by sifting litter or using flight intercept traps (Lawrence & Newton 1980; Newton 1984; Leschen 1994; Stephenson *et al.* 1994; Löbl & Leschen 2003b; Tang *et al.* 2014; Löbl 2018; Löbl *et al.* 2021).

Although the Neotropical Region has the ideal conditions for supporting a rich diversity of scaphidiines, at present only about 200 species (of the approximately 2000 known) have been recorded from there. In Brazil, the situation is even more limited. Despite the large forest areas, the country has only 41 known species, distributed among the following seven genera: *Cyparium* Erichson, 1845 (13 spp.), *Scaphidium* Olivier, 1790 (12 spp.), *Alexidia* Reitter, 1880 (1 sp.), *Amalocera* Erichson, 1845 (5 spp.), *Baeocera Erichson, 1845* (1 sp.), *Scaphisoma* Leach, 1815 (8 spp.) and *Toxidium* LeConte, 1860 (1 sp.) (Löbl 2018; von Groll & Lopes-Andrade 2021, 2022; von Groll 2023).

Previous studies have shown that this low number is unrelated to the absence of these beetles in Brazil (von Groll & Lopes-Andrade 2021). It is more likely related to the lack of knowledge regarding this subfamily and the lack of interest in studying small beetles, although such beetles can commonly be found in miscellaneous collections, in alcohol or dry (pers. obs.). However, beetles in miscellaneous collections were usually collected using generic methods (e.g., FIT), which do not allow for host associations.

With this paper, my aim is to enhance our understanding of the Brazilian shining fungus beetle fauna, focusing on specimens collected directly from their hosts (2018–2023, with a few exceptions) in remnants of the Atlantic Forest in Minas Gerais, southeastern Brazil. Hence, an illustrated key to the seven Brazilian genera and their descriptions is provided. Additionally, 20 new species, distributed across five genera, are described: *Cyparium* (1 sp. nov.), *Alexidia* (2 spp. nov.), *Baeocera* (6 spp. nov.), *Scaphisoma* (4 spp. nov.), and *Toxidium* (7 spp. nov.).

The descriptions include host information, illustrations of internal and external morphology of males and females (when available), and detailed measurements of the specimens. Finally, an updated checklist of the Brazilian species is provided.

Material and methods

The studied material is deposited at the Entomological Collection of the Laboratory of Systematics and Biology of Coleoptera, UFV, Viçosa, Minas Gerais (MG), Brazil (CELC). Specimens were collected (with few exceptions) during expeditions that took place between 2019 and 2023 in Viçosa, in the state of Minas Gerais, southeastern Brazil: Viçosa, "Mata da Biologia" (20°45′32″ S, 42°51′49″ W; 75 ha. of Atlantic Forest) (Fig. 1A–D); Viçosa, "Vila Gianetti" (20°45′16″ S, 42°52′21″ W; sidewalk in front of an avenue) (Fig. 1A–B, E–F); Viçosa, "Estação de Pesquisa, Treinamento e Educação Ambiental Mata do Paraíso (EPTEA)" (20°48′05″ S, 42°51′58″ W; 194 ha. of Atlantic Forest) (Fig. 1A–B, G); and Parque Estadual da Serra do Brigadeiro, city of Araponga (20°39′54″ S, 42°31′18″ W; 14.984 ha. of Atlantic Forest) (Fig. 1A–B).

Scaphisomatiini beetles from Viçosa (*Alexidia*, *Baeocera*, *Scaphisoma*, and *Toxidium*) were collected using a DIY mouth aspirator (Fig. 1G) directly from the host. The single *Cyparium* specimen was collected manually. The method used to collect the specimens of *Toxidium* from Araponga is unknown – these specimens were included in this manuscript because other individuals belonging to the same species were collected during the same expeditions mentioned above.

After collecting, beetles were kept in the freezer for a few hours, mounted on card triangles, and then dried in an oven for approximately 24 hours. They were then labelled, sorted by genera, and kept in drawers containing camphor. Primary identifications were conducted using original descriptions and the key to genera provided by Leschen & Löbl (2005), supplemented by personal communications with Dr Ivan Löbl (MHNG).

For dissection, beetles were immersed in warm water until the tissues were softened. Larger parts were separated and then boiled in a solution of KOH for tissue clarification. After that, the structures were placed in 10% acetic acid and washed in water. Subsequently, small structures were dissected and photographed in temporary slides using glycerine or KY®. After the process, all parts were washed and kept in genitalia vials or 0.2 ml Eppendorf tubes containing glycerine. Photographs follow von Groll & Lopes-Andrade (2022). Measurements were obtained using a Zeiss Stemi 2000C stereo microscope (2× objective) with calibrated ocular micrometer. Legs and antennae were photographed using a Zeiss AxioLab microscope with digital camera attachment, measured digitally using tpsDig2 (ver. 2.32), with range, mean and standard deviation calculated in PAST..

Fig. 1. Collection sites. **A–B**. Distribution maps of Scaphidiinae Latreille, 1806. **A**. South America. **B**. Minas Gerais (part). **C–D**. Entrance of Mata da Biologia (Viçosa, MG). **E–F**. Vila Gianetti (Viçosa, MG). **G**. Collecting from *Ceratiomyxa fruticulosa* T.Macbr. on a fallen tree (Mata do Paraíso, Viçosa, MG).

Measurement results are provided as ratios for the antennomeres (when measurable) and in millimetres (mm) for other structures.Abbreviations follow von Groll & Lopes-Andrade (2021) and von Groll (2023).

Maps were generated using ArcGIS 10. The coordinates were obtained via Google Earth Pro. Illustrations for the identification key were produced in Adobe Illustrator 2023, based on photographs provided in this paper, except for (1) *Amalocera* sp., dorsal (based on a photo taken of a specimen deposited at CELC); (2) *Scaphidium peckorum* Fierros-López, 2005, frontal (based on a photo of the holotype deposited in the Field Museum of Natural History, available from https://collections-zoology.fieldmuseum.org/); and (3) antenna of *Scaphidium* (based on Fierros-López 2005: fig. 11). Plates were created using Adobe Photoshop CC 2018.

The following code is used in the 'Material examined' sections: '*' stands for specimens with the abdomen and genitalia removed, and '**' for entirely dissected beetles. All dissected parts are preserved in a genitalia vial or an Eppendorf tube, filled with glycerine, and pinned along with the beetle. All paratypes are labelled "PARATYPUS + '♂' / '♀'", or just "PARATYPUS" – when the sex is unknown – on yellow paper. All holotypes are labelled "HOLOTYPUS ♂", on red paper, except for *Alexidia solitaria* sp. nov., which still needs a "HOLOTYPUS ♀" label. More detailed information regarding the examined material (e.g., number and data information of each specimen) can be found in the Supp. file 1.

The key to genera is based on Leschen & Löbl (1995, 2005), and the descriptions of the Brazilian genera follow Löbl & Leschen (2003b) and Leschen & Löbl (2005), supplemented by specific papers mentioned after each description. The synonymy list is based on Löbl (2018). Terminology follows Ogawa & Löbl (2013) for external morphology, and male and female terminalia; Naomi (1988a, 1988b), Leschen *et al.* (1990), Leschen & Löbl (2005), Lawrence & Ślipiński (2013), and von Groll & Lopes-Andrade (2022) for external morphology; Harris (1979) for microsculpture; Jałoszyński (2012) for the internal structure of the prothorax; Friedrich & Beutel (2006) for the mesonotum; Lawrence *et al.* (2021) for the hind wing venation; Crowson (1938), Naomi (1989a), and Hübler & Klass (2013), von Groll & Lopes-Andrade (2022) for the metendosternite; Naomi (1989b) for the abdominal segments; and Naomi (1990) for the male terminalia.

Results

Key to the Scaphidiinae Latreille, 1806 genera occurring in Brazil

1. Antennae robust; antennomeres VII–XI forming a distinct club (Fig. 2A–B) 2
– Antennae slender; antennomeres VII–XI slender, forming a loose club (Fig. 2C–D) 3

2. Eyes emarginate near antennal insertion (Fig. 2E), tibiae smooth (not spinose) ..... ***Scaphidium*** Olivier, 1790
– Eyes not emarginate near antennal insertion (Fig. 2F), tibiae spinose (Fig. 2G) ..... ***Cyparium*** Erichson, 1845

3. Profemora with ctenidium (Fig. 2H) 4
– Profemora without ctenidium 5

4. Antennomere III very short, triangular (Fig. 2C); last apical palpomere normal (almost the same width as previous and gradually tapering towards the apex) (Fig. 2I) ..... ***Scaphisoma*** Leach, 1815
– Antennomere III not distinctly shorter than IV (Fig. 2D); last apical palpomere aciculate (much narrower than the previous or abruptly narrowed at the apex) (Fig. 2J) ..... ***Baeocera*** Erichson, 1845

5. Body laterally compressed, strongly convex dorsally (in lateral view) (Fig. 2K); elytral basal striae absent; maxillary palpi normal (Fig. 2I) ..... ***Toxidium*** LeConte, 1860
– Body not compressed laterally, and just normally convex dorsally (in lateral view); elytral basal striae present (Fig. 2L–M) 6

6. Scutellum visible in dorsal view (Fig. 2L); mesotibiae with two inner apical spines (Fig. 2N); prothoracic corbiculum absent..... ***Amalocera*** Erichson, 1845
– Scutellum concealed in dorsal view (Fig. 2M); mesotibiae with just one inner apical spine (Fig. 2O); prothoracic corbiculum present (Fig. 2P) ..... ***Alexidia*** Reitter, 1880

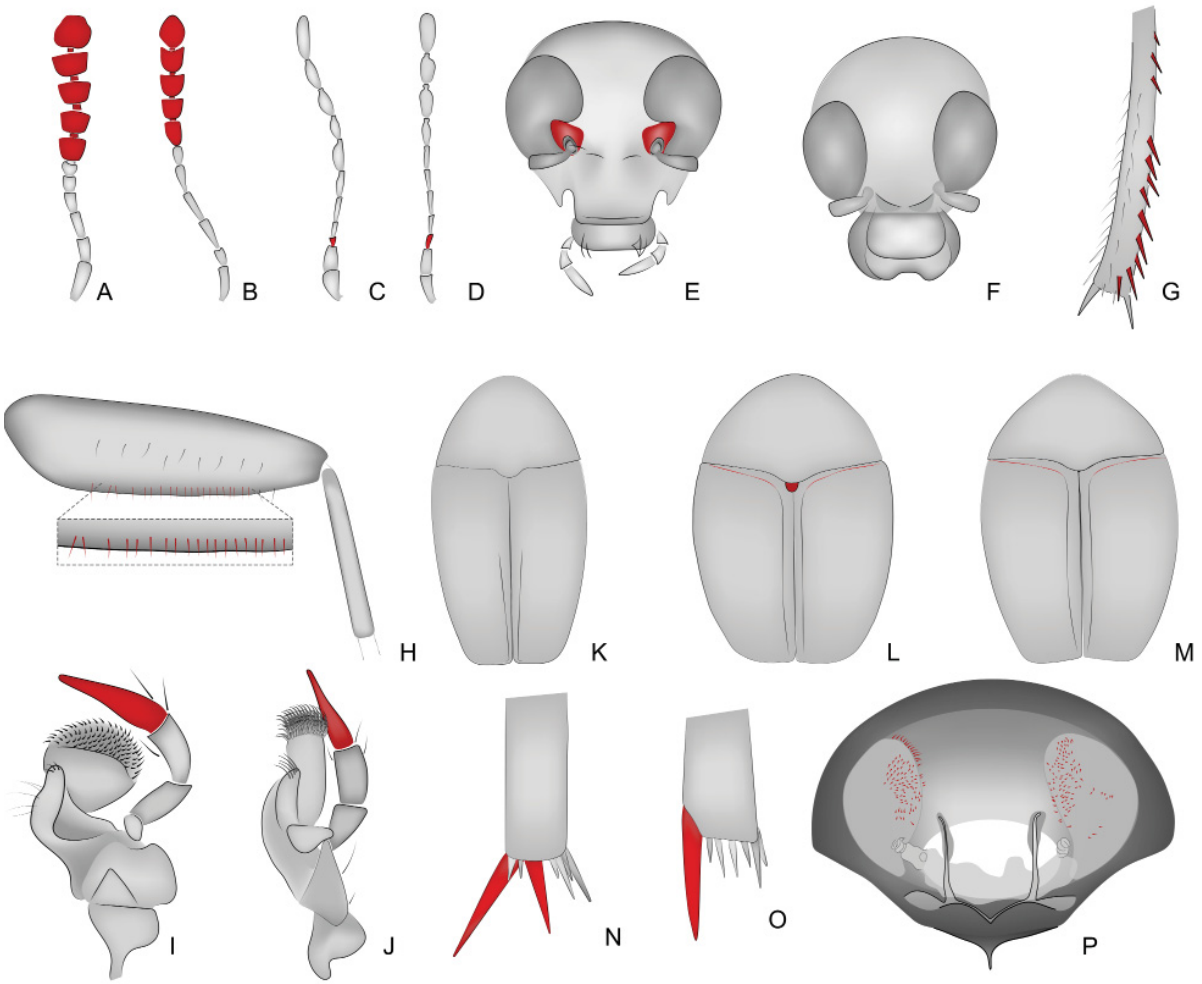

Fig. 2. Scaphidiinae Latreille, 1806, morphology. In red: pertinent characteristics. **A–D**. Antennae. **A**. *Cyparium fugitivum* sp. nov. **B**. *Scaphidium* sp., adapted from Fierros-López (2005). **C**. *Scaphisoma hilarum* sp. nov. **D**. *Baeocera inusitata* sp. nov. **E–F**. Heads, frontal views. **E**. *Scaphidium peckorum* Fierros-López, 2005. **F**. *Cyparium fugitivum* sp. nov. **G**. *Cyparium* sp., tibia. **H**. *Scaphisoma hilarum* sp. nov., ctenidium. **I–J**. Mandible. **I**. *Toxidium speratum* sp. nov. **J**. *Baeocera facilis* sp. nov. **K–M**. Habitus, dorsal views. **K**. *Toxidium speratum* sp. nov. **L**. *Amalocera* sp. **M**. *Alexidia convivalis* sp. nov. **N–O**. Inner spines of mesotibiae. **N**. *Amalocera* sp. **O**. *Alexidia convivalis* sp. nov. **P**. *Alexidia convivalis* sp. nov., prothoracic corbiculum.

Descriptions of new species

Class Insecta Linnaeus, 1758
Order Coleoptera Linnaeus, 1758
Family Staphylinidae Latreille, 1802
Subfamily Scaphidiinae Latreille, 1806
Tribe Cyparіini Achard, 1924

Genus ***Cyparium*** Erichson, 1845
Figs 2A, F–G, 3–5

Cyparium Erichson, 1845: 3. Type species: *Cyparium palliatum* Erichson, 1845; by monotypy.
Yparicum Achard, 1920: 126. Type species: *Yparicum yunnanum* Achard, 1920; by monotypy.

Cyparium, the only genus of the tribe Cyparіini, comprises 62 species, 5 subspecies, and one "potential new species", with the majority occuring in the Neotropical Region (23 spp. and 3 subspecies), of which 13 are from Brazil (Löbl 2018; von Groll & Lopes-Andrade 2021; Löbl & Cosandey 2023). While it was once considered "notably absent from southern South America, the western part of the Palearctic, and Australia" (Löbl & Leschen 2003b), it is now understood that the low number of species in Brazil is a result of the lack of studies/collections involving Scaphidiinae (von Groll & Lopes-Andrade 2022). Throughout my field trips in Minas Gerais, Brazil, it was very common to collect specimens of *Cyparium*. Although this paper includes the description of only one new species, it should be noted that several others have been collected.

General description (Leschen & Löbl 2005)

Head. Mandible with two apical teeth and subapical serrations present on the left mandible. Maxillary palp normal. Galea narrow, with paniculate brush. Inner and basal setae of lacinia absent. Last labial palp straight. Eyes anteriorly entire, not notched. Antennae clubbed; antennomeres VII–XI symmetrical.

Prothorax. Prothoracic corbiculum absent. Hypomeron visible in lateral view; apex acute and not extending beyond pronotum.

Mesothorax. Mesoventral lines impunctate. Secondary lines present. Scutellum visible in dorsal view. Mesoventral process carinate. Mesepimeron absent. Meso- and metaventrite separate.

Metathorax. Submesocoxal lines parallel to coxae, punctate. Metaventral setose patch absent. Primary seta present.

Wings. Sutural and apical serrations of the elytra present. Lateral stria present.

Legs. Profemoral ctenidium absent. Tibiae spinose. Mesotibiae with two inner apical spines, equal in length.

Abdomen. Submetacoxal bead on abdominal process absent. Submetacoxal space absent.

Cyparium fugitivum sp. nov.
urn:lsid:zoobank.org:act:C00D14F8-67BE-4DBB-8E05-CBF79D7920BC
Figs 1A–D, 2A, F–G, 3–5, 93A–B

Diagnosis

Body length: 4.40 mm, robust. Black, laterals of pronotum, hypomere and humeral region reddish; very shining. Seven rows of coarse elytral punctures. Lacking microsculpture. Medium lobe strongly curved in lateral view; parameres thin.

Etymology

The species epithet is a Latin word meaning ‘runaway’, because the holotype almost escaped when I tried to collect it.

Material examined

Holotype

BRAZIL • ♂*; Minas Gerais, Viçosa, Mata da Biologia; 15 May 2021; E. von Groll and A. Orsetti leg.; “Fungo 44 / Em *Agaricales* indet. / Dissecado em 15.xii.2022 / HOLOTYPUS ♂”; CELC. (Fig. 3D–E).

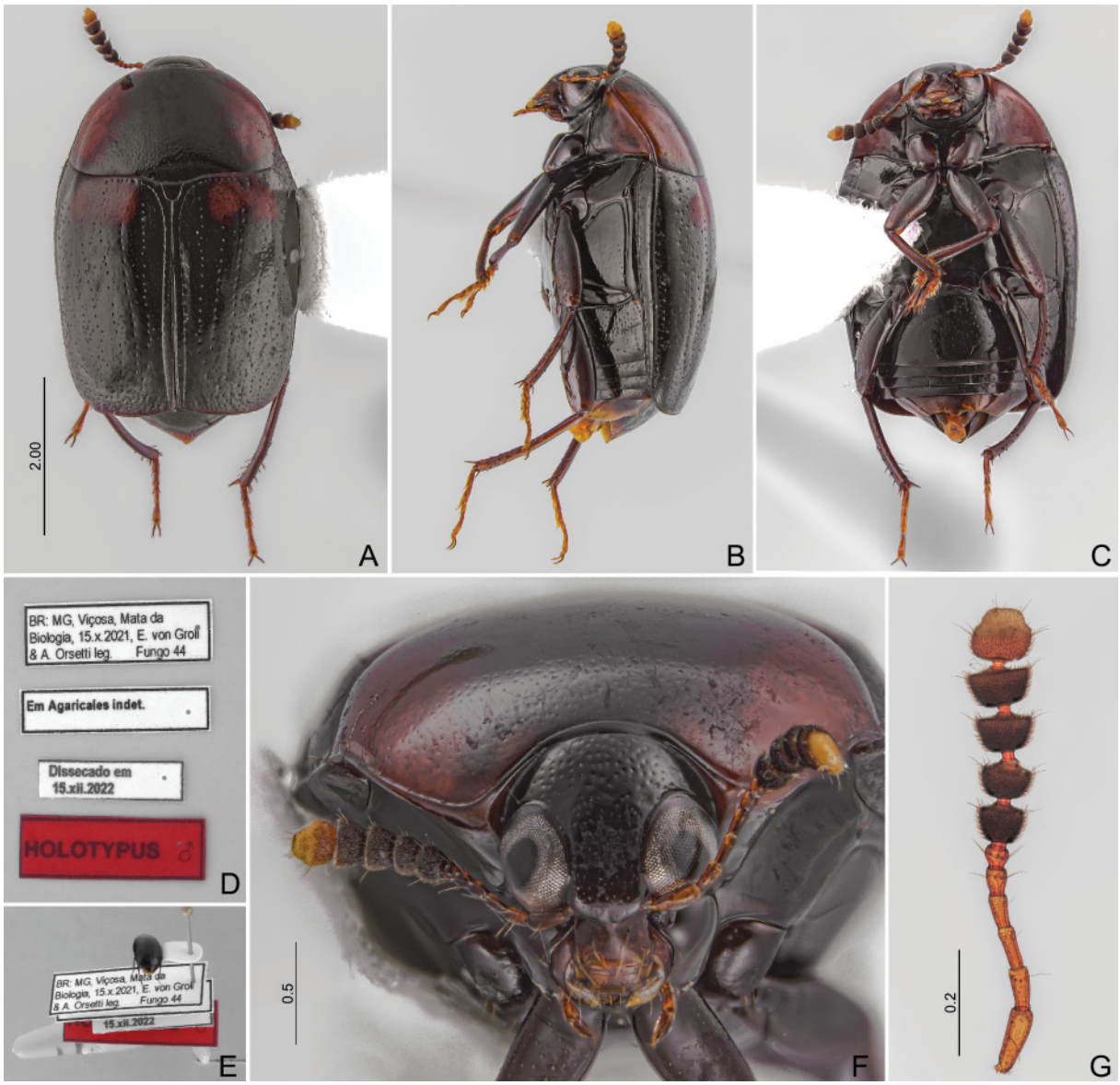

Fig. 3. *Cyparium fugitivum* sp. nov., holotype, ♂ (CELC). **A**. Dorsal view. **B**. Lateral view. **C**. Ventral view. **D**. Labels. **E**. Pinned. **F**. Frontal view. **G**. Antennae. Scales in mm.

Fig. 4. *Cyparium fugitivum* sp. nov., holotype, ♂ (CELC). **A**. Prothorax, dorsal view. **B**. Oblique view. **C–E**. Legs. **C**. Fore. **D**. Middle. **E**. Hind. **F–H**. Tarsi. **F**. Pro. **G**. Meso. **H**. Meta. **I**. Apical spine of mesotibiae. **J**. Apical spine of metatibiae. **K**. Apex of elytra. **L**. Abdomen, dorsal view. Scales in mm.

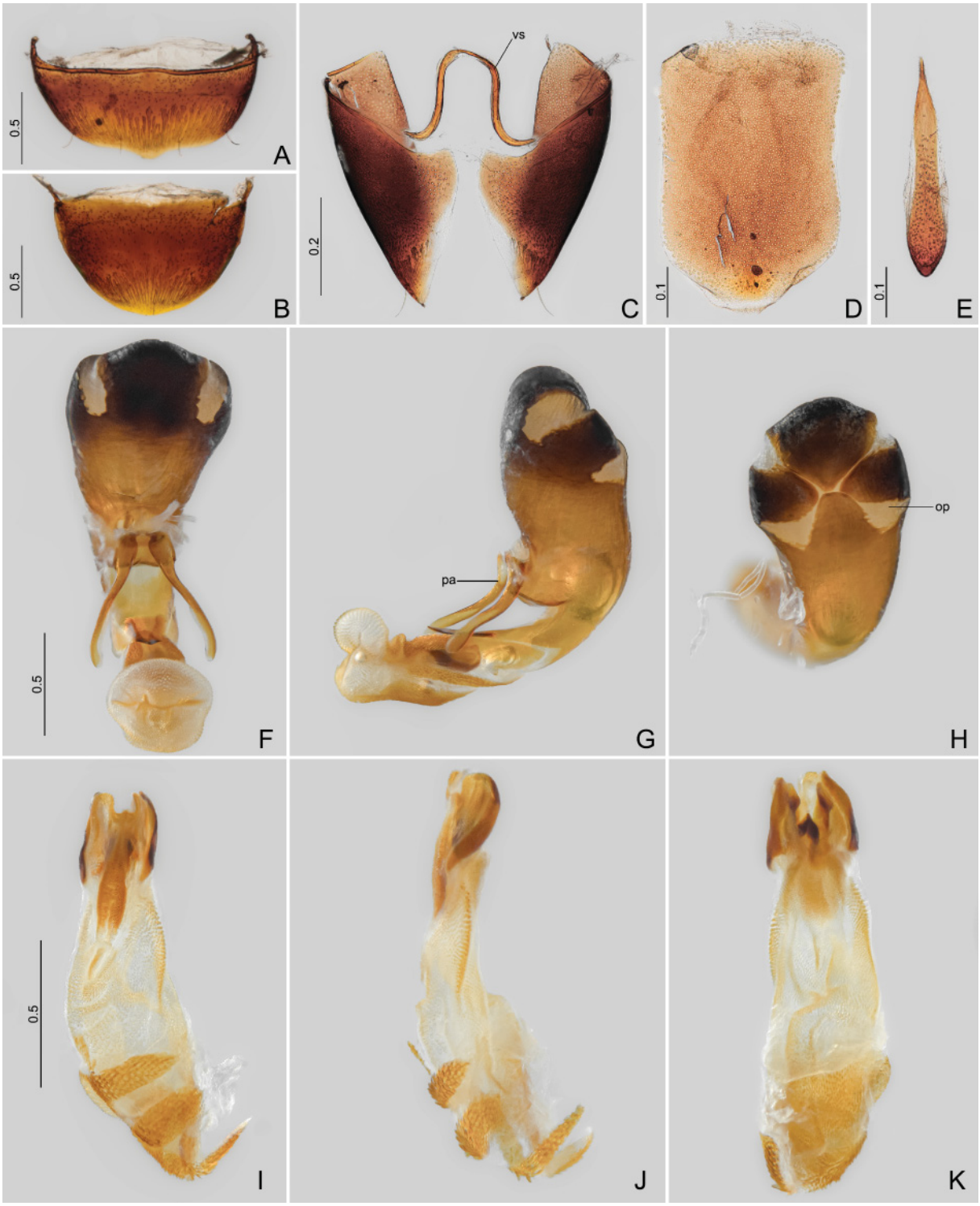

Fig. 5. *Cyparium fugitivum* sp. nov., holotype, ♂ (CELC). **A**. Sternite VIII. **B**. Tergite VIII. **C**. Tergite IX. **D**. Tergite X. **E**. Sternite IX. **F–H**. Aedeagi. **F**. Frontal view. **G**. Lateral view. **H**. Dorsal view. **I–K**. Sclerite of the internal sac. **I**. Frontal view. **J**. Lateral view. **K**. Dorsal view. Abbreviations: op = opening; pa = parameres; vs = ventral strut. Scales in mm.

Description

Colouration. Black. Humeral region, laterals of pronotum and hypomeron reddish (Figs 3A–C, F, 4A–B). Legs dark red-purplish (Fig. 4C–E). Antennomeres I–VI and XI, mouthparts, and tarsi ochreous (Figs 3F, 4F–H).

Head. Frons with dense and coarse punctate; eyes very prominent (Fig. 3F). Antennomeres VIII–XI wide; ratios: I 127/45 : II 83/38 : III 86/33 : IV 63/36 : V 55/40 : VI 40/46 : VII 69/85 : VIII 62/93 : IX 70/102 : X 67/110 : XI 103/112 (Fig. 3G).

Thorax. Pronotum coarse and shallowly punctate (Fig. 4A). Hypomeron smooth (Fig. 4B). Scutellum rounded posteriorly (Fig. 4A). Ventral sclerites of thorax smooth and almost glabrous; metaventrite with sparse coarse punctures laterally (Fig. 4B–C). Submesocoxal lines parallel to coxae, with few coarse punctures (Fig. 4B).

Wings. Elytra rectangular, longer than wide; sutural and basal striae connected; basal stria punctate, reaching almost middle of elytra (Fig. 3A). Seven rows of coarse punctures (Fig. 3A). Epipleuron coarsely punctate (Fig. 4B). Apical spines small (Fig. 4K).

Legs. Femora sparsely and coarsely punctate (Fig. 4C–E). Meso- and metatibiae curved (Fig. 4D–E), with two large apical spines (Fig. 4I–J).

Abdomen. Abdominal ventrite I coarsely punctate, denser laterally; submetacoxal bead with close and coarse punctures (Figs 3B–C, 4B). Propygidium and pygidium micropunctured and with coarse punctures; disc with strigulate microsculpture anteriorly (Fig. 4L).

Male

Sternite VIII rectangular with a rounded projection (Fig. 5A). Tergite VIII wide and rounded (Fig. 5B). Tergite IX with rectangular-shaped ventral struts (Fig. 5C). Tergite X (Fig. 5D) as long as wide. Sternite IX thicker posteriorly (Fig. 5E).

Aedeagus. Strongly sclerotized. Basal bulb large; apical lobe curved in lateral view (Fig. 5F–H); dorsal openings forming an upside-down triangle (Fig. 5H). Parameres thin and short, slightly sinuous (Fig. 5F–G). Internal sac with irregular sclerites (Fig. 5I–K).

Measurements (n = 1; in mm). TL 4.40, SY 0.37, HW 1.09, IS 0.44, WA 0.27, PL 1.56, PA 1.41, PB 2.75, SL 0.24, SW 0.28, EI 2.70, EL 3.12, EW 1.60, EH 1.09, MSW 0.55, MEL 0.31, MEW 0.13, MB 0.71, MC 1.22, VL 1.00, VL2 0.66. Legs: PrF 1.53, PrT 0.91, MsF 1.34, MsT 1.09, MtF 1.59, MtT 1.56.

Host

Collected from an undetermined mushroom on the border of a field trail (Fig. 93A–B)**.**

Remarks

The humeral reddish area is similar to *C. pici* von Groll & Lopes-Andrade, 2021 and *C. loebli* von Groll & Lopes-Andrade, 2021 but differs by the larger size and by the pronotal lateral reddish marks. The pronotum colouration resembles *C. anale* Reitter, 1880 but the elytral colouration is different. The aedeagus is similar to that of *C. pici* but it is less robust and the sclerites are in a different shape. The aedeagus is also similar to that of *C. lescheni* von Groll & Lopes-Andrade, 2021 but it is larger and more robust.

Distribution

Mata da Biologia, Universidade Federal de Viçosa, campus of Viçosa, state of Minas Gerais, Southeast Brazil (Fig. 1A–D).

Scaphidiini Latreille, 1806

Genus ***Scaphidium*** Olivier, 1790
Fig. 2B, E

Scaphidium Olivier, 1790: 20: 1. Type species: *Scaphidium quadrimaculatum* Olivier, 1790; fixation by Latreille 1810.
Ascaphidium Pic, 1915a: 24. Type species: *Ascaphidium sikorai* Pic, 1915; by monotypy.
Cribroscaphium Pic, 1920b: 93 (subgenus of *Scaphidium*). Type species: *Scaphidium irregulare* Pic, 1920; by monotypy.
Hemiscaphium Achard, 1922a: 12. Type species: *Scaphidium striatipenne* Gestro, 1879; by original designation.
Hyposcaphidium Achard, 1922a: 12 (subgenus of *Scaphidium*). Type species: *Scaphidium rufopygum* Lewis, 1893, designated by Löbl 2015: 21.
Isoscaphium Achard, 1922a: 12 (subgenus of *Scaphidium*). Type species: *Scaphidium quadriguttatum* Say, 1823, designated by Löbl 2015: 21.
Pachyscaphidium Achard, 1922a: 12 (subgenus of *Scaphidium*). Type species: *Scaphidium arrowi* Achard, 1920; by monotypy.
Scaphidiolum Achard, 1922a: 12. Type species: *Scaphidium basale* Laporte, 1840; by original designation.
Scaphidopsis Achard, 1922a: 12. Type species: *Scaphidium pardale* Laporte, 1840; by original designation.
Falsoascaphidium Pic, 1923: 16. Type species: *Scaphidium subdepressum* Pic, 1921; by original designation.
Parascaphium Achard, 1923: 97. Type species: *Scaphium optabile* Lewis, 1893; by monotypy.

There are 13 species of *Scaphidium* known from Brazil. During my field trips, it was possible to collect only one specimen, *Scaphidium* cf. *gounellei*. Nonetheless, this single specimen was not included in this manuscript due to limited time.

General description (Leschen & Löbl 2005)

Head. Mandible with two apical teeth and serrations present. Maxillary palp normal. Galea wide with radulate brush. Inner and basal setae of lacinia present. Last labial palp straight. Eyes anteriorly notched (Fig. 2E). Antennae clubbed; antennomeres VII–XI symmetrical (Fig. 2B).

Prothorax. Prothoracic corbiculum absent. Hypomeron visible in lateral view; apex subacute and not extending beyond pronotum.

Mesothorax. Mesoventral lines impunctate. Secondary lines present. Scutellum visible in dorsal view. Mesoventral process carinate. Mesepimeron absent. Meso- and metaventrite separate.

Metathorax. Submesocoxal lines parallel to coxae. Metaventral setose patch present. Primary seta absent.

Wings. Sutural and apical serrations of elytra present. Basal stria absent; lateral stria present.

Legs. Profemoral ctenidium absent. Tibiae not spinose. Mesotibiae with two inner apical spines, equal in length.

Abdomen. Submetacoxal bead on abdominal process absent. Submetacoxal space absent.

Tribe Scaphisomatini Casey, 1893

Genus ***Alexidia*** Reitter, 1880
Figs 2M, O–P, 6–13

Alexidia Reitter, 1880: 43. Type species: *Alexidia rogenhoferi* Reitter, 1880; by monotypy.

Alexidia comprises four known species, all of them distributed in the Neotropical Region. Only *A. plaumanni* Löbl & Leschen, 2003a is reported from Brazil (state of Santa Catarina). During my field trips, two species of *Alexidia* were discovered and are described here: (1) *A. convivalis* sp. nov. represented by 19 specimens, and (2) *A. solitaria* sp. nov. represented by a single female. No more specimens belonging to this genus were collected.

General description

Body large, oval.

Head. Labral setae present. Mandible apically bidentate (Fig. 7B–C). Maxillary palp aciculate (Fig. 7D). Galea wide, with radulate brush (Fig. 7D). Inner and basal setae of lacinia absent (Fig. 7D). Setae on adoral surface of hypopharynx spinose (Fig. 7E–F). Last labial palpomere curved (Fig. 7E–F). Submaxillary ducts present (Fig. 7G). Gular suture not reaching submentum. Frontoclypeal suture present (Figs 6H, 12E). Antennomeres III and IV elongate; VII–X with a long basal stalk (Figs 6J–K, 12F).

Prothorax. Prothoracic corbiculum present (Fig. 7L). Hypomeron visible in lateral view; apex subacute and not extending beyond pronotum (Figs 6B, 12B).

Mesothorax. Mesoventral lines impunctate and connected to mesocoxal cavity (Fig. 8D). Median and secondary lines absent. Prepectus present. Scutellum concealed in dorsal view (Fig. 8A–B). Mesoventral process paxillate (Fig. 8G). Meso- and metaventrite not fused (Fig. 8D).

Metathorax. Submesocoxal lines arcuate (Figs 8F, 12D). Metaventral setose patch absent (Fig. 8E). Intercoxal plates present.

Wings. Elytra lacking apical serrations (Figs 9H, 12H); basal and lateral striae present (Fig. 8A).

Legs. Profemoral ctenidium absent. Mesotibiae with a single inner apical spine (Fig. 9E).

Abdomen. Submetacoxal bead meeting in middle; punctate (Fig. 8E). Submetacoxal area absent.

Males. Aedeagal sclerites tripartite (Fig. 10E–J) (Löbl & Leschen 2003b; Leschen & Löbl 2005).

Alexidia convivalis sp. nov.
urn:lsid:zoobank.org:act:15C92174-46F7-4EAB-8406-88CEA582294F
Figs 1A–B, G, 6–11

Diagnosis

Body length: 1.41–1.55 mm. Oval, in dorsal view, and convex in lateral. Brown to dark brown, edges of some sclerites reddish; shining. Sutural, basal, and lateral striae joined. Almost glabrous and lacking coarse punctures. Submetacoxal area short.

Etymology

The species epithet is a Latin word meaning ‘feast’, ‘banquet’, because of the great feast they were having, all the time specimens were collected among other *Alexidia* and many *Baeocera* species.

Material examined

Holotype

BRAZIL • ♂; Minas Gerais, Viçosa, EPTEA Mata do Paraíso; 24 Mar. 2022; E. von Groll *et al.* leg.; "Fungo 20 / Em *Ceratiomyxa fruticulosa* em *Pinus* / HOLOTYPE ♂"; CELC. (Fig. 6D–E)

Paratypes

BRAZIL • 1 ex.; same locality as for holotype; 12 Nov. 2019; LabCol leg.; "Fungo 10 / Em *Ceratiomyxa fruticulosa*"; CELC • 6 ♂♂, 7 ♀♀ (1 ♂*, 1 ♂**, 1 ♀**,); same locality as for holotype; 10 Mar. 2022; LabCol leg.; "Falcon 26 / Em *Ceratiomyxa fruticulosa* em *Pinus*"; CELC • 1 ♂, 1 ♀; same locality as for holotype; 24 Mar. 2022; E. von Groll *et al.* leg.; "Fungo 20 / Em *Ceratiomyxa fruticulosa* em *Pinus*"; CELC • 1 ♂, 1 ♀; same locality as for holotype; 14 Apr. 2022; LabCol leg.; "Falcon 42 / Em *Ceratiomyxa fruticulosa* em *Pinus*"; CELC.

Description

Colouration. Dark brown, edges of some sclerites reddish; distal part of femora and tibiae lighter, tarsi, mouthparts and antennomeres I–VI yellow (Fig. 6A–C, H). Variation: light brown and not reddish (Fig. 6F–G).

Head. Frons smooth, subglabrous, devoid of punctures (Fig. 6H). Clypeus longer than wide (Fig. 6H–I). Labrum rounded apically (Fig. 7A). Mandible elongate (Fig. 7B–C). Last maxillary palpomere 1.70× as long as previous (Fig. 7D). Last labial palpomere not strongly curved (Fig. 7E–F). Mentum laterally constricted (Fig. 7F). Three submaxillary ducts (Fig. 7G). Gular region with strigulate microsculpture and few and sparse gular pores; gular suture short, more than 2× distant from submentum (Fig. 7G). Antennomeres VIII, IX, and XI slender. Antennomere proportions (n = 2): I 98/32 : II 88/36 : III 56/16 : IV 84/16 : V 98/17 : VI 89/17 : VII 97/25 : VIII 77/17 : IX 112/27 : X 105/35 : XI 113/35 (Fig. 6J–K).

Prothorax. Smooth, lacking microsculpture (Figs 6A, F, 7H–I, 11A). Pronotum strongly curved in lateral view (Figs 6B, G, 11B); punctation very fine; pubescence sparse and short; posterior angles not trespassing mesenepisternum. Hypomeron almost glabrous (Figs 6G, 11C). Notosternal suture curved inward (Fig. 7J). Prosternal process long and acute (Fig. 7K). Profurca thin and elongate (Fig. 7L). Prothoracic corbiculum shortly pubescent (Fig. 7L).

Mesothorax. Lacking microsculpture, almost glabrous (Figs 6B, G, 8E–F, 11B–C). Scutellar lines straight in middle, forming two lateral lobes (Fig. 8C). Mesepimeron short and oblique (Fig. 8F). Procoxal rests triangular, wide (Fig. 8D). Mesoventral lines oblique (Fig. 8D). Median and secondary lines absent. Mesoventral process sinuous (Fig. 8G).

Metathorax. Metaventrite smooth, devoid of punctures; pubescence sparse (Figs 6B, G, 8E–F, 11B–C). Submesocoxal lines punctate; submesocoxal area micropunctured; length: 0.04–0.05 (Figs 6A, G, 8F, 11C). Metanepisternum mostly covered by elytra (Figs 6A, G, 8F, 11C). Metanotum with alacrista triangular and wide; median membranous area wide; scutoscutellar suture oval and flattened (Fig. 8H). Metepimeron distinct, smooth. Intercoxal plates rectangular (Figs 6A, G, 8F, 11B–C). Metendosternite thick; stalk, and ventral longitudinal flange elongate (Fig. 8I–K).

Wings. Elytra wider anteriorly; shining; lacking microsculpture; finely punctate; moderately pubescent (Figs 6A, F, 8L–M, 11A). Sutural striae joined to basal and then, to lateral striae (Figs 6A–B, F–G, 7H). Adsutural area wider near posterior ⅔. Epipleura impunctate (Fig. 8F). Hind wings fully developed (Fig. 9A).

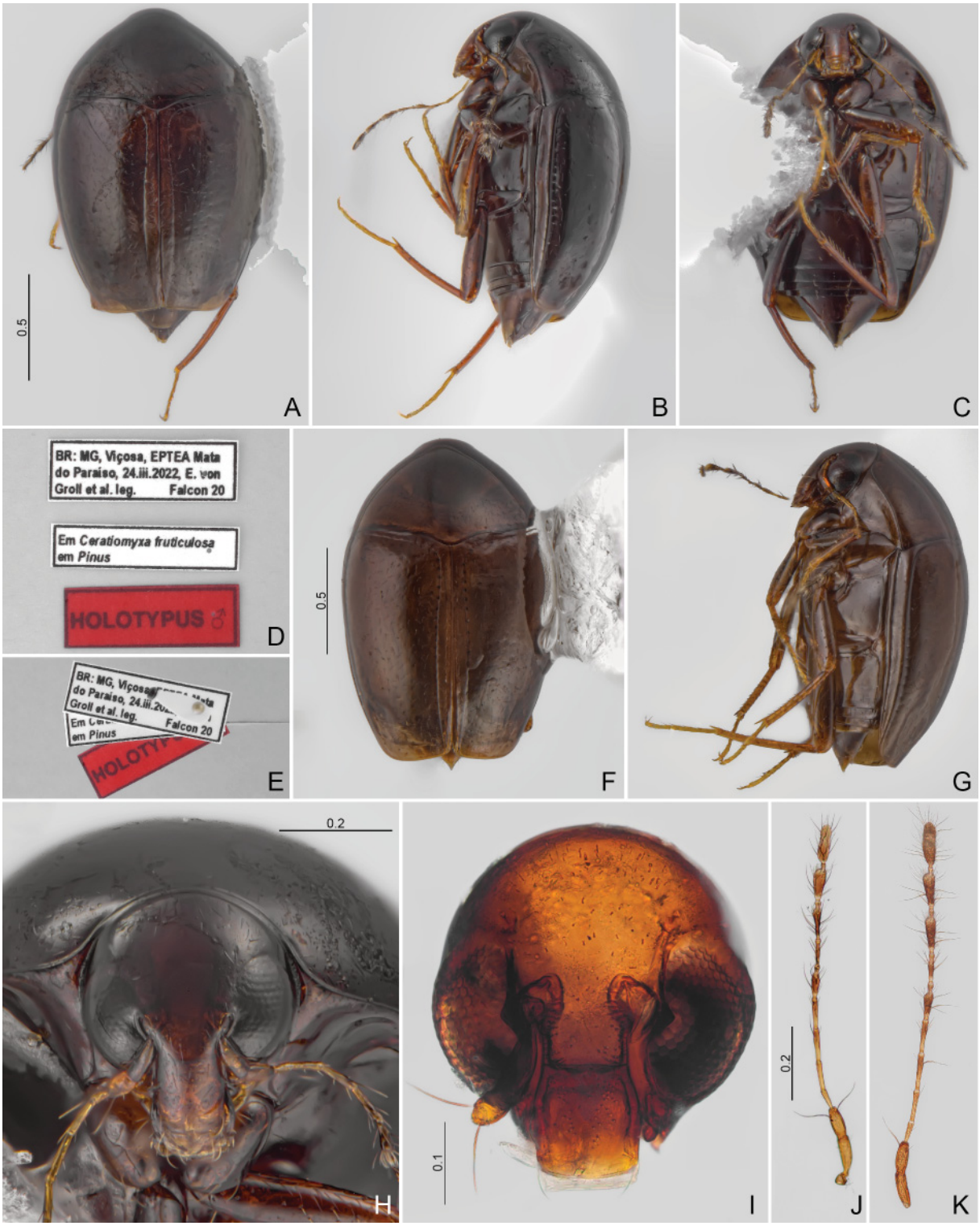

Fig. 6. *Alexidia convivalis* sp. nov. (CELC). **A–E, H**. Holotype, ♂. **A**. Dorsal view. **B**. Lateral view. **C**. Ventral view. **D**. Labels. **E**. Pinned. **F–G**. Paratype, teneral (#09). **F**. Dorsal view. **G**. Lateral view. **H**. Head, frontal view. **I**. Paratype, ♂ (#05), dissected head, frontal view. **J–K**. Antennae. **J**. Paratype, ♂ (#11). **K**. Paratype, ♀ (#07). Scales in mm.

Legs (Figs 9B–G, 11D–I). Pro- and mesofemora sparse and coarsely punctate. Femora narrow. Meso- and metatibiae bearing a long apical spine.

Abdomen. Subglabrous, shining; primary setae present. Lateral of ventrite I and tergite VI with micropuncture (Figs 6B, 11B). Tergite VI bearing few setae (Figs 9H, 11J).

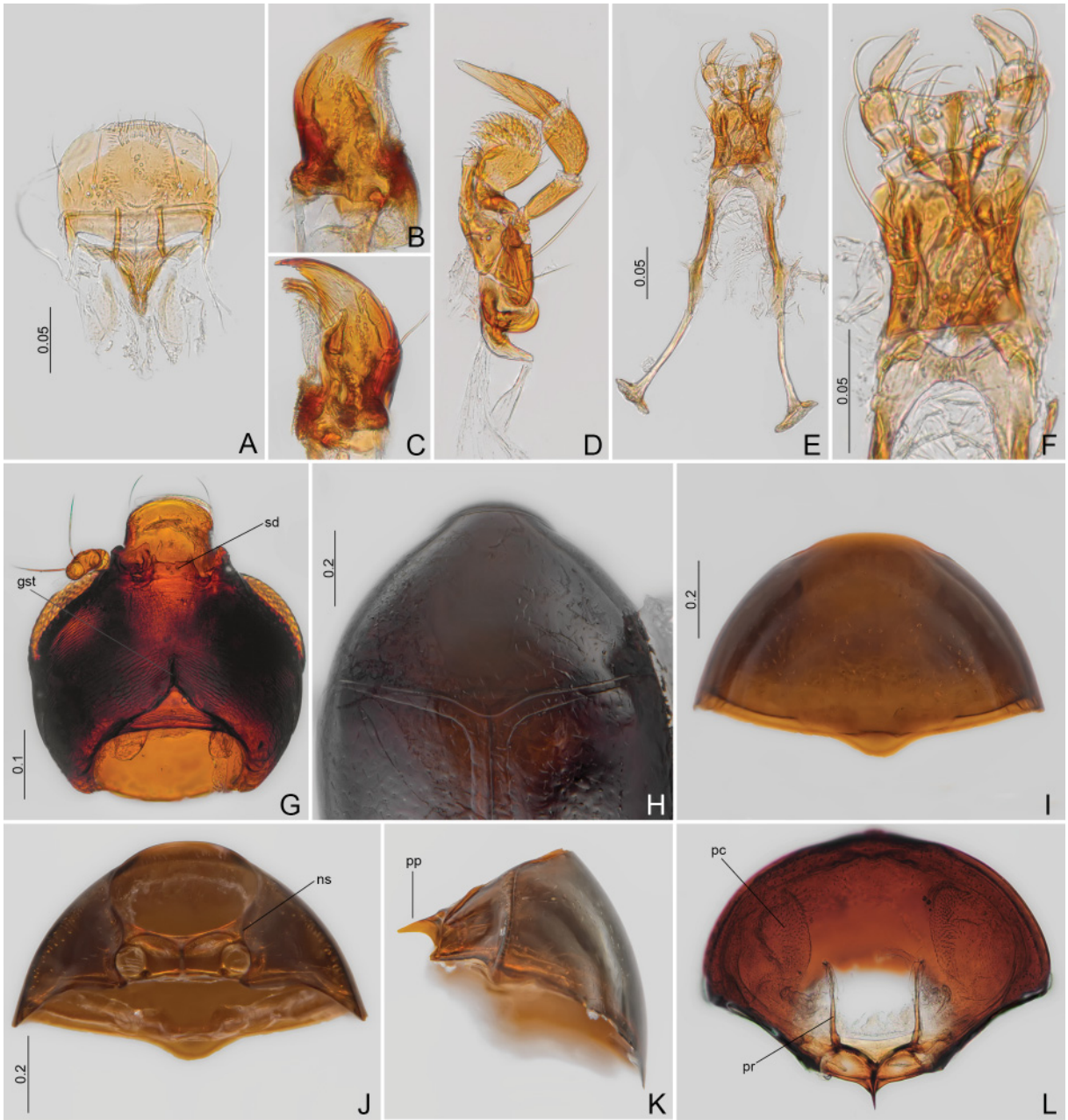

Fig. 7. *Alexidia convivalis* sp. nov. (CELC). **A–G**. Paratype, ♂ (#05). **A**. Labrum. **B–C**. Mandibles. **D**. Maxilla. **E–F**. Labium. **G**. Dissected head, ventral view. **H**. Holotype, ♂, prothorax, dorsal view. **I–K**. Paratype, ♂ (#05), prothorax. **I**. Dorsal view. **J**. Ventral view. **K**. Lateral view. **L**. Paratype (#08), prothorax, inner view. Abbreviations: gst = gular suture; ns = notosternal suture; pc = prothoracic corbiculum; pp = prosternal process; pr = profurca; sd = submaxillary duct. Scales in mm.

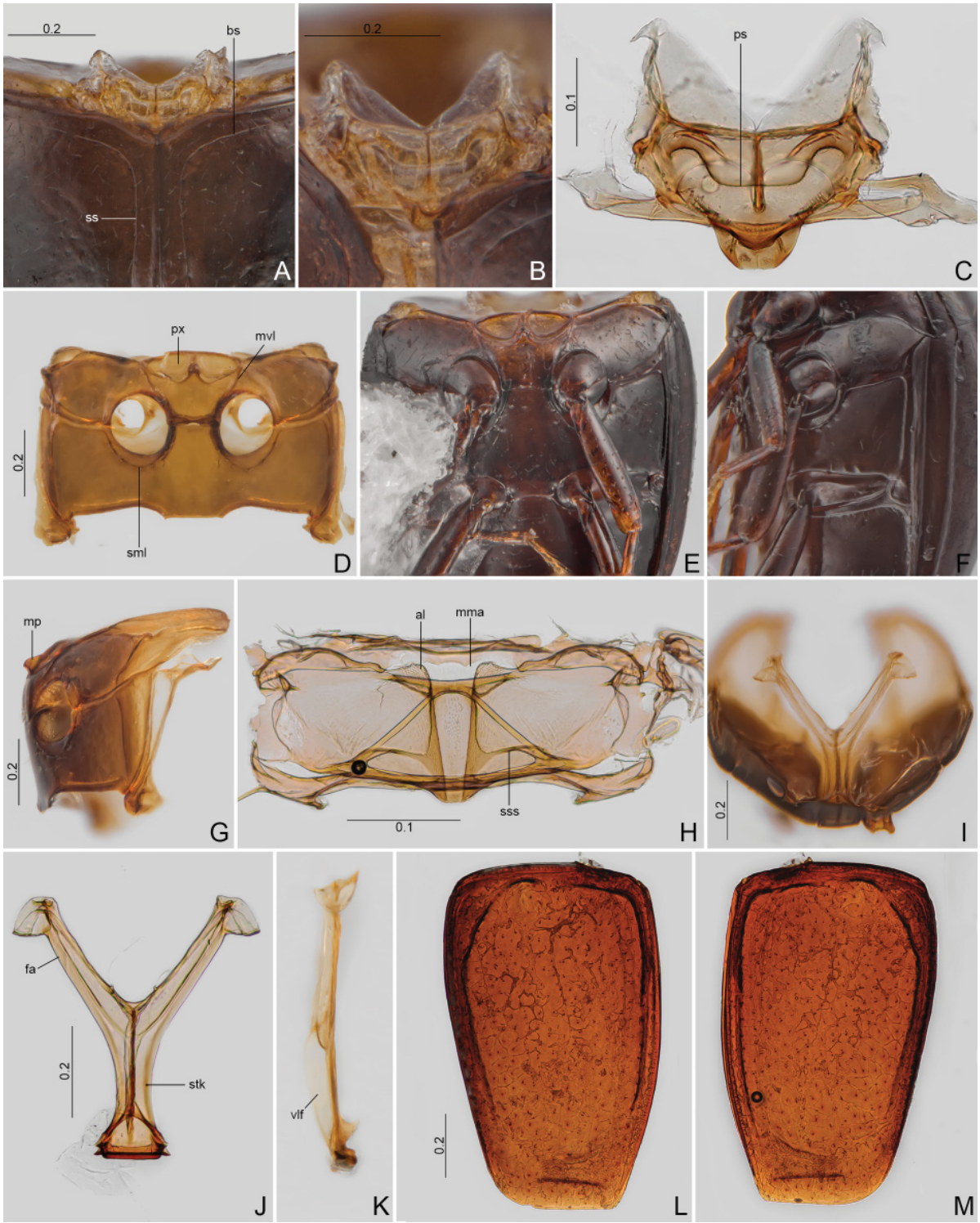

Fig. 8. *Alexidia convivalis* sp. nov. (CELC). **A–C**. Scutellar shield. **A–B**. Paratype ♂ (#08). **C**. Paratype, ♂ (#11). **D–G**. Meso- and metathorax. **D**. Paratype, ♂ (#11), dissected, ventral view. **E**. Paratype (#08), ventral view. **F**. Holotype, ♂, oblique view. **G**. Paratype, ♂ (#11), lateral view. **H**. Paratype, ♂ (#11), metanotum. **I–K**. Metendosternite. **I**. Paratype, ♂ (#05), connected to the thorax. **J**. Paratype, ♂ (#11), dorsal view. **K**. Paratype, ♂ (#11), lateral view. **L–M**. Paratype, ♂ (#05), elytra. Abbreviations: al = alacrista; bs = basal stria; fa = furcal arms; mma = median membranous area; mp = mesoventral process; mvl = mesoventral line; ps = prescutellar line; px = procoxal rest; sml = submesocoxal line; ss = sutural stria; sss = scutoscutellar suture; stk = stalk; vlf = ventral longitudinal flange. Scales in mm.

Males

Antennae slightly thinner than in females (Fig. 6J–K). Pro- and mesotarsomeres I–III slightly widened, bearing tenent setae (Fig. 9C, E). Metatibia arcuate (Fig. 9F). Ventrite VIII with a short posterior projection (Fig. 9I); tergite VIII straight posteriorly (Fig. 9J); both tergite and ventrites VIII punctate and not microsculptured. Tergite IX with rounded ventral struts (Fig. 9K); sternite IX thick, with strigulate microsculpture (Fig. 9L); tergite X triangular (Fig. 9M).

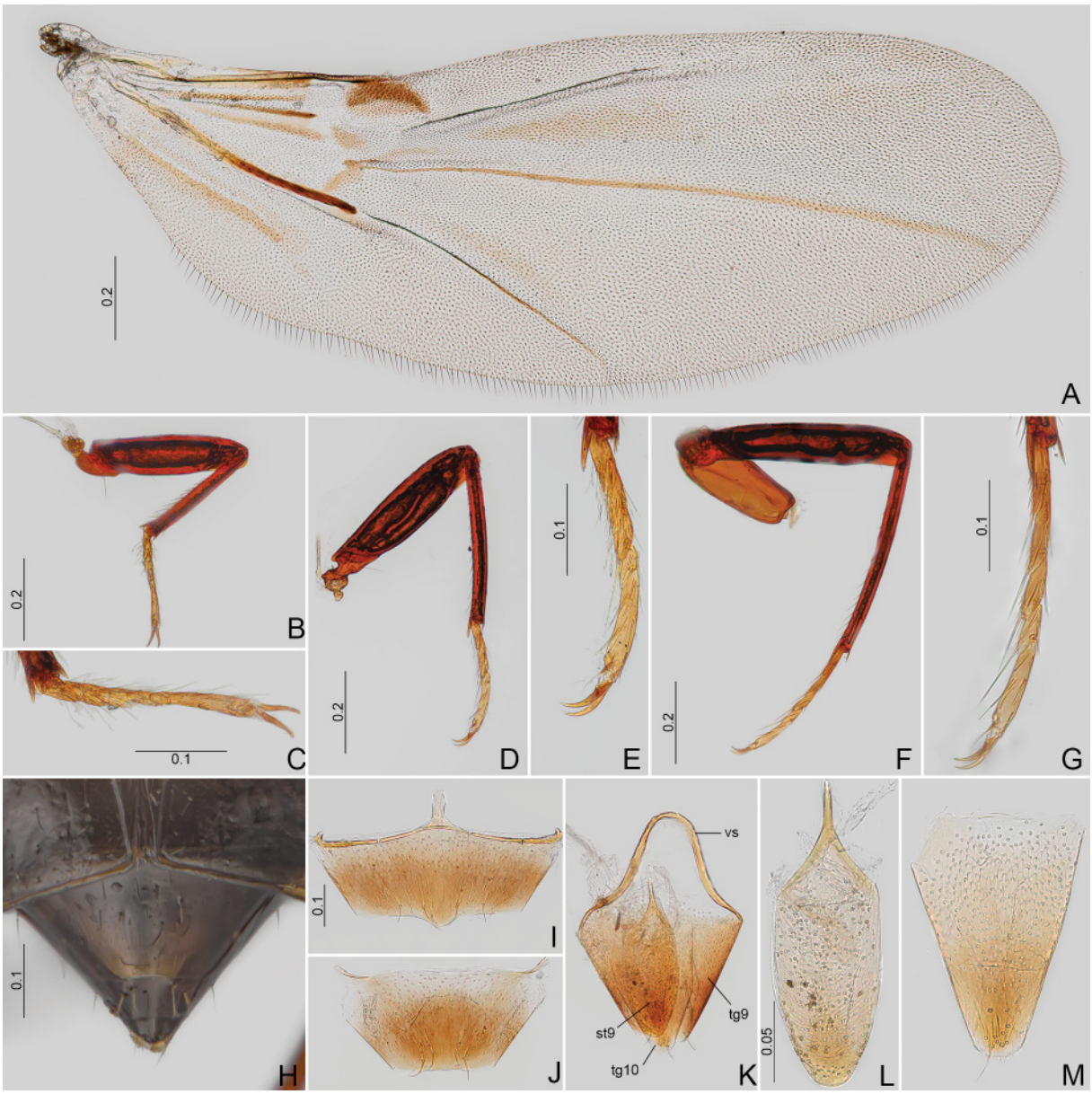

Fig. 9. *Alexidia convivalis* sp. nov. (CELC). **A–G**. Paratype, ♂ (#11). **A**. Hind wing. **B**. Foreleg. **C**. Protibiae. **D**. Middle leg. **E**. Mesotibiae. **F**. Hind leg. **G**. Metatibiae. **H**. Holotype, ♂, abdomen, dorsal view. **I–M**. Paratype, ♂ (#05). **I**. Sternite VIII. **J**. Tergite VIII. **K**. Tergite IX. **L**. Sternite IX. **M**. Tergite X. Abbreviations: st9 = sternite IX; tg9 = tergite IX; tg10 = tergite X; vs = ventral struts. Scales in mm.

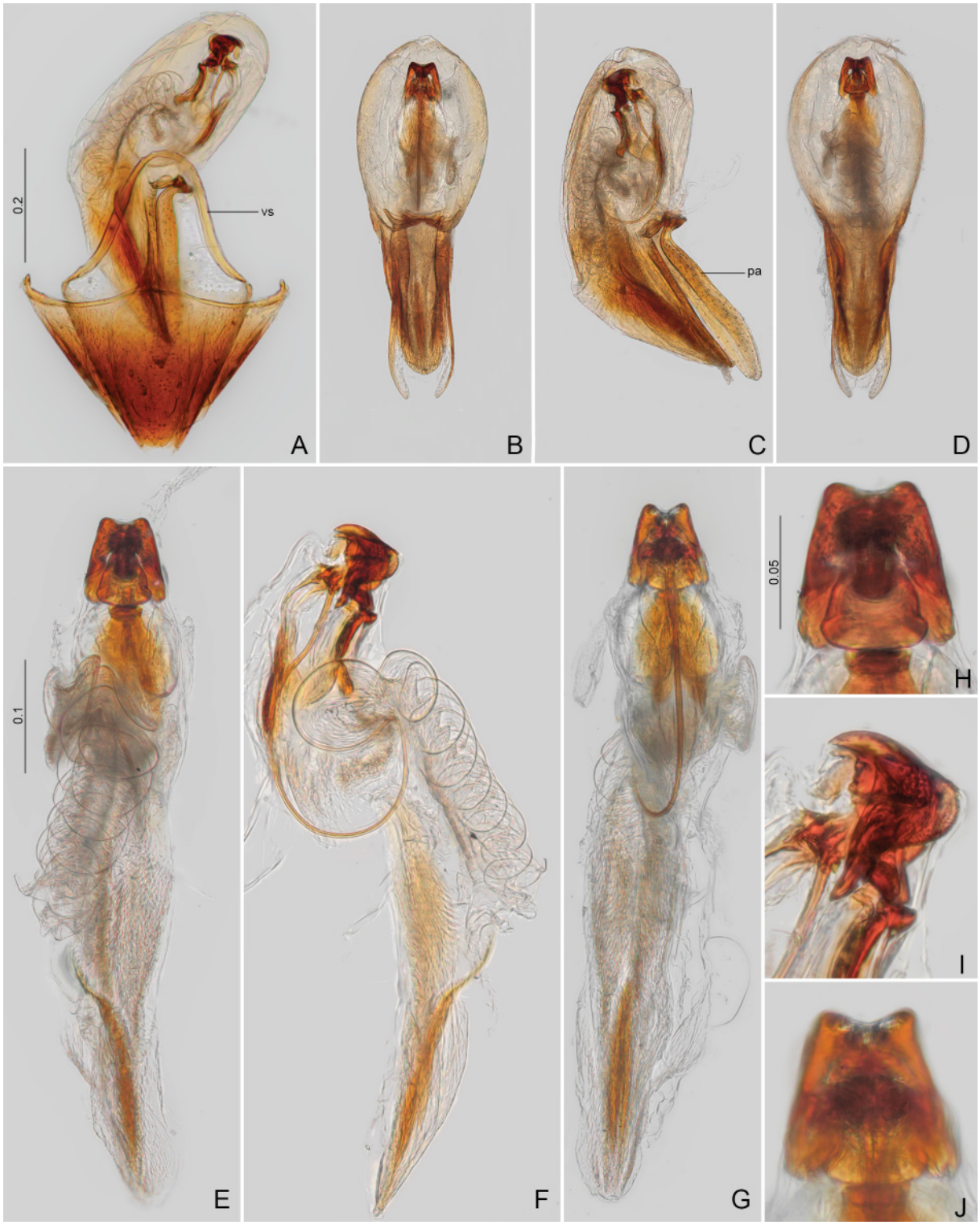

Fig. 10. *Alexidia convivalis* sp. nov. (CELC). **A–J**. Paratype, ♂ (#05). **A**. Terminalia **B–D**. Aedeagi. **B**. Frontal view. **C**. Lateral view. **D**. Dorsal view. **E–G**. Sclerite of the internal sac. **E**. Frontal view. **F**. Lateral view. **G**. Dorsal view. **H–J**. Detail of sclerite of the internal sac. **H**. Frontal view. **I**. Lateral view. **J**. Dorsal view. Abbreviations: pa = parameres; vs = ventral struts. Scales in mm.

Fig. 11. *Alexidia convivalis* sp. nov. (CELC). **A–C**. Paratype, ♀. **A**. Dorsal view. **B**. Lateral view. **C**. Oblique view (#6). **D–N**. Paratype ♀ (#7). **D–F**. Legs. **D**. Fore. **E**. Middle. **F**. Hind. **G–I**. Tarsi. **G**. Pro. **H**. Meso. **I**. Meta. **J**. Abdomen, dorsal view. **K**. Sternite VIII. **L**. Tergite VIII. **M**. Genitalia. **N**. Ovipositor. Abbreviations: dg = distal gonocoxites; gs = gonostyli; sd = spermathecal duct; sp = spermatheca. Scales in mm.

Aedeagus (Fig. 10A–J). Curved in lateral view; basal bulb poorly sclerotized; apical lobe sclerotized. Parameres long and thin; sclerite tripartite and symmetrical (Fig. 10E–J).

Measurements (n = 9, including holotype, unless otherwise specified; in mm). TL (n = 8) 1.44–1.50 (1.46 ± 0.02), SY 0.17–0.20 (0.18 ± 0.01), HW 0.36–0.40 (0.39 ± 0.01), IS 0.18–0.22 (0.19 ± 0.01), WA 0.10–0.13 (0.12 ± 0.01), PL (n = 8) 0.54–0.60 (0.57 ± 0.02), PA 0.42–0.47 (0.44 ± 0.02), PB 0.93–0.97 (0.95 ± 0.01), EI 0.96–1.05 (1.00 ± 0.03), EL 1.05–1.12 (1.08 ± 0.03), EW 0.48–0.54 (0.50 ± 0.02), EH 0.42–0.49 (0.46 ± 0.02), MsW 0.20–0.26 (0.23 ± 0.02), MeL 0.06–0.12 (0.09 ± 0.02), MeW (n = 8) 0.03–0.04 (0.03 ± 0.01), MB 0.10–0.13 (0.12 ± 0.01), MC 0.30–0.35 (0.32 ± 0.02), ML 0.04–0.05 (0.04 ± 0.005), VL 0.25–0.28 (0.26 ± 0.01), VL2 (n = 8) 0.22–0.27 (0.25 ± 0.02); PrF 0.37–0.42 (0.40 ± 0.02), PrT 0.25–0.31 (0.29 ± 0.02), MsF 0.40–0.47 (0.44 ± 0.02), MsT 0.35–0.41 (0.38 ± 0.02), MtF 0.44–0.50 (0.49 ± 0.02), MtT 0.43–0.49 (0.47 ± 0.02).

Females (Fig. 11)

Tarsi not enlarged and lacking tenent setae (Fig. 11G–I). Ventrite VIII with a triangular projection (Fig. 11K) and tergite VIII straight posteriorly (Fig. 11L) – both microsculptured. Spermatheca elongate and twisted, forming a circular structure; spermathecal duct filiform (Fig. 11M). Distal gonocoxite long and slender, somewhat arcuate (Fig. 11M–N). Gonostylus about 2 × as long as wide, tapering posteriorly (Fig. 11M–N).

Measurements (n = 9, in mm). TL 1.41–1.55 (1.50 ± 0.04), SY 0.15–0.19 (0.18 ± 0.01), HW 0.39–0.41 (0.40 ± 0.01), IS 0.18–0.21 (0.19 ± 0.01), WA 0.11–0.14 (0.12 ± 0.01), PL 0.54–0.63 (0.59 ± 0.03), PA 0.43–0.47 (0.45 ± 0.01), PB 0.88–0.98 (0.95 ± 0.03), EI 0.95–1.04 (1.01 ± 0.03), EL 1.03–1.14 (1.11 ± 0.03), EW 0.44–0.55 (0.51 ± 0.04), EH 0.43–0.49 (0.46 ± 0.02), MsW 0.20–0.27 (0.24 ± 0.02), MeL 0.05–0.13 (0.09 ± 0.02), MeW 0.02–0.04 (0.03 ± 0.01), MB 0.10–0.14 (0.12 ± 0.01), MC 0.29–0.38 (0.33 ± 0.03), ML 0.04–0.06 (0.05 ± 0.01), VL 0.25–0.33 (0.28 ± 0.02), VL2 0.24–0.28 (0.26 ± 0.01), PrF 0.39–0.42 (0.41 ± 0.01), PrT 0.28–0.31 (0.30 ± 0.01), MsF 0.42–0.46 (0.45 ± 0.01), MsT 0.35–0.41 (0.38 ± 0.02), MtF 0.45–0.50 (0.48 ± 0.02), MtT 0.45–0.49 (0.48 ± 0.01).

Host

Collected from *Ceratiomyxa fruticulosa* T.Macbr. (Protozoa) on a fallen *Pinus* sp. tree (Fig. 1G).

Remarks

The aedeagus is very similar to that of *A. plaumanni* but it can be easily distinguished by the external morphology: smaller body length, the metaventrite and abdomen are not punctate, and the elytral punctation is not coarse.

Distribution

Mata do Paraíso, Universidade Federal de Viçosa, campus of Viçosa, state of Minas Gerais, Southeast Brazil (Fig. 1A–B, G).

Alexidia solitaria sp. nov.

urn:lsid:zoobank.org:act:237D02EA-01BB-4B94-9EAA-F2181F24BE55

Figs 1A–B, 12–13, 93C

Diagnosis

Body length: 1.74 mm. Dark wine-brown; legs lighter; tarsi and posterior laterals of elytra yellow; very shining. Somewhat flattened in lateral view. Sutural, basal, and lateral striae joined. Antennomere IX distinctly enlarged. Spermatheca C-shaped. Gonostylus short.

Etymology

The species epithet is a Latin word meaning ‘alone’, because the single known specimen was collected alone.

Material examined

Holotype

BRAZIL • ♀*; Minas Gerais, Viçosa, Recanto das Cigarras (Mata da Biol.); 20 Nov. 2019; Labcol leg.; “Fungo 14 / Dissecado em 07 Oct. 2022 /”; CELC. Lacking the “HOLOTYPUS ♀” label.

Description

Colouration. Dark wine-brown; frons, coxae, femora and tibiae lighter (Fig. 12A–C). Antennae, tarsi, posterior laterals of elytra, propygidium and pygidium yellow (Fig. 12A–H).

Head. Frons smooth, sparsely pubescent, devoid of punctures; one fovea above each eye (Fig. 12E). Clypeus longer than wide (Fig. 12E). Labrum rounded apically (Fig. 12E). Antennomere VIII sinuate (Fig. 12F); antennomere proportions (n = 1): I missing : II 106/39 : III 66/18 : IV 94/16 : V 109/18 : VI 94/20 : VII 108/35 : VIII 88/22 : IX 124/38 : X 112/42 : XI 119/46.

Prothorax. Smooth, lacking microsculpture (Fig. 12A–D, G). Pronotum not strongly curved in lateral view (Fig. 12B); punctation very fine; pubescence somewhat dense; posterior angles not trespassing mesenepisternum (Fig. 12B). Hypomeron poorly pubescent (Fig. 12D).

Mesothorax (Fig. 12B–D). Lacking microsculpture. Mesoventral line oblique. Secondary lines absent (Fig. 12D). Mesepimeron short and oblique (Fig. 12D).

Metathorax (Fig. 12B–D). Metaventrite smooth, lacking punctures, and sparsely pubescent. Submesocoxal lines punctate; submesocoxal area length: 0.05 mm. Metanepisternum mostly covered by elytra. Metepimeron distinct, smooth.

Wings (Fig. 12A–D, G–H). Elytra wider anteriorly; shining, lacking microsculpture, finely punctate, and moderately pubescent. Sutural striae joined to basal, and then, to the lateral – distinctly punctate (Fig. 12A–B). Epipleura impunctate (Fig. 12D).

Legs (Fig. 12B–D). Pro- and mesofemora with sparse and coarse punctures. Femora narrow. Meso- and metatibiae bearing a long apical spine.

Abdomen (Fig. 12B–D, H). Ventrite I impunctate, shining; primary setae present. Tergite VI with micropuncture and sparsely pubescent.

Terminalia. Ventrite VIII with a triangular projection (Fig. 13A); tergite VIII straight posteriorly (Fig. 13B) – both microsculptured. Bursa copulatrix spinose (Fig. 13C–D). Spermatheca large, C-shaped; spermathecal duct filiform (Fig. 13C). Distal gonocoxite thick on posterior area, arcuate (Fig. 13C–D). Gonostylus very short (Fig. 13C–D).

Measurements (n = 1, holotype). TL 1.70, SY 0.22, HW 0.44, IS 0.22, WA 0.15, PL 0.65, PA 0.50, PB 1.10, EI 1.16, EL 1.26, EW 0.53, EH 0.50, MB 0.11, MC 0.40, ML 0.05, VL 0.50, VL2 0.31, PrF 0.47, PrT 0.34, MsF 0.48, MsT 0.42, MtF 0.55, MtT 0.53.

Host

Collected from an undetermined young orange-white fungus/myxomycete on a decaying tree (Fig. 93C).

Fig. 12. *Alexidia solitaria* sp. nov., holotype, ♀ (CELC). **A**. Dorsal view. **B**. Lateral view. **C**. Ventral view. **D**. Oblique view. **E**. Head, frontal view. **F**. Antenna. **G**. Prothorax, dorsal view. **H**. Elytral apex. Scales in mm.

Remarks

The morphology is similar to that of *A. convivalis* sp. nov. but can be distinguished by the longer, wider, and more flattened body shape. The elytra present a distinct colouration on the posterior laterals and the adsutural area is not distinctly wide at the posterior ⅔. The antennomeres are thicker than those of *A. convivalis*. Regarding the female genitalia, the spermatheca of *A. solitaria* sp. nov. is larger and not entirely twisted, the distal gonocoxite is more curved, and the gonostylus is shorter than in *A. convivalis*.

Distribution

Mata da Biologia, Universidade Federal de Viçosa, campus of Viçosa, state of Minas Gerais, Southeast Brazil (Fig. 1A–D).

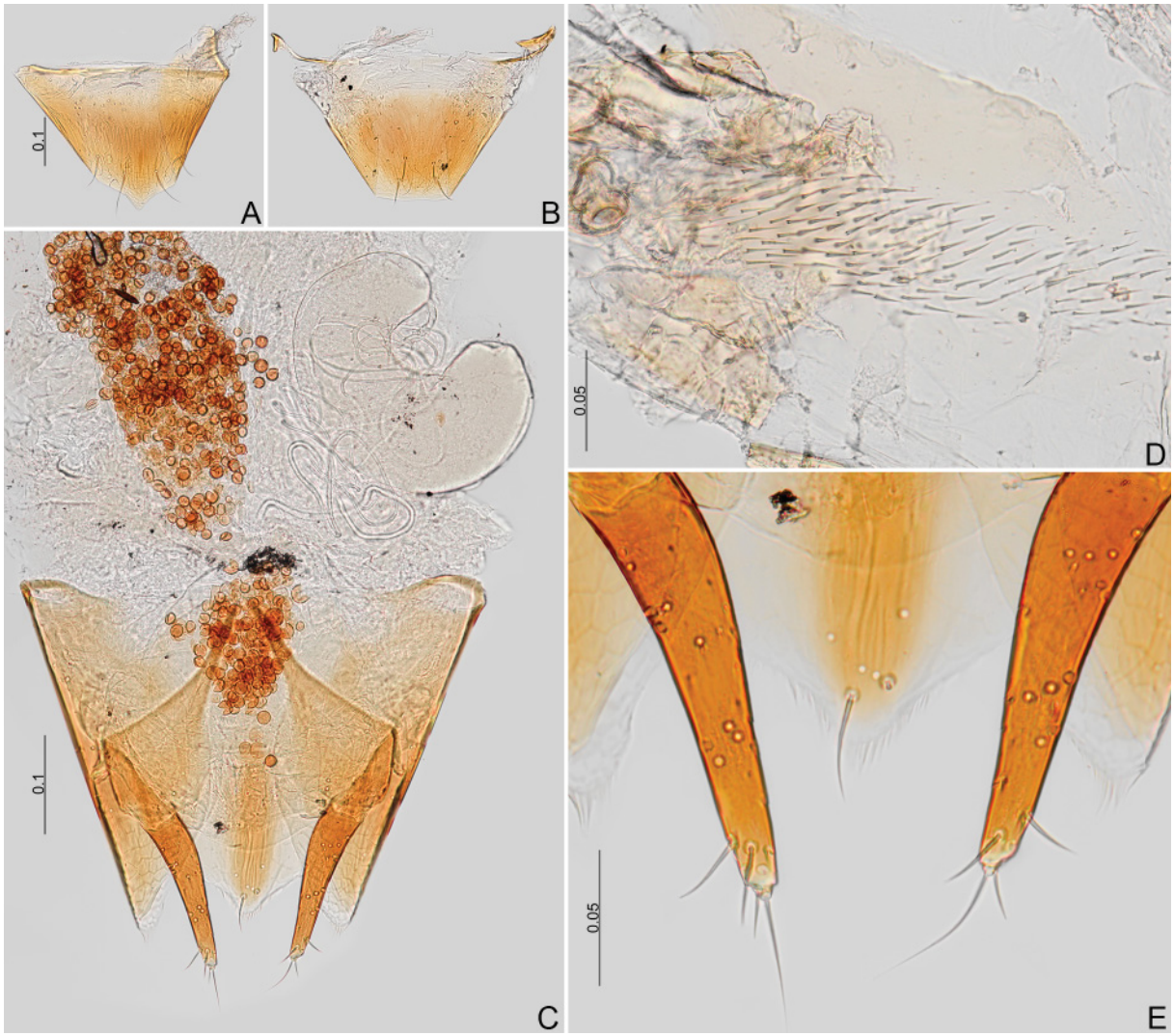

Fig. 13. *Alexidia solitaria* sp. nov., holotype, ♀ (CELC). **A**. Sternite VIII. **B**. Tergite VIII. **C**. Genitalia. **D**. Bursa copulatrix. **E**. Ovipositor. Scales in mm.

Genus ***Amalocera*** Erichson, 1845
Fig. 2L, N

Amalocera Erichson, 1845: 4. Type species: *Amalocera picta* Erichson, 1845; by monotypy.

Amalocera is represented by only five known species – all of them registered for Brazil. Until the development of this paper, the CELC collection counted only two specimens (male and female) of this genus. The two specimens belong to the same new species and are not included here due to limited time.

General description (Löbl 1974; Leschen & Löbl 2005)

Body wide (Fig. 2L).

Head. Labral setae present. Mandible apically bidentate, with apical serrations. Maxillary palp normal. Galea wide, with radulate brush. Inner and basal setae of lacinia absent. Setae on adoral surface of hypopharynx absent. Last labial palpomere curved. Submaxillary ducts present. Gular suture not reaching submentum. Frontoclypeal suture present. Eyes entire – not notched. Antennae filiform, antennomeres III and IV elongate; VII–XI asymmetrical.

Prothorax. Prothoracic corbiculum absent. Hypomeron visible in lateral view; apex subacute and not extending beyond pronotum.

Mesothorax. Mesoventral lines impunctate and not connected to the mesocoxal cavity. Secondary and median lines absent. Prepectus present. Scutellum quite visible in dorsal view. Meso- and metaventrite partially fused. Mesoventral process carinate. Mesepimeron absent.

Metathorax. Submesocoxal lines parallel to coxae. Metaventral setose patch absent. Intercoxal plates present.

Wings. Elytra with apical serrations; basal and lateral striae present and connected. Profemoral ctenidium absent. Metatibiae with a single spine. Mesotibiae with two apical spines, unequal in length (Fig. 2N).

Abdomen. Submetacoxal bead punctate, meeting in middle; submetacoxal space present; submetaxocal lines parallel to coxae. Primary setae of ventrite I absent.

Males. Tibiae bearing secondary sexual characteristics.

Genus ***Baeocera*** Erichson, 1845
Figs 2D, J, 14–43

Baeocera Erichson, 1845: 4. Type species: *Baeocera falsata* Achard, 1920.
Sciatrophes Blackburn, 1903: 100. Type species: *Sciatrophes latens* Blackburn, 1903; by monotypy.
Cyparella Achard, 1924: 28. Type species: *Scaphisoma rufoguttatum* Fairmaire, 1898; by original designation.
Amaloceroschema Löbl, 1967: 1 (as subgenus). Type species: *Baeocera freudei* Löbl, 1967; by original designation.
Eubaeocera Cornell, 1967: 2, fig. 1. Type species: *Baeocera abdominalis* Casey, 1900; by original designation.

With over 300 described species, *Baeocera* is one of the largest Scaphidiinae genera, which can be found on all continents. However, to date, Brazil has only one known species: *Baeocera freudei* Löbl, 1967 (state of Amazonas). In this work, six new species are described, and one species group is proposed.

The six new species present a similar external morphology and were collected simultaneously (same host and days), making them difficult to distinguish. In this context, associating females with their respective species proved particularly challenging, as the most diagnostic characters are found in the male genitalia. This issue was partially resolved through complete dissections, enabling comparison of additional structures (e.g., metendosternite, profurca).

General description (* = variable characters within the genera, but not variable in the species below; Löbl & Leschen 2003b; Leschen & Löbl 2005)

Head. Labral setae simple* (Fig. 15A). Mandible unidentate* (Fig. 15B–C). Last maxillary palpomere aciculate; galea narrow (longer than wide), with paniculate brush; lacinia lacking basal setae (Fig. 15D). Setae on adoral surface of hypopharynx setose; last labial palpomere thin (Fig. 15E). Antennomere III and IV not shortened (Fig. 14J). Gular pores present. Frontoclypeal suture present (Fig. 14H).

Prothorax. Hypomeron visible in lateral view*; pronotal angles acute and slightly extending anapleural suture* (Fig. 14B). Prothoracic corbiculum present (Fig. 15K).

Mesothorax. Mesoventral process paxillate (Fig. 16A). Mesoventral space (prepectus) absent. Mesoventral lines connected to mesocoxal cavity; impunctate* (Fig. 15M). Secondary lines absent. Mesanepisternum finely and sparsely punctate and pubescent*. Mesepimeron exposed* (Fig. 14B).

Metathorax. Metanepisternum exposed (Fig. 14C). Submesocoxal lines present. Metacoxal process short*. Metaventral setose patch present* (Fig. 14G).

Wings. Hind wings developed (Fig. 16I). Basal and sutural elytral striae connected*; lateral striae present*; apical serrations present*.

Legs. Profemoral ctenidium present (Fig. 2H). Mesotibiae bearing outer spines and two ventral spines.

Abdomen. Submetacoxal lines parallel to coxae; punctate*. Membranes of abdominal ventrites with brick-wall pattern.

Baeocera facilis sp. nov.
urn:lsid:zoobank.org:act:DE609417-1EBA-4468-8315-576FC53CDBEE
Figs 1A–B, G, 14–18

Diagnosis

Body length: 1.00–1.18 mm; somewhat narrow in dorsal view; moderately convex in lateral view. Brown to dark brown; mouthparts, antennae, and legs ochreous. Mesepimeron width approximately 0.72 of the mesanepisternum width, and 3.60 × as wide as long. Submesocoxal lines arcuate and punctate. Metanepisternal suture straight or moderately curved; punctate. Basal striae connected to sutural and reaching approximately the outer ⅔ of the basal width. Femora with strigulate microsculpture. Aedeagus with parameres with apex slightly thinner, sclerite of internal sac asymmetrical and undefined. Distal gonocoxite and gonostylus elongate.

Etymology

The species epithet is a Latin word meaning ‘easy’, referring of the simplicity of distinguishing this species from others.

Fig. 14. *Baeocera facilis* sp. nov. (CELC). **A–E, H**. Holotype, ♂. **A**. Dorsal view. **B**. Lateral view. **C**. Ventral view. **D**. Labels. **E**. Pinned. **F–G**. Paratype, ♀ (#51), teneral. **F**. Dorsal view. **G**. Lateral view. **H**. Head, frontal view. **I**. Paratype, ♂ (#102), head, frontal view, dissected, arrow: fovea. **J–K**. Antennae. **J**. Paratype, ♂ (#102). **K**. Paratype, ♀ (#49). Abbreviation: mta = metanepisternum. Scales in mm.

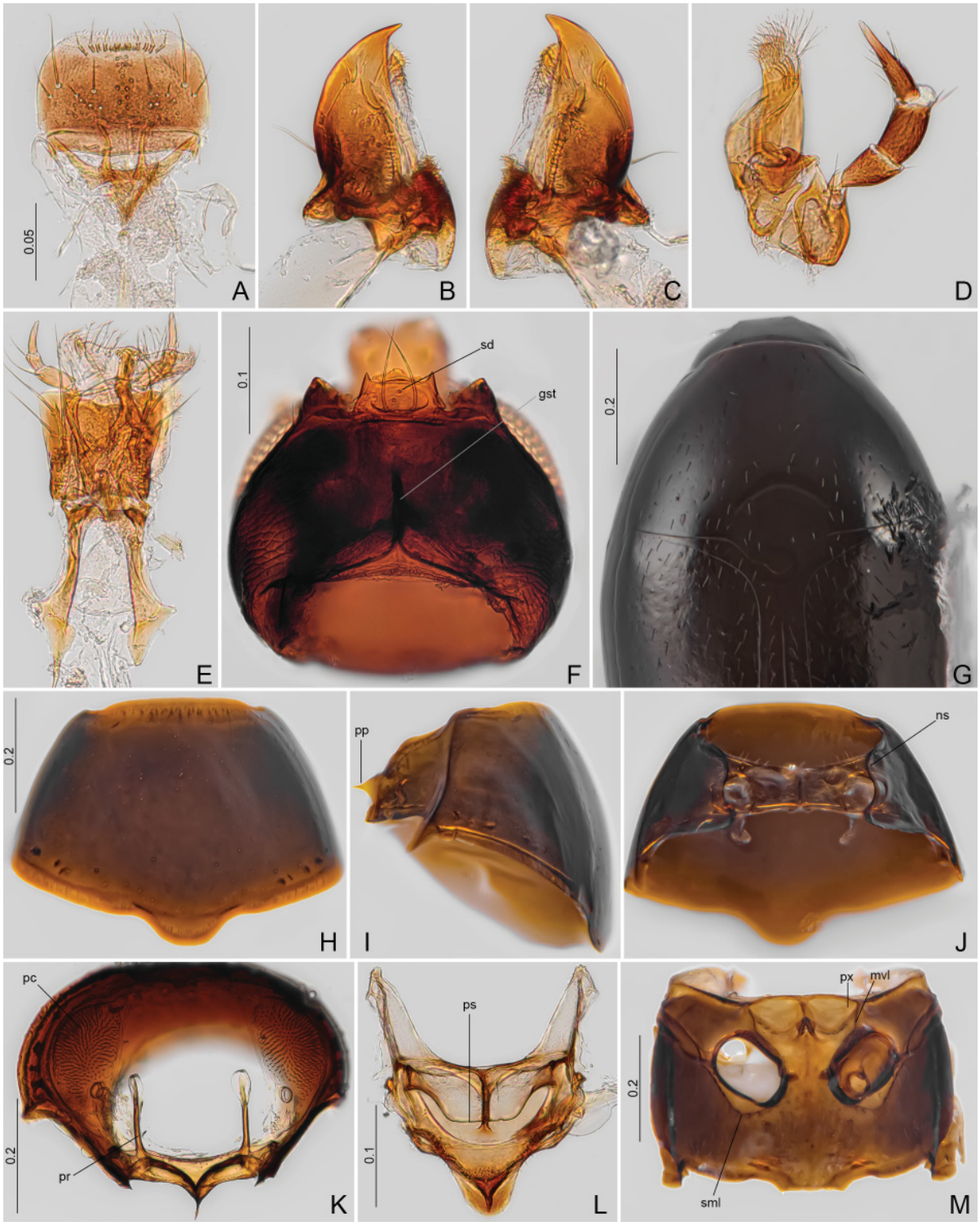

Fig. 15. *Baeocera facilis* sp. nov. (CELC). **A**. Paratype, ♂ (#102), labrum. **B–C**. Paratype, ♀ (#49), mandibles. **D–F**. Paratype, ♂ (#102). **D**. Maxilla. **E**. Labium. **F**. Head, ventral view. **G**. Holotype, ♂, prothorax, dorsal view. **H–M**. Paratype, ♂ (#102). **H–K**. Prothorax. **H**. Dorsal view. **I**. Lateral view. **J**. Ventral view. **K**. Inner view. **L**. Scutellar shield. **M**. Meso- and metathorax, ventral view. Abbreviations: gst = gular suture; mvl = mesoventral line; ns = notosternal suture; pc = prothoracic corbiculum; pp = prosternal process; pr = profurca; ps = prescutellar line; px = procoxal rest; sd = submaxillary duct; sml = submesocoxal line. Scales in mm.

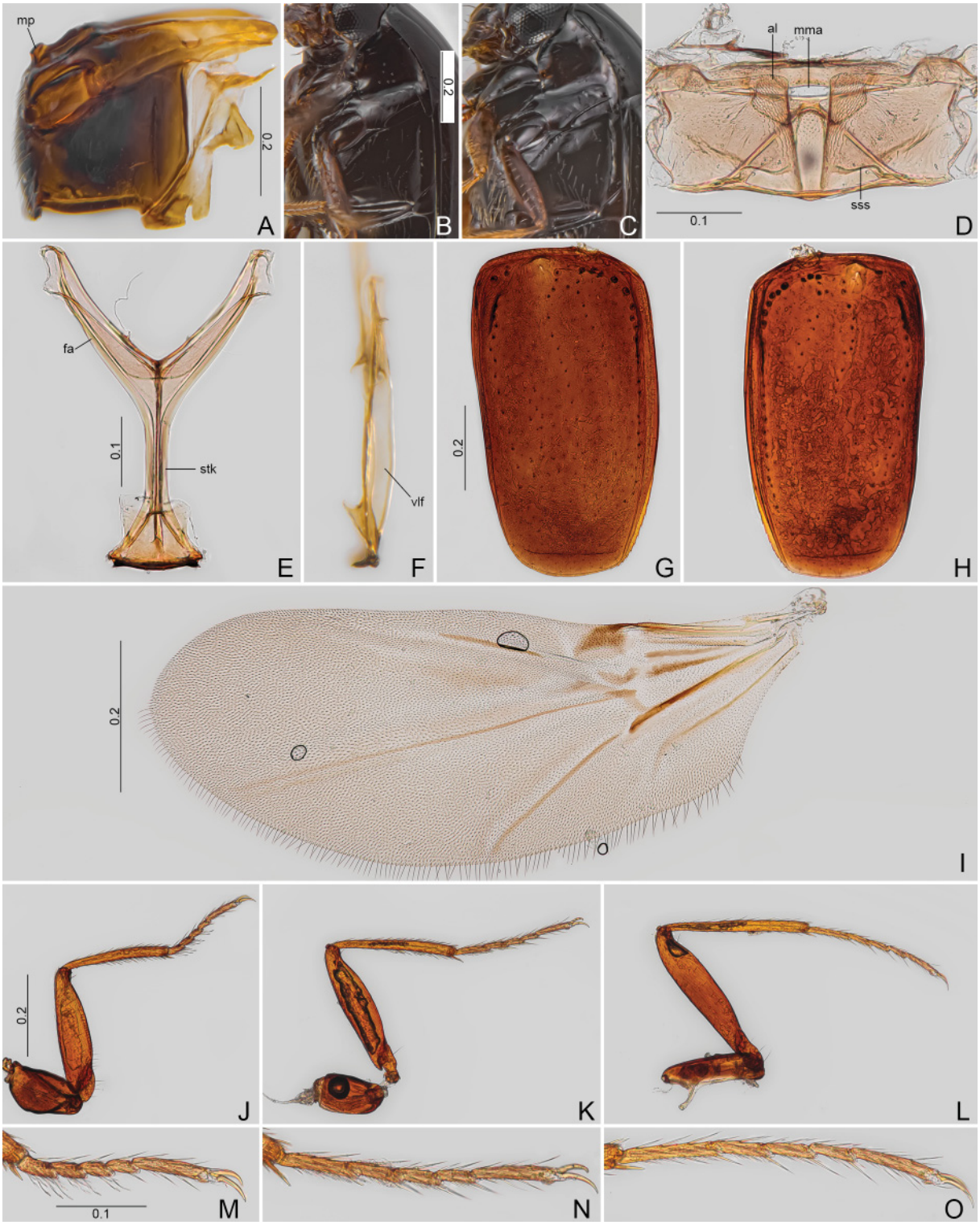

Fig. 16. *Baeocera facilis* sp. nov. (CELC). **A–C**. Meso- and metathorax, lateral views. **A**. Paratype, ♂ (#102), dissected. **B**. Holotype, ♂. **C**. Paratype, ♀ (#53). **D**. Paratype, ♂ (#102), metanotum. **E–F**. Paratype, ♀ (#49), metendosternite. **E**. Dorsal view. **F**. Lateral view. **G–O**. Paratype, ♂ (#102). **G–H**. Elytra. **I**. Hind wing. **J–L**. Legs. **J**. Fore. **K**. Middle. **L**. Hind. **M–O**. Tarsi. **M**. Pro. **N**. Meso. **O**. Meta. Abbreviations: al = alacrista; fa = furcal arm; mma = median membranous area; mp = mesoventral process; sss = scutoscutellar suture; stk = stalk; vlf = ventral longitudinal flange. Scales in mm.

Material examined

Holotype

BRAZIL • ♂; Minas Gerais, Viçosa, EPTEA Mata do Paraíso; 24 Mar. 2022; E. von Groll *et al.* leg.; "Falcon 20 / Em *Ceratiomyxa fruticulosa* em *Pinus* / HOLOTYPUS ♂"; CELC. (Fig. 14D–E)

Paratypes

BRAZIL • 2 ♂♂, 5 ♀♀ (1 ♂**, 1 ♀**); same data as for holotype; CELC.

Description

Colouration. Dark brown; mouthparts, antennae, clypeus, and anterior part of femora dark ochreous; tibiae and tarsi light ochreous (Fig. 14A–C, H). Variation: all structures paler (Fig. 14F–G).

Head (Figs 14H–I, 15A–F). Finely punctate; pubescence sparse; one fovea above each eye (Fig. 14H–I). Labrum slightly curved posteriorly (Fig. 15A). Mandibles not strongly curved (Fig. 15B–C). Last labial palpomere distinctly elongate, curved; mentum concave posteriorly (Fig. 15E). Gular pores absent; gular suture wide near ostium; gular region with strigulate microsculpture (Fig. 15F). Antennae elongate (Fig. 14J–K), antennomere VII thin and longer than VIII, XI elongate and oval; antennomere proportions (n = 2): I 76/30 : II 69/30 : III 35/14 : IV 45/13 : V 58/14 : VI 51/14 : VII 70/19 : VIII 63/21 : IX 77/28 : X 75/34 : XI 101/40.

Prothorax (Fig. 15G–K). Punctation sparse and fine; pubescence sparse (Figs 14A, 15G, 18A). Hypomeron almost glabrous, with few coarse punctation (Fig. 16B), absent in some specimens (Fig. 16C). Prosternal process narrow and spinose (Fig. 15I). Profurca thin and elongate (Fig. 15K).

Mesothorax (Figs 15G, L, 16A–C). Scutellum visible in dorsal view, wider than long (Fig. 15G); tip rounded; scutellar lines oblong laterally (Fig. 15L). Mesoventral lines angulate; coxal rests large; median lines short and open (Fig. 15M). Mesepimeron about 3.60 × as wide as long, and about 0.72 × the width of the mesanepisternum (Fig. 16B–C).

Metathorax (Figs 15M, 16A–F). Metaventrite smooth, shining, and with little pubescence laterally (Fig. 16B–C). Submesocoxal lines arcuate and punctate; submesocoxal area length: 0.03–0.04 mm (Figs 15M, 16B–C, 18C). Metanepisternal suture punctate, curvature variable (Figs 16B–C, 18C). Metanotum with large alacrista; scutoscutellar suture not trespassing apodeme (Fig. 16D). Stalk of metendosternite narrower than arms (Fig. 16E–F).

Wings (Figs 14A, F, 16G–I, 18A). Elytra with coarse and sparse punctures; pubescence fine and sparse. Basal striae connected to sutural, impunctate, and reaching about basal mid-width of elytra (Fig. 15G). Lateral striae fine, impunctate, and slightly curved near humeral region (Figs 14B, G, 18B).

Legs. Elongate; femora with distinct strigulate microsculpture (Figs 14C, G, 16J–L, 18D–F).

Abdomen. Ventral surface shining, finely punctate; pubescence moderately dense and elongate (Figs 14B, G, 18B–C). Pro- and pygidium with fine and sparse pubescence (Figs 17A, 18J). Posterior area of ventrite I, ventrites II–VI, and tergites with imbricate microsculpture (Figs 14B, G, 18C).

Males

Pro- and mesotarsomeres I–III slightly widened, bearing few and elongate tenent setae (Fig. 16J–O). Sternite VIII with a distinct elongate posterior projection (Fig. 17B). Tergite VIII triangular, with a smooth posterior projection (Fig. 17C). Tergite IX with ventral struts curved, and forming an acute angle (Fig. 17D). Sternite IX with elongate anterior sclerotized projection (Fig. 17D–E). Tergite X triangular (Fig. 17D, F).

Aedeagus (Fig. 17G–K). Median lobe poorly sclerotized and slightly curved in lateral view (Fig. 17I). Parameres more sclerotized than apical lobe; almost parallel but apex slightly thinner. Sclerite of internal sac asymmetric and undefined (Fig. 17G–K).

Measurements (n = 3, including holotype; in mm). TL 1.05–1.13 (1.08 ± 0.04), SY 0.11–0.13 (0.12 ± 0.01), HW 0.30–0.31 (0.30 ± 0.01), IS 0.13–0.14 (0.14 ± 0.01), WA 0.06–0.08 (0.07 ± 0.01), PL 0.40–0.45 (0.42 ± 0.03), PA 0.30–0.35 (0.32 ± 0.03), PB 0.59–0.60 (0.60 ± 0.01), SL 0.01–0.02 (0.02 ± 0.01), SW 0.04–0.05 (0.05 ± 0.01), EI 0.64–0.70 (0.67 ± 0.03), EL 0.75–0.78 (0.77 ± 0.02), EW 0.33–0.36 (0.35 ± 0.02), EH 0.26–0.35 (0.31 ± 0.05), MsW 0.18–0.20 (0.19 ± 0.01), MeL 0.03–0.04 (0.04 ± 0.01), MeW 0.13–0.15 (0.14 ± 0.01), MB 0.10–0.14 (0.13 ± 0.02), MC 0.24–0.27 (0.26 ± 0.02), ML 0.03–0.04 (0.04 ± 0.01), VL 0.13–0.16 (0.15 ± 0.02), PrF 0.32–0.33 (0.32 ± 0.01), PrT 0.25–0.26 (0.26 ± 0.01), MsF 0.33–0.36 (0.34 ± 0.02), MsT 0.30–0.31 (0.31 ± 0.01), MtF 0.39–0.40 (0.40 ± 0.01), MtT 0.34–0.37 (0.36 ± 0.02).

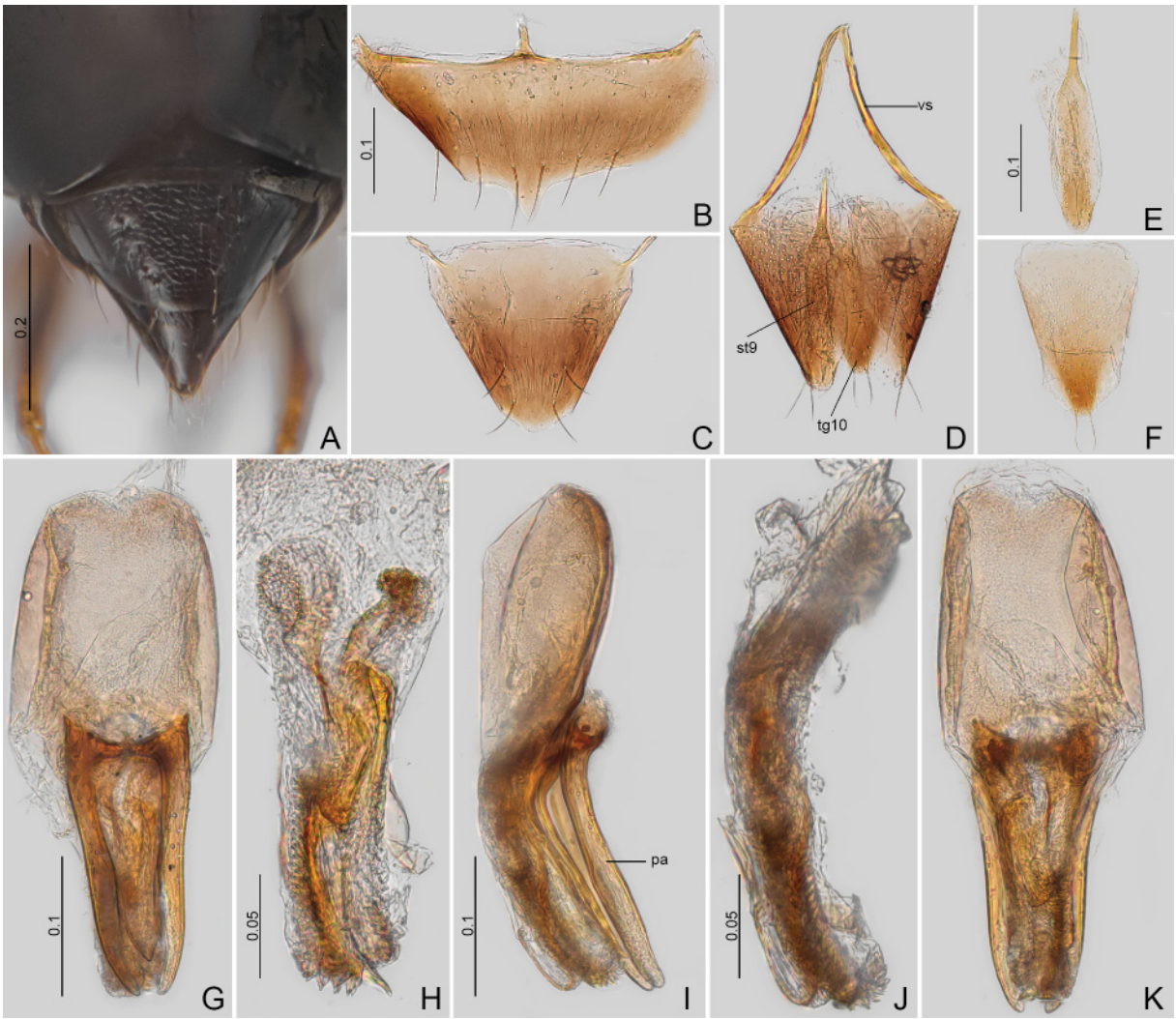

Fig. 17. *Baeocera facilis* sp. nov. (CELC). **A**. Holotype, ♂, abdomen, dorsal view. **B–K**. Paratype, ♂ (#102). **B**. Sternite VIII. **C**. Tergite VIII. **D**. Tergite IX. **E**. Sternite IX. **F**. Tergite X. **G–K**. Aedeagi. **G**. Frontal view. **H**. Sclerite of internal sac, frontal view. **I**. Lateral view. **J**. Sclerite of internal sac, lateral view. **K**. Dorsal view. Abbreviations: pa = parameres; st9 = sternite IX; tg10 = tergite X; vs = ventral struts. Scales in mm.

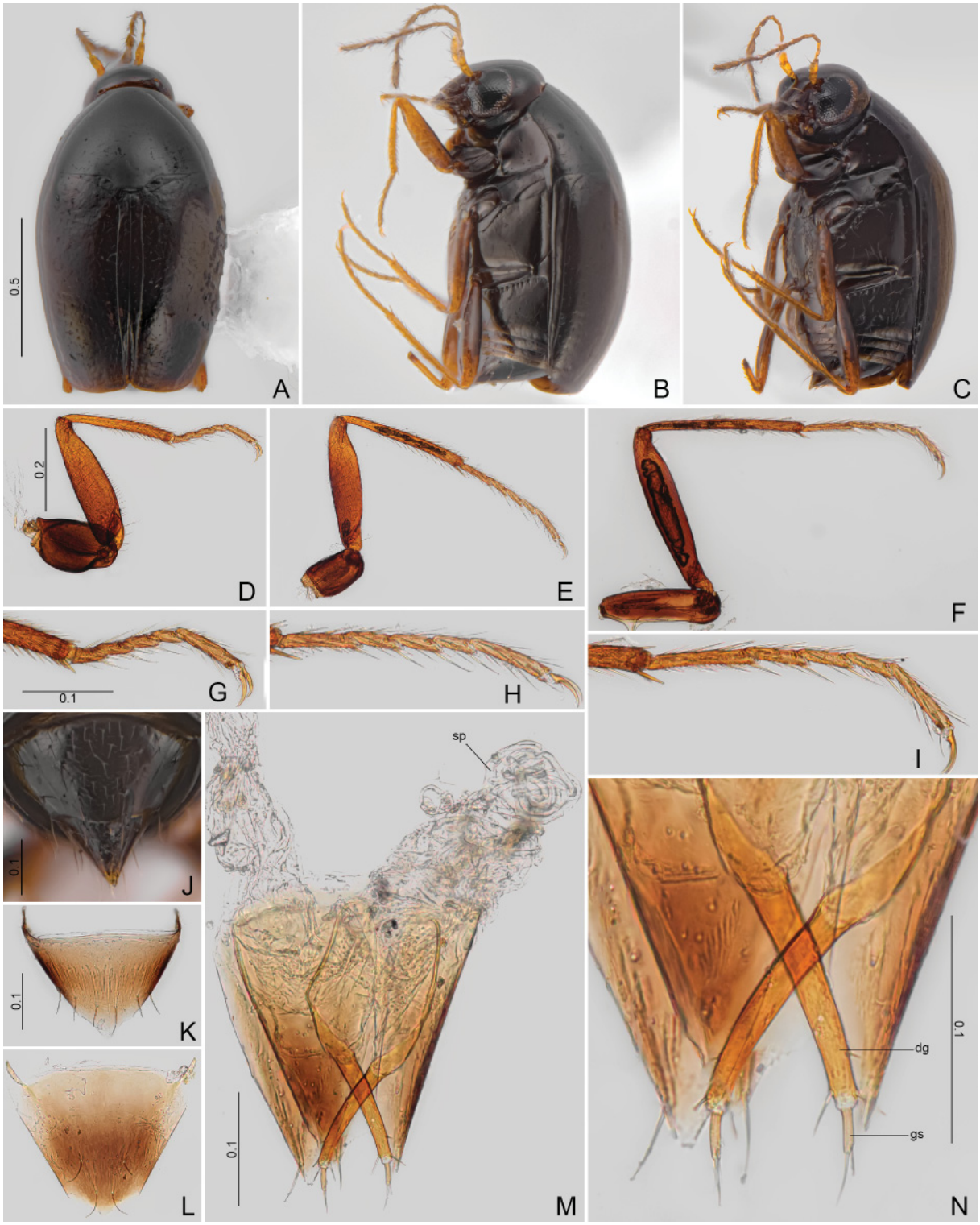

Fig. 18. *Baeocera facilis* sp. nov. (CELC). **A–C**. Paratype, ♀ (#49). **A**. Dorsal view. **B**. Lateral view. **C**. Oblique view. **D–N**. Paratype, ♀ (#53). **D–F**. Legs. **D**. Fore. **E**. Middle. **F**. Hind. **G–I**. Tarsi. **G**. Pro. **H**. Meso. **I**. Meta. **J**. Abdomen, dorsal view. **K**. Sternite VIII. **L**. Tergite VIII. **M**. Terminalia. **N**. Ovipositor. Abbreviations: dg = distal gonocoxites; gs = gonostyli; sp = spermatheca. Scales in mm.

Females (Fig. 18)

Ventrite and tergite VIII with a triangular posterior projection (Fig. 18K–L). Spermatheca elongate, filiform (Fig. 18M). Distal gonocoxite elongate and slightly curved; gonostylus 6× as long as wide (Fig. 18M–N).

Measurements (n = 5; in mm). TL 1.00–1.18 (1.10 ± 0.06), SY 0.11–0.14 (0.13 ± 0.01), HW 0.29–0.32 (0.31 ± 0.01), IS 0.12–0.16 (0.14 ± 0.01), WA 0.07–0.08 (0.07 ± 0.01), PL 0.38–0.45 (0.42 ± 0.03), PA 0.29–0.39 (0.33 ± 0.04), PB 0.55–0.67 (0.62 ± 0.04), SL 0.01–0.02 (0.02 ± 0), SW 0.04–0.05 (0.05 ± 0.01), EI 0.64–0.74 (0.71 ± 0.04), EL 0.72–0.82 (0.79 ± 0.04), EW 0.30–0.41 (0.35 ± 0.05), EH 0.27–0.36 (0.30 ± 0.04), MsW 0.16–0.22 (0.18 ± 0.02), MeL 0.03–0.05 (0.04 ± 0.01), MeW 0.13–0.15 (0.14 ± 0.01), MB 0.11–0.14 (0.13 ± 0.01), MC 0.22–0.32 (0.28 ± 0.04), ML 0.04, VL 0.15–0.17 (0.16 ± 0.01), PrF 0.31–0.35 (0.33 ± 0.02), PrT 0.24–0.28 (0.26 ± 0.02), MsF 0.33–0.40 (0.36 ± 0.03), MsT 0.30–0.33 (0.31 ± 0.02), MtF 0.38–0.45 (0.41 ± 0.03), MtT 0.35–0.39 (0.37 ± 0.02).

Host

Collected together from *Ceratiomyxa fruticulosa* on a fallen *Pinus* sp. tree (Fig. 1G).

Remarks

The ovipositor is similar to species belonging to *Xotidium* Löbl, 1992 (Ogawa & Löbl 2016), e.g., *X. montanum* (Löbl, 1971). However, *B. facilis* sp. nov. can be separated by the larger body and by the not approximate meso- and metacoxae. *Baeocera facilis* can be easily distinguished from the other species of *Baeocera* described in this manuscript by the femora with strigulate microsculpture and by the elongate distal gonocoxite and gonostylus in females.

Distribution

Mata do Paraíso, Universidade Federal de Viçosa, campus of Viçosa, state of Minas Gerais, Southeast Brazil (Fig. 1A–B).

Baeocera inusitata sp. nov.

urn:lsid:zoobank.org:act:FDC769FE-16E8-4DC5-BC8F-BD494B65DCE1

Figs 1A–B, 19–24, 93D

Diagnosis

Body length: 1.09–1.31 mm; body oblong; dark brown. Antennae elongate, almost reaching metacoxae. Mesepimeron about 4.5× as wide as long. Submesocoxal lines slightly arcuate, punctate; submesocoxal area short. Basal striae entire (connected to sutural and lateral ones). Parameres of aedeagus enlarged posteriorly in lateral view. Females with distal gonocoxite rounded cone-shaped, bearing one long apical seta; gonostylus absent.

Etymology

The species epithet is a Latin word meaning ‘unusual’, referring to the distinctive morphology of the female ovipositor.

Material examined

Holotype

BRAZIL • ♂; Minas Gerais, Viçosa, EPTEA Mata do Paraíso; 24 Mar. 2022; E. von Groll *et al.* leg.; “Falcon 20 / Em *Ceratiomyxa fruticulosa* em *Pinus* / HOLOTYPUS ♂”; CELC. (Fig. 19D–E)

Fig. 19. *Baeocera inusitata* sp. nov. (CELC). **A–F**. Holotype, ♂. **A**. Dorsal view. **B**. Lateral view, arrow: lateral impression. **C**. Ventral view. **D**. Labels. **E**. Pinned. **F**. Head, frontal view. **G–H**. Antennae. **G**. Paratype, ♂ (#95). **H**. Paratype, ♀ (#103). **I–M**. Paratype, ♂ (#95). **I**. Labrum. **J–K**. Mandibles. **L**. Maxilla. **M**. Labium, arrow: lateral concavities. Scales in mm.

Fig. 20. *Baeocera inusitata* sp. nov. (CELC). **A**. Holotype, ♂, prothorax, dorsal view. **B–H**. Paratype, ♂ (#95). **B–E**. Prothorax. **B**. Dorsal view. **C**. Lateral view. **D**. Ventral view. **E**. Inner view. **F**. Scutellar shield. **G–H**. Meso- and metathorax. **G**. Ventral view. **H**. Lateral view. **I**. Holotype, ♂, oblique view. **J–L**. Paratype, ♂ (#95). **J**. Metanotum. **K–L**. Metendosternite. **K**. Dorsal view. **L**. Lateral view. Abbreviation: ml = median line. Scales in mm.

Paratypes

BRAZIL • 7 ♂♂, 6 ♀♀ (3 ♂♂*, 2 ♂♂**, 1 ♀*); same collection data as for holotype; CELC • 8 ♂♂, 3 ♀♀ (1 ♂*, 1 ♀*); same collection data as for holotype; 26 Mar. 2022; "Falcon 26 / Em *Ceratiomyxia fruticulosa* em *Pinus*"; CELC • 5 ♂♂, 6 ♀♀ (1 ♂**, 1 ♀*); same collection data as for holotype; 31 Mar. 2022; E. von Groll *et al*. leg.; "Falcon 19 / Em *Ceratiomyxia fruticulosa* no tronco caído"; CELC • 1 ♂, 5 ♀♀ (1 ♀*); same collection data as for holotype; 14 Apr. 2022; Falcon 42; CELC • 3 ♂♂, 2 ♀♀ (2 ♂♂*, 2 ♀♀*); Minas Gerais, Viçosa, UFV, Mata da Biologia; 12 Apr. 2022; E. von Groll and G.J Figueiredo leg.; "Falcon 04 / Em *Ceratiomyxia fruticulosa* no tronco caído"; CELC • 1 ♂; same data collection as for preceding; "Falcon 01 / Em *Ceratiomyxia fruticulosa* no tronco caído"; CELC.

Description

Colouration. Dark brown; antennomeres I–VI, tibiae, tarsi, apex of each abdominal ventrites light ochreous; coxae, femora, and clypeus dark ochreous (Fig. 19A–C, F). Variation: all structures paler.

Head (Fig. 19F–M). Frons finely punctate; pubescence sparse (Fig. 19F). Labrum slightly curved posteriorly (Fig. 19I). Mandibles strongly curved; tooth elongate (Fig. 19J–K). Last maxillary palpomere remarkably thin (Fig. 19L). Labial palpomere II shortened, wider than long; IV almost straight, thin; posterior portion of mentum with three concavities: one large in middle and two small laterally (Fig. 19M). Antennae (Fig. 19G–H) elongate, almost reaching metacoxae (Fig. 20I); antennomeres thin, antennomere VII slightly oblong; proportions (n = 13): I 69/33 : II 69/33 : III 39/14 : IV 48/14 : V 59/14 : VI 59/16 : VII 58/22 : VIII 78/26 : IX 89/32 : X 89/34 : XI 95/35.

Prothorax (Fig. 20A–E). Shining, lacking microsculpture; punctation fine and moderately sparse. Pronotum with a distinct anterior bead (Fig. 20A). Prosternal process thick in lateral view (Fig. 20C). Profurca slightly robust and elongate (Fig. 20E).

Mesothorax (Fig. 20F–I). Scutellum visible in dorsal view, wider than long (Fig. 20A); tip rounded (Fig. 20F). Mesoventral lines very curved; coxal rests large; median lines open (Fig. 20G). Mesepimeron about 4.5 × as wide as long, and about 0.73 × the width of the mesanepisternum (Fig. 20I).

Metathorax (Fig. 20G–L). Metaventrite smooth, shining, and with few pubescence laterally (Fig. 20I). Submesocoxal lines slightly arcuate coxae, punctate; submesocoxal area short, length: 0.02–0.04 mm (Figs 20G–I, 23C). Metanepisternal suture punctate, curvature variable (Figs 20I, 23C). Metanotum with trapezoidal alacrista and scutoscutellar suture just slightly longer than apodeme (Fig. 20J). Metendosternite with stalk and arms similar in thickness (Fig. 20K–L).

Wings (Figs 19A, 21A–C, 23A). Elytra with coarse and moderately sparse punctures. Basal striae connected to sutural and lateral ones; all impunctate.

Legs. Elongate, not microsculptured (Figs 21D–I, 23D–I).

Abdomen. Submetacoxal lines distinctly coarse punctate (Figs 20I, 23C). Ventral surface shining; pubescence sparse, denser posteriorly, punctures moderately coarse (Figs 19B–C, 23B). Ventrite I with (Fig. 19B) or without (Fig. 23B) a lateral curved impression – unrelated to sex, collection date, or life stage (including teneral specimens). Pro- and pygidium with hardly visible micropuncture; sparsely pubescent (Fig. 21J).

Males

Pro- and metatibiae slightly curved (Fig. 21D–E). Pro- and mesotarsomeres I–III slightly widened, protarsomeres bearing few and elongate tenent setae (Fig. 21G–H). Both sternite and tergite VIII with triangular-rounded posterior projection (Fig. 21K–L). Tergite IX with ventral struts curved (Fig. 21M). Sternite IX oblong (Fig. 21M). Tergite X wide and triangular.

Aedeagus (Fig. 22A–H). Median lobe slightly curved in lateral view (Fig. 22C, H), basal bulb poorly sclerotized, apical lobe moderately sclerotized, almost same length as basal bulb. Parameres more (Fig. 22C) or less (Fig. 22H) wide posteriorly in lateral view. Sclerite of internal sac with two elongate and twisted sclerotized plates (Fig. 22E–G).

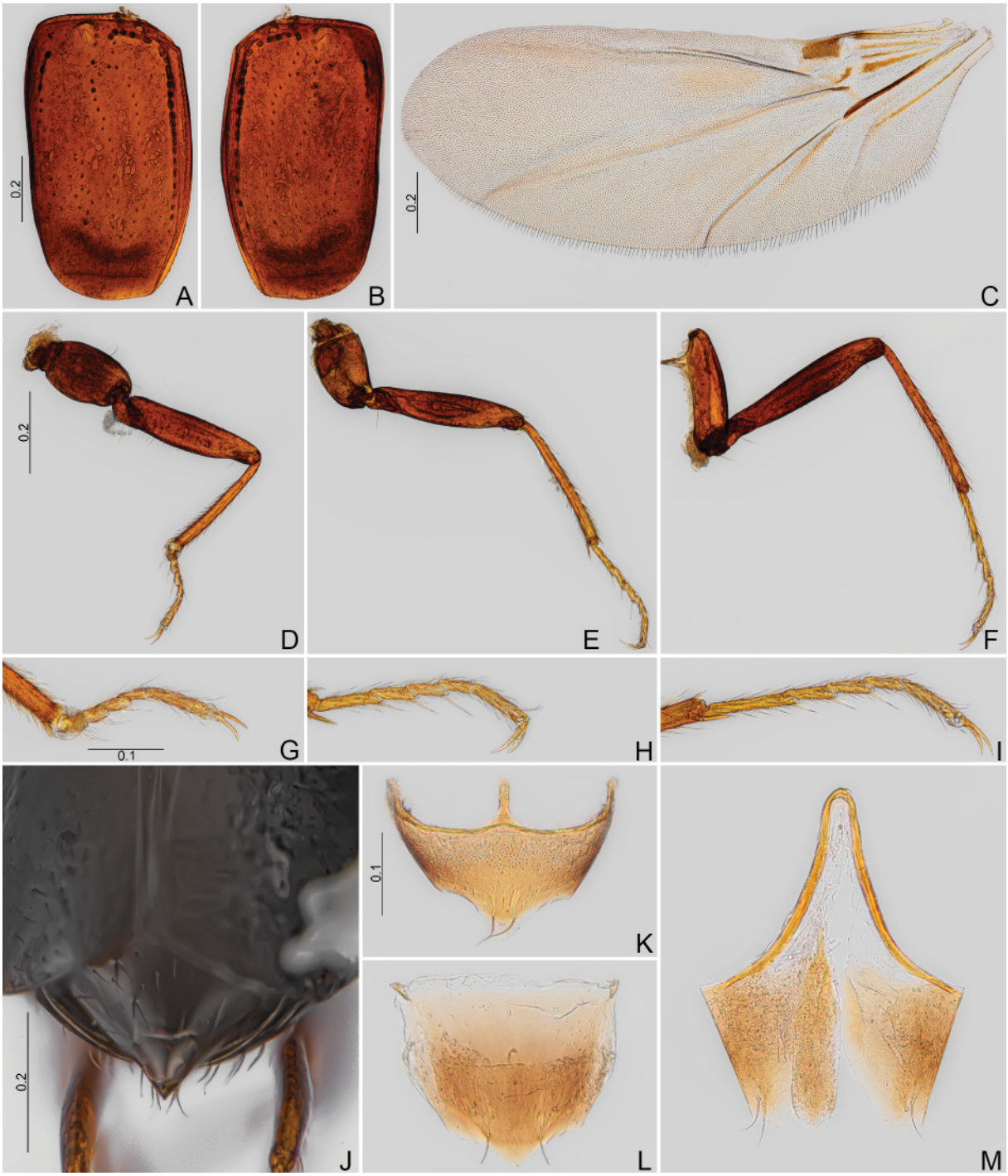

Fig. 21. *Baeocera inusitata* sp. nov. (CELC). **A–I**. Paratype, ♂ (#95). **A–B**. Elytra. **C**. Hind wing. **D–F**. Legs. **D**. Fore. **E**. Middle. **F**. Hind. **G–I**. Tarsi. **G**. Pro. **H**. Meso. **I**. Meta. **J**. Holotype, ♂, abdomen, dorsal view. **K–M**. Paratype, ♂ (#95). **K**. Sternite VIII. **L**. Tergite VIII. **M**. Tergite IX. Scales in mm.

Measurements (n = 14, including holotype, unless otherwise specified; in mm). TL (n = 26) 1.11–1.27 (1.18 ± 0.04), SY 0.13–0.17 (0.14 ± 0.01), HW 0.31–0.36 (0.33 ± 0.01), IS (n = 13) 0.14–0.18 (0.16 ± 0.01), WA 0.08–0.12 (0.09 ± 0.01), PL 0.40–0.48 (0.44 ± 0.02), PA 0.35–0.42 (0.38 ± 0.02), PB 0.62–0.76 (0.68 ± 0.03), SL 0.01–0.02 (0.02 ± 0), SW 0.04–0.05 (0.05 ± 0), EI 0.71–0.83 (0.77 ± 0.04), EL 0.80–0.93 (0.86 ± 0.04), EW 0.33–0.43 (0.38 ± 0.03), EH 0.29–0.36 (0.33 ± 0.02), MsW 0.17–0.21 (0.19 ± 0.01), MeL 0.03–0.04 (0.03 ± 0), MeW 0.11–0.16 (0.14 ± 0.02), MB 0.11–0.16 (0.14 ± 0.01), MC 0.27–0.31 (0.29 ± 0.02), ML 0.03–0.04 (0.03 ± 0), VL 0.15–0.22 (0.18 ± 0.02), VL2 0.21–0.27 (0.24 ± 0.02), PrF 0.31–0.40 (0.36 ± 0.02), PrT 0.25–0.31 (0.28 ± 0.02), MsF 0.32–0.41 (0.37 ± 0.02), MsT 0.30–0.36 (0.32 ± 0.02), MtF 0.39–0.45 (0.42 ± 0.02), MtT 0.35–0.44 (0.39 ± 0.03).

Females (Figs 23–24)

Sternite VIII with a wide and rounded posterior projection (Fig. 23J). Tergite VIII triangular, lacking posterior projection (Fig. 23K). Distal gonocoxite rounded cone-shaped, bearing one long apical seta, gonostylus absent (Figs 23L–M, 24A–D).

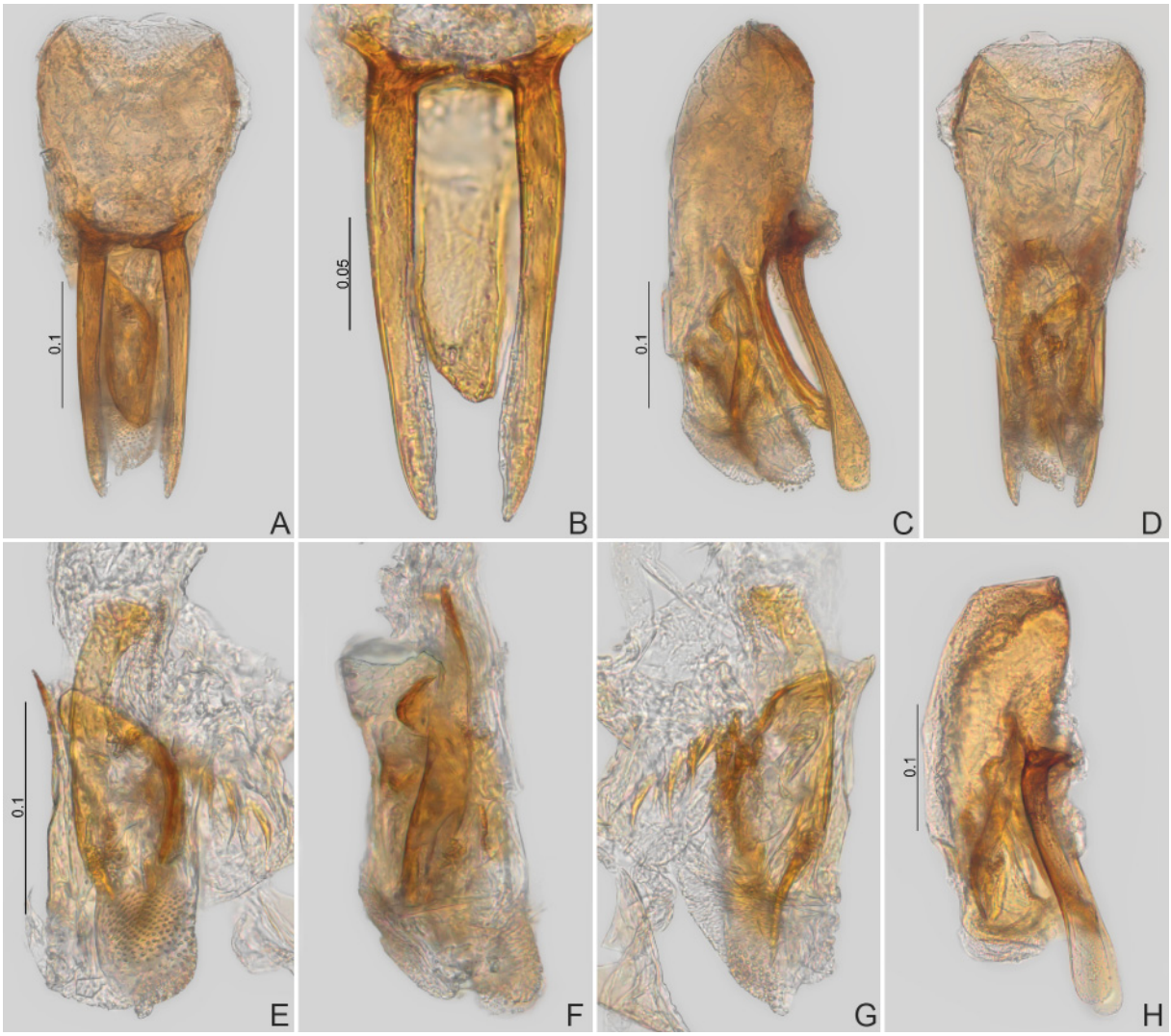

Fig. 22. *Baeocera inusitata* sp. nov. (CELC). **A–G**. Paratype, ♂ (#95). **A–D**. Aedeagi. **A**. Frontal view. **B**. Parameres, frontal view. **C**. Lateral view. **D**. Dorsal view. **E–G**. Sclerite of internal sac. **E**. Frontal view. **F**. Lateral view. **G**. Dorsal view. **H**. Paratype, ♂ (#86), aedeagi, lateral view. Scales in mm.

Measurements (n = 14, unless otherwise specified; in mm). TL (n = 22) 1.09–1.31 (1.22 ± 0.05), SY 0.13–0.17 (0.15 ± 0.01), HW 0.31–0.35 (0.33 ± 0.01), IS 0.15–0.20 (0.18 ± 0.02), WA 0.08–0.12 (0.10 ± 0.01), PL 0.43–0.50 (0.47 ± 0.02), PA 0.35–0.42 (0.39 ± 0.02), PB (n = 12) 0.65–0.75 (0.70 ± 0.03), SL 0.02–0.03 (0.02 ± 0), SW 0.04–0.06 (0.05 ± 0), EI 0.70–0.86 (0.80 ± 0.05), EL 0.81–0.95 (0.89 ± 0.04), EW 0.34–0.44 (0.38 ± 0.03), EH 0.29–0.39 (0.35 ± 0.03), MsW 0.17–0.22 (0.19 ± 0.01), MeL (n = 13) 0.03–0.04 (0.03 ± 0), MeW (n = 13) 0.13–0.17 (0.14 ± 0.01), MB 0.13–0.18 (0.15 ± 0.01), MC 0.27–0.32 (0.3 ± 0.01), ML 0.02–0.04 (0.03 ± 0), VL 0.11–0.22 (0.19 ± 0.03), VL2 0.22–0.27 (0.25 ± 0.02),

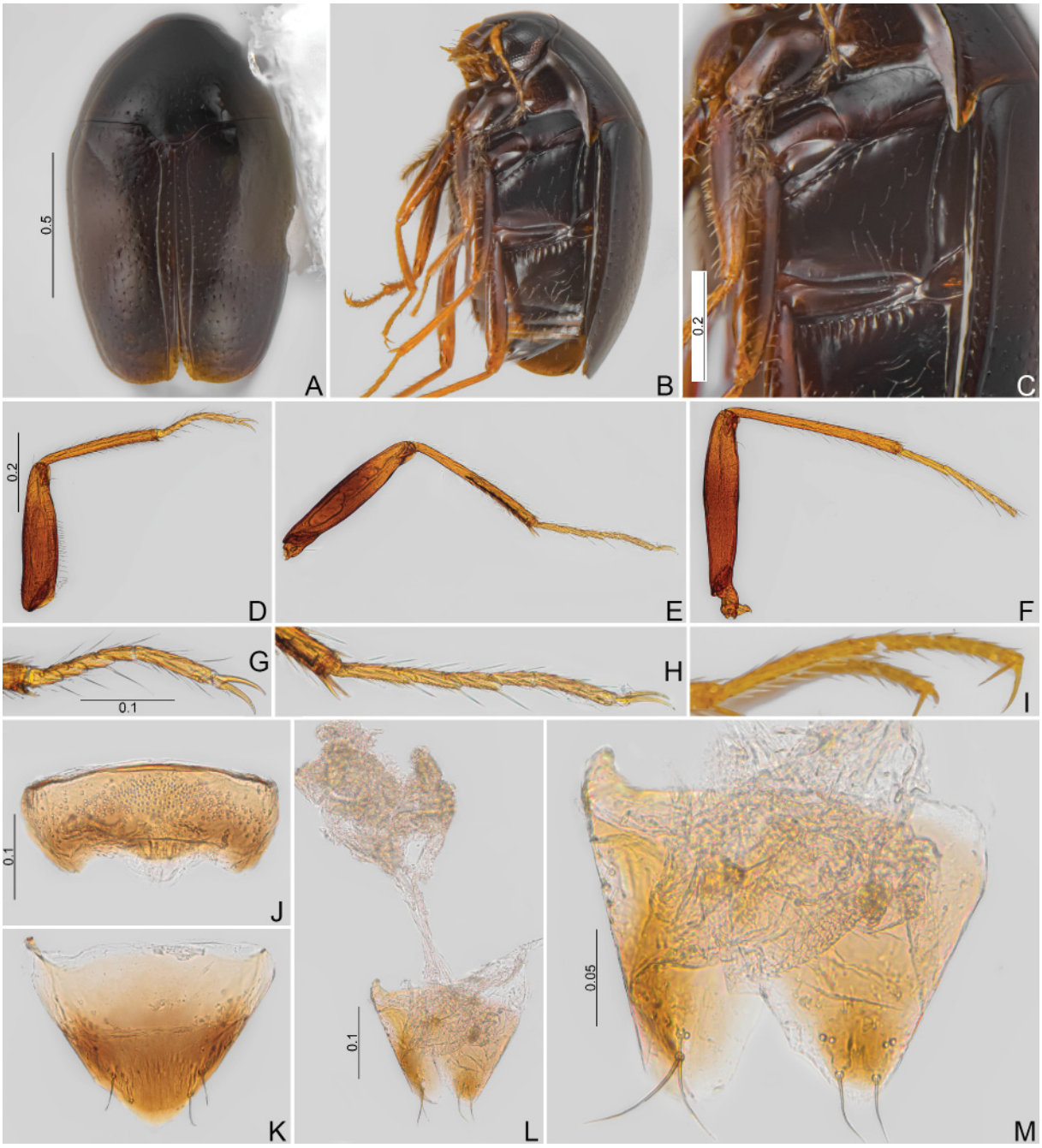

Fig. 23. *Baeocera inusitata* sp. nov., paratype, ♀ (#103) (CELC). **A**. Dorsal view. **B**. Oblique view. **C**. Thorax, oblique view. **D–F**. Legs. **D**. Fore. **E**. Middle. **F**. Hind. **G–I**. Tarsi. **G**. Pro. **H**. Meso. **I**. Meta. **J**. Sternite VIII. **K**. Tergite VIII. **L**. Genitalia. **M**. Ovipositor. Scales in mm.

PrF 0.34–0.41 (0.37±0.02), PrT 0.26–0.32 (0.29±0.02), MsF 0.36–0.40 (0.39±0.01), MsT 0.31–0.36 (0.34±0.02), MtF 0.41–0.47 (0.44±0.02), MtT 0.35–0.45 (0.41±0.02).

Host

Collected from *Ceratiomyxa fruticulosa* on a fallen *Pinus* sp. (Fig. 1G) and other two logs, also covered with *C. fruticulosa* (Fig. 93D).

Remarks

This species is similar to *B. colibri* sp. nov. but differs mainly by the entire basal striae, and by the more elongate antennae, with thinner antennomeres. Other differences are the very short submesocoxal area and the much thinner last maxillary palpomere. Regarding the genitalia, *B. inusitata* sp. nov. can be easily distinguished from *B. colibri* sp. nov. by the straight parameres in males and by the distinct shape of the ovipositor in females. The absence of gonostylus was also recorded to the *B. lenta* species group (e.g., *B. caliginosa* Löbl, 1984) (Ogawa & Löbl 2013) but *B. inusitata* sp. nov. differs by the much shorter distal gonocoxite.

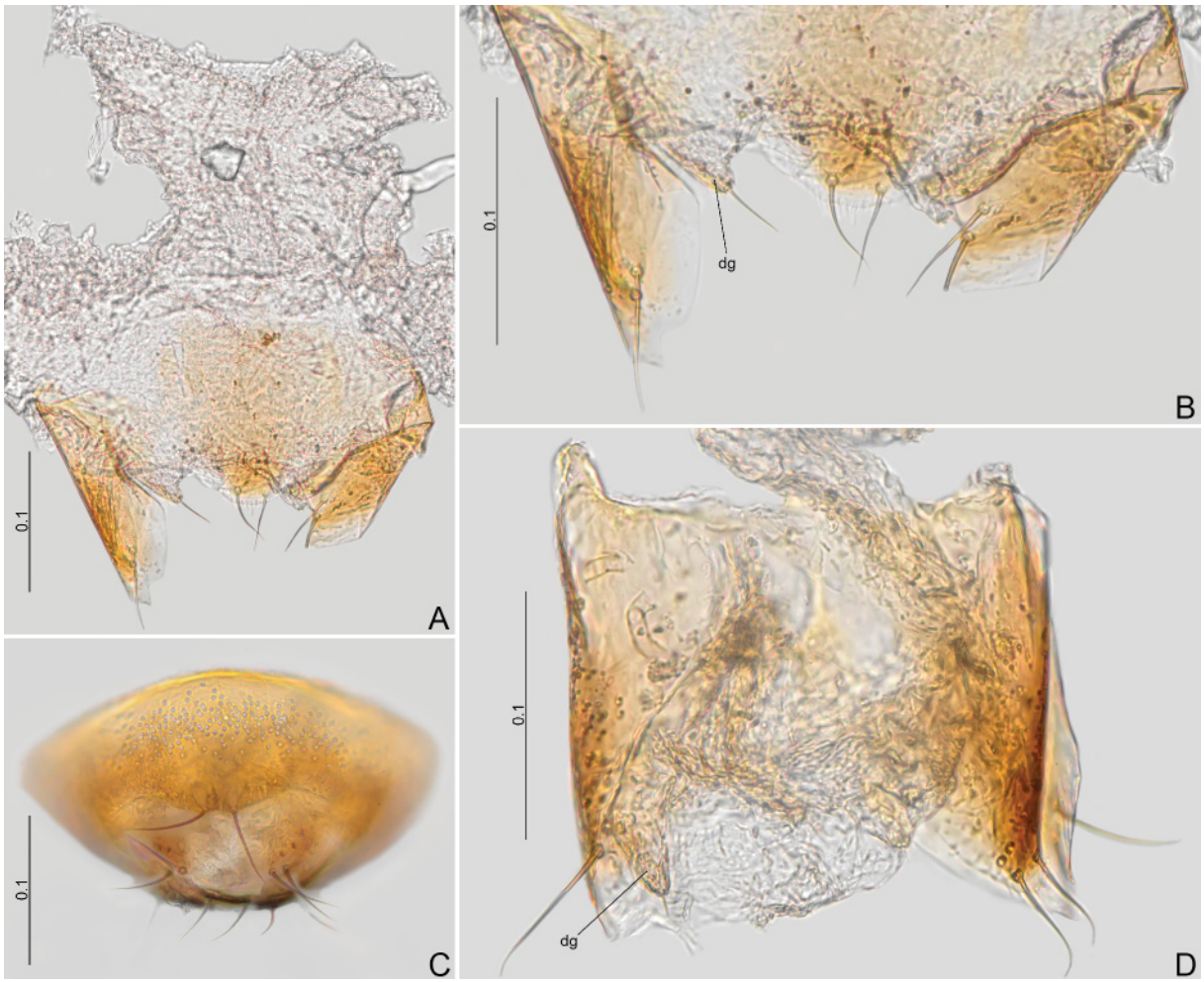

Fig. 24. *Baeocera inusitata* sp. nov., paratypes, ♀♀ (CELC). **A**. Genitalia (#134). **B**. Ovipositor (#134). **C**. Apex, abdomen with genitalia (#126). **D**. Genitalia (#23). Abbreviation: dg=distal gonocoxite. Scales in mm.

Distribution

Mata do Paraíso and Mata da Biologia, Universidade Federal de Viçosa, campus of Viçosa, state of Minas Gerais, Southeast Brazil (Fig. 1A–B).

Baeocera ardua species group

Group formed by four species with small body, dark brown colouration, submesocoxal lines arcuate, flagellum elongate, basal striae connected to the sutural one, but not to the lateral, and reaching approximately the outer ⅔ of the basal width.

Baeocera ardua sp. nov.
urn:lsid:zoobank.org:act:2B0B23CC-680A-44F3-86B5-32EDD6D5F138
Figs 1A–B, G, 25–28

Diagnosis

Small, body length: 1.11 mm. Not strongly oblong in dorsal view; dark brown. Mesepimeron width approximately 0.75 of the mesanepisternum width, and 3.18× as wide as long. Submesocoxal lines arcuate and punctate. Basal striae connected to sutural and reaching approximately the outer 2.12/3 of the basal width. Parameres thin, lobed posteriorly, tip oblong. Female unknown.

Etymology

The species epithet is a Portuguese adjective in apposition, meaning 'difficult', 'hard', referring to the challenging study of this morphologically uniform group, and in particular this species.

Material examined

Holotype
BRAZIL • ♂*; Minas Gerais, Viçosa, EPTEA Mata do Paraíso; 10 Mar. 2022; E. von Groll *et al.* leg.; "Falcon 26 / Em *Ceratiomyxia fruticulosa* em *Pinus* / Dissecado em 21.x.2022 / HOLOTYPUS ♂"; CELC. (Fig. 25D–E)

Paratype
BRAZIL • 1 ♂**; same collection data as for holotype; CELC.

Description

Colouration. Dark brown; mouthparts, antennomeres I–VI, and legs ochreous; tarsi, posterior part of abdominal ventrites yellow (Fig. 25A–C, F).

Head (Fig. 25F–O). Frons finely punctate; pubescence fine (Fig. 25F). Labrum almost straight posteriorly; laterals rounded (Fig. 25J). Mandibles not strongly curved; tooth somewhat elongate (Fig. 25K–L). Maxillary palpomere III somewhat oblong (Fig. 25M). Labial palpomeres elongate and very thin; palpomere II curved; mentum concave posteriorly (Fig. 25N). Gular pores absent (Fig. 25O). Antennae (Fig. 25H–I) elongate, antennomeres III–VI thick; antennomere VII longer than VIII; XI elongate, with sides parallel; antennomere proportions (n = 2): I 75/32 : II 62/32 : III 33/14 : IV 47/14 : V 51/15 : VI 47/16 : VII 57/22 : VIII 50/23 : IX 72/33 : X 75/38 : XI 110/34.

Prothorax (Fig. 26A–E, I). Punctation moderately sparse and fine; pubescence sparse (Fig. 26A). Pronotum constricted laterally. Hypomeron poorly pubescent (Fig. 26I). Prosternal process strongly acute in lateral view (Fig. 26C). Profurca tapering apically (Fig. 26E).

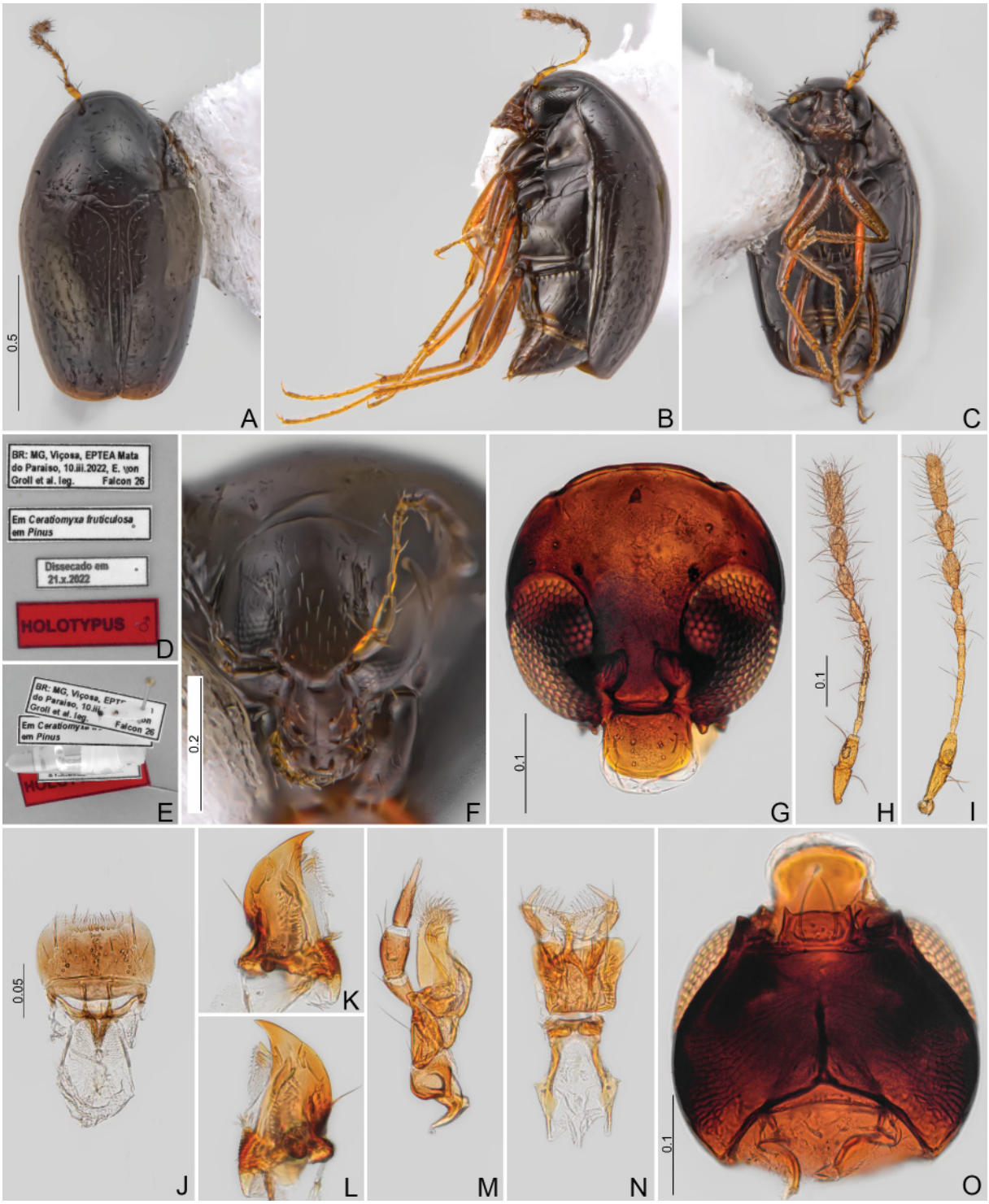

Fig. 25. *Baeocera ardua* sp. nov. (CELC). **A–F**. Holotype, ♂. **A**. Dorsal view. **B**. Lateral view. **C**. Ventral view. **D**. Labels. **E**. Pinned. **F**. Head, frontal view. **G**. Paratype, ♂ (#33), head, frontal view. **H–I**. Antennae. **H**. Holotype, ♂. **I**. Paratype, ♂ (#33). **J–O**. Paratype, ♂ (#33). **J**. Labrum. **K–L**. Mandibles. **M**. Maxilla. **N**. Labium. **O**. Head, ventral view. Scales in mm.

Mesothorax (Fig. 26F–I). Scutellum visible in dorsal view, wider than long; tip rounded (Fig. 26F). Mesoventral lines strongly curved (Fig. 26G). Mesepimeron about 3.18× as wide as long, and about 0.75× the width of the mesanepisternum (Fig. 26I). Mesoventral process truncated in lateral view (Fig. 26H).

Metathorax (Fig. 26G–I). Metaventrite smooth, shining, pubescence moderately sparse laterally (Fig. 26I). Submesocoxal lines arcuate and punctate; submesocoxal area length: 0.05–0.06 mm (Fig. 26G–I). Metanepisternal suture dashed, curvature variable (Fig. 26H–I). Metanotum with alacrista trapezoidal-shaped, with distinct sides; scutoscutellar suture elongate and slightly longer than apodeme (Fig. 26J). Stalk of metendosternite narrower than arms (Fig. 27A–B).

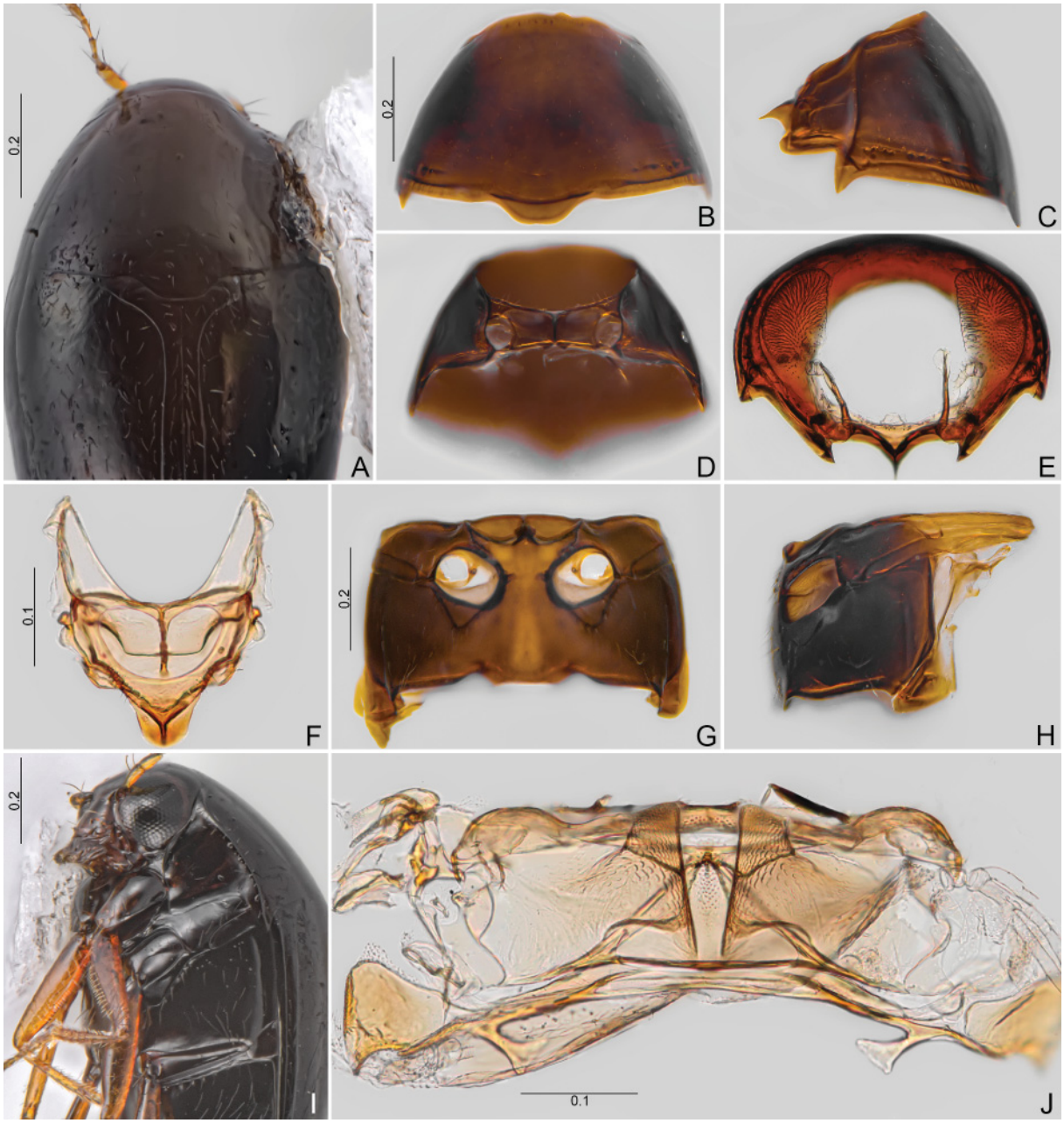

Fig. 26. *Baeocera ardua* sp. nov. (CELC). **A**. Holotype, ♂, prothorax, dorsal view. **B–H**. Paratype, ♂ (#33). **B–E**. Prothorax. **B**. Dorsal view. **C**. Lateral view. **D**. Ventral view. **E**. Inner view. **F**. Scutellar shield. **G–I**. Meso- and metathorax. **G**. Ventral view. **H**. Lateral view. **I**. Holotype, ♂, oblique view. **J**. Paratype, ♂ (#33), metanotum. Scales in mm.

Wings (Figs 25A, 27C–D). Elytra tapering toward apex; punctation moderately coarse and sparse. Basal striae connected to sutural, impunctate, and reaching approximately the outer 2.12/3 of the basal width (Fig. 26A). Lateral striae fine, impunctate, and curved near humeral region (Fig. 26I).

Legs. Thin, elongate, not microsculptured

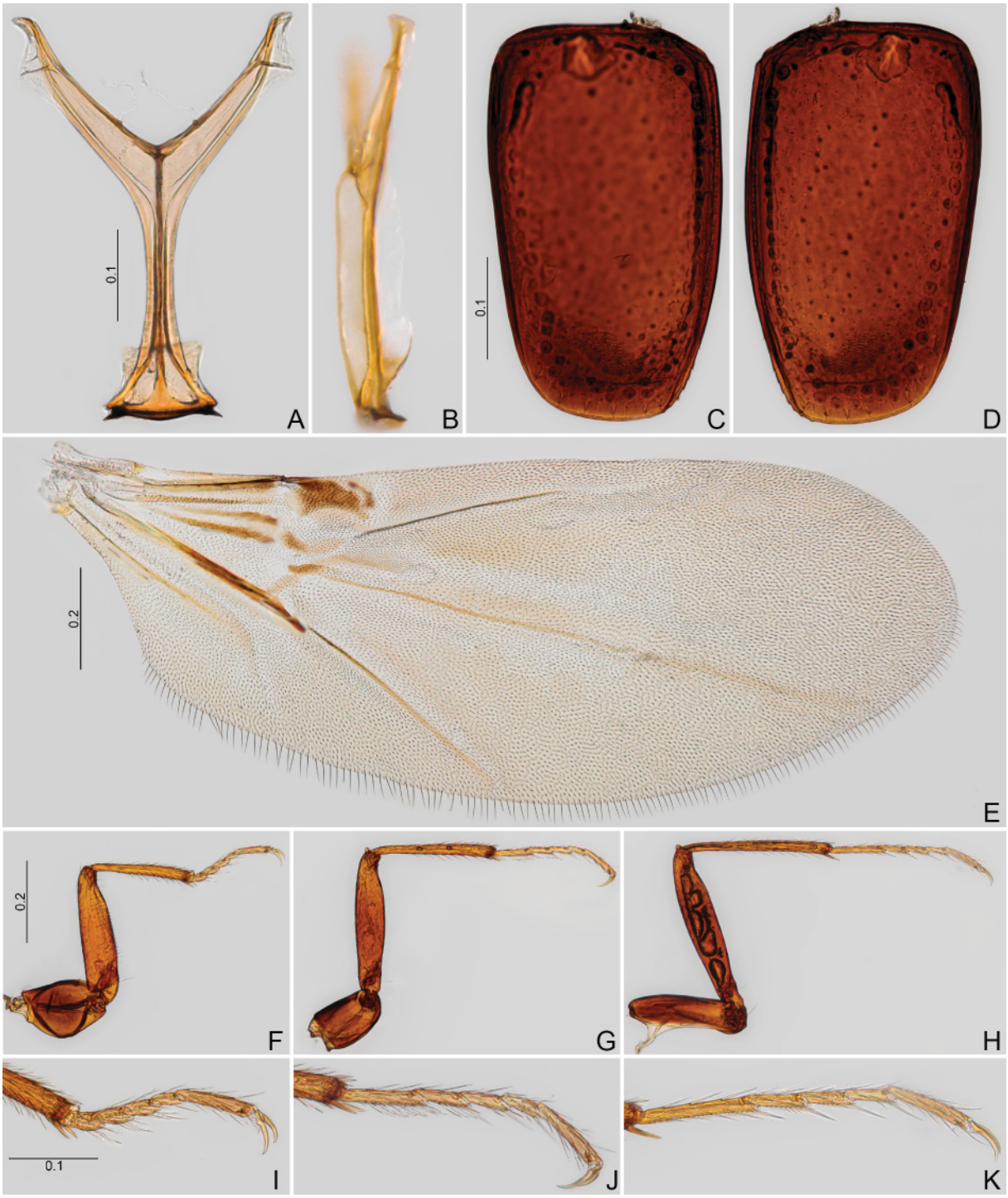

Fig. 27. *Baeocera ardua* sp. nov., paratype, ♂ (#33) (CELC). **A–B**. Metendosternite. **A**. Dorsal view. **B**. Lateral view. **C–D**. Elytra. **E**. Hind wing. **F–H**. Legs. **F**. Fore. **G**. Middle. **H**. Hind. **I–K**. Tarsi. **I**. Pro. **J**. Meso. **K**. Meta. Scales in mm.

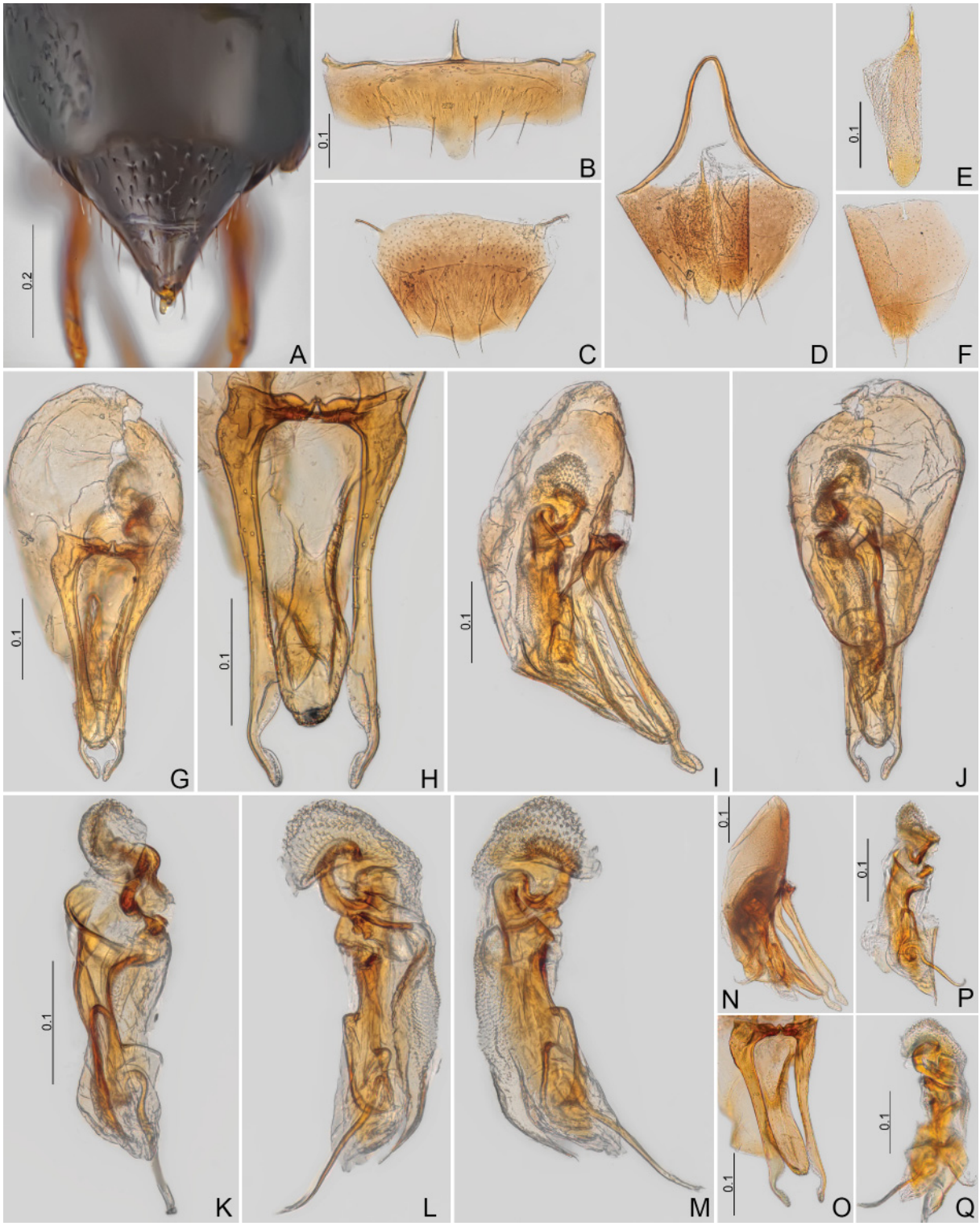

Fig. 28. *Baeocera ardua* sp. nov. (CELC). **A–M**. Holotype, ♂. **A**. Abdomen, dorsal view. **B**. Sternite VIII. **C**. Tergite VIII. **D**. Tergite IX. **E**. Sternite IX. **F**. Tergite X. **G–J**. Aedeagi. **G**. Frontal view. **H**. Parameres, ventral view. **I**. Lateral view. **J**. Dorsal view. **K–M**. Sclerites of internal sac. **K**. Frontal view. **L**. Lateral view-1. **M**. Lateral view-2. **N–Q**. Paratype, ♂ (#33), aedeagi. **N**. Lateral view. **O**. Parameres, oblique view. **P**. Sclerite, oblique view. **Q**. Sclerite, lateral view. Scales in mm.

Abdomen. Submetacoxal lines with sparse and coarse punctures (Figs 25B, 26I). Ventral surface shining; pubescence dense; punctures fine. Propygidium dense and coarsely punctate; micropunctured; pubescence dense (Fig. 28A).

Males

Pro- and mesotarsomeres I–III widened, bearing tenent setae (Fig. 27F–K). Sternite VIII with a large posterior projection (Fig. 28B). Tergite VIII with a small posterior projection (Fig. 28C). Tergite IX with strongly curved ventral struts (Fig. 28D). Sternite IX slightly constricted centrally, microsculptured (Fig. 28E). Tergite X triangular (Fig. 28F).

Aedeagus (Fig. 28G–Q). Median lobe poorly sclerotized; basal bulb longer than apical lobe; apex truncate (Fig. 28H). Parameres also poorly sclerotized, but more than median lobe; thin, with a lobe near apex, tip wide (Fig. 28G, J, N–O). Sclerite of internal sac with distinct curvatures, flagellum thin (Fig. 28K–M, P–Q).

Measurements (n = 2, including holotype; in mm; * = invariant). TL 1.11*, SY 0.10*, HW 0.31–0.32 (0.32 ± 0.01), IS 0.15–0.16 (0.16 ± 0.01), WA 0.07*, PL 0.43–0.44 (0.44 ± 0.01), PA 0.31–0.36 (0.34 ± 0.04), PB 0.63–0.67 (0.65 ± 0.03), SL 0.02*, SW 0.04*, EI 0.69–0.70 (0.70 ± 0.01), EL 0.76–0.78 (0.77 ± 0.01), EW 0.32–0.34 (0.33 ± 0.01), EH 0.30–0.33 (0.32 ± 0.02), MsW 0.15–0.16 (0.16 ± 0.01), MeL 0.04–0.05 (0.05 ± 0.01), MeW 0.12*, MB 0.10*, MC 0.27–0.28 (0.28 ± 0.01), ML 0.05–0.06 (0.06 ± 0.01), VL 0.13–0.15 (0.14 ± 0.01), PrF 0.29–0.30 (0.30 ± 0.01), PrT 0.24*, MsF 0.32–0.37 (0.35 ± 0.04), MsT 0.29*, MtF 0.38*, MtT 0.35–0.36 (0.36 ± 0.01).

Host

Collected from *Ceratiomyxa fruticulosa* on a fallen *Pinus* sp. tree (Fig. 1G).

Remarks

Similar to *B. bottine* sp. nov. but differs by the smaller size, the submetacoxal line less arcuate, the femora not distinctly darker near the coxae, the slender antennomeres, and by the more elongate and parallel antennomere XI. Regarding the male terminalia, *B. ardua* sp. nov. can be separated by the wider apical projection of sternite VIII, the more parallel sides of tergite IX, and by the lobed parameres.

Distribution

Mata do Paraíso, Universidade Federal de Viçosa, campus of Viçosa, state of Minas Gerais, Southeast Brazil (Fig. 1A–B).

Baeocera bottine sp. nov.
urn:lsid:zoobank.org:act:8ECC11F2-94CB-49C9-8EB6-6688882705A1
Figs 1A–B, G, 29–33

Diagnosis

Body length: 1.16–1.22 mm. Dark brown; legs ochreous, femora darker on anterior ⅔. Antennomeres IX–XI oblong. Mesepimeron width approximately 0.62 of the mesanepisternum width, and 2.90 × as wide as long. Submesocoxal lines arcuate, punctate; submesocoxal area = 0.05 mm. Basal striae connected to sutural and reaching approximately the outer ⅔ of the basal width. Aedeagus with thin parameres, with a shallow lobe near apex in frontal view. Tergite VIII in females with posterior projection. Distal gonocoxite triangular, elongate.

Etymology

The species epithet is a French noun in apposition, meaning ‘boot’, in allusion to the female ovipositor’s resemblance to Victorian ladies’ boots.

Fig. 29. *Baeocera bottine* sp. nov. (CELC). **A–E**. Holotype, ♂. **A**. Dorsal view. **B**. Lateral view. **C**. Ventral view. **D**. Labels. **E**. Pinned. **F–G**. Paratype, ♀ (#52). **F**. Dorsal view. **G**. Lateral view. **H**. Holotype, ♂, head, frontal view. **I**. Paratype, ♀ (#31), head, frontal view, dissected. **J**. Holotype, ♂, head, frontal view. **K–M**. Antennae. **K**. Holotype, ♂. **L**. Paratype, ♀ (#31). **M**. Paratype, ♀ (#52). Scales in mm.

Material examined

Holotype

BRAZIL • ♂*; Minas Gerais, Viçosa, EPTEA Mata do Paraíso; 14 Apr. 2022; E. von Groll *et al.* leg.; "Falcon 42 / Em *Ceratiomyxa fruticulosa* em *Pinus* / Dissecado em 21.x.2022 / HOLOTYPUS ♂"; CELC. (Fig. 29D–E)

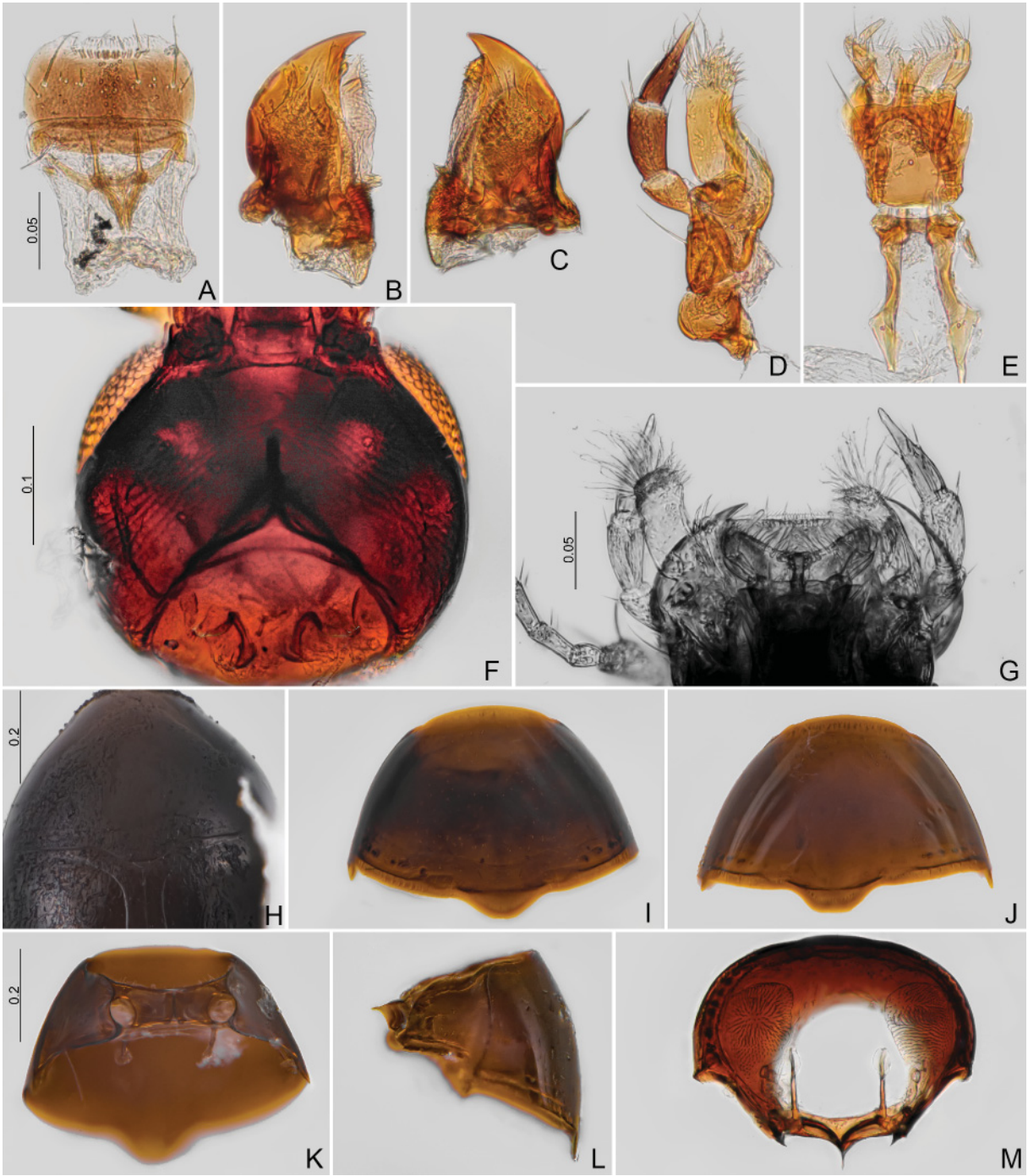

Fig. 30. *Baeocera bottine* sp. nov. (CELC). **A–E**. Paratype, ♀ (#31). **A**. Labrum. **B–C**. Mandibles. **D**. Maxilla. **E**. Labium. **F–I**. Holotype, ♂. **F**. Head, ventral view. **G**. Mouth parts. **H**. Prothorax, dorsal view. **I**. Prothorax, dorsal view, dissected. **J–M**. Paratype, ♀ (#31), prothorax. **J**. Dorsal view. **K**. Ventral view. **L**. Lateral view. **M**. Inner view. Scales in mm.

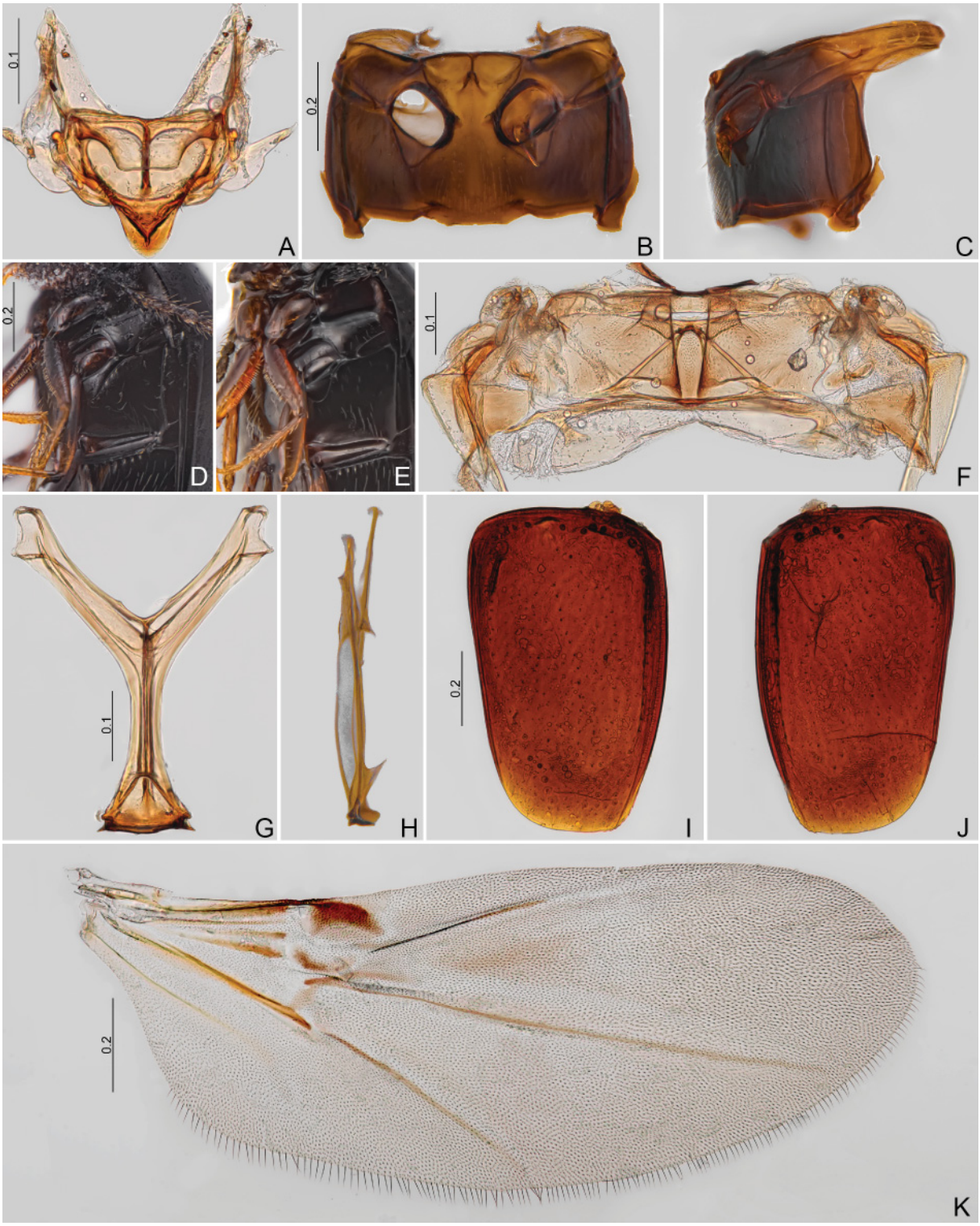

Fig. 31. *Baeocera bottine* sp. nov. (CELC). **A–C**. Paratype, ♀ (#31). **A**. Scutellar shield. **B–E**. Meso- and metathorax. **B**. Ventral view. **C**. Lateral view. **D**. Holotype, ♂, oblique view. **E**. Paratype, ♀ (#52), oblique view. **F–K**. Paratype, ♀ (#31). **F**. Metanotum. **G–H**. Metendosternite. **G**. Dorsal view. **H**. Lateral view. **I–J**. Elytra. **K**. Hind wing. Scales in mm.

Fig. 32. *Baeocera bottine* sp. nov., holotype, ♂ (CELC). **A–C**. Legs. **A**. Fore. **B**. Middle. **C**. Hind. **D**. Abdomen, dorsal view. **E**. Sternite VIII. **F**. Tergite VIII. **G**. Tergite IX. **H**. Sternite IX. **I**. Tergite X. **J–L**. Aedeagi. **J**. Frontal view. **K**. Lateral view. **L**. Dorsal view. **M–O**. Sclerites of internal sac. **M**. Frontal view. **N**. Lateral view-1. **O**. Lateral view-2. Scales in mm.

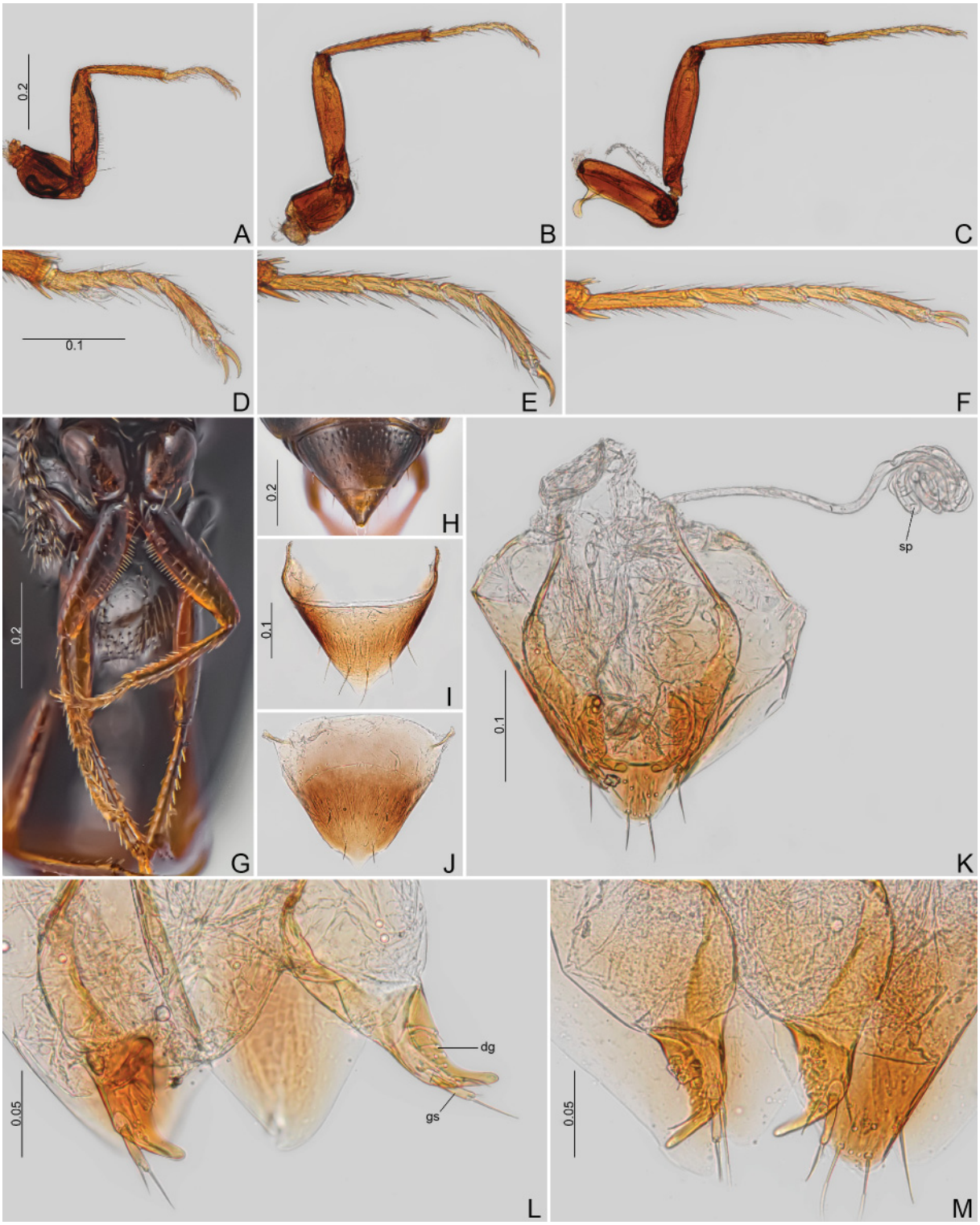

Fig. 33. *Baeocera bottine* sp. nov. (CELC). **A–F**. Paratype, ♀ (#31). **A–C**. Legs. **A**. Fore. **B**. Middle. **C**. Hind. **D–F**. Tarsi. **D**. Pro. **E**. Meso. **F**. Meta. **G–H**. Paratype, ♀, (#52). **G**. Forelegs. **H**. Abdomen, dorsal view. **I–L**. Paratype, ♀ (#31). **I**. Sternite VIII. **J**. Tergite VIII. **K**. Genitalia. **L**. Ovipositor. **M**. Paratype, ♀ (#52), ovipositor. Abbreviations: dg = distal gonocoxites; gs = gonostyli; sp = spermatheca. Scales in mm.

Paratypes

BRAZIL • 1 ♀**; same collection data as for holotype; 10 Mar. 2022; E. von Groll *et al.* leg.; "Falcon 26 / Em *Ceratiomyxia fruticulosa* em *Pinus*"; CELC • 1 ♀**; same collection data as for holotype; 24 Mar. 2022; E. von Groll *et al.* leg.; "Falcon 20 / Em *Ceratiomyxia fruticulosa* em *Pinus*"; CELC.

Description

Colouration. Dark brown; mouthparts and tarsi yellow; antennae, posterior area of femora, and tibiae, ochreous; frons, coxae, and anterior ⅔ of femora dark ochreous (Fig. 29A–C, F–G, 32A–D, 33G). Variations: (1): all structures paler; (2) abdominal ventrites III–VI ochreous (Figs 29G, 33H). Colouration of legs varies with viewing angle; for example, Figures 29G and 33G show the same specimen photographed at different angles. In Figure 33G, the leg coloration appears darker and more accurate.

Head (Figs 29H–M, 30A–G). Frons with sparse punctures; one fovea above each eye. Labrum almost straight posteriorly (Fig. 30A). Maxillary palpomere III elongate and not distinctly curved; IV, thin (Fig. 30D, G). Labial palpomere II curved; mentum slightly concave posteriorly (Fig. 30E, G). Gular pores sparse (Fig. 30F). Antennae not distinctly elongate (Fig. 29K–M). Antennomere VII just slightly longer than VIII; IX–XI oblong; antennomere proportions (n = 3): I 71/32 : II 63/32 : III 30/15 : IV 39/14 : V 45/14 : VI 39/15 : VII 46/22 : VIII 44/22 : IX 62/35 : X 64/38 : XI 90/40.

Prothorax (Fig. 30H–M). Punctation sparse; pubescence short. Hypomeron subglabrous, impunctate (Fig. 31D–E). Prosternal process acute in lateral view (Fig. 30L). Profurca thin and short (Fig. 30M).

Mesothorax (Fig. 31A–E). Scutellum visible in dorsal view (Fig. 30H), wider than long; slightly triangular (Fig. 31A). Mesoventral lines smoothly curved (Fig. 31B). Median lines curved and open (Fig. 31B). Mesepimeron 2.90 × as wide as long and about 0.62 × the width of the mesanepisternum; variations: 2.33 × as wide as long and about 0.67 × the width of the mesanepisternum. (Fig. 31D–E). Mesoventral process oblong in lateral view (Fig. 31C).

Metathorax (Fig. 31B–C). Metaventrite smooth, shining, pubescence moderately sparse. Submesocoxal lines strongly arcuate; punctate; submesocoxal area length: 0.05–0.06 mm (Fig. 31D–E). Metanepisternal suture dashed, more or less convex (Fig. 31D–E). Metanotum with alacrista trapezoidal-shaped, longer than wide; scutoscutellar suture lateral end at same position as apodeme (Fig. 31F). Arms of metendosternite slightly thicker than stalk (Fig. 31G–H).

Wings (Fig. 29A, F, I–K). Elytra with sparse and fine punctures – similar to pronotum; pubescence short. Basal striae connected to sutural, impunctate, and reaching approximately the outer ⅔ of the basal width (Fig. 29F). Lateral striae fine, impunctate, and curved near humeral region (Fig. 29C, G).

Legs. Thin, elongate, not microsculptured (Figs 32A–C, 33A–F).

Abdomen. Submetacoxal lines coarse punctate (Fig. 29B, G). Ventrite I shining; pubescence dense; finely punctate. Propygidium dense and coarsely punctate; micropunctured; pubescence dense (Figs 32D, 33H).

Males

Protibiae slightly curved (Fig. 32A). Pro- and mesotarsomeres I–III widened, bearing tenent setae (Fig. 32A–B). Sternite VIII with an acute posterior projection (Fig. 32E). Tergite VIII with a small projection (Fig. 32F). Tergite IX with curved ventral struts (Fig. 32G). Sternite IX elongate and oblong posteriorly (Fig. 32H). Tergite X triangular (Fig. 32I).

Aedeagus (Fig. 32J–O). Median lobe slightly curved in lateral view; basal bulb similar in length as apical lobe, and poorly sclerotized; apical lobe more sclerotized (Fig. 32J–L). Parameres thin and parallel, with a small posterior constriction in frontal view (Fig. 32J). Sclerite of internal sac curved, flagellum thin and very elongate (Fig. 32M–O).

Measurements (n = 1, holotype; in mm). TL 1.16, SY 0.12, HW 0.32, IS 0.14, WA 0.06, PL 0.49, PA 0.32, PB 0.66, SL 0.01, SW 0.04, EI 0.76, EL 0.81, EW 0.37, EH 0.32, MsW 0.17, MeL 0.04, MeW 0.16, MB 0.10, MC 0.27, ML 0.05, VL 0.14, PrF 0.27, PrT 0.20, MsF 0.32, MsT 0.28, MtF 0.37, MtT 0.32.

Females (Figs 29L–M, 33)

Antennomeres VI–X thicker than those of males (Fig. 29L–M). Ventrite and tergite VIII with a triangular posterior projection (Fig. 33I–J). Spermatheca filiform (Fig. 33K). Distal gonocoxite triangular and distinctly longer than wide, gonostylus rectangular (Fig. 33K–M).

Measurements (n = 2; in mm; * = invariant). TL 1.22*, SY 0.11*, HW 0.32–0.34 (0.33 ± 0.01), IS 0.15–0.16 (0.16 ± 0.01), WA 0.08–0.10 (0.09 ± 0.01), PL 0.47–0.51 (0.49 ± 0.03), PA 0.35*, PB 0.69–0.70 (0.70 ± 0.01), SL 0.02–0.03 (0.03 ± 0.01), SW 0.05–0.06 (0.06 ± 0.01), EI 0.76–0.77 (0.77 ± 0.01), EL 0.83–0.85 (0.84 ± 0.01), EW 0.38–0.40 (0.39 ± 0.01), EH 0.36–0.38 (0.37 ± 0.01), MsW 0.17–0.18 (0.18 ± 0.01), MeL 0.03–0.04 (0.04 ± 0.01), MeW 0.12–0.17 (0.15 ± 0.04), MB 0.11–0.12 (0.12 ± 0.01), MC 0.27–0.28 (0.28 ± 0.01), ML 0.05–0.06 (0.06 ± 0.01), VL 0.18–0.19 (0.19 ± 0.01), PrF 0.29*, PrT 0.21–0.22 (0.22 ± 0.01), MsF 0.34–0.35 (0.35 ± 0.01), MsT 0.24–0.27 (0.26 ± 0.02), MtF 0.36–0.37 (0.37 ± 0.01), MtT 0.31–0.32 (0.32 ± 0.01).

Host

Collected from *Ceratiomyxa fruticulosa* on a fallen *Pinus* sp. tree (Fig. 1G).

Remarks

Similar to *B. pulga* sp. nov. but differs by the smaller body length, the more oblong antennomeres VII–XI, the spoon-like sternite IX, the more parallel parameres, the curved sclerite of internal sac, and the more elongate distal gonocoxite in females.

Distribution

Mata do Paraíso, Universidade Federal de Viçosa, campus of Viçosa, state of Minas Gerais, Southeast Brazil (Fig. 1A–B).

Baeocera colibri sp. nov.

urn:lsid:zoobank.org:act:9216244A-A10C-4B93-8894-7148CF8DC7EE

Figs 1A–D, G, 34–38

Diagnosis

Body length: 1.08–1.22 mm; oblong. Dark brown. Mesepimeron approximately 0.65 the width of the mesanepisternum, and 2.75 × as wide as long. Submesocoxal lines strongly arcuate, punctate. Basal striae connected to sutural and reaching approximately the outer ⅔ of the basal width. Propygidium dense and coarsely punctate. Aedeagus with parameres strongly sinuous, constricted posteriorly; sclerites twisted, hummingbird-shaped. Tergite VIII in females lacking posterior projection. Distal gonocoxite robust.

Etymology

The species epithet is a Spanish noun in apposition, meaning ‘hummingbird’, alluding to the hummingbird-like male sclerite of the internal sac.

Material examined

Holotype

BRAZIL • ♂; Minas Gerais, Viçosa, EPTEA Mata do Paraíso; 12 Nov. 2019; LabCol leg.; "Fungo 06 / Fotos: 0751-0753 / Em *Ceratiomyxia fruticulosa* / HOLOTYPUS ♂"; CELC. (Fig. 34D–E)

Fig. 34. *Baeocera colibri* sp. nov. (CELC). **A–F**. Holotype, ♂. **A**. Dorsal view. **B**. Lateral view. **C**. Ventral view. **D**. Labels. **E**. Pinned. **F**. Head, frontal view. **G**. Paratype, ♀ (#48), head, frontal view. **H–I**. Antennae. **H**. Paratype, ♂ (#09). **I**. Paratype, ♀ (#22). **J–M**. Paratype, ♂ (#13). **J**. Labrum. **K–L**. Mandibles. **M**. Maxilla. **N**. Paratype, ♀ (#16), labium. Scales in mm.

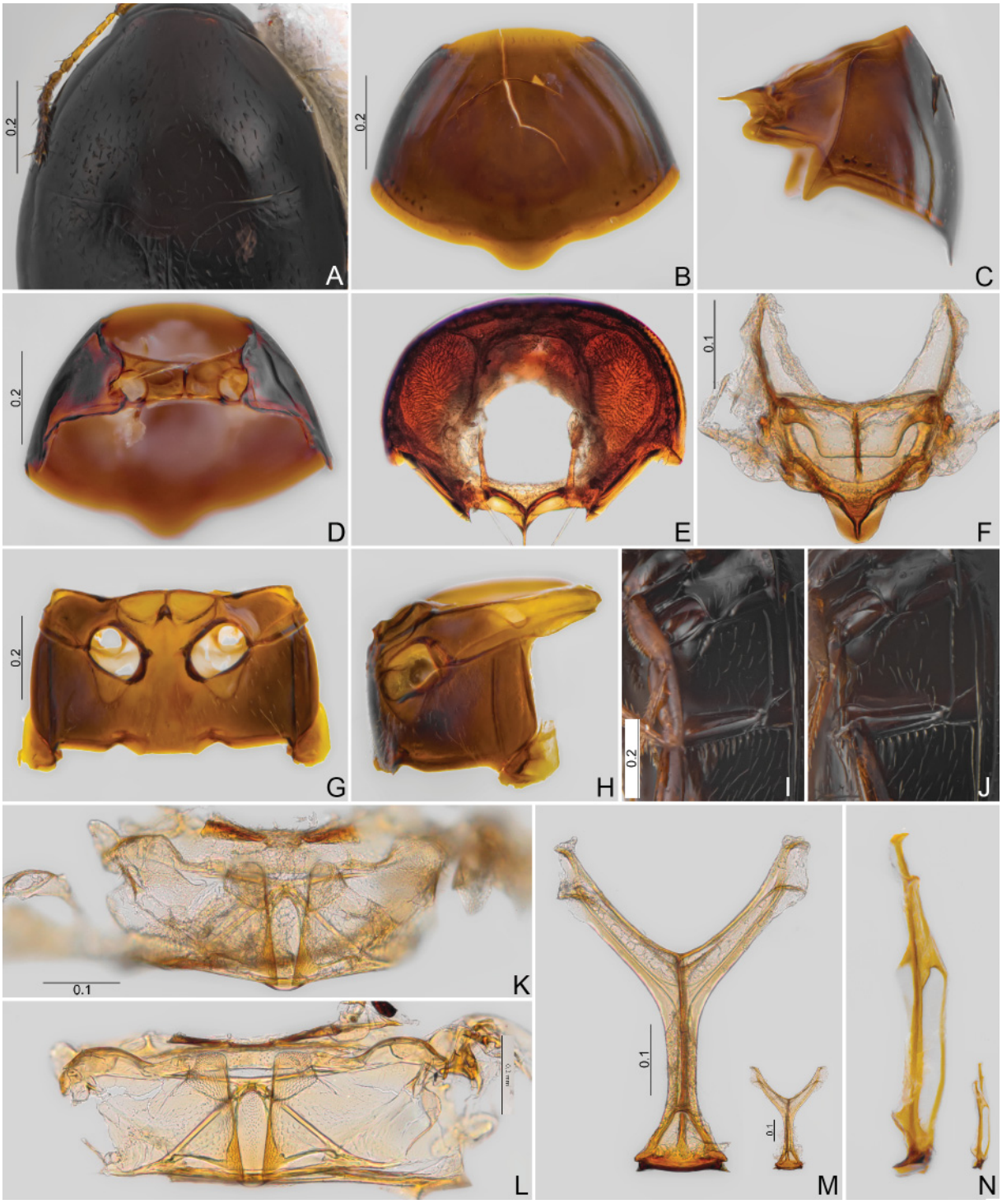

Fig. 35. *Baeocera colibri* sp. nov. (CELC). **A**. Holotype, ♂, prothorax, dorsal view. **B–H**. Paratype, ♂ (#13). **B–E**. Prothorax. **B**. Dorsal view. **C**. Lateral view. **D**. Ventral view. **E**. Inner view. **F**. Scutellar shield. **G–J**. Meso- and metathorax. **G**. Ventral view. **H**. Lateral view. **I**. Holotype, ♂, oblique view. **J**. Oblique view (paratype, ♂, #55). **K–L**. Metanotum. **K**. Paratype, ♂ (#13). **L**. Paratype, ♀ (#16). **M–N**. Metendosternite (paratypes; large figures = ♂, #13; small = ♀, #16). **M**. Dorsal view. **N**. Lateral view. Scales in mm.

Paratypes

BRAZIL • 2 ♂♂, 3 ♀♀ (1 ♂**, 1 ♀*, 1 ♀**); same collection data as for holotype; CELC • 1 ♀*; same collection data as for holotype; "Fungo 31 / Em *Xylodon flaviporus*"; CELC • 4 ♂♂ (1 ♂*), 1 ♀*, 2 ex.; same collection data as for holotype; "Fungo 10 / Em *Ceratiomyxia fruticulosa*"; CELC • 1 ♂*, 1 ♀, 1 ex.; same collection data as for holotype; 14 Nov. 2019; LabCol leg.; "Fungo 34 / Fotos: 0783-0790; Em *Ceratiomyxa fruticulosa*"; CELC • 1 ♂*, 1 ♀*; same collection data as for holotype; 24 Mar. 2022; E. von Groll *et al.* leg.; "Falcon 20 / Em *Ceratiomyxia fruticulosa* em *Pinus*"; CELC.

Description

Colouration. Dark brown, with reddish nuances, angle dependent; clypeus, coxae, tip of elytra, and anterior part of femora ochreous; antennomeres I–VI, mouthparts, tibiae, apex of each ventral ventrite, and tarsi yellow (Figs 34A–C, F–G, 38A–C). Variations: sclerites from light to dark brown.

Head (Fig. 34F–N). Frons with punctation sparse, some coarser than other (Fig. 34F–G). Labrum straight posteriorly (Fig. 34J). Mandibles with tooth not distinctly elongate (Fig. 34K–L). Maxillary palpomere III somewhat oblong, IV thick (Fig. 34M). Labial palpomere II elongate; IV thin and curved; mentum concave posteriorly (Fig. 34N). Antennomeres VII and XI elongate (Fig. 34H–I); antennomere proportions (n = 6): I 74/30 : II 57/27 : III 31/14 : IV 37/14 : V 42/14 : VI 39/16 : VII 43/22 : VIII 45/24 : IX 71/36 : X 73/38 : XI 106/39.

Prothorax (Fig. 35A–E). Punctation sparse and fine; pubescence sparse and short. Hypomeron subglabrous, impunctate (Figs 34B, 38B). Prosternal process distinctly elongate and spinose in lateral view (Fig. 35C). Profurca short and thick (Fig. 35E).

Mesothorax (Fig. 35F–J). Scutellum visible in dorsal view, wider than long; tip rounded (Fig. 35A). Mesoventral lines curved; median lines short, straight, and open (Fig. 35G). Mesepimeron 2.75 × as wide as long and about 0.65 × the width of the mesanepisternum (Fig. 35G–J). Mesoventral process with a small posterior ridge (Fig. 35H).

Metathorax (Fig. 35G–N). Metaventrite smooth, shining, pubescence moderately sparse laterally (Fig. 35I–J). Submesocoxal lines strongly arcuate, punctate; submesocoxal area length: 0.04–0.07 mm (Fig. 35G–J). Metanepisternal suture dashed, with variable curvature (Fig. 35I–J). Metanotum with alacrista trapezoidal-shaped; scutoscutellar suture short, and not trespassing apodeme (Fig. 35K–L). Stalk of metendosternite slightly narrower than arms (Fig. 35M–N).

Wings (Figs 34A, 36A–B, 38A). Elytra dense and coarsely punctured. Basal striae connected to sutural, impunctate, and reaching approximately the outer ⅔ of the basal width (Fig. 35A). Lateral striae fine, impunctate, and curved near humeral region (Fig. 34B).

Legs. Thin, elongate, not microsculptured (Figs 36D–I, 38D–I).

Abdomen. Submetacoxal lines with coarse punctures (Fig. 35I–J). Ventral surface shining; pubescence dense; punctures fine (Fig. 35I–J). Propygidium dense and coarsely punctate; micropunctured; pubescence dense (Figs 36J, 38J).

Males

Pro- and mesotarsomeres I–III widened, bearing tenent setae (Fig. 36G–I). Sternite VIII with an elongate posterior projection (Fig. 36K). Tergite VIII triangular with a smooth and wide posterior projection (Fig. 36L). Tergite IX with curved ventral struts. Sternite IX constricted centrally (Fig. 36M). Tergite X triangular, wide (Fig. 36M).

Aedeagus (Fig. 37A–N). Median lobe with basal bulb larger than apical lobe; apical lobe bent and moderately sclerotized. Parameres distinctly sclerotized and sinuous in frontal view; with a constriction near apex (Fig. 37B). Internal sac formed by a twisted sclerite that forms a short and curved main

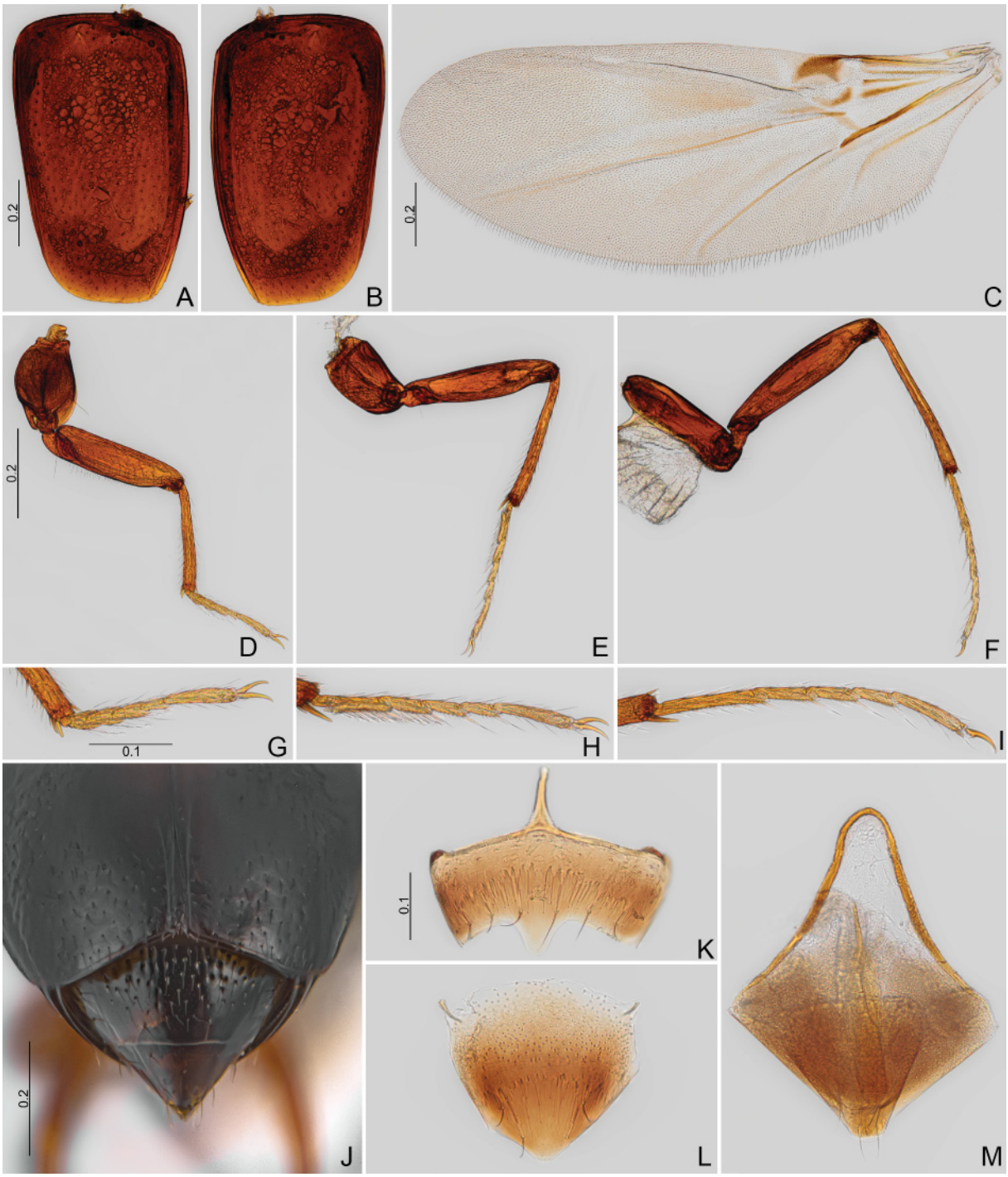

Fig. 36. *Baeocera colibri* sp. nov. (CELC). **A–B**. Paratype, ♀ (#16), elytra. **C–I**. Paratype, ♂ (#13). **C**. Hind wing. **D–F**. Legs. **D**. Fore. **E**. Middle. **F**. Hind. **G–I**. Tarsi. **G**. Pro. **H**. Meso. **I**. Meta. **J**. Holotype, ♂, abdomen, dorsal view. **K–M**. Paratype, ♂ (#09). **K**. Sternite VIII. **L**. Tergite VIII. **M**. Tergite IX. Scales in mm.

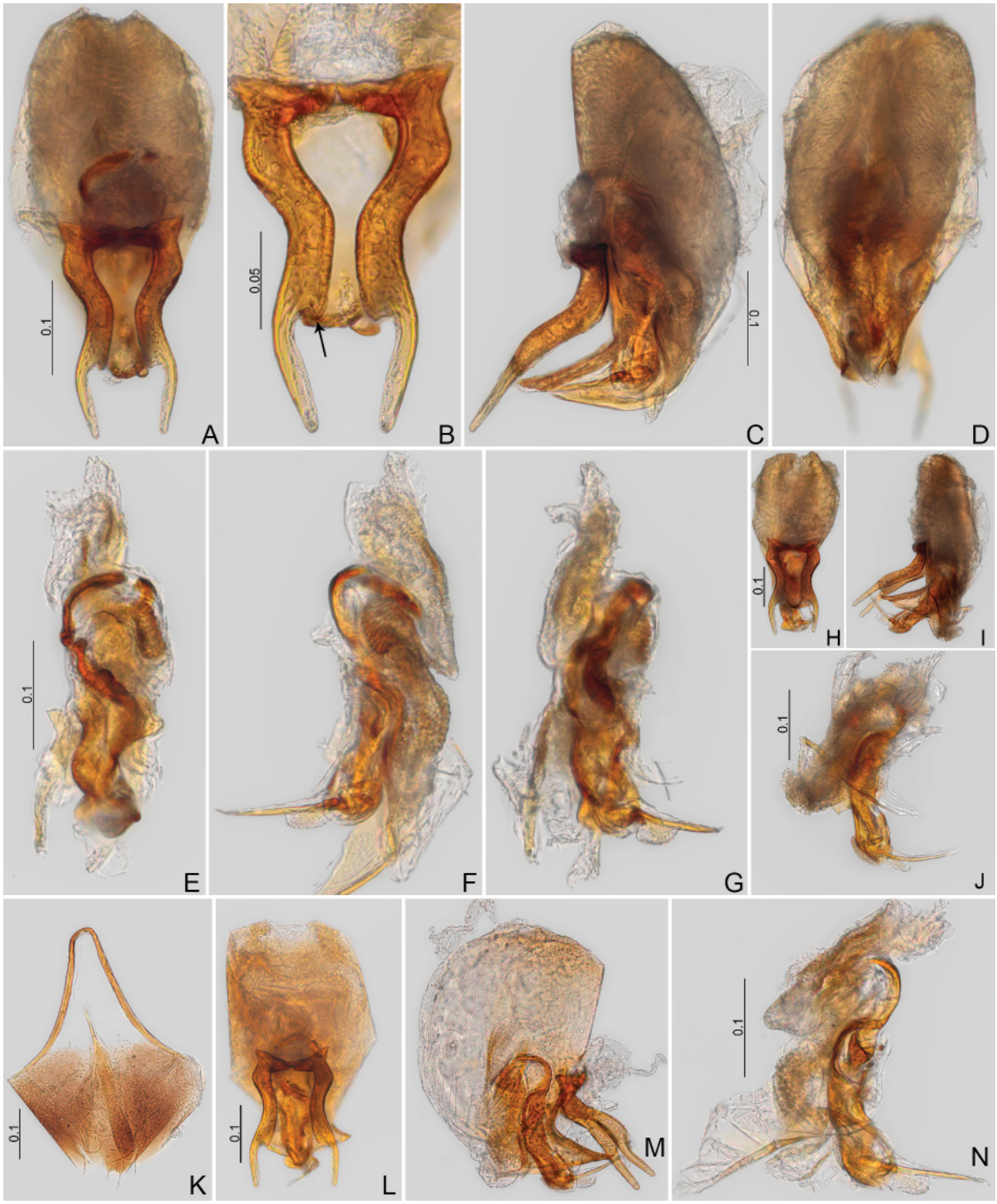

Fig. 37. *Baeocera colibri* sp. nov. (CELC). **A–G**. Paratype, ♂ (#13). **A–D**. Aedeagi. **A**. Frontal view. **B**. Parameres, frontal view, arrow: constriction. **C**. Lateral view. **D**. Dorsal view. **E–G**. Sclerite of internal sac. **E**. Frontal view. **F**. Lateral view-1. **G**. Lateral view-2. **H–J**. Paratype, ♂ (#09). **H**. Frontal view. **I**. Lateral view. **J**. Sclerite of internal sac, lateral view. **K–N**. Paratype, ♂ (#55). **K**. Tergite IX. **L**. Aedeagi, frontal view. **M**. Aedeagi, lateral view. **N**. Sclerite of internal sac, lateral view. Scales in mm.

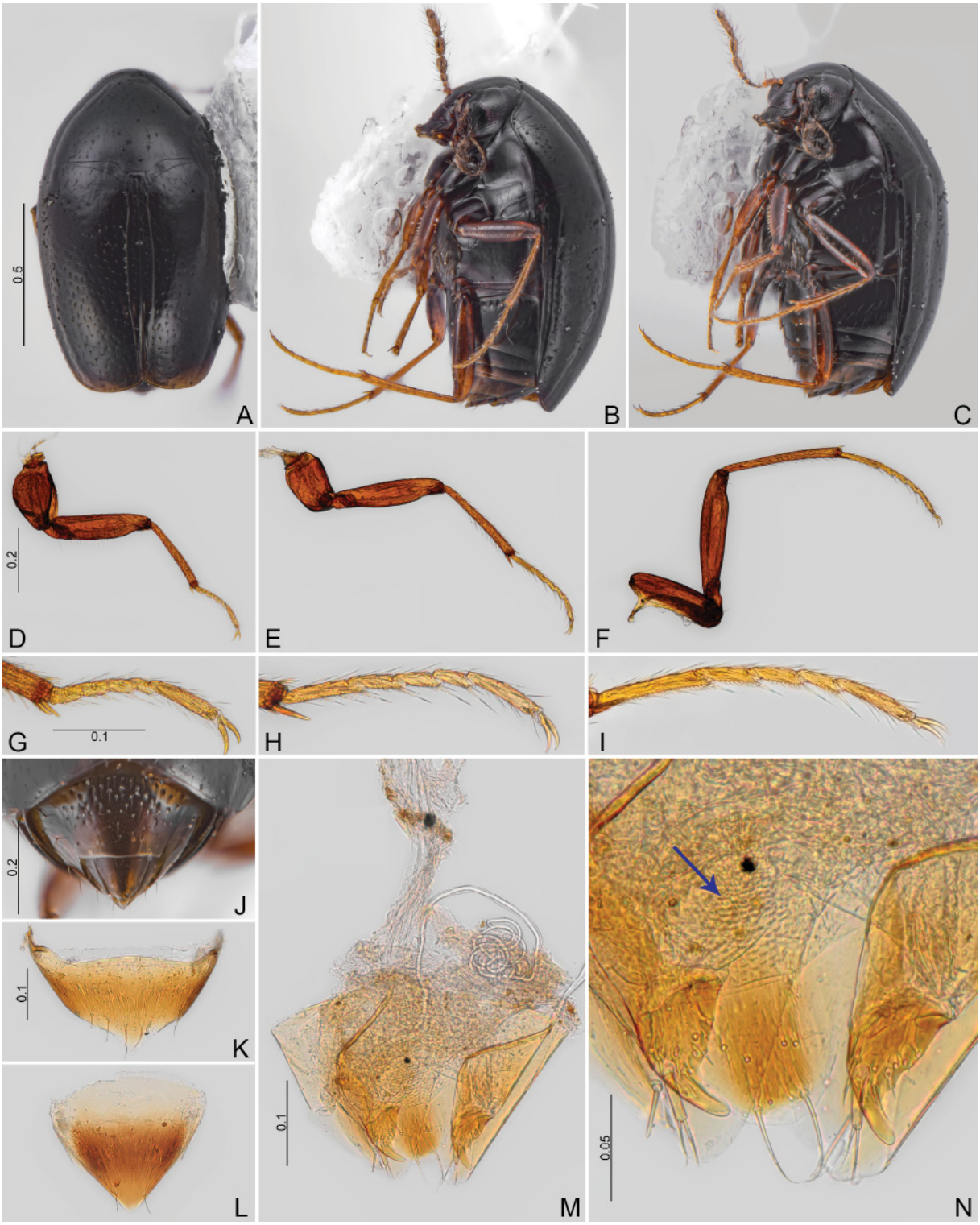

Fig. 38. *Baeocera colibri* sp. nov. (CELC). **A–C**. Paratype, ♀ (#12). **A**. Dorsal view. **B**. Lateral view. **C**. Oblique view. **D–I**. Paratype, ♀ (#16). **D–F**. Legs. **D**. Fore. **E**. Middle. **F**. Hind. **G–I**. Tibiae. **G**. Pro. **H**. Meso. **I**. Meta. **J**. Paratype, ♀ (#12), abdomen, dorsal view. **K–N**. Paratype, ♀ (#16). **K**. Sternite VIII. **L**. Tergite VIII. **M**. Genitalia. **N**. Ovipositor, arrow: sclerites. Scales in mm.

structure; terminal part of flagellum extending obliquely from main part, that resembles a hummingbird (Fig. 37E–G, J, N).

Measurements (n = 9, including holotype, unless otherwise specified; in mm). TL 1.08–1.22 (1.18 ± 0.04), SY (n = 8) 0.08–0.12 (0.11 ± 0.01), HW (n = 8) 0.30–0.35 (0.33 ± 0.02), IS (n = 8) 0.15–0.18 (0.17 ± 0.01), WA (n = 8) 0.06–0.10 (0.08 ± 0.01), PL 0.43–0.51 (0.47 ± 0.03), PA 0.33–0.39 (0.35 ± 0.02), PB 0.64–0.72 (0.68 ± 0.03), SL 0.02–0.03 (0.02 ± 0), SW (n = 8) 0.04–0.05 (0.04 ± 0), EI 0.68–0.78 (0.75 ± 0.03), EL 0.74–0.85 (0.82 ± 0.03), EW 0.34–0.40 (0.37 ± 0.02), EH 0.33–0.38 (0.36 ± 0.02), MsW 0.15–0.18 (0.17 ± 0.01), MeL 0.04–0.05 (0.04 ± 0), MeW 0.11–0.15 (0.13 ± 0.01), MB 0.09–0.12 (0.10 ± 0.01), MC 0.25–0.30 (0.28 ± 0.02), ML 0.05–0.07 (0.06 ± 0.01), VL 0.13–0.18 (0.15 ± 0.01), PrF 0.29–0.34 (0.31 ± 0.02), PrT 0.20–0.29 (0.24 ± 0.03), MsF (n = 8) 0.32–0.37 (0.35 ± 0.01), MsT 0.28–0.32 (0.30 ± 0.02), MtF 0.35–0.41 (0.39 ± 0.02), MtT 0.32–0.37 (0.35 ± 0.02).

Females (Fig. 38)

Ventrite VIII with a triangular posterior projection (Fig. 38K). Tergite VIII triangular, lacking a posterior projection (Fig. 38L). Bursa copulatrix with small sclerites (Fig. 38N). Spermatheca filiform (Fig. 38M). Distal gonocoxite triangular, robust; gonostylus elongate (Fig. 38M–N).

Measurements (n = 9, unless otherwise specified in mm). TL 1.11–1.25 (1.20 ± 0.04), SY 0.10–0.12 (0.11 ± 0.01), HW 0.32–0.36 (0.34 ± 0.01), IS 0.16–0.19 (0.17 ± 0.01), WA 0.07–0.10 (0.08 ± 0.01), PL 0.43–0.51 (0.48 ± 0.03), PA 0.35–0.38 (0.36 ± 0.01), PB 0.64–0.76 (0.70 ± 0.04), SL (n = 7) 0.02–0.03 (0.02 ± 0), SW (n = 8) 0.03–0.06 (0.04 ± 0.01), EI 0.73–0.80 (0.76 ± 0.03), EL 0.78–0.88 (0.84 ± 0.03), EW (n = 8) 0.34–0.42 (0.38 ± 0.03), EH (n = 8) 0.34–0.42 (0.37 ± 0.03), MsW 0.14–0.20 (0.17 ± 0.02), MeL 0.04–0.05 (0.04 ± 0), MeW (n = 8) 0.10–0.15 (0.13 ± 0.02), MB 0.09–0.14 (0.11 ± 0.02), MC 0.24–0.32 (0.28 ± 0.03), ML 0.04–0.06 (0.05 ± 0.01), VL 0.12–0.17 (0.15 ± 0.02), PrF (n = 8) 0.26–0.32 (0.3 ± 0.02), PrT 0.20–0.25 (0.23 ± 0.02), MsF 0.32–0.36 (0.34 ± 0.01), MsT 0.27–0.30 (0.29 ± 0.01), MtF (n = 8) 0.35–0.41 (0.38 ± 0.02), MtT 0.31–0.36 (0.35 ± 0.02).

Host

Collected from *Ceratiomyxa fruticulosa* on a fallen *Pinus* sp., *Xylodon flaviporus* (Berk. & M.A.Curtis ex Cooke) Riebesehl & Langer (Schizoporaceae), and from unknown fungi on logs (Fig. 1G).

Remarks

Similar to *B. pulga* sp. nov. and *B. bottine* sp. nov. Differs by the more robust body, the coarser and denser elytral punctures, and by the shape of the antennomeres. The male terminalia can be distinguished by the strongly sinuous parameres, which bear a distinct posterior constriction. Females are distinguished by tergite IX lacking a posterior projection, and by the less elongate distal gonocoxite.

Distribution

Mata do Paraíso and Mata da Biologia, Universidade Federal de Viçosa, campus of Viçosa, state of Minas Gerais, Southeast Brazil (Fig. 1A–D).

Baeocera pulga sp. nov.
urn:lsid:zoobank.org:act:DD0E4C47-48F1-4615-A269-D62D7A1B01D4
Figs 1A–B, G, 39–43

Diagnosis

Body length: 1.23–1.25 mm; moderately oblong. Dark brown. Antennomeres VII and VIII oblong, IX–XI distinctly larger than remaining. Mesepimeron 0.73 the width of the mesanepisternum, and 2.73 ×

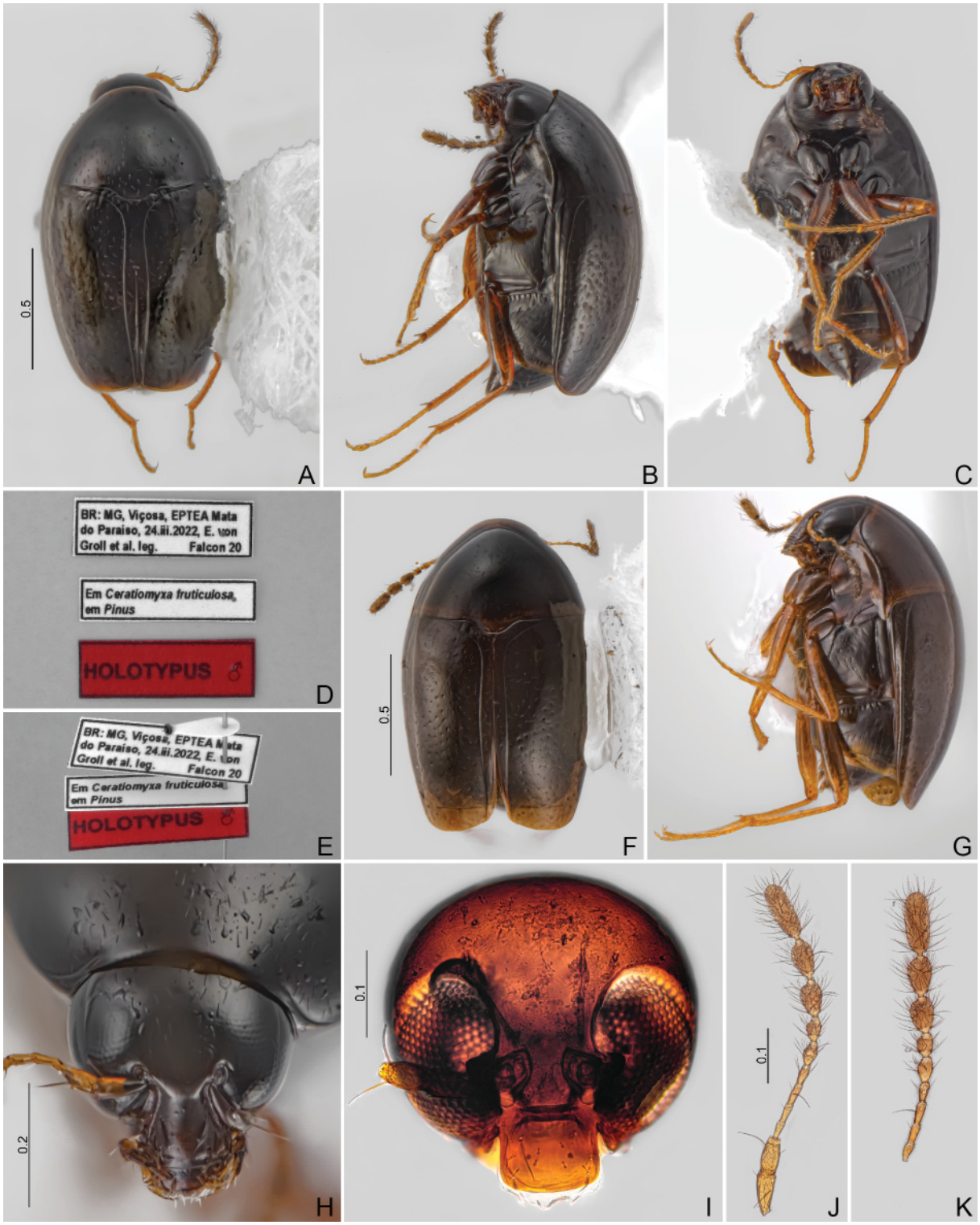

Fig. 39. *Baeocera pulga* sp. nov. (CELC). **A–E**. Holotype, ♂. **A**. Dorsal view. **B**. Lateral view. **C**. Ventral view. **D**. Labels. **E**. Pinned. **F–G**. Paratype, ♂ (#36), teneral. **F**. Dorsal view. **G**. Lateral view. **H–I**. Heads, frontal views. **H**. Holotype, ♂. **I**. Paratype, ♂ (#35). **J–K**. Antennae. **J**. Paratype, ♂ (#35). **K**. Paratype, ♀ (#57). Scales in mm.

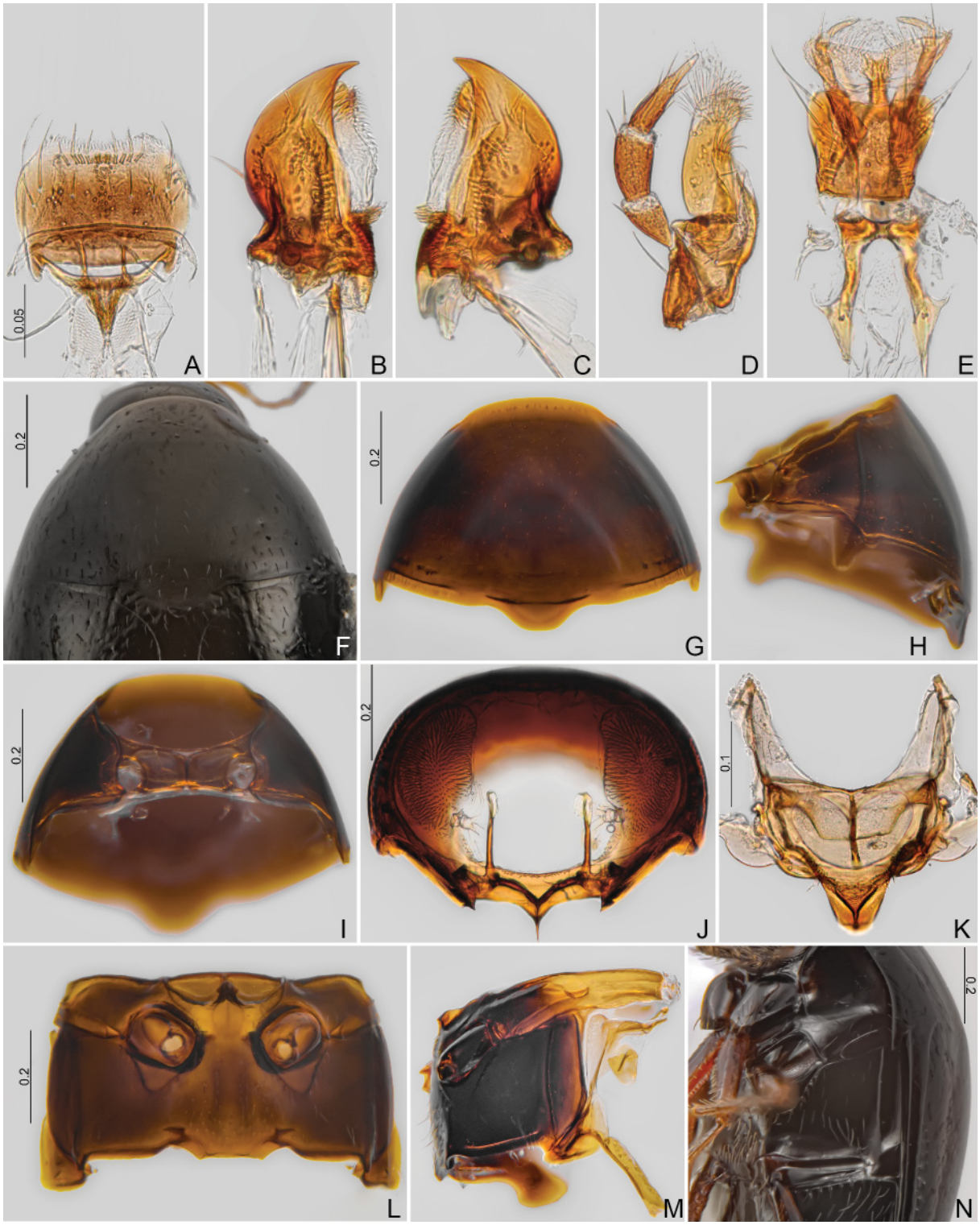

Fig. 40. *Baeocera pulga* sp. nov. (CELC). **A–E**. Paratype, ♂ (#35). **A**. Labrum. **B–C**. Mandibles. **D**. Maxilla. **E**. Labium. **F**. Holotype, ♂, prothorax, dorsal view. **G–M**. Paratype, ♂ (#35). **G–J**. Prothorax. **G**. Dorsal view. **H**. Lateral view. **I**. Ventral view. **J**. Inner view. **K**. Scutellar shield. **L–N**. Meso- and metathorax. **L**. Ventral view. **M**. Lateral view. **N**. Holotype, ♂, oblique view. Scales in mm.

as wide as long. Submesocoxal lines strongly arcuate, punctate. Basal striae connected to sutural and reaching approximately the outer ⅔ of the basal width. Aedeagus with parameres sinuous. Internal sac formed by twisted sclerites that form an elongate and just slightly curved shape; terminal part of flagellum extends at a right angle from main part, forming an 'L-shaped' structure. Tergite VIII in females with a small posterior projection. Distal gonocoxite triangular, moderately elongate.

Etymology

The species epithet is a Portuguese noun in apposition, referring to friends' humorous observations that the author studies fleas rather than beetles.

Material examined

Holotype

BRAZIL • ♂; Minas Gerais, Viçosa, EPTEA Mata do Paraíso; 24 Mar. 2022; E. von Groll *et al.* leg.; "Falcon 20 / Em *Ceratiomyxia fruticulosa* em *Pinus* / HOLOTYPUS ♂"; CELC. (Fig. 39D–E)

Paratypes

BRAZIL • 3 ♂♂ (1 ♂*, 1 ♂**); same collection data as for holotype; 10 Mar. 2022; E. von Groll *et al.* leg.; "Falcon 26 / Em *Ceratiomyxia fruticulosa* em *Pinus*"; CELC • 1 ♀*; same collection data as for holotype; "Falcon 42 / Em *Ceratiomyxia fruticulosa* em *Pinus*"; CELC.

Description

Colouration. Dark brown; clypeus, tip of elytra, and femora dark ochreous; antennomeres, mouthparts, tibiae, apex of each ventral ventrite, and tarsi yellow (Figs 39A–C, 43A–D). Variations: brown, with ochreous parts paler.

Head (Figs 39H–K, 40A–E). Frons with punctation sparse and fine. Labrum curved posteriorly (Fig. 40A). Maxillary palpomeres elongate and moderately thin (Fig. 40D). Labial palpomeres distinctly thin and curved; mentum concave posteriorly (Fig. 40E). Antennomeres VII and VIII oblong (Fig. 39J–K); antennomere proportions (n=2): I 69/32 : II 68/34 : III 33/17 : IV 36/16 : V 42/16 : VI 37/17 : VII 47/27 : VIII 45/29 : IX 69/44 : X 76/44 : XI 110/44.

Prothorax (Fig. 40F–J). Punctation sparse and very fine; pubescence sparse. Hypomeron subglabrous, impunctate (Fig. 40N). Prosternal process distinctly elongate and spinose in lateral view (Fig. 40H). Profurca thin (Fig. 40J).

Mesothorax (Fig. 40K–N). Scutellum visible in dorsal view (Fig. 40F), wider than long; tip rounded (Fig. 40K). Mesoventral lines smoothy curved; median lines closed (Fig. 40L). Mesepimeron 2.73 × as wide as long and about 0,73 × the width of the mesanepisternum (Fig. 40N). Mesoventral process with a posterior ridge in lateral view (Fig. 40M).

Metathorax (Figs 40L–N, 41A–C). Metaventrite smooth, shining, pubescence moderately sparse (Fig. 40N). Submesocoxal lines arcuate and punctate; submesocoxal area length: 0.04–0.06 mm (Fig. 40L–M). Metanepisternal suture punctate, more or less convex (Fig. 40N). Metanotum with alacrista trapezoidal-shaped; scutoscutellar suture trespassing the apodeme (Fig. 41A). Arms of metendosternite slightly ticker than stalk (Fig. 41B–C).

Wings (Figs 39A–C, F–G, 41D–F). Elytra with coarse and sparse punctures – coarser than pronotum. Basal striae connected to sutural, impunctate, and reaching approximately the outer ⅔ of the basal width (Fig. 40F). Lateral striae fine, impunctate, and curved near humeral region (Fig. 40N).

Legs. Thin, elongate, not microsculptured (Figs 41G–L, 43C–D).

Abdomen. Ventrite I with (Fig. 39C) or without (Fig. 43B) a lateral curved impression – unrelated to sex, collection date, or life stage (including teneral specimens). Submetacoxal lines coarse punctate (Figs 39B, 43B). Ventral surface shining; pubescence dense; punctures fine (Figs 39B, 43B). Propygidium dense and coarsely punctate; micropunctured; pubescence dense (Figs 42A, 43E).

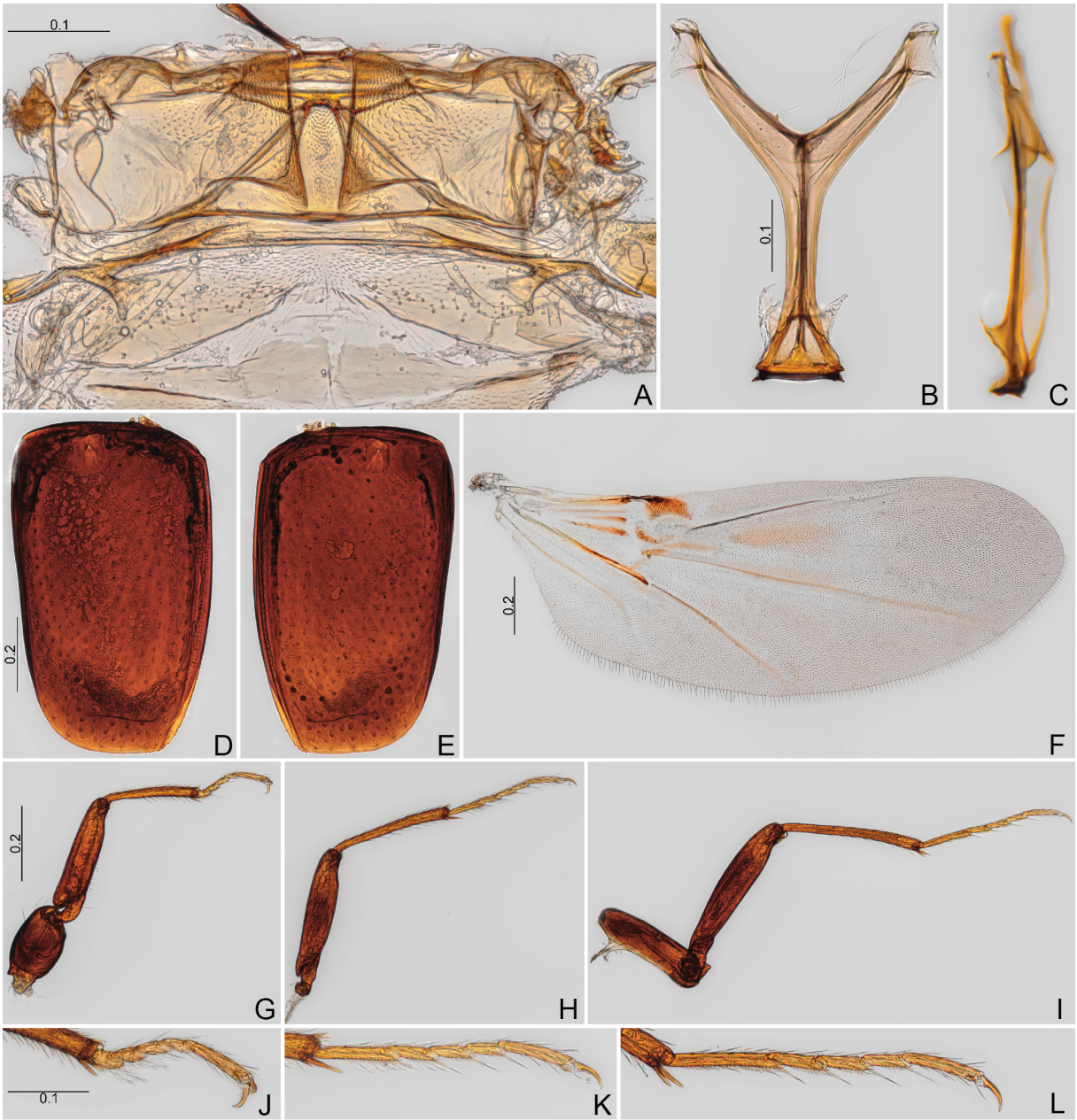

Fig. 41. *Baeocera pulga* sp. nov., paratype, ♂ (#35) (CELC). **A**. Metanotum. **B–C**. Metendosternite. **B**. Dorsal view. **C**. Lateral view. **D–E**. Elytra. **F**. Hind wing. **G–I**. Legs. **G**. Fore. **H**. Middle. **I**. Hind. **J–L**. Tibiae. **J**. Pro. **K**. Meso. **L**. Meta. Scales in mm.

Fig. 42. *Baeocera pulga* sp. nov. (CELC). **A**. Holotype, ♂, abdomen, dorsal view. **B–N**. Paratype, ♂ (#35). **B**. Sternite VIII. **C**. Tergite VIII. **D**. Tergite IX. **E**. Terminalia. **F**. Sternite IX. **G**. Tergite X. **H–K**. Aedeagi. **H**. Frontal view. **I**. Parameres, ventral view. **J**. Lateral view. **K**. Dorsal view. **L–N**. Sclerites of internal sac. **L**. Frontal view. **M**. Lateral view-1. **N**. Lateral view-2. **O–P**. Paratype, ♂ (#35), aedeagi. **O**. Frontal view. **P**. Parameres, frontal view. **Q-R**. Paratype, ♂ (#30). **Q**. Lateral view. **R**. Lateral view (sclerite). Scales in mm.

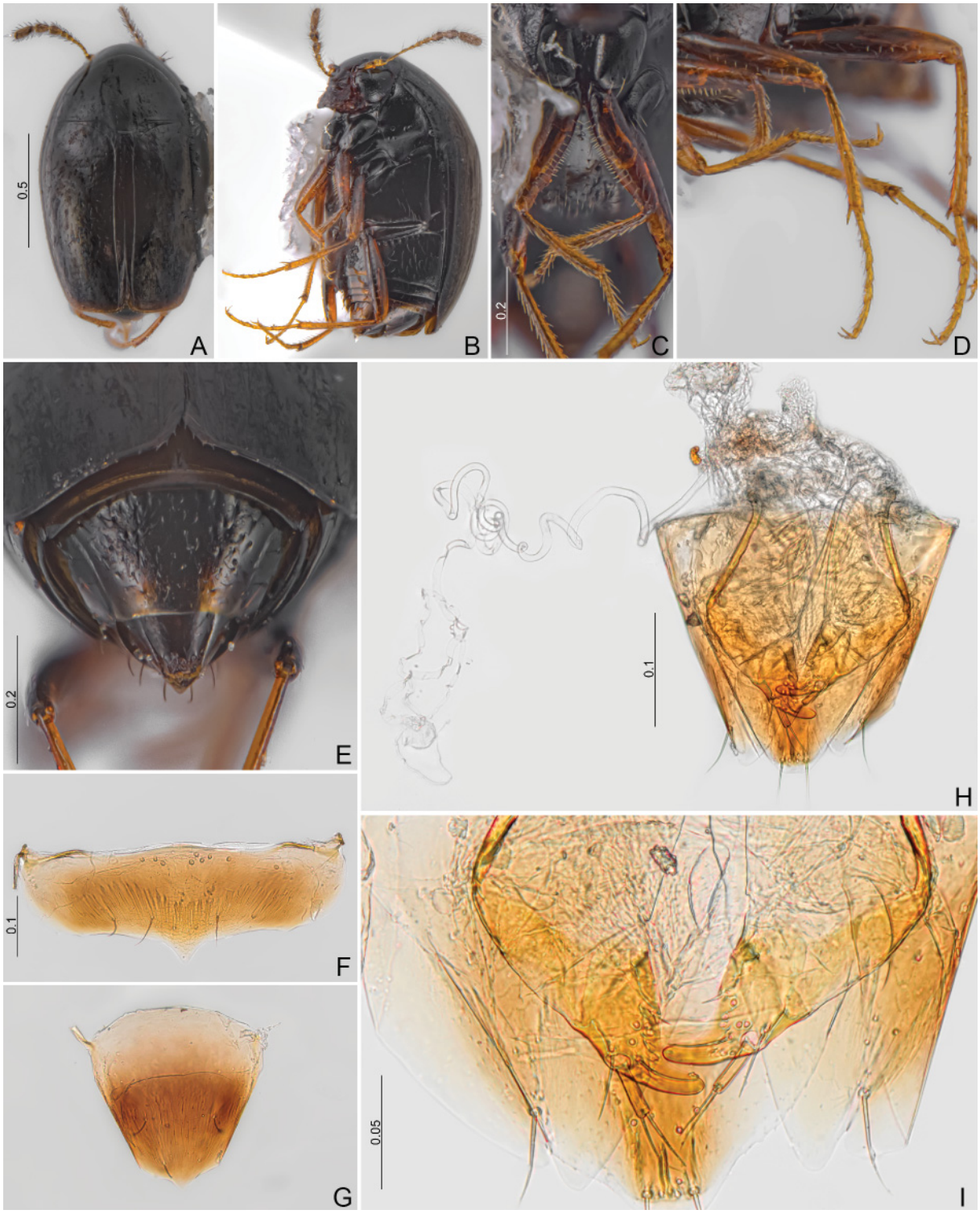

Fig. 43. *Baeocera pulga* sp. nov., paratype, ♀ (#57) (CELC). **A**. Dorsal view. **B**. Oblique view. **C**. Forelegs. **D**. Middle and hind legs. **E**. Abdomen, dorsal view. **F**. Sternite VIII. **G**. Tergite VIII. **H**. Genitalia. **I**. Ovipositor. Scales in mm.

Males

Tibiae slightly arcuate (Fig. 41G–I). Pro- and mesotarsomeres I–III widened, bearing tenent setae (Fig. 41J–L). Sternite VIII with a large triangular posterior projection (Fig. 42B). Tergite VIII triangular, lacking posterior projection (Fig. 42C). Tergite IX with curved ventral struts (Fig. 42D–E). Sternite IX somewhat acute posteriorly, elongate (Fig. 42F). Tergite X triangular, wide (Fig. 42G).

Aedeagus (Fig. 42H–R). Median lobe with basal bulb membranous, oval, and longer than apical lobe; apical lobe bent in lateral view (Fig. 42J, Q). Parameres thin and sinuous in frontal view (Fig. 42I, P). Internal sac formed by a twisted sclerite that forms an elongate and just slightly curved main structure; terminal part of flagellum extending at a right angle from main part, forming an 'L-shaped' structure (Fig. 42L–N, Q–R).

Measurements (n = 4, including holotype). TL 1.23–1.27 (1.25 ± 0.01), SY 0.10–0.11 (0.11 ± 0.01), HW 0.35–0.36 (0.35 ± 0.01), IS 0.16–0.18 (0.17 ± 0.01), WA 0.07–0.12 (0.09 ± 0.02), PL 0.51–0.55 (0.53 ± 0.02), PA 0.35–0.40 (0.37 ± 0.02), PB 0.72–0.76 (0.74 ± 0.02), SL 0.02–0.03 (0.02 ± 0.01), SW 0.04–0.05 (0.05 ± 0.01), EI 0.75–0.80 (0.78 ± 0.02), EL 0.87–0.90 (0.88 ± 0.01), EW 0.39–0.44 (0.41 ± 0.02), EH 0.32–0.38 (0.36 ± 0.03), MsW 0.19–0.20 (0.20 ± 0.01), MeL 0.03–0.05 (0.04 ± 0.01), MeW 0.14–0.15 (0.15 ± 0.01), MB 0.11–0.14 (0.13 ± 0.01), MC 0.26–0.30 (0.28 ± 0.02), ML 0.04–0.06 (0.05 ± 0.01), VL 0.16–0.17 (0.17 ± 0.01), PrF 0.31–0.32 (0.32 ± 0.01), PrT 0.23–0.25 (0.24 ± 0.01), MsF 0.34–0.35 (0.35 ± 0.01), MsT 0.28–0.32 (0.30 ± 0.02), MtF 0.39–0.41 (0.41 ± 0.01), MtT 0.32–0.37 (0.35 ± 0.02).

Female (Fig. 43)

Antennae thicker than those of the males (Fig. 39K). Sternite VIII with a triangular posterior projection (Fig. 43F). Tergite VIII elongate, bearing a small posterior triangular projection (Fig. 43G). Spermatheca filiform. Triangular distal gonocoxite; gonostylus rectangular (Fig. 43H–I).

Measurements (n = 1; in mm). TL 1.25, SY 0.12, HW 0.34, IS 0.19, WA 0.11, PL 0.50, PA 0.36, PB 0.72, SL 0.02, SW 0.04, EI 0.77, EL 0.83, EW 0.40, EH 0.36, MsW 0.20, MeL 0.04, MeW 0.14, MB 0.12, MC 0.30, ML 0.05, VL 0.15, PrF 0.30, PrT 0.25, MsF 0.34, MsT 0.30, MtF 0.40, MtT 0.38.

Host

Collected from *Ceratiomyxa fruticulosa* on a fallen *Pinus* sp. tree (Fig. 1G).

Remarks

Resembles *B. bottine* sp. nov. and *B. colibri* sp. nov. Differs from both species by the oblong antennomeres VII and VIII, and by the more elongate and thinner last labial palpomere. It differs from *B. bottine* by the more sinuous parameres in frontal view, the shorter flagellum, and the less curved sclerite of internal sac. It can be distinguished from *B. colibri* by the straighter parameres, lacking a distinct posterior constriction. Females can be distinguished by the proportions of the distal gonocoxite: not distinctly elongate as *B. bottine*, and not strongly robust as *B. colibri*.

Distribution

Mata do Paraíso, Universidade Federal de Viçosa, campus of Viçosa, state of Minas Gerais, Southeast Brazil (Fig. 1A–B).

Genus ***Scaphisoma*** Leach, 1815

Figs 2C, H, 44–64

Scaphisoma Leach, 1815: 89. Type species: *Silpha agaricina* Linnaeus, 1758; by monotypy.
Scaphosoma Agassiz, 1846: 332.
Caryoscapha Ganglbauer, 1899: 343 (as subgenus of *Scaphisoma*). Type species: *Scaphisoma limbatum* Erichson, 1945; by monotypy.

Scaphiomicrus Casey, 1900: 58. Type species: *Scaphisoma pusilla* LeConte, 1860; by original designation.
Pseudoscaphosoma Pic, 1915b: 31. Type species: *Pseudoscaphosoma testaceomaculatum* Pic, 1915; by original designation.
Scutoscaphosoma Pic, 1916a: 3 (as subgenus of *Scaphosoma*). Type species: *Scaphisoma* (*Scutoscaphosoma*) *rouyeri* Pic, 1916a; by monotypy.
Scaphella Achard, 1924: 29. Type species: *Scaphisoma antennatum* Achard, 1920; by original designation.
Macrobaeocera Pic, 1925: 195. Type species: *Scaphisoma phungi* Pic, 1922, by monotypy.
Macroscaphosoma Pic, 1928a: 33. Type species: *Macroscaphosoma collarti* Pic, 1928; by monotypy.
Mimoscaphosoma Pic, 1928b: 49 (as subgenus of *Scaphisoma*). Type species: *Scaphisoma bruchi* Pic, 1928; by original designation.
Metalloscapha Löbl, 1975a: 384. Type species: *Metalloscapha papua* Löbl, 1975; by original designation.
[*Macroscaphosoma* Löbl, 1997: xi. Type species *Macroscaphosoma collarti* Pic, 1928 (credited to Löbl 1970)].

Scaphisoma, with approximately 800 species, is the largest genus of Scaphidiinae. However, it is likely that this number, as with other Scaphidiinae genera, is still underestimated, especially in Brazil. The Brazilian fauna comprises only seven known species – a number that is now understood (pers. obs.) to be substantially divergent from reality. With continued research on Scaphidiinae, this number should increase exponentially.. To exemplify, in less than 30 short field trips it was possible to collect more than 500 specimens; and about 200 still need to be studied.

General description (* = variable characters within the genera, but not variable in the species below; Löbl & Leschen 2003b; Leschen & Löbl 2005)

Head. Labral setae simple* (Fig. 45E). Mandible unidentate; lacking serrations* (Fig. 45F–G). Maxillary palp normal; galea wide, with radulate brush; lacinia with basal setae (Fig. 45H). Setae on adoral surface of hypopharynx setose; last labial palpomere curved and thick (Fig. 45I). Eyes notched*. Antennomere III short and triangular (Fig. 2C). Gular pores present*. Frontoclypeal suture present (Fig. 45A).

Prothorax. Prepectus present. Hypomeron visible in lateral view; extending beyond pronotum* (Fig. 44B). Prothoracic angle acute. Prothoracic corbiculum absent (Fig. 46B).

Mesothorax. Mesoventral process paxillate (Fig. 46E). Scutellum tip exposed*. Mesoventral lines not connecting to mesocoxal cavity. Mesepimeron exposed* (Fig. 45J). Meso- and metaventrite fused (Fig. 46D).

Metathorax. Metepimeron and metanepisternum exposed; metepimeral lines impunctate (Fig. 46F). Intercoxal plates absent. Metacoxal process digitate. Metaventral setose patch absent*.

Wings. Lateral striae present. Elytral apical serration present (Fig. 47H). Hind wings developed (Fig. 46L).

Legs. Profemoral ctenidium present (Fig. 2H, 44C). Mesotibiae with two apical spines.

Abdomen. Submetacoxal lines punctate* (Fig. 47G). Membranes of abdominal ventrites lacking brick-wall pattern.

Scaphisoma hilarum sp. nov.
urn:lsid:zoobank.org:act:2467E5AF-9F4A-49B8-926C-C6027AA689B8
Figs 1A–B, E–F, 44–49, 94C–D

Diagnosis

Body length: 1.25–1.41 mm. Blackish. Each elytron with a large dark ochreous macula, near apex yellow. Basal striae absent; adsutural area notably widened and not angulate anteriorly. Clypeus, coxae, femora, metaventrite, and abdomen with strigulate microsculpture. Aedeagus with trifid apex. Females with distal gonocoxite thick.

Fig. 44. *Scaphisoma hilarum* sp. nov. (CELC). **A–E**. Holotype, ♂. **A**. Dorsal view. **B**. Lateral view. **C**. ventral view. **D**. Labels. **E**. Pinned. **F–G**. Paratype, ♂ (#37). **F**. Dorsal view. **G**. Lateral view. **H–J**. Paratype, ♂ (#40). **H**. Dorsal view. **I**. Lateral view. **J**. Ventral view. Scales in mm.

Etymology

The species epithet is a Latin word meaning ‘cheerful’, ‘merry’, referring to its merry colouration.

Material examined

Holotype

BRAZIL • ♂; Minas Gerais, Viçosa, UFV, Vila Gianetti; 24 Mar. 2022; E. von Groll leg.; “Falcon 43 / Em *Inonotus* sp. (Hymenochaetaceae) / HOLOTYPUS ♂”; CELC. (Fig. 44D–E)

Fig. 45. *Scaphisoma hilarum* sp. nov. (CELC). **A**. Holotype, ♂, head, frontal view. **B**. Paratype, ♂ (#58), head, frontal view. **C–D**. Antennae. **C**. Paratype, ♂ (#58). **D**. Paratype, ♀ (#55). **E–I**. Paratype, ♂ (#58). **E**. Labrum. **F–G**. Mandibles. **H**. Maxilla. **I**. Labium. **J**. Holotype, ♂, prothorax, dorsal view. **K–L**. Paratype, ♂ (#58), prothorax. **K**. Dorsal view. **L**. Lateral view. Abbreviation: pp = prosternal process. Scales in mm.

Paratypes

BRAZIL • 2 ♂♂; 1 ♀ (1 ♂*); same collection data as for holotype; 10 Mar. 2022; E. von Groll leg.; "Falcon 36/ Em *Inonotus* sp. (Hymenochaetaceae)"; CELC • 2 ♂♂; 3 ♀♀; same collection data as for holotype; 10 Mar. 2022; E. von Groll leg.; "Falcon 42 / Em *Inonotus* sp. (Hymenochaetaceae)"; CELC • 3 ♂♂, 1 ♀; same collection data as for holotype; 23 Mar. 2022; E. von Groll leg.; "Falcon 42 / Em *Inonotus* sp. (Hymenochaetaceae)"; CELC • 1 ♂, 2 ♀♀ (1 ♀*); same collection data as for holotype; 23 Mar. 2022; E. von Groll leg.; "Falcon 36 / Em *Inonotus* sp. (Hymenochaetaceae)"; CELC • 4 ♂♂, 1 ex. (1 ♂*, 1 ♂**); same collection data as for holotype; 24 Mar. 2022; E. von Groll leg.; Falcon 43; CELC • 1 ♀; same collection data as for holotype; 25 Mar. 2022; E. von Groll leg.; "Falcon 29 / Em *Inonotus* sp. (Hymenochaetaceae)"; CELC • 2 ♂♂; 1 ♀; same collection data as for holotype; 1 Apr. 2022; "Falcon 03 / Em *Inonotus* sp."; CELC • 1 ♂, 1 ex.; same collection data as for holotype; 1 Apr. 2022; E. von Groll leg.; "Falcon 26 / Em *Inonotus* sp."; CELC • 10 ♂♂, 17 ♀♀, 3 ex. (1 ♂*); same collection data as for holotype; 26 Apr. 2022; E. von Groll leg.; "/ Em *Inonotus* sp."; CELC.

Description

Colouration. Blackish; each elytron with a large dark reddish-ochreous macula, apex yellow; head, thoracic ventrites, and abdominal ventrite I dark ochreous-brown; legs, mouthparts, and apex of abdominal ventrites II–VII light ochreous (Figs 44A–C, 45A). Variations: (1) paler tonalities (Fig. 44F–G); (2) elytral macula absent (Fig. 44H–J).

Head (Fig. 45A–I). Wide (0.41–0.45 mm); punctures very fine; pubescence moderately sparse. Clypeus transverse microsculptured (Fig. 45A–B). Labrum shallowly concave posteriorly (Fig. 45E). Last labial palpomere not strongly curved; mentum practically square-shaped (Fig. 45I). Antennomeres VII–IX wide (Fig. 45C–D); antennomere proportions (n = 3): I 81/46 : II 68/39 : III 25/16 : IV 40/14 : V 64/17 : VI 71/21 : VII 90/33 : VIII 62/25 : IX 82/31 : X 84/29 : XI 117/35.

Prothorax (Figs 45J–L, 46A–B). Not microsculptured. Pronotum shining; punctures coarse, more visible near posterior bead; pubescence short and moderately dense (Fig. 45J). Hypomeron shining, glabrous; prothoracic angle extending about 2 × mesepimeron length beyond anapleural line (Fig. 44B, G, I). Prosternal process arcuate (Fig. 45L). Profurca with robust and slightly curved stalk (Fig. 45B).

Mesothorax (Fig. 46C–F). Visible part of scutellum with length similar to width; tip acute (Figs 45J, 46C). Mesanepisternum moderately coarse punctate, densely pubescent (Fig. 46F). Mesepimeron about 4.20 × as wide as long (Fig. 46E–F). Procoxal rests wider than long; mesoventral lines coarse punctate; secondary lines absent (Fig. 46D). Mesoventral process with similar length sides in lateral view (Fig. 46E).

Metathorax (Fig. 46D–I). Metaventrite with strigulate microsculpture, finely punctate, and densely pubescent (Fig. 46F). Submesocoxal lines slightly arcuate, punctate; submesocoxal area length: 0.03–0.05 mm (Fig. 46D–F). Metanepisternum and metepimeron shining, bearing fine and dense pubescence (Fig. 46F). Metanotum alacrista longer than wide (Fig. 46G). Metendosternite with arms somewhat oblong (Fig. 46H–I).

Wings (Figs 44A–C, 46J–L). Elytra elongate, narrowed posteriorly, coarse punctate – coarser than pronotum –, and moderately pubescent; lateral contours arcuate. Lateral ridge visible in dorsal view. Sutural stria strongly widened and not curved anteriorly; adsutural area wider anteriorly; basal stria absent (Fig. 44A). Lateral stria not curving at humeral area (Fig. 44B).

Legs. Femora with strigulate microsculpture (Fig. 44C). Metafemora fusiform (Figs 47A–C, 49D–F).

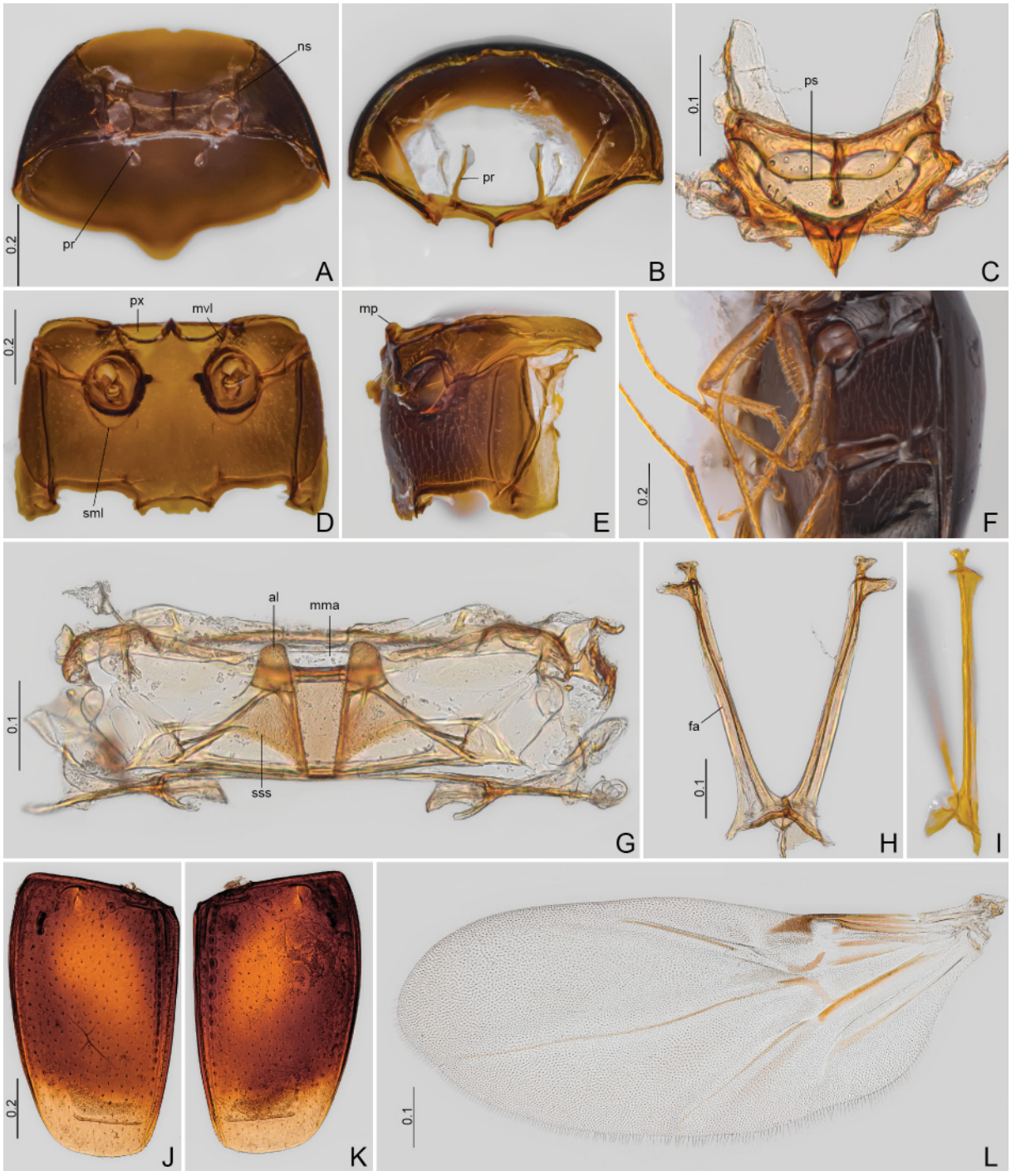

Fig. 46. *Scaphisoma hilarum* sp. nov. (CELC). **A–E**. Paratype, ♂ (#58). **A–B**. Prothorax. **A**. Ventral view. **B**. Inner view. **C**. Scutellar shield. **D–E**. Meso- and metathorax. **D**. Ventral view. **E**. Lateral view. **F**. Holotype, ♂, oblique view. **G–L**. Paratype, ♂ (#58). **G**. Metanotum. **H–I**. Metendosternite. **H**. Dorsal view. **I**. Lateral view. **J–K**. Elytra. **L**. Hind wing. Abbreviations: al = alacrista; fa = furcal arm; mma = median membranous area; mp = mesoventral process; mvl = mesoventral line; ns = notosternal suture; pr = profurca; ps = prescutellar line; px = procoxal rest; sml = submesocoxal line; sss = scutoscutellar suture. Scales in mm.

Abdomen. Strigulate microsculptured (Figs 47G–H, 49J). Ventrite I with finely punctate and densely pubescent (Fig. 44B). Submetacoxal lines arcuate, punctate; submetacoxal area length = 0.07–0.10 mm (Fig. 47G). Tergite VI sparsely and finely punctate; pubescence sparse (Figs 47H, 49J).

Males

Pre- and mesotarsomeres I–III enlarged, with tenent setae (absent in mesotarsomere I) (Fig. 47D–F). Sternite and tergite VIII strigulate microsculptured. Sternite VIII with a shallow triangular projection (Fig. 47I). Tergite VIII straight posteriorly (Fig. 47J). Tergite IX with short-angled ventral struts (Fig. 47K). Sternite IX very elongate, fusiform (Fig. 47K). Tergite X triangular (Fig. 47L).

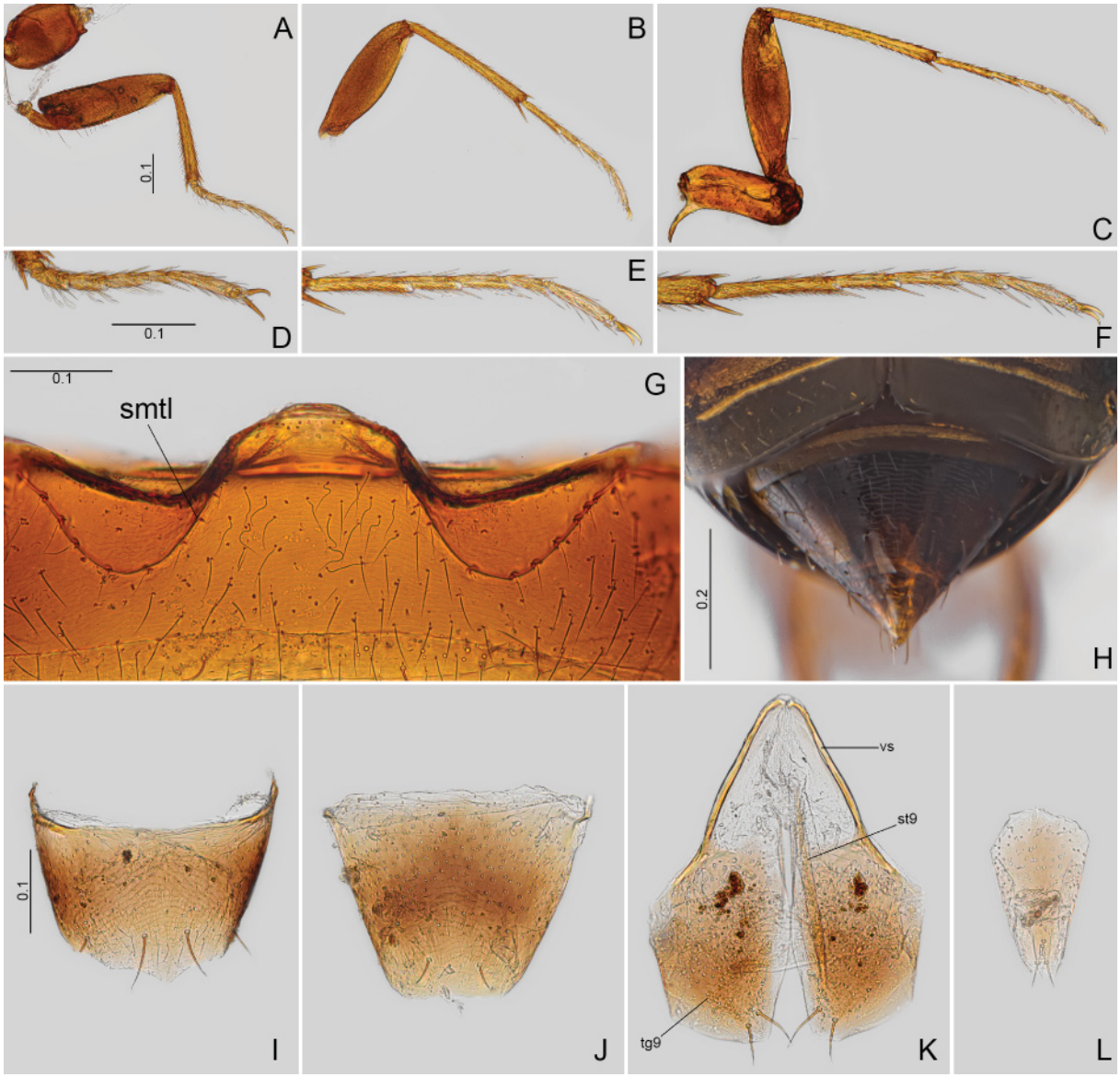

Fig. 47. *Scaphisoma hilarum* sp. nov. (CELC). **A–G**. Paratype, ♂ (#58). **A–C**. Legs. **A**. Fore. **B**. Middle. **C**. Hind. **D–F**. Tibiae. **D**. Pro. **E**. Meso. **F**. Meta. **G**. Ventrite. **H**. Holotype, ♂, abdomen, dorsal view. **I–L**. Paratype, ♂ (#58). **I**. Sternite VIII. **J**. Tergite VIII. **K**. Tergite IX. **L**. Tergite X. Abbreviations: smtl = submetacoxal line; st9 = sternite IX; tg9 = tergite IX; vs = ventral struts. Scales in mm.

Aedeagus (Fig. 48A–J). Median lobe poorly sclerotized; basal bulb oval (when inflate) and longer than apical lobe; apical lobe slightly curved in lateral view (Fig. 48C). Parameres more sclerotized near basal bulb, elongate, and narrowed apically. Internal sac with symmetrical sclerites; sclerite with an apical forceps-shaped structure that connects to aedeagus apex, forming a tripartite apex – this structure can be more or less closed.

Measurements (n=8, including holotype, unless otherwise specified; in mm; *=invariant). TL 1.25–1.41 (1.31±0.05), SY 0.16–0.20 (0.19±0.02), HW 0.41–0.45 (0.42±0.01), IS 0.18–0.23 (0.20±0.01), WA 0.11–0.16 (0.14±0.02), PL 0.50–0.55 (0.53±0.02), PA 0.45–0.51 (0.49±0.03), PB 0.74–0.88 (0.82±0.04), SL (n=4) 0.02*, SW (n=4) 0.01–0.02 (0.02±0.01), EI 0.75–0.86 (0.80±0.04), EL 0.86–0.99 (0.91±0.04), EW 0.40–0.50 (0.44±0.03), EH 0.28–0.36 (0.32±0.02), Me 0.17–0.23 (0.20±0.02), MeL 0.10–0.14 (0.12±0.01), MeW 0.02–0.04 (0.03±0.01), MB 0.14–0.20 (0.16±0.02), MC 0.34–0.40 (0.37±0.02), ML 0.03–0.05 (0.04±0.01), MA 0.06–0.10 (0.08±0.02), MA2 0.12–0.15 (0.13±0.01),

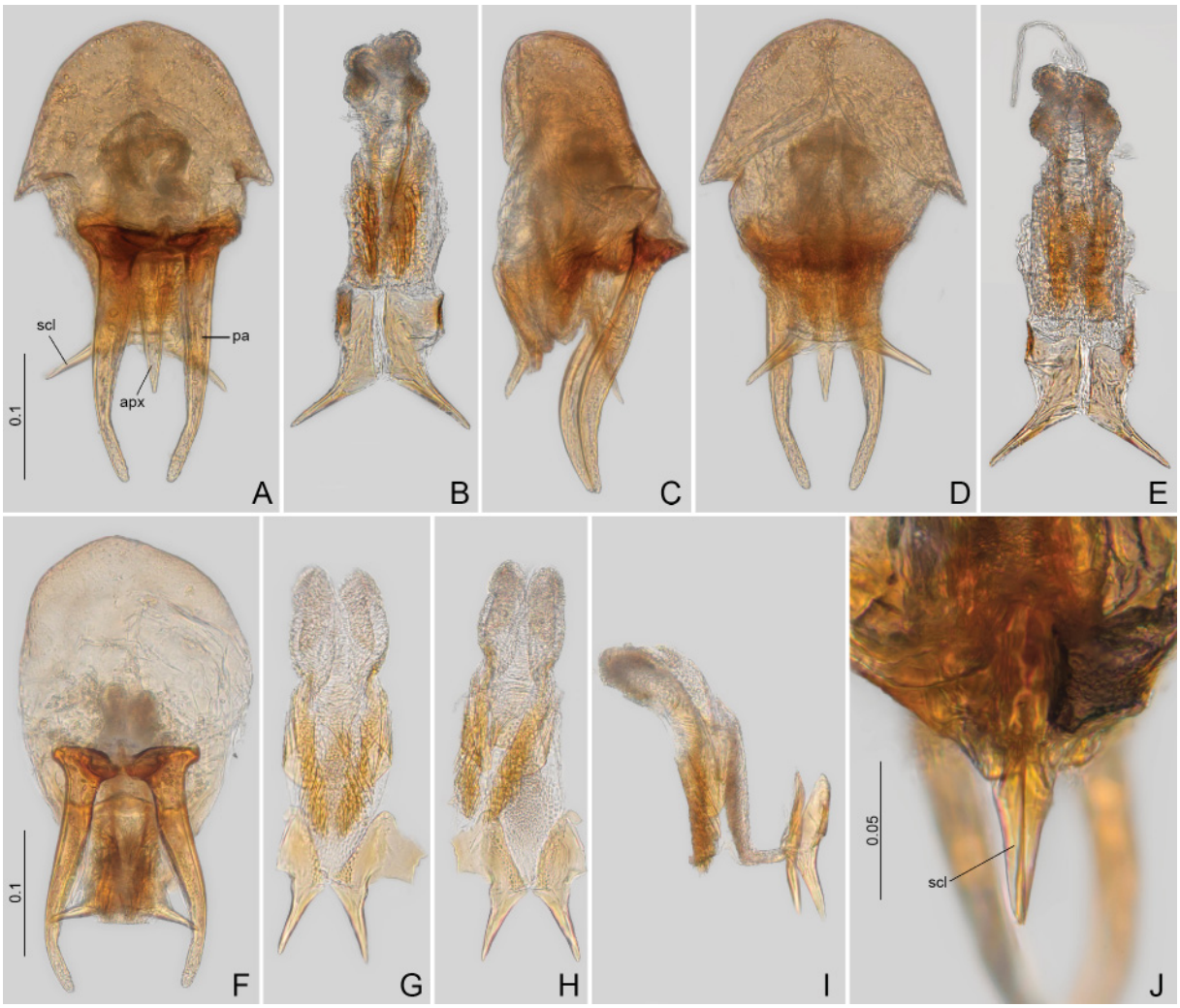

Fig. 48. *Scaphisoma hilarum* sp. nov., aedeagus (CELC). **A–E**. Paratype, ♂ (#58). **A**. Frontal view. **B**. Sclerite of internal sac, frontal view. **C**. Lateral view. **D**. Dorsal view. **E**. Sclerite of internal sac, dorsal view. **F–I**. Paratype, ♂ (#57). **F**. Frontal view. **G–J**. Sclerite of internal sac. **G**. Frontal view. **H**. Doral view. **I**. Lateral view. **J**. Paratype, ♂ (#16), dorsal view. Abbreviations: apx=apex of aedeagi; pa=parameres; scl=sclerite of internal sac. Scales in mm.

Fig. 49. *Scaphisoma hilarum* sp. nov. (CELC). **A–C**. Paratype, ♀ (#13). **A**. Dorsal view. **B**. Lateral view. **C**. Ventral view. **D–I**. Paratype, ♀ (#55). **D–F**. Legs. **D**. Fore. **E**. Middle. **F**. Hind. **G–I**. Tarsi. **G**. Pro. **H**. Meso. **I**. Meta. **J**. Paratype, ♀ (#13), abdomen, dorsal view. **K–N**. Paratype, ♀ (#55). **K**. Sternite VIII. **L**. Tergite VIII. **M**. Genitalia. **N**. Ovipositor. Abbreviations: dg = distal gonocoxites; gs = gonostyli. Scales in mm.

VL 0.23–0.27 (0.25±0.01), VL2 0.24–0.28 (0.26±0.01), PrF 0.34–0.35 (0.35±0), PrT 0.23–0.26 (0.25±0.01), MsF 0.34–0.36 (0.35±0.01), MsT 0.30–0.36 (0.33±0.02), MtF 0.40–0.46 (0.43±0.02), MtT 0.40–0.46 (0.43±0.02).

Females (Fig. 49)
Ventrite VIII slightly convex posteriorly (Fig. 49K). Tergite VIII shallowly concave, posteriorly (Fig. 49L). Distal gonocoxite thick, slightly curved; gonostylus fusiform (Fig. 49M–N).

Measurements (n=8, unless otherwise specified; in mm; *=invariant). TL 1.25–1.41 (1.32±0.05), SY 0.17–0.20 (0.18±0.01), HW 0.42–0.45 (0.43±0.01), IS 0.20–0.22 (0.21±0.01), WA 0.12–0.16 (0.14±0.01), PL 0.46–0.55 (0.52±0.03), PA 0.45–0.54 (0.50±0.03), PB 0.75–0.85 (0.81±0.03), SL (n=2) 0.02*, SW (n=2) 0.02–0.03 (0.03±0.01), EI 0.76–0.89 (0.81±0.04), EL 0.84–0.94 (0.90±0.04), EW 0.44–0.46 (0.45±0.01), EH 0.27–0.33 (0.31±0.03), Me 0.18–0.22 (0.20±0.01), MeL 0.09–0.13 (0.10±0.02), MeW 0.03–0.04 (0.03±0), MB 0.15–0.19 (0.17±0.01), MC 0.33–0.38 (0.35±0.02), ML 0.03–0.05 (0.04±0), MA 0.07–0.08 (0.07±0.01), MA2 0.12–0.16 (0.14±0.01), VL 0.22–0.26 (0.24±0.01), VL2 (n=7) 0.24–0.27 (0.26±0.01), PrF 0.32–0.37 (0.35±0.01), PrT 0.24–0.27 (0.25±0.01), MsF 0.34–0.37 (0.35±0.01), MsT 0.29–0.34 (0.32±0.02), MtF 0.40–0.44 (0.41±0.02), MtT 0.40–0.44 (0.42±0.01).

Host

Collected from *Inonotus* sp. (Hymenochaetaceae) (Figs 1A–B, E–F, 94A–D).

Remarks

The species belongs to the *S. haemorrhoidale* group (Löbl 1970), being more similar in size and aedeagus shape to *S. jacobsoni* Löbl, 1975b. However, it differs by the rather widened adsutural area and the sutural striae not angulate anteriorly. It is also similar to *S. jacqi* Löbl & Ramage, 2022 (Ramage & Löbl 2022), differing by the angle of the sutural striae, and by strigulate microsculpture of the metaventrite, absent in *S. jacqi*.

Distribution

Universidade Federal de Viçosa, campus of Viçosa, state of Minas Gerais, Southeast Brazil (Figs 1A–B, E–F).

Scaphisoma infinitum sp. nov.

urn:lsid:zoobank.org:act:5AC7D322-BA4B-4282-A157-B8B772D51C4B
Figs 1A–D, 50–54, 93F–J

Diagnosis

Body length: 1.09–1.36 mm. Brown to dark brown. Very shining, lacking microsculpture. Antennomere IX elongate. Submesocoxal lines slightly arcuate and punctate. Basal stria absent; sutural striae curved anteriorly. Aedeagus distinctly small; apical elongate and triangular; sclerite of internal sac simple. Distal gonocoxite in females elongate.

Etymology

The species epithet is a Latin word meaning ‘endless’, due to the large number of beetles that have been collected.

Material examined

Holotype
BRAZIL • ♂; Minas Gerais, Viçosa, Mata da Biologia; 23 Nov. 2021; E. von Groll and G.L.N. Martins leg.; “/ Em fungo branco ressupinado no tronco caído / HOLOTYPUS ♂”; CELC. (Fig. 50D–E)

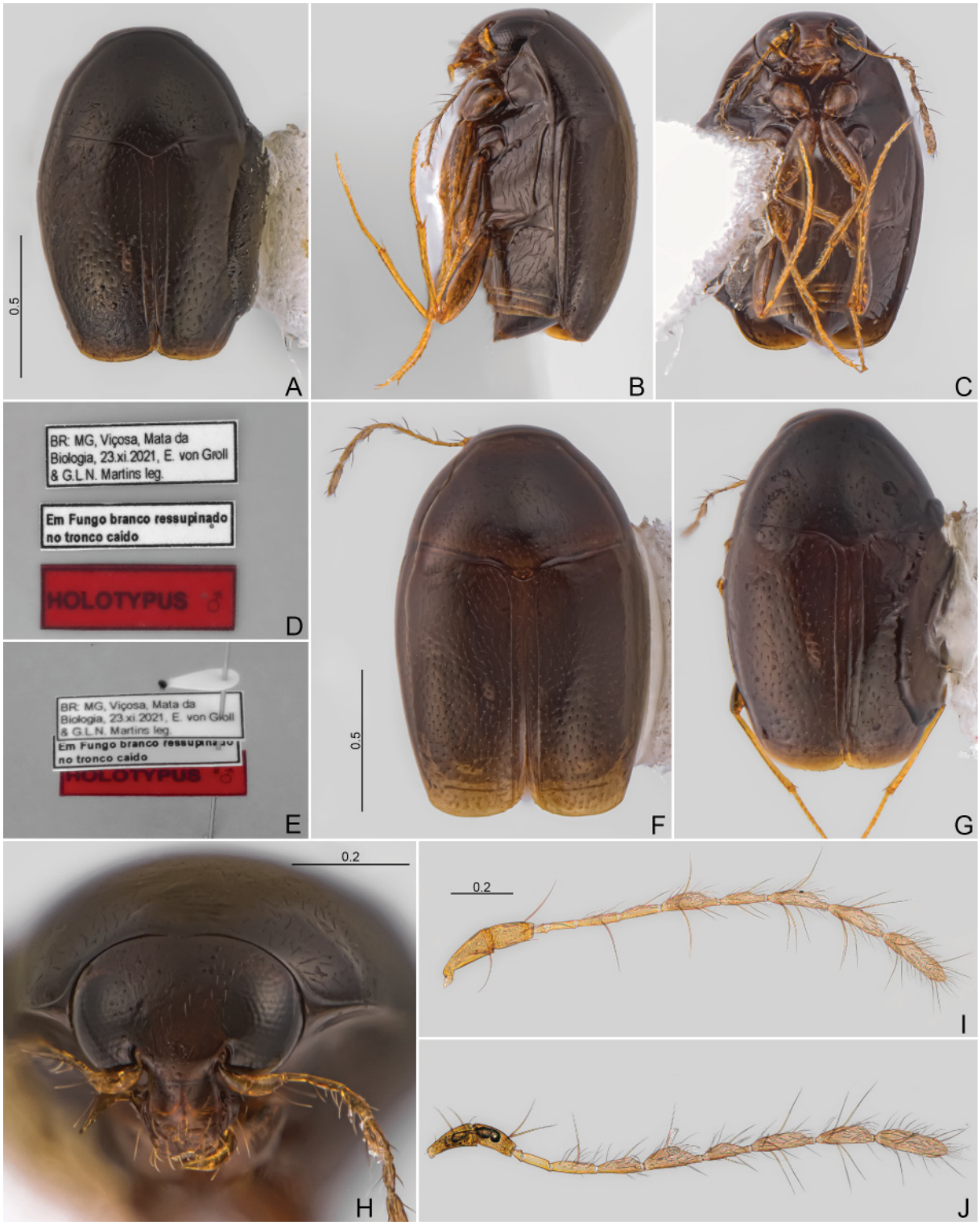

Fig. 50. *Scaphisoma infinitum* sp. nov. (CELC). **A–E**. Holotype, ♂. **A**. Dorsal view. **B**. Lateral view. **C**. Ventral view. **D**. Labels. **E**. Pinned. **F**. Paratype (#50), dorsal view. **G**. Paratype, ♀ (#55), dorsal view. **H**. Holotype, ♂, head, frontal view. **I–J**. Antennae. **I**. Paratype, ♂ (#54). **J**. Paratype, ♀ (#07). Scales in mm.

Paratypes

BRAZIL • 3 ♂♂, 3 ex. (1 ♂*); same collection data as for holotype; EPTEA Mata do Paraíso; 12 Nov. 2019; LabCol leg.; "Fungo 02 / Em fungo branco ressupinado em tronco indet."; CELC • 2 ♂♂, 4 ♀♀, 2 ex. (1 ♀*); same collection data as for holotype; EPTEA Mata do Paraíso; 12 Nov. 2019; LabCol leg.; "Fungo 10 / Em *Ceratiomyxa fruticulosa*"; CELC • 12 ♂♂, 8 ♀♀, 2 ex. (1 ♂*, 1 ♂**, 2 ♀♀**); same collection data as for holotype; 13 Nov. 2019; E. von Groll *et al.* leg.; "Fungo 16 / Em fungo amarelado ressupinado em tronco caído indet."; CELC • 25 ♂♂, 18 ♀♀, 12 ex. (5 ♂♂**, 1 ♀**); same collection data as for holotype; EPTEA Mata do Paraíso; 14 Nov. 2019; LabCol leg.; "Fungo 07 / Em fungo branco ressupinado em tronco indet."; CELC • 3 ♂♂, 1 ♀, 1 ex. (1 ♂*); same collection data as for holotype; EPTEA Mata do Paraíso; 14. Nov. 2019; LabCol leg.; "Fungo 13 / Em fungo ressupinado indet. no tronco caído e em *Ceratiomyxa fruticulosa* no solo"; CELC • 8 ♂♂, 17 ♀♀, 3 ex. (2 ♂♂**, 2 ♀♀**); same collection data as for holotype; EPTEA Mata do Paraíso; 14. Nov. 2019; LabCol leg.; "Fungo 23 / Em fungo branco ressupinado em tronco indet."; CELC • 2 ♂♂, 3 ♀♀, 2 ex. (1 ♂*); same collection data as for holotype; 20 Nov. 2019; E. von Groll *et al.* leg.; "Fungo 31 / Em fungo amarelado ressupinado em tronco caído indet."; CELC • 9 ♂♂, 4 ♀♀, 3 ex. (1 ♂*); same collection data as for holotype; 20 Nov. 2019; E. von Groll *et al.* leg.; "Fungo 20 / Em fungo branco ressupinado em tronco indet."; CELC • 3 ♂♂, 4 ♀♀, 3 ex. (1 ♂*); same collection data as for holotype; EPTEA Mata do Paraíso; 26 Nov. 2019; LabCol leg.; "Fungo 27 / Em fungo branco ressupinado em tronco indet."; CELC • 17 ♂♂, 10 ♀♀, 13 ex. (1 ♂*, 1 ♀*, 1 ♂**); same collection data as for holotype; 23 Nov. 2021; E. von Groll and G.L.N. Martins leg.; "/ Em fungo branco ressupinado no tronco caído"; CELC.

Description

Colouration. Dark brown. Antennae, mouthparts, legs, tip of elytra, and abdominal ventrites II–VI yellow (Fig. 50A–B, H). Variations: (1) light brown (Fig. 50F); (2) medium brown; (3) pronotum darker than elytra (Fig. 50G).

Head (Figs 50H–J, 51A–E). Punctation fine, sparse; pubescence sparse (Fig. 50H). Labrum conspicuously concave posteriorly (Fig. 51A). Last maxillary palpomere elongate, about 6× as long as wide (Fig. 51D). Last labial palpomere strongly curved; posterior-lateral sides of mentum concave (Fig. 51E). Antennomeres VIII–XI elongate; antennomere proportions (n=3): I 83/40 : II 70/36 : III 23/17 : IV 48/14 : V 72/18 : VI 71/21 : VII 96/30 : VIII 79/21 : IX 99/25 : X 97/27 : XI 124/30.

Prothorax (Fig. 51F–J). Pronotum lacking microsculpture; punctures dense and moderately coarse; pubescence fine and short. Hypomeron shining, glabrous; posterior angle not extending significantly beyond anapleural line (Fig. 52B). Prosternal process thick (Fig. 51H). Membranous part of profurca almost rounded (Fig. 51J).

Mesothorax (Fig. 51K–N). Visible part of scutellum longer than wide (Fig. 51F); scutellar lines rising laterally; tip acute (Fig. 51K). Mesepimeron about 3.70× as wide as long (Fig. 51N). Mesoventral lines not curved; punctate; secondary lines absent; median lines short, opened (Fig. 51L). Mesoventral process elongate in lateral view (Fig. 51M).

Metathorax (Figs 51L–N, 52A–C). Metaventrite smooth, punctures fine and sparse; pubescence moderately long (Fig. 51N). Submesocoxal lines slightly arcuate; punctate; submesocoxal area length about 0.04 mm (Fig. 51L–N). Metendosternite arms straight, forming an acute V-shape (<40°). (Fig. 52B–C).

Wings (Figs 50A–C, 52D–F). Elytra not strongly narrowed apically; punctures coarser than pronotum, pubescence sparse and short. Sutural stria curved near base; basal stria absent (Fig. 51F). Lateral stria slightly curving at humeral area (Fig. 50B).

Legs. Lacking microsculpture (Figs 52G–L, 54D–I).

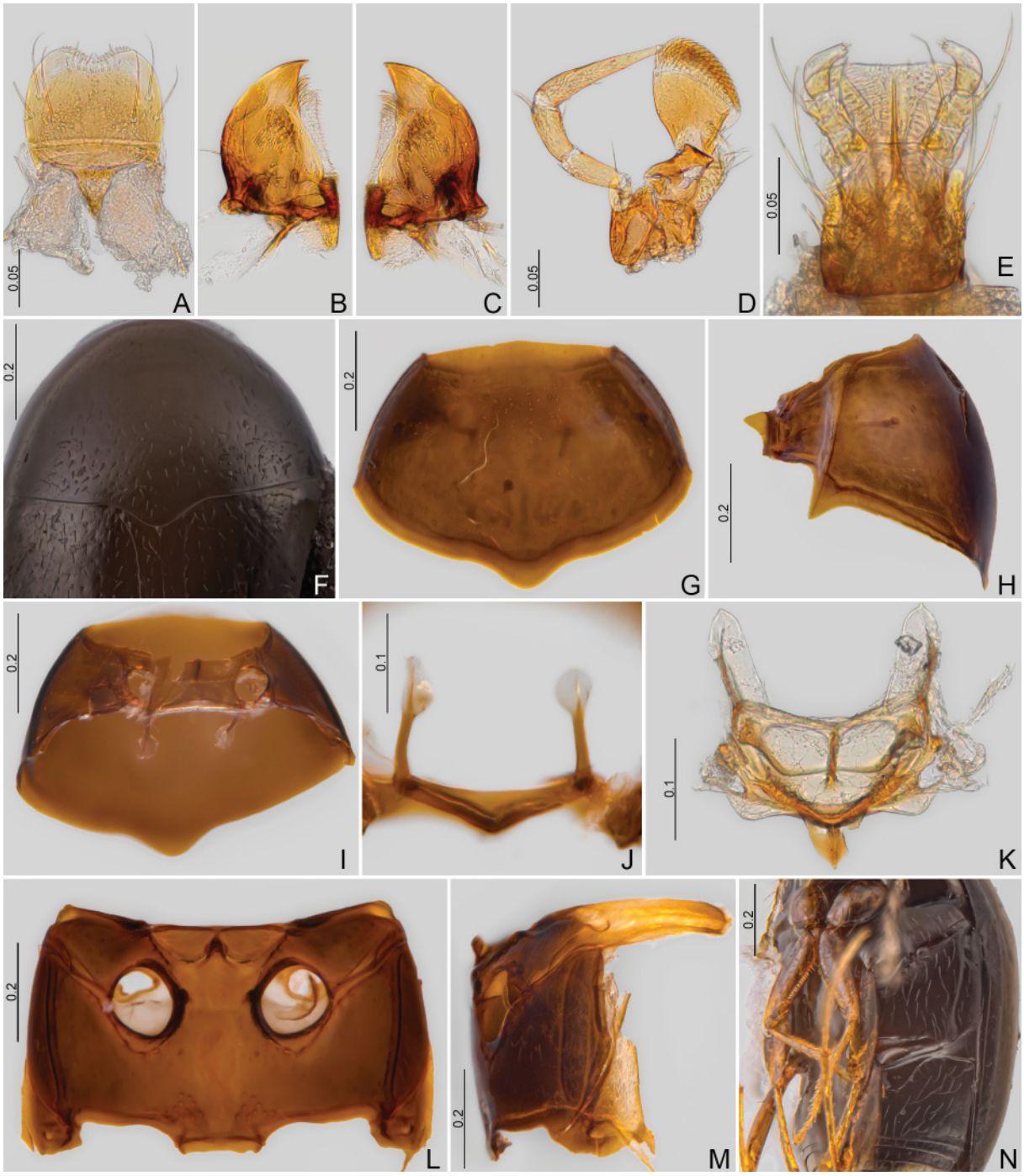

Fig. 51. *Scaphisoma infinitum* sp. nov. (CELC). **A**. Paratype, ♂ (#36), labrum. **B–C**. Paratype, ♂ (#73), mandibles. **D–E**. Paratype, ♂ (#36). **D**. Maxilla. **E**. Labium. **F**. Holotype, ♂, prothorax, dorsal view. **G–M**. Paratype, ♂ (#36). **G–J**. Prothorax. **G**. Dorsal view. **H**. Lateral view. **I**. Ventral view. **J**. Profurca. **K**. Scutellar shield. **L–N**. Meso- and metathorax. **L**. Ventral view. **M**. Lateral view. **N**. Holotype, ♂, oblique view. Scales in mm.

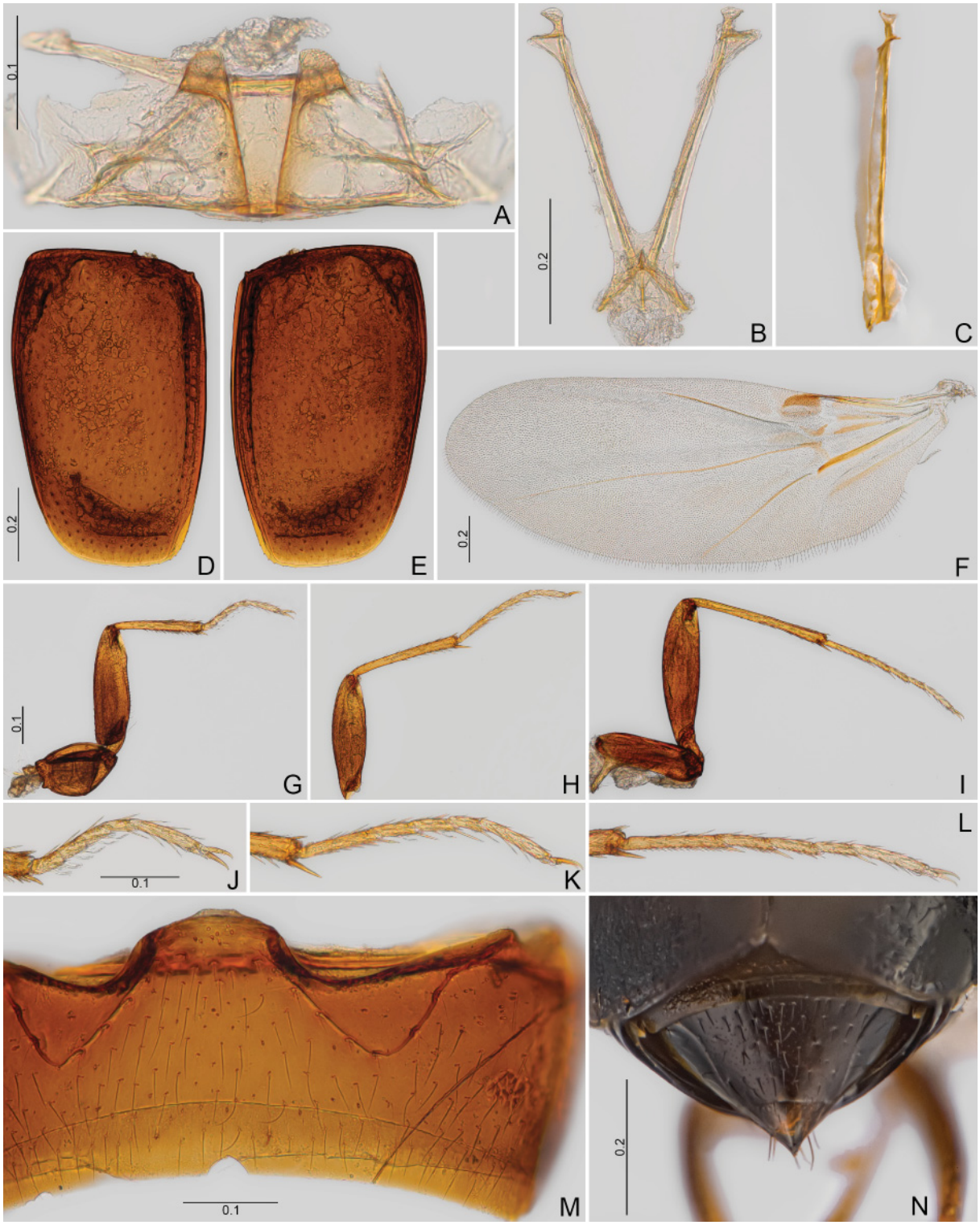

Fig. 52. *Scaphisoma infinitum* sp. nov. (CELC). **A–M**. Paratype, ♂ (#36). **A**. Metanotum. **B–C**. Metendosternite. **B**. Dorsal view. **C**. Lateral view. **D–E**. Elytra. **F**. Hind wing. **G–I**. Legs. **G**. Fore. **H**. Middle. **I**. Hind. **J–L**. Tibiae. **J**. Pro. **K**. Meso. **L**. Meta. **M**. Ventrite I. **N**. Holotype, ♂, abdomen, dorsal view. Scales in mm.

Abdomen. Lacking microsculpture, smooth, ventrites with very fine punctures, pubescence like metaventrite (Figs 51N, 52M). Submetacoxal lines arcuate, with sparse punctures; submetacoxal area length = 0.05–0.07 mm (Fig. 52M). Tergite VI with micro- and coarse punctures (Figs 52N, 54J).

Males

Pro- and mesotarsomeres I–III slightly wide, with few tenent setae (except for mesotarsomere I) (Fig. 52J–L). Sternite and tergite VIII lacking microsculpture. Sternite VIII with a small projection (Fig. 53A). Tergite VIII straight apically (Fig. 53B). Sternite IX elongate and with parallel sides (Fig. 53C).

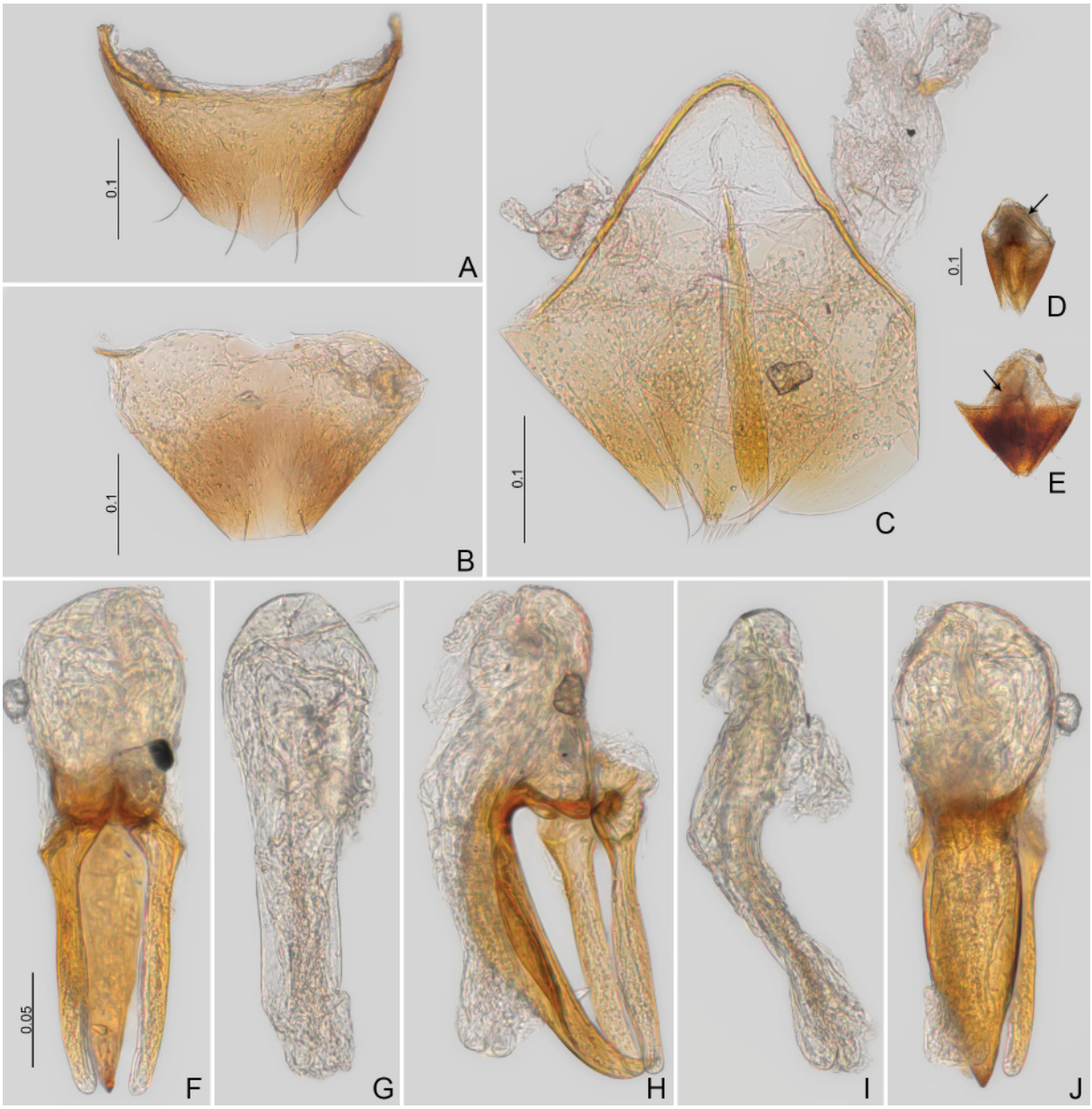

Fig. 53. *Scaphisoma infinitum* sp. nov. (CELC). **A–C**. Paratype, ♂ (#36). **A**. Sternite VIII. **B**. Tergite VIII. **C**. Tergite and sternite IX. **D–E**. Terminalia not dissected, arrow: aedeagus. **D**. Paratype, ♂ (#14). **E**. Paratype, ♂ (#109). **F–J**. Paratype, ♂ (#36). **F–J**. Aedeagi. **F**. Frontal view. **G**. Sclerite of internal sac, frontal view. **H**. Lateral view. **I**. Sclerite of internal sac, lateral view. **J**. Dorsal view. Scales in mm.

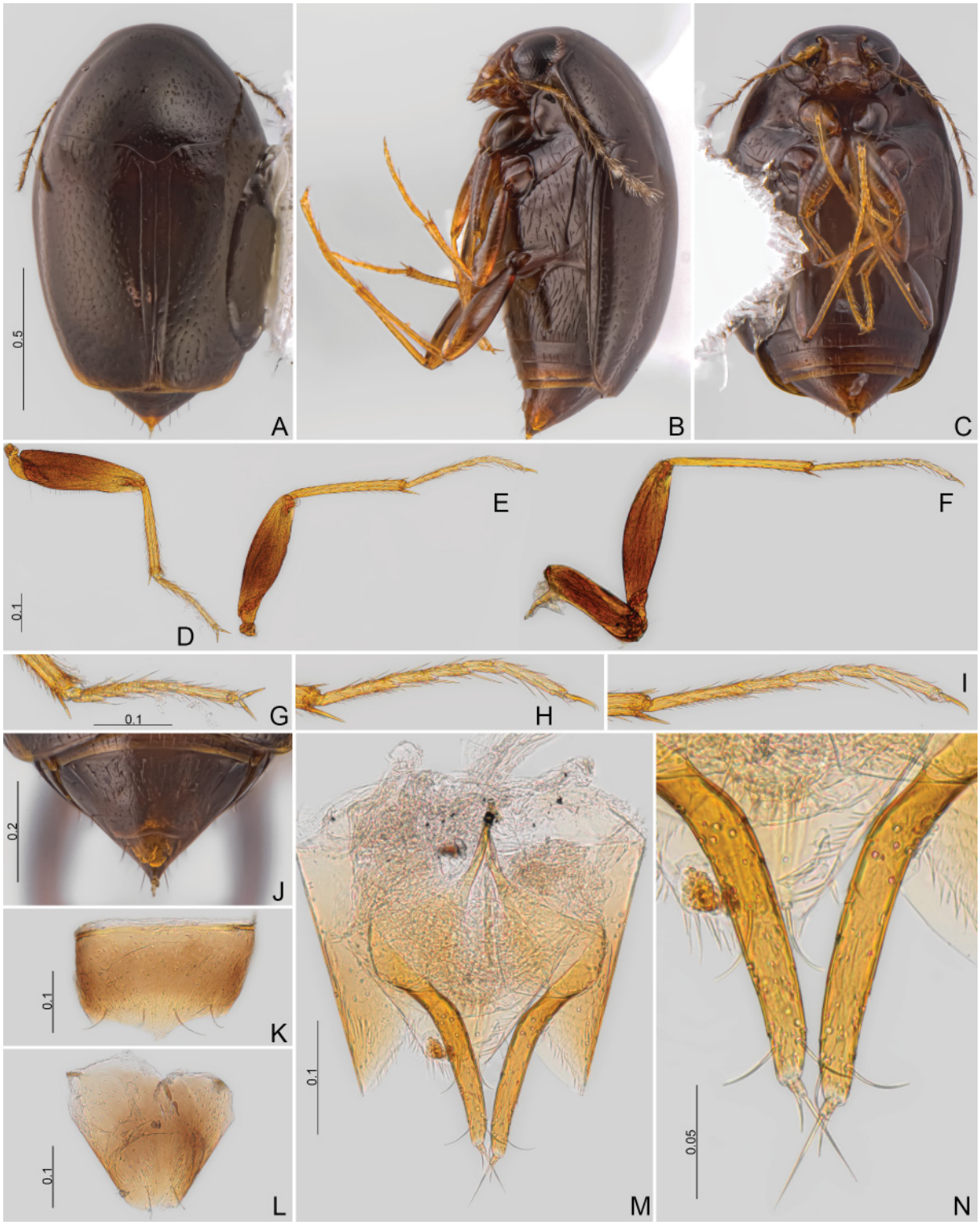

Fig. 54. *Scaphisoma infinitum* sp. nov. (CELC). **A–C**. Paratype, ♀ (#33). **A**. Dorsal view. **B**. Lateral view. **C**. Ventral view. **D–I**. Paratype, ♀ (#07). **D–F**. Legs. **D**. Fore. **E**. Middle. **F**. Hind. **G–I**. Tarsi. **G**. Pro. **H**. Meso. **I**. Meta. **J**. Paratype, ♀ (#33), abdomen, dorsal view. **K–N**. Paratype, ♀ (#07). **K**. Sternite VIII. **L**. Tergite VIII. **M**. Genitalia. **N**. Ovipositor. Scales in mm.

Aedeagus (Fig. 53D–J). Very small, hardly visible between terminal tergites and ventrites (Fig. 53D–E). Median lobe with elongate apical lobe and small and membranous basal bult; apical lobe triangular and sclerotized in ventral and dorsal view (Fig. 53F, J). Parameres almost straight, angulate anteriorly, in frontal view (Fig. 53F). Internal sac membraneous, completely filling median lobe (Fig. 53G, I).

Measurements (n = 5, including holotype, unless otherwise specified; in mm). TL (n = 35) 1.09–1.31 (1.21 ± 0.06), SY 0.15–0.18 (0.16 ± 0.01), HW 0.36–0.44 (0.41 ± 0.03), IS 0.17–0.23 (0.19 ± 0.02), WA 0.11–0.14 (0.12 ± 0.01), PL 0.44–0.53 (0.47 ± 0.03), PA 0.44–0.51 (0.46 ± 0.03), PB 0.68–0.80 (0.76 ± 0.05), EI 0.71–0.84 (0.78 ± 0.05), EL 0.78–0.95 (0.86 ± 0.07), EW 0.36–0.44 (0.41 ± 0.03), EH 0.29–0.35 (0.32 ± 0.02), Me 0.19–0.22 (0.20 ± 0.02), MeL 0.09–0.12 (0.11 ± 0.01), MeW 0.02–0.03 (0.02 ± 0), MB 0.12–0.15 (0.13 ± 0.01), MC 0.27–0.35 (0.31 ± 0.04), ML 0.03–0.05 (0.04 ± 0.01), MA 0.06–0.07 (0.06 ± 0.01), MA2 0.12–0.17 (0.14 ± 0.02), VL2 0.19–0.26 (0.22 ± 0.03), VL 0.22–0.29 (0.26 ± 0.03), PrF 0.28–0.35 (0.32 ± 0.03), PrT 0.22–0.27 (0.24 ± 0.02), MsF 0.30–0.36 (0.33 ± 0.03), MsT 0.27–0.36 (0.30 ± 0.04), MtF 0.33–0.42 (0.37 ± 0.04), MtT 0.33–0.42 (0.37 ± 0.04).

Females (Fig. 54)

Sternite VIII with a small posterior projection (Fig. 54K). Tergite VIII slightly concave posteriorly (Fig. 54L). Distal gonocoxite slender, curved; gonostylus small, rectangular (Fig. 54M–N).

Measurements (n = 8; unless otherwise specified; in mm). TL (n = 34) 1.17–1.36 (1.26 ± 0.05), SY 0.16–0.18 (0.16 ± 0.01), HW 0.40–0.43 (0.41 ± 0.01), IS 0.19–0.21 (0.20 ± 0.01), WA 0.11–0.15 (0.12 ± 0.01), PL 0.46–0.56 (0.50 ± 0.04), PA 0.40–0.51 (0.46 ± 0.04), PB 0.70–0.83 (0.76 ± 0.04), EI 0.75–0.89 (0.82 ± 0.05), EL 0.84–0.96 (0.89 ± 0.05), EW 0.41–0.45 (0.44 ± 0.02), EH 0.31–0.34 (0.33 ± 0.01), Me 0.18–0.23 (0.21 ± 0.02), MeL 0.09–0.11 (0.10 ± 0.01), MeW 0.02–0.03 (0.02 ± 0), MB 0.11–0.16 (0.13 ± 0.02), MC 0.29–0.36 (0.32 ± 0.03), ML 0.03–0.05 (0.04 ± 0.01), MA 0.05–0.07 (0.06 ± 0.01), MA2 0.12–0.16 (0.15 ± 0.01), VL 0.22–0.26 (0.24 ± 0.02), VL2 0.25–0.29 (0.27 ± 0.01), PrF 0.31–0.35 (0.33 ± 0.01), PrT 0.21–0.25 (0.23 ± 0.01), MsF 0.32–0.36 (0.34 ± 0.02), MsT: 0.28–0.32 (0.30 ± 0.01), MtF (n = 7): 0.35–0.42 (0.39 ± 0.02), MtT (n = 7): 0.35–0.42 (0.39 ± 0.02).

Host

Collected from undetermined resupinate and/or crust fungi (Fig. 93F–J). Few specimens collected from a small decomposing log with *Ceratiomyxa fruticulosa*.

Remarks

Species similar to *S. minutipenis* Löbl & Ogawa, 2016 due to colour pattern, elongate sternite IX, small aedeagus, and the internal sac lacking sclerite and flagellum. However, it can be easily distinguished by the smaller body length, the slender antennomeres, the more arcuate submetacoxal lines, the longer submetacoxal area, and the absence of ventral abdominal microsculpture.

Distribution

Mata do Paraíso and Mata da Biologia, Universidade Federal de Viçosa, campus of Viçosa, state of Minas Gerais, Southeast Brazil (Fig. 1A–D).

Scaphisoma mutabile sp. nov.
urn:lsid:zoobank.org:act:3E14760B-CE18-4AF6-AD89-F83374F45C2F
Figs 1A–B, 55–59

Diagnosis

Body length: 1.28–1.52 mm. Brown-reddish; pronotum darker than elytra. Pronotum and elytra iridescent. Elytra, thorax, legs, and abdomen with distinct strigulate microsculpture. Sutural striae

parallel to suture; basal striae absent. Submesocoxal lines nearly parallel; punctate. Submetacoxal lines arcuate. Parameres widened apically; sclerite of internal sac simple. Females with spermatheca large and twisted; distal gonocoxite curved.

Etymology

The species epithet is a Greek word meaning 'change', due to the change of colour depending on the position.

Material examined

Holotype

BRAZIL • ♂; Minas Gerais, Viçosa, Mata da Biologia; 30 Oct. 2019; E von Groll and I.S. Pecci-Madalena leg.; "Fungo 25 / Em *Xylodon flaviporus* / HOLOTYPUS ♂"; CELC. (Fig. 55D–E)

Paratypes

BRAZIL • 3 ♂♂, 4 ♀♀, 2 ex. (1 ♂**, 1 ♀*); same collection data as for holotype; 30 Oct. 2019; E von Groll and I.S. Pecci-Madalena leg.; "Fungo 25 / Em *Xylodon flaviporus* /"; CELC • 2 ♂♂ (1 ♂*); same collection data as for holotype; 12 Nov. 2019; LabCol leg.; "Fungo 03 / Em fungo branco ressupinado em tronco indet."; CELC.

Description

Colouration. Elytra, thorax, and ventrite I reddish-brown; pronotum and posterior part of elytra darker (Fig. 55A–C); mouthparts, antennae, legs, apex of elytra, and abdominal segments III–VII yellow (Fig. 55C, H). Pronotum and elytra iridescent, more visible under direct light (Fig. 55F–G). Variations: (1) darker tonalities (Fig. 55F); (2) lighter tonalities (Fig. 55G); (3) iridescence variably distributed; (4) ventrite also iridescent.

Head (Figs 55H–K, 56A–E). Frons with punctures somewhat coarse; pubescence moderately sparse. Clypeus wider than long (Fig. 55I). Labrum shallowly concave posteriorly (Fig. 56A). Maxillary palpomeres conspicuously elongate (Fig. 56D). Last labial palpomere not strongly curved, thick; mentum elongate, with a posterior angulate concavity (Fig. 56E). Antennomere VII enlarged (Fig. 55J–K); antennomere proportions (n = 2): I missing : II 73/45 : III 34/18 : IV 63/16 : V 80/21 : VI 81/21 : VII 102/31 : VIII 83/24 : IX 110/33 : X 105/32 : XI 128/36.

Prothorax (Fig. 56F–J). Lacking microsculpture, smooth. Pronotum with punctures fine and moderately sparse; pubescence short and sparse (Fig. 56F). Hypomeron shining, glabrous; posterior angles angulate extending beyond anapleural line (Figs 55B, 59B). Prosternal process concave (Fig. 56H). Profurca short, curved (Fig. 56J).

Mesothorax (Fig. 56K–N). With strigulate microsculpture (Figs 56N, 59B). Visible part of scutellum longer than wide (Fig. 56F); scutellar line sinuous; tip acute (Fig. 56K). Mesanepisternum with sparse pubescence (Figs 55B, 56N, 59B). Mesepimeron wide, 4.39× as wide as long; almost uneven due to strigulate microsculpture of mesanepisternum (Fig. 56N). Mesoventral lines not curved; punctate; secondary and median lines absent (Fig. 56L). Mesoventral process longer than wide and curved in lateral view (Fig. 56M).

Metathorax (Figs 56L–N, 57A–C). With strigulate microsculpture (Figs 56N, 56B). Metaventrite with moderately coarse punctures; pubescence sparse (Fig. 56N). Submesocoxal lines nearly parallel, punctate; submesocoxal length about 0.04 mm (Fig. 56L–N). Metanepisternum conspicuously wider near metacoxae (Fig. 56N). Metendosternite arms widely separated (Fig. 57B–C).

Wings (Fig. 57D–G). Elytra with strigulate microsculpture (Fig. 57D–F); not strongly narrowed apically; punctation coarse – coarser than pronotum. One longitudinal carina on disc of each elytron (Fig. 59A) – weakly marked (but distinct) on holotype (Fig. 55A). Sutural striae slightly curved anteriorly; basal striae absent (Fig. 55A). Curvature of lateral striae shortened at humeral area (Fig. 55B).

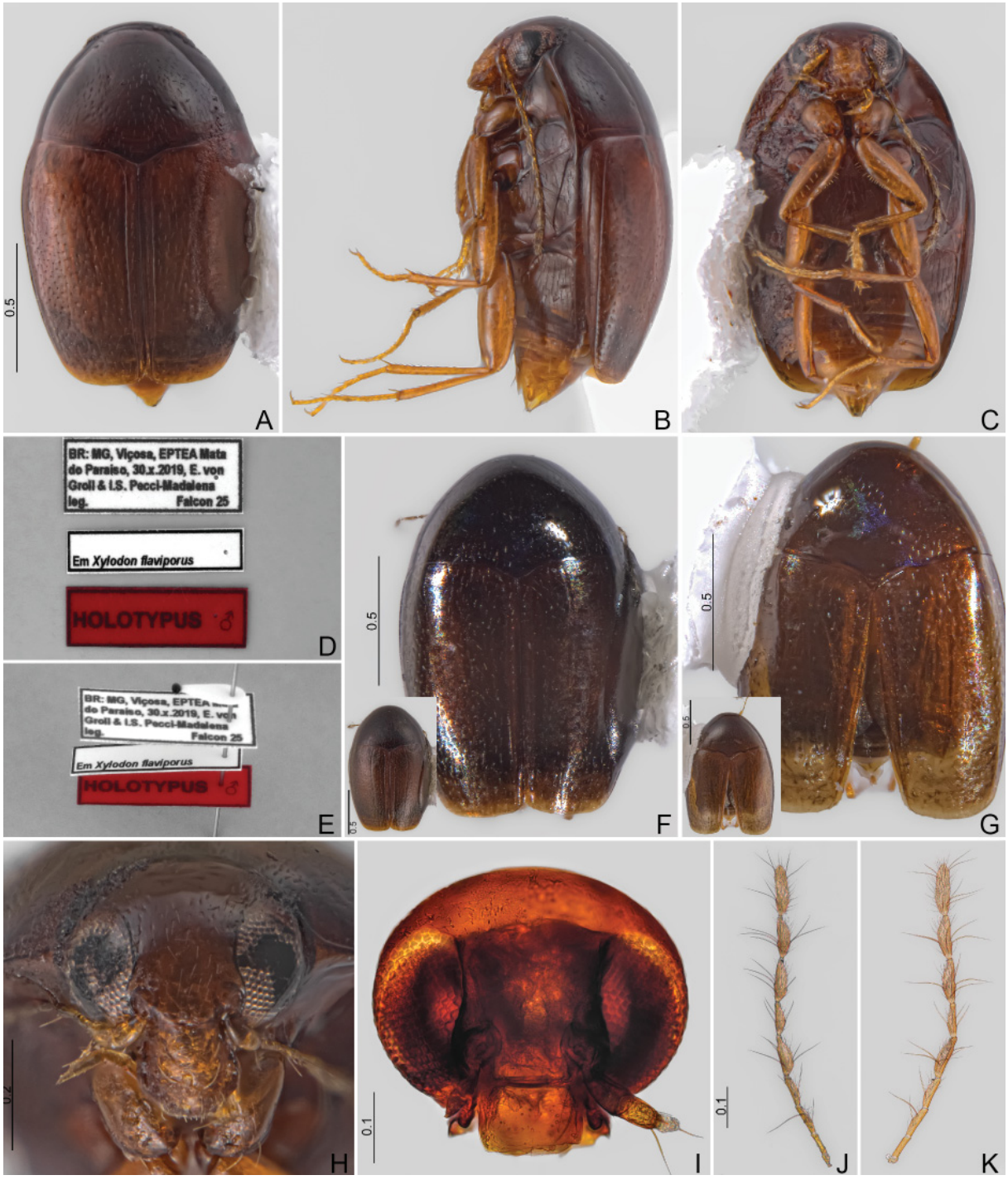

Fig. 55. *Scaphisoma mutabile* sp. nov. **A–E**. Holotype, ♂ (CELC). **A**. Dorsal view. **B**. Lateral view. **C**. Ventral view. **D**. Labels. **E**. Pinned. **F**. Paratype, ♂ (#67). **G**. Paratype (#72). **H–I**. Head, frontal view. **H**. Holotype, ♂. **I**. Paratype, ♂ (#69). **J–K**. Antennae. **J**. Paratype, ♂ (#69). **K**. Paratype, ♀ (#75). F–G. Specimens photographed without diffuser (large image); with diffuser (small image). Scales in mm.

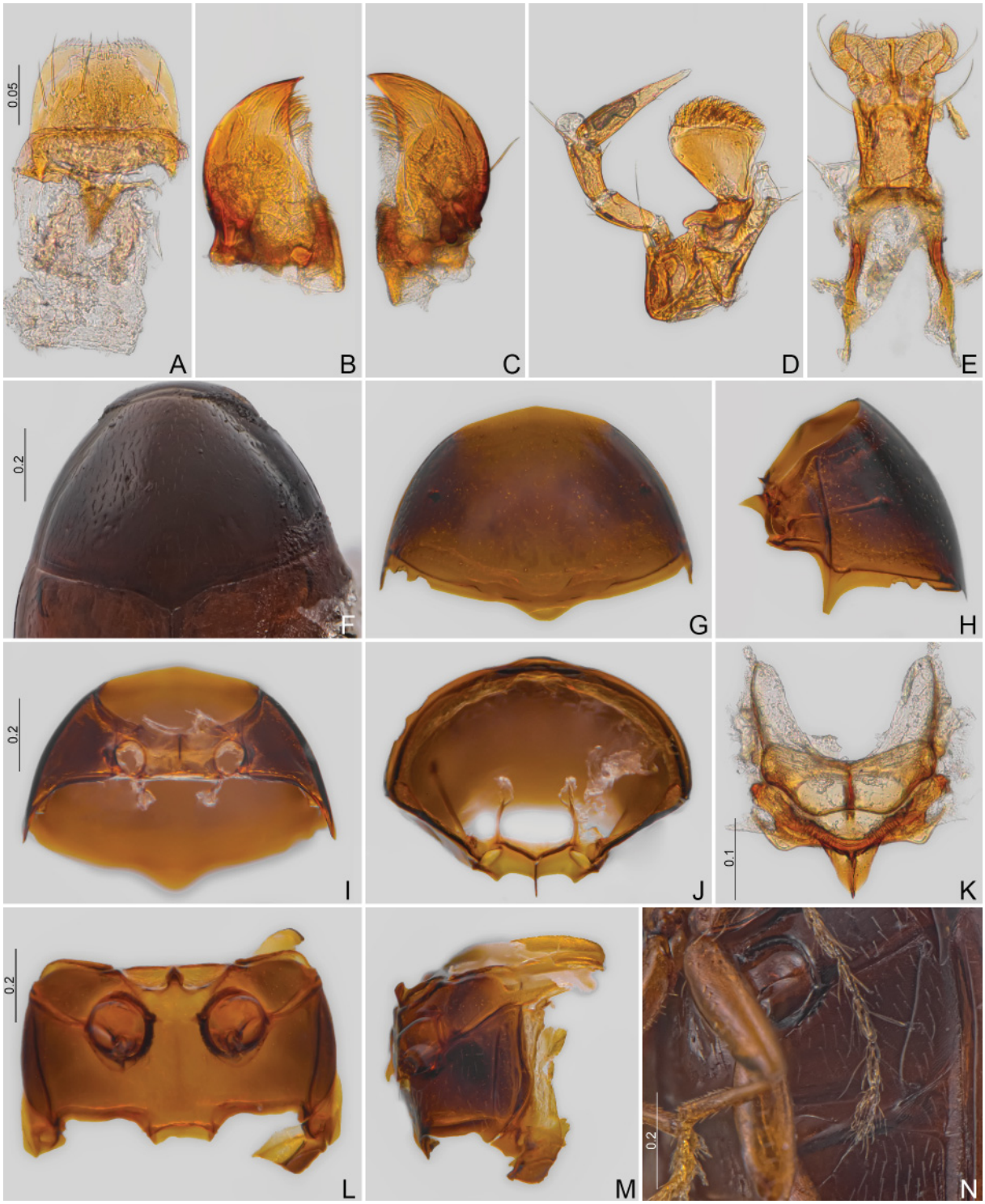

Fig. 56. *Scaphisoma mutabile* sp. nov. (CELC). **A–E**. Paratype, ♂ (#69). **A**. Labrum. **B–C**. Mandibles. **D**. Maxilla. **E**. Labium. **F**. Holotype, ♂, prothorax, dorsal view. **G–M**. Paratype, ♂ (#69). **G–J**. Prothorax. **G**. Dorsal view. **H**. Lateral view. **I**. Ventral view. **J**. Inner view. **K**. Scutellar shield. **L–N**. Meso- and metathorax. **L**. Ventral view. **M**. Lateral view. **N**. Holotype, ♂, oblique view. Scales in mm.

Legs (Figs 56N, 57H–M, 59D–I). With strigulate microsculpture.

Abdomen. Ventrites with strigulate microsculpture; pubescence dense (Figs 55B–C, 58A, 59B–C). Submetacoxal lines arcuate and punctate; submetacoxal area length = 0.06–0.10 mm (Fig. 58A). Tergite VI and VII with imbricate microsculpture (Fig. 58B).

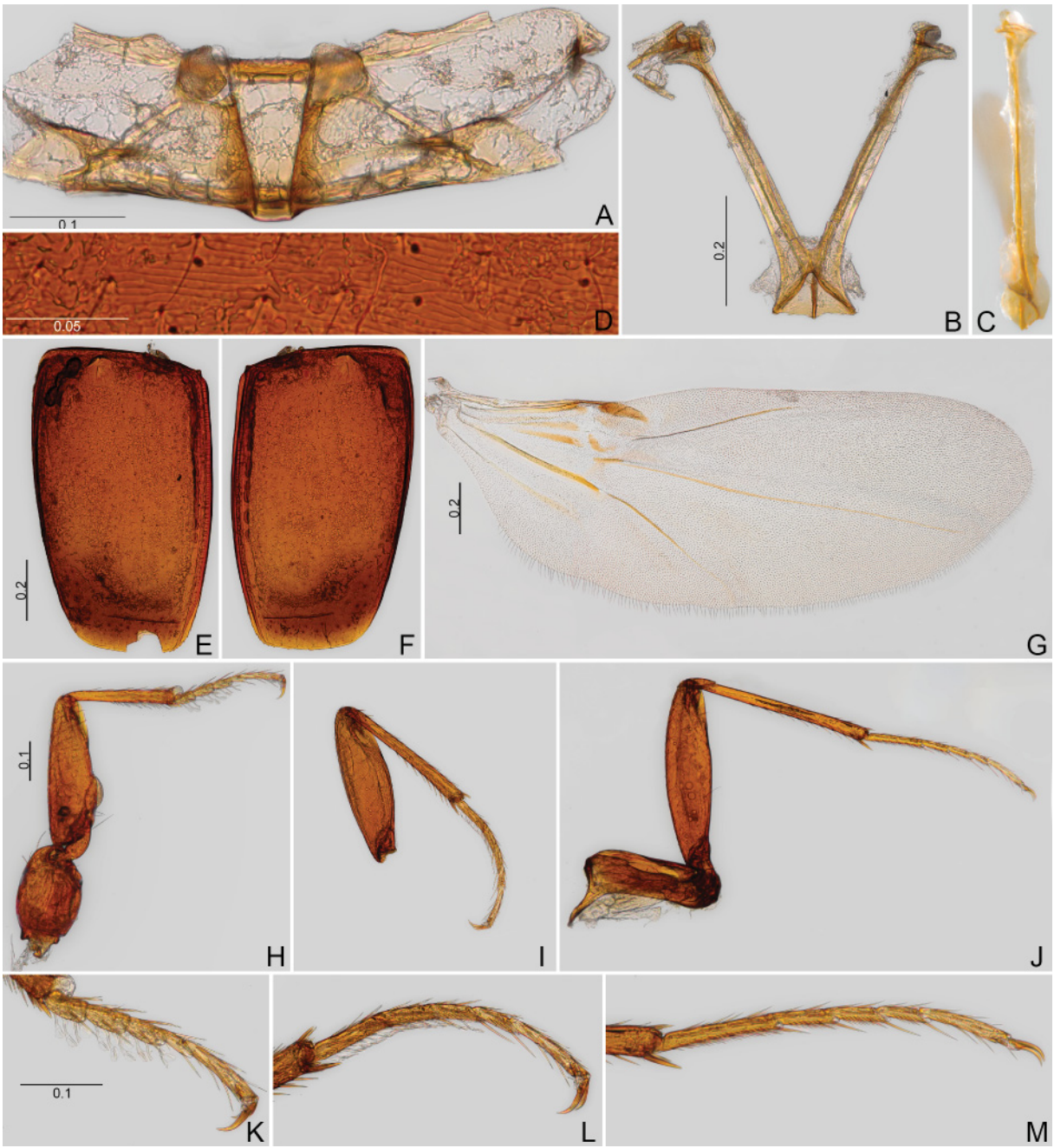

Fig. 57. *Scaphisoma mutabile* sp. nov., paratype, ♂ (#69) (CELC). **A**. Metanotum. **B–C**. Metendosternite. **B**. Dorsal view. **C**. Lateral view. **D–F**. Elytra. **D**. Detail. **E**. Left. **F**. Right. **G**. Hind wing. **H–J**. Legs. **H**. Fore. **I**. Middle. **J**. Hind. **K–M**. Tibiae. **K**. Pro. **L**. Meso. **M**. Meta. Scales in mm.

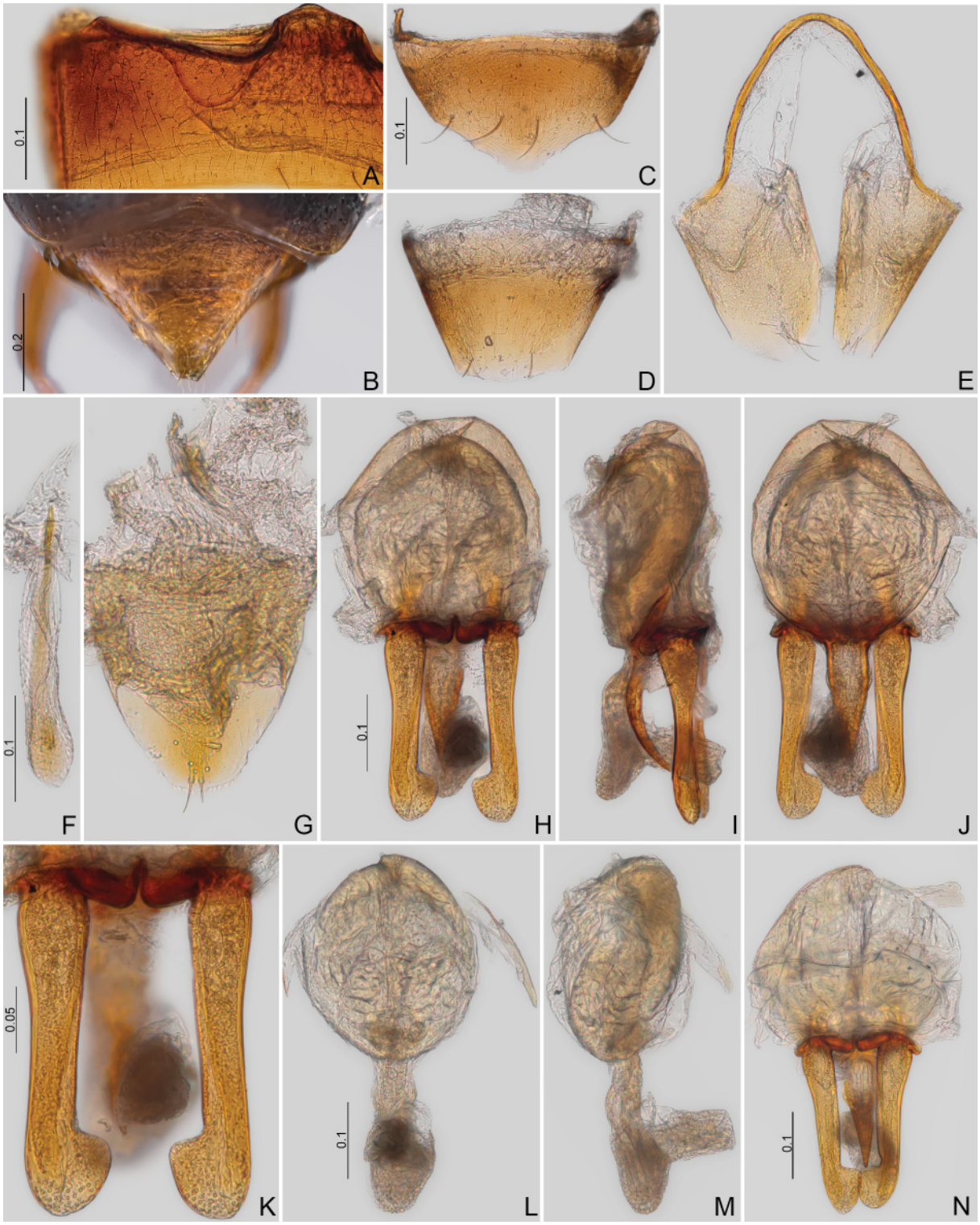

Fig. 58. *Scaphisoma mutabile* sp. nov. (CELC). **A**. Paratype, ♂ (#69), ventrite I. **B**. Holotype, ♂, abdomen, dorsal view. **C–M**. Paratype, ♂ (#69). **C**. Sternite VIII. **D**. Tergite VIII. **E**. Tergite IX. **F**. Sternite IX. **G**. Tergite X. **H–N**. Aedeagi. **H**. Frontal view. **I**. Lateral view. **J**. Dorsal view. **K**. Parameres, frontal view. **L–M**. Sclerite of internal sac. **L**. Frontal view. **M**. Lateral view. **N**. Paratype, ♂ (#67), frontal view. Scales in mm.

Males

Pro- and mesotarsomeres I–III widened, with dense tenent setae, especially mesotarsomeres (Fig. 57K–M). Sternite and tergite VIII with strigulate microsculpture. Sternite VIII with a wide posterior projection (Fig. 58C). Tergite VIII slightly convex posteriorly (Fig. 58D). Tergite IX with oblong ventral struts (Fig. 58E). Sternite IX wider posteriorly (Fig. 58F). Tergite X oval (Fig. 58G).

Aedeagus (Fig. 58H–N). Basal bulb and apical lobe very distinct. Basal bulb remarkably rounded (Fig. 58H); apical lobe triangular, small, sclerotized, curved, and shorter than basal bulb (Fig. 58I). Parameres elongate; tip wide in frontal view (Fig. 58K). Internal sac membranous and similar to the median lobe shape: rounded with a projection (Fig. 58L–M).

Measurements (n = 6 including holotype, unless otherwise specified; in mm). TL 1.28–1.45 (1.38 ± 0.07), SY (n = 5) 0.16–0.20 (0.19 ± 0.02), HW 0.40–0.45 (0.43 ± 0.02), IS 0.20–0.23 (0.21 ± 0.01), WA 0.12–0.15 (0.13 ± 0.01), PL 0.53–0.60 (0.56 ± 0.03), PA 0.44–0.55 (0.50 ± 0.04), PB 0.77–0.91 (0.84 ± 0.06), EI 0.79–0.94 (0.87 ± 0.06), EL 0.90–1.01 (0.95 ± 0.05), EW 0.40–0.54 (0.46 ± 0.05), EH 0.31–0.38 (0.34 ± 0.02), Me 0.18–0.25 (0.23 ± 0.02), MeL (n = 5) 0.13–0.14 (0.13 ± 0.01), MeW (n = 5) 0.03, MB 0.11–0.18 (0.14 ± 0.02), MC 0.31–0.39 (0.35 ± 0.03), ML 0.02–0.04 (0.03 ± 0.01), MA 0.06–0.10 (0.07 ± 0.02), MA2 0.13–0.19 (0.15 ± 0.02), VL 0.23–0.31 (0.26 ± 0.03), VL2 0.23–0.34 (0.27 ± 0.04), PrF 0.35–0.39 (0.37 ± 0.01), PrT 0.24–0.30 (0.27 ± 0.02), MsF 0.34–0.40 (0.37 ± 0.03), MsT 0.25–0.36 (0.31 ± 0.04), MtF 0.38–0.46 (0.43 ± 0.03), MtT 0.38–0.45 (0.42 ± 0.02).

Females (Fig. 59)

Sternite and tergite VIII. Sternite VIII with a projection (Fig. 59J). Tergite VIII bearing a small projection (Fig. 59K). Spermatheca remarkably enlarged and twisted (Fig. 59L). Distal gonocoxite thick and curved; gonostylus distinctly small (Fig. 59M).

Measurements (n = 3; in mm). TL 1.48–1.52 (1.50 ± 0.02), SY 0.19–0.20 (0.19 ± 0.01), HW 0.45–0.47 (0.46 ± 0.01), IS 0.21–0.24 (0.22 ± 0.02), WA 0.14–0.16 (0.15 ± 0.01), PL 0.58–0.65 (0.62 ± 0.04), PA 0.45–0.55 (0.5 ± 0.05), PB 0.88–0.94 (0.90 ± 0.03), EI 0.92–0.99 (0.95 ± 0.04), EL 1.01–1.05 (1.03 ± 0.02), EW 0.48–0.58 (0.52 ± 0.05), EH 0.39–0.40 (0.39 ± 0.01), Me 0.26–0.27 (0.27 ± 0.01), MeL 0.13–0.15 (0.14 ± 0.01), MeW 0.03–0.04 (0.03 ± 0.01), MB 0.14–0.15 (0.14 ± 0.01), MC 0.34–0.40 (0.37 ± 0.04), ML 0.04–0.05 (0.04 ± 0.01), MA 0.07–0.11 (0.09 ± 0.02), MA2 0.15–0.18 (0.17 ± 0.02), VL 0.26–0.28 (0.27 ± 0.01), VL2 0.30–0.32 (0.31 ± 0.01), PrF 0.38–0.40 (0.39 ± 0.01), PrT 0.25–0.27 (0.26 ± 0.01), MsF 0.37–0.40 (0.39 ± 0.02), MsT 0.31–0.36 (0.34 ± 0.03), MtF 0.43–0.46 (0.45 ± 0.02), MtT 0.41–0.45 (0.43 ± 0.02).

Host

Collected from *Xylodon flaviporus* and an undetermined crust/resupinate fungus.

Remarks

Similar to *S. iridescens* Löbl & Ogawa, 2016 due to the presence of iridescence, the shape of the sutural striae, and the absence of basal striae. The submesocoxal lines are also similar in both species. Nonetheless, *S. iridescens* presents the iridescence on the ventral surface, while *S. mutabile* sp. nov. always presents it on the dorsal surface (pronotum and elytra) and rarely ventrally. *Scaphisoma mutabile* sp. nov. can also be easily distinguished by the smaller body length, the elytra with strigulate microsculpture, and by the different shape of parameres.

Distribution

Mata do Paraíso, Universidade Federal de Viçosa, campus of Viçosa, state of Minas Gerais, Southeast Brazil (Fig. 1A–B).

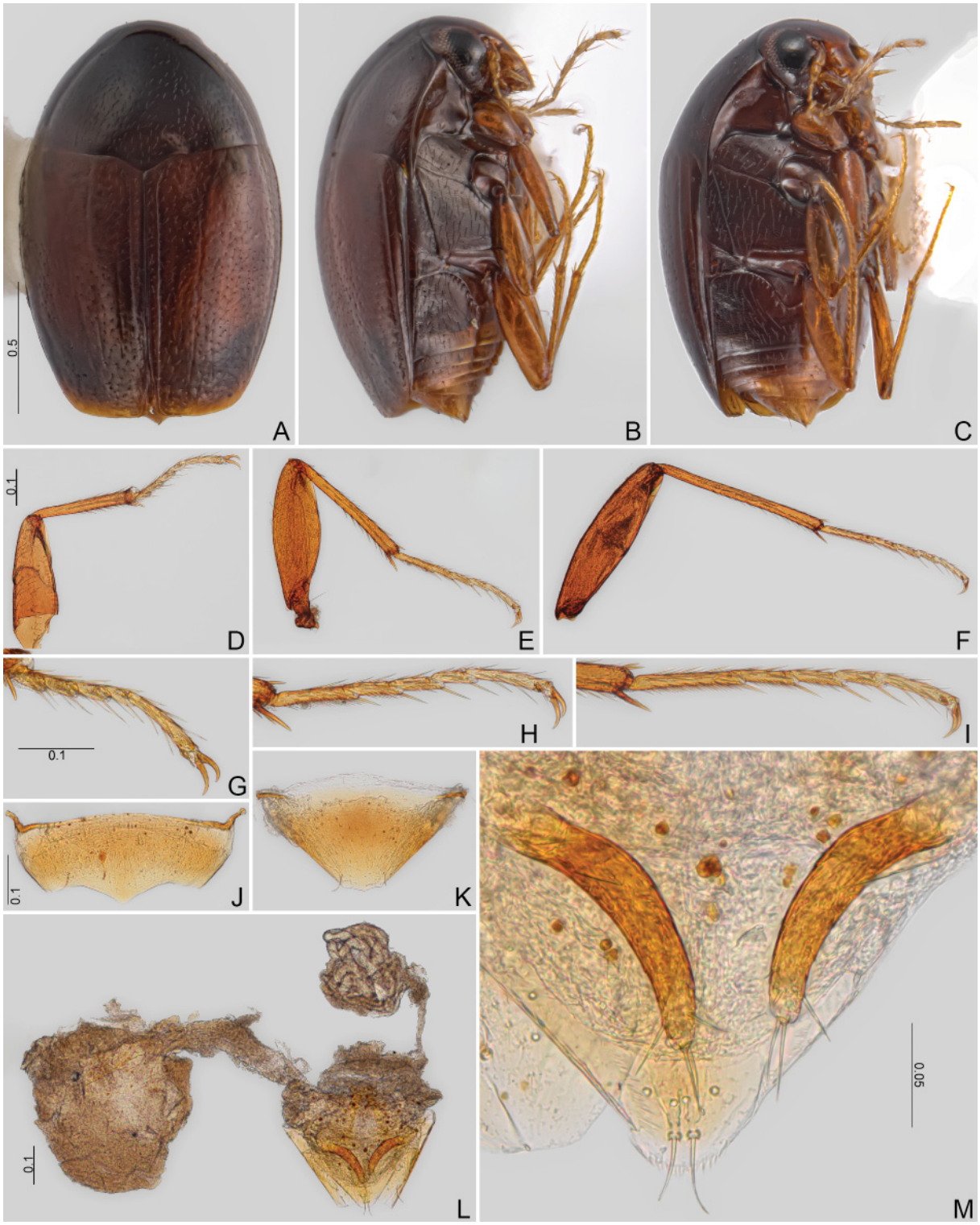

Fig. 59. *Scaphisoma mutabile* sp. nov. (CELC). **A–C**. Paratype, ♀ (#74). **A**. Dorsal view. **B**. Lateral view. **C**. Oblique view. **D–M**. Paratype, ♀ (#75). **D–F**. Legs. **D**. Fore. **E**. Middle. **F**. Hind. **G–I**. Tarsi. **G**. Pro. **H**. Meso. **I**. Meta. **J**. Sternite VIII. **K**. Tergite VIII. **L**. Genitalia. **M**. Ovipositor. Scales in mm.

Scaphisoma peculiare sp. nov.
urn:lsid:zoobank.org:act:21613515-84E8-49AA-9560-B65537EB8CDE
Figs 1A–D, 60–64, 93E–F

Diagnosis

Body length: 1.46–1.70 mm. Oblong; brown, appendages yellow. Last maxillary palpomere modified, flattened apically. Sutural stria present and connected to basal. Mesocoxal lines slightly arcuate; submesocoxal area very short. Metacoxal lines parallel to metacoxae; submetacoxal area very short. Males lacking tenent setae. Abdominal ventrite I with punctures coarse and dense; densely pubescent. Median lobe, parameres, and sclerite of internal sac elongate and curved in frontal view. Apex of parameres irregular denticulate. Distal gonocoxite fusiform.

Etymology

The species epithet is a Latin word meaning 'singular', due to the different characteristics of the species.

Material examined

Holotype

BRAZIL • ♂; Minas Gerais, Viçosa, Mata da Biologia; 12 Nov. 2020; E von Groll and G.L.N. Martins leg.; "/ Em fungo branco ressupinado em tronco caído / HOLOTYPUS ♂"; CELC. (Fig. 60D–E)

Paratypes

BRAZIL • 4 ♂♂, 6 ♀♀, 6 ex. (1 ♂*, 1 ♀*, 1 ♂**, 1 ♀**); same collection data as for holotype; 12 Nov. 2020; E von Groll and G.L.N. Martins leg.; "/ Em fungo branco ressupinado em tronco caído"; CELC • 5 ♂♂, 6 ♀♀, 12 ex. (1 ♂*, 1 ♂**,1 ♀*); 15 Oct. 2021; E. von Groll and A. Orsetti leg.; "Fungo 30 / Em fungo branco ressupinado no tronco caído"; CELC.

Description

Colouration. Brown; antennae, legs, mouthparts, apex of elytra, and posterior bead of abdominal ventrites and tergites yellow (Figs 60A–C, H, 63B). Variation: (1) paler tonalities (Fig. 60F–G).

Head (Figs 60H–K, 61A–E). Frons finely punctate; area between antennae with coarse punctures; pubescence moderately dense (Fig. 60H). Clypeus widened posteriorly (Fig. 60I). Distance between antennal insertion less than 2 × the size of the insertion, easily seen in dissected heads (Fig. 60I). Labrum conspicuously concave posteriorly (Fig. 61A). Mandibles not strongly curved, thick (Fig. 61B–C). Last maxillary palpomere with truncate apex (Fig. 61D). Last labial palpomere distinctly curved; mentum with sides similar in length (Fig. 61E). Antennomeres elongate (Fig. 60J–K); antennomere proportions (n = 6): I 85/50 : II 88/44 : III 29/19 : IV 38/15 : V 78/18 : VI 94/20 : VII 117/37 : VIII 90/23 : IX 124/31 : X 117/33 : XI 123/30.

Prothorax (Fig. 61F–J). Pronotum with punctures fine and sparse; pubescence short, fine (Fig. 61F). Hypomeron shining, almost glabrous; posterior angle extending just a little beyond anapleural line (Fig. 61C). Prosternal process forming a just slightly arcuate curvature (Fig. 61H). Profurca elongate, straight (Fig. 61J).

Mesothorax (Figs 61K, 62A–C). Visible part of scutellum with similar sides (Fig. 61F), tip not strongly acute (Fig. 61K). Mesoventral process short in lateral view (Fig. 62B). Mesanepisternum with few punctures (Fig. 62C). Mesepimeron about 2.59 × as wide as long (Fig. 62C). Mesoventral lines straight, impunctate (Fig. 62A); secondary lines present, curved (Fig. 60B).

Fig. 60. *Scaphisoma peculiare* sp. nov. (CELC). **A–E**. Holotype, ♂. **A**. Dorsal view. **B**. Lateral view. **C**. ventral view. **D**. Labels. **E**. Pinned. **F–G**. Paratype (#223), teneral. **F**. Dorsal view. **G**. Lateral view. **H–I**. Heads, frontal views. **H**. Holotype, ♂. **I**. Paratype, ♂ (#236). **J–K**. Antennae. **J**. Paratype, ♂ (#236). **K**. Paratype, ♀ (#220). Scales in mm.

Metathorax (Fig. 62A–F). Metaventrite with punctures moderately coarse, pubescence dense and thick (Fig. 62C). Submesocoxal lines slightly arcuate; submesocoxal area short, length = 0.03 mm (Figs 62A–C, 64C). Metanepisternum less pubescent than metaventrite, wider near metacoxae (Fig. 62C). Metepimeron densely pubescent. Metanotum with alacrista 'P-shaped' laterally (Fig. 62D). Metendosternite with wide ventral lamina, arms forming an angle of approximately of 40° (Fig. 62E–F).

Fig. 61. *Scaphisoma peculiare* sp. nov. (CELC). **A–E**. Paratype, ♂ (#236). **A**. Labrum. **B–C**. Mandibles. **D**. Maxilla. **E**. Labrum. **F**. Holotype, ♂, prothorax, dorsal view. **G–J**. Paratype, ♂ (#202). **G–J**. Prothorax. **G**. Dorsal view. **H**. Lateral view. **I**. Ventral view. **J**. Inner view. **K**. Paratype, ♂ (#236), scutellar shield. Scales in mm.

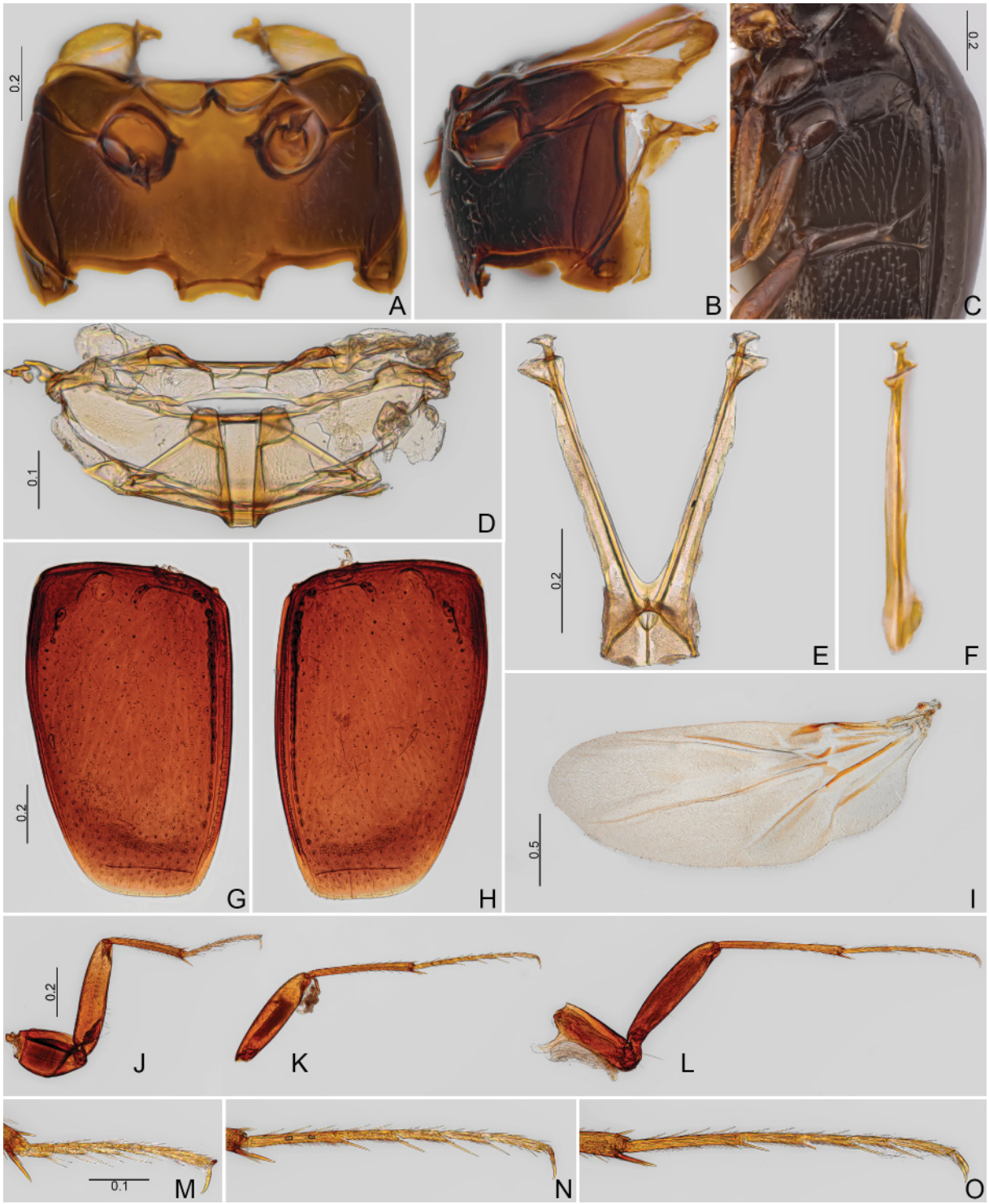

Fig. 62. *Scaphisoma peculiare* sp. nov. (CELC). **A–B**. Paratype, ♂ (#236), meso- and metathorax. **A**. Ventral view. **B**. Lateral view. **C**. Holotype, ♂, oblique view. **D**. Paratype, ♂ (#236), metanotum. **E–F**. Paratype, ♂ (#202), metendosternite. **E**. Dorsal view. **F**. Lateral view. **G–O**. Paratype, ♂ (#236). **G–H**. Elytra. **I**. Hind wing. **J–L**. Legs. **J**. Fore. **K**. Middle. **L**. Hind. **M–O**. Tibiae. **M**. Pro. **N**. Meso. **O**. Meta. Scales in mm.

Wings (Fig. 62G–I). Elytra narrowed apically; punctation coarse and sparse. Sutural stria connected to basal (Fig. 61F). Adsutural area narrow (Fig. 60A). Basal stria impunctate and reaching about basal mid-width of elytra. Lateral stria punctate, curved at humeral area (Figs 60B, 64B).

Legs (Figs 62J–O, 64D–I). Femora elongate and thin, not microsculptured. Apical spine of protibiae I longer than tarsomere I.

Abdomen. Ventrites conspicuously coarse with dense punctures and pubescence (Figs 60B–C, G, 64B). Submetacoxal lines parallel to coxae, coarse and densely punctate (Figs 62C, 63A). Submetacoxal area remarkably short: 0.01–0.04 mm (Fig. 62C). Tergite VI coarse punctate and densely pubescent; micropunctured (Figs 63B, 64J).

Males

Tibiae slightly curved. Protarsomeres I–III just a slightly wider – visible only under microscope; lacking tenet setae (Fig. 62M–O). Sternite and tergite VIII lacking microsculpture and both with a wide apical projection (Fig. 63C–D). Tergite IX with ventral struts forming a flat plate (Fig. 63E). Sternite IX guitar-shape (Fig. 63F). Tergite X ellipsoidal (Fig. 63G).

Aedeagus (Fig. 63H–M). Median lobe with basal bulb membranous and rounded; apical lobe distinctly elongate and thin, longer than basal bulb (Fig. 63H–J, L–M); apical lobe and parameres curved in frontal view (Fig. 63J). Parameres more (Fig. 63M) or less (Fig. 63L) separated, with irregular denticulate apex, resembling broken structures (Fig. 63J). Internal sac thin, elongate and curved (Fig. 63K).

Measurements (n = 8, including holotype, unless otherwise specified; in mm). TL (n = 10) 1.52–1.66 (1.58 ± 0.04), SY 0.17–0.19 (0.18 ± 0.01), HW 0.49–0.50 (0.49 ± 0.01), IS 0.21–0.22 (0.22 ± 0), WA 0.13–0.15 (0.14 ± 0.01), PL 0.59–0.65 (0.62 ± 0.02), PA 0.50–0.56 (0.53 ± 0.02), PB 0.93–1.04 (0.96 ± 0.04), SL (n = 7) 0.01–0.03 (0.02 ± 0.01), EI 0.94–1.06 (1.00 ± 0.04), EL 1.05–1.15 (1.10 ± 0.03), EW 0.54–0.59 (0.55 ± 0.02), EH 0.38–0.45 (0.41 ± 0.02), Me 0.23–0.27 (0.24 ± 0.01), MeL 0.03–0.05 (0.04 ± 0.01), MeW 0.10–0.12 (0.11 ± 0.01), MB 0.19–0.23 (0.21 ± 0.01), MC 0.30–0.37 (0.33 ± 0.03), ML 0.03–0.04 (0.03 ± 0.01), MA 0.02–0.03 (0.02 ± 0), VL 0.24–0.29 (0.26 ± 0.02); VL2 (n = 7) 0.28–0.31 (0.29 ± 0.01), PrF 0.43–0.47 (0.45 ± 0.02), PrT 0.30–0.35 (0.31 ± 0.02), MsF 0.45–0.49 (0.47 ± 0.02), MsT 0.39–0.45 (0.43 ± 0.02), MtF 0.48–0.52 (0.50 ± 0.01), MtT 0.48–0.52 (0.50 ± 0.01).

Females (Fig. 64)

Sternite and tergite VIII with a wide apical projection (Fig. 64K–L). Tergite VIII imbricate microsculpture (Fig. 64L). Distal gonocoxite fusiform and curved; gonostylus wide, triangular (Fig. 64M–N). Spermatheca not detected.

Measurements (n = 7, unless otherwise specified; in mm). TL (n = 12) 1.46–1.70 (1.62 ± 0.08), SY 0.16–0.19 (0.18 ± 0.01), HW 0.46–0.51 (0.49 ± 0.02), IS 0.20–0.24 (0.22 ± 0.01), WA 0.13–0.17 (0.15 ± 0.01), PL 0.59–0.68 (0.64 ± 0.03), PA 0.50–0.58 (0.54 ± 0.03), PB 0.89–1.06 (0.98 ± 0.06), SL 0.02–0.03 (0.02 ± 0), EI 0.95–1.13 (1.04 ± 0.06), EL 1.06–1.19 (1.13 ± 0.04), EW 0.54–0.6 (0.57 ± 0.02), EH 0.39–0.46 (0.43 ± 0.03), Me 0.24–0.27 (0.25 ± 0.01), MeL 0.04–0.05 (0.04 ± 0), MeW 0.10–0.11 (0.10 ± 0.01), MB 0.19–0.23 (0.21 ± 0.02), MC 0.30–0.39 (0.33 ± 0.04), ML 0.03–0.04 (0.03 ± 0.01), MA 0.01–0.04 (0.03 ± 0.01), VL 0.26–0.31 (0.28 ± 0.02), VL2 0.28–0.34 (0.30 ± 0.02), PrF 0.41–0.47 (0.45 ± 0.02), PrT (n = 6) 0.28–0.40 (0.32 ± 0.04), MsF 0.43–0.47 (0.46 ± 0.01), MsT 0.38–0.45 (0.42 ± 0.03), MtF 0.47–0.54 (0.5 ± 0.02), MtT 0.47–0.54 (0.50 ± 0.02).

Host

Collected from undetermined resupinate and/or crust fungi (Fig. 93E–F).

Remarks

The punctation of submeso- and submetacoxal lines, the sutural and basal striae are similar to *S. repandum* Casey, 1893. Nonetheless, *S. peculiare* sp. nov. can be easily distinguished by the unusual shape of the last maxillary palpomere and more variable body length range.

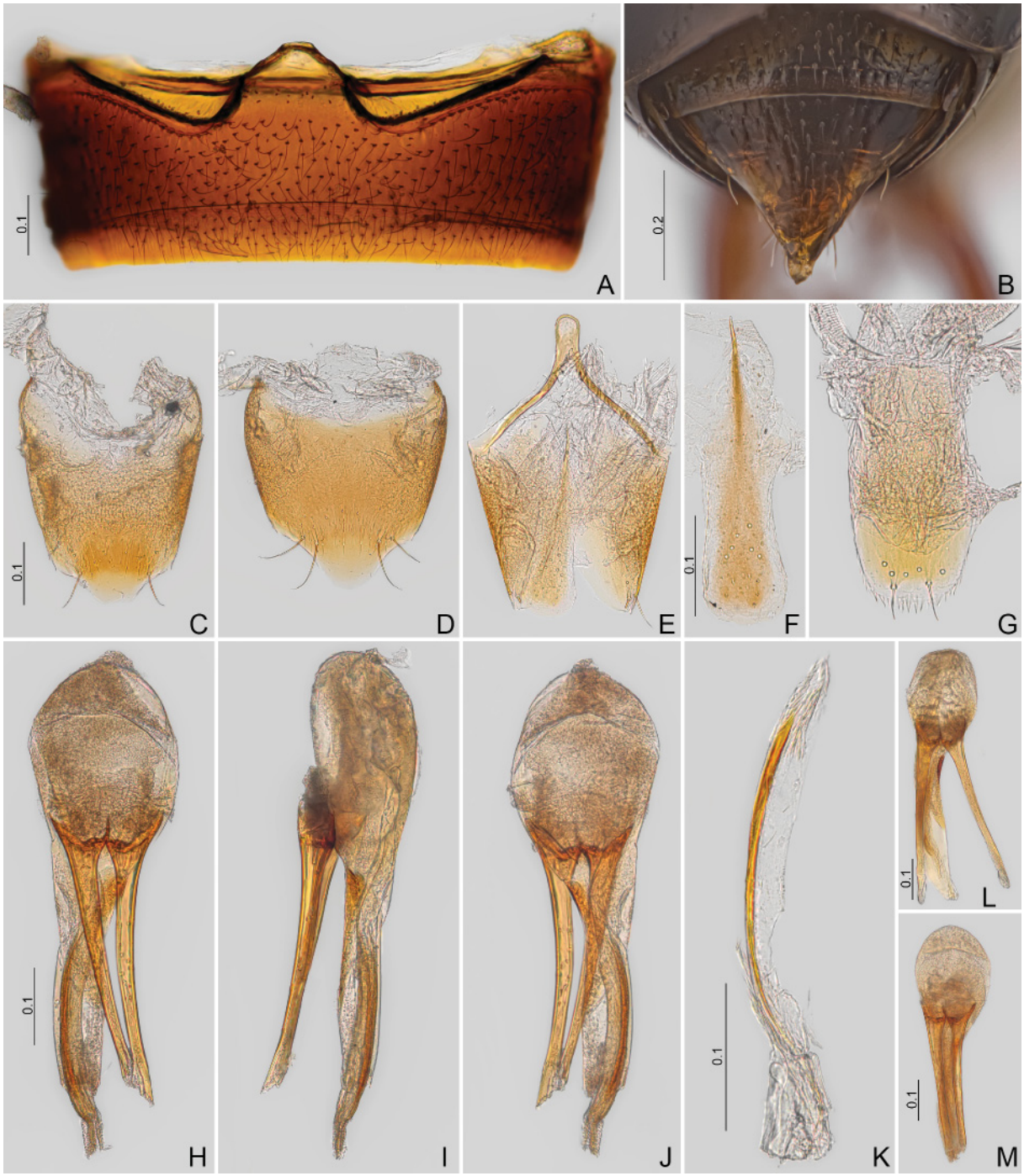

Fig. 63. *Scaphisoma peculiare* sp. nov. (CELC). **A**. Paratype, ♂ (#236), ventrite I. **B**. Holotype, ♂, abdomen, dorsal view. **C–K**. Paratype, ♂ (#236). **C**. Sternite VIII. **D**. Tergite VIII. **E**. Tergite IX. **F**. Sternite IX. **G**. Tergite X. **H–M**. Aedeagus. **H**. Frontal view. **I**. Lateral view. **J**. Dorsal view. **K**. Sclerite of internal sac. **L**. Paratype, ♂ (#202), frontal view. **M**. Paratype, ♂ (#215), frontal view. Scales in mm.

Fig. 64. *Scaphisoma peculiare* sp. nov. (CELC). **A–C**. Paratype, ♀ (#234) (CELC). **A**. Dorsal view. **B**. Lateral view. **C**. Ventral view. **D–I**. Paratype, ♀ (#220). **D–F**. Legs. **D**. Fore. **E**. Middle. **F**. Hind. **G–I**. Tarsi. **G**. Pro. **H**. Meso. **I**. Meta. **J**. Paratype, ♀ (#234), abdomen, dorsal view. **K–N**. Paratype, ♀ (#220). **K**. Sternite VIII. **L**. Tergite VIII. **M**. Genitalia. **N**. Ovipositor. Scales in mm.

Distribution

Mata da Biologia, Universidade Federal de Viçosa, campus of Viçosa, state of Minas Gerais, Southeast Brazil (Fig. 1A–D).

Genus ***Toxidium*** LeConte, 1860

Figs 2I, K, 65–92

Toxidium LeConte, 1860: 324. Type species: *Toxidium gammaroides* LeConte, 1860; by monotypy.

Toxidium comprises only 34 described species, of which seven are from the Neotropical Region. Only *T. acuminatum* Pic, 1920c is reported to Brazil. In this paper, seven new species are described for Minas Gerais, Brazil. These new species represent just about half of the collected species.

General description (* = variable characters within the genera, but not variable in the species below; Löbl & Leschen 2003b; Leschen & Löbl 2005)

Body compressed laterally (Figs 2K, 65A).

Head. Frontoclypeal suture present (Fig. 65H). Labral setae simple (Fig. 66A). Mandibles with two apical teeth and subapical serrations (Fig. 66B–C). Maxillary palpomeres normal; galea wide, with radulate brush (Fig. 66D). Eyes anteriorly notched (Fig. 65I). Antennomeres III and IV elongate (Fig. 65J).

Prothorax. Hypomeron visible in lateral view, not extending beyond pronotum (Fig. 65B). Prothoracic carinae prominent. Prothoracic corbiculum absent.

Mesothorax. Median lines absent. Mesoventral space (prepectus) present. Mesoventral lines impunctate, connecting to mesocoxal cavity (Fig. 67B). Secondary lines present (Fig. 67D). Mesoventral process paxillate (Fig. 67C). Mesepimeron absent (Fig. 71B). Meso- and metaventrite not fused (Fig. 67B).

Metathorax. Mesocoxal lines parallel to coxae, impunctate (Fig. 67D). Lacking metaventral setose patch. Intercoxal plates present. Metacoxae contiguous.

Wings. Hind wings developed (Fig. 67L). Elytral basal stria absent*. Sutural striae shortened* (Fig. 2K). Apical serrations on elytra absent.

Legs. Profemoral ctenidium absent. Mesotibiae with two apical spines, very distinct in length (Fig. 90F). Metatarsi about as long as metatibiae (Fig. 65B).

Abdomen. Submetacoxal space absent. Submetacoxal bead punctate (Fig. 72D). Membranes of abdominal ventrites with brick-wall pattern (Fig. 86H).

Toxidium brigadeirense sp. nov.

urn:lsid:zoobank.org:act:60631403-F38E-4222-8688-A789842C7CCE

Figs 1A–B, 65–70

Diagnosis

Body length: 2.18–2.33 mm. Dark brown, some areas dark reddish; femora and tibiae wine red; tarsi yellow. Shining; strongly curved in lateral view. Sutural striae extending from the apex to approximately 0.80 of the elytral sutural length; elytral punctation sparse. Pronotum length exceeding hypomeron. Metanepisternal suture almost straight. Metaventrite with few coarse punctures near anapleural lines – absent in some specimens. Posterior region of abdominal ventrite I and ventrites II–VI with imbricate microsculpture. Parameres with a hock-shaped posterior projection. Sclerite of internal sac J-shaped. Distal gonocoxite remarkably elongate.

Etymology

The species epithed is derived from the name of the type locality, Parque Estadual da Serra do Brigadeiro.

Material examined

Holotype

BRAZIL • ♂; Minas Gerais, Araponga; Parque Estadual da Serra do Brigadeiro; 25 Oct. 2015; Araújo, S.L. *et al.* leg.; "/ HOLOTYPUS ♂"; em tronco; CELC. (Fig. 65D–E)

Paratypes

BRAZIL • 1 ♂, 1 ♀ (1 ♂**, 1 ♀*); same collection data as for holotype; 25 Oct. 2015; CELC • 1 ♂*; Viçosa, EPTEA Mata do Paraíso; 7 Apr. 2022; E. von Groll and C. Lopes-Andrade leg.; "Falcon 03 / Em Fungo branco ressupinado no tronco caído"; CELC.

Description

Colouration. Dark brown; some areas dark reddish; antennae, maxillary and labial palpomeres, tarsi, and apical ventral segments and elytra yellow; mouthparts, coxae, femora, and tibiae wine red (Fig. 65A–C, H). Variation: brown with lighter tonalities – not reddish (Fig. 65F–G).

Head (Figs 65H–L, 66A–E). Frons densely and moderately coarse punctate; pubescence dense. Clypeus almost squared (Fig. 65I). Mandibles strongly curved (Fig. 66B–C). Last maxillary palpomere about 4× as long as wide; lacinia with moderately dense apical and basal pubescence (Fig. 66D). Last labial palpomere short and thick; mentum concave posteriorly (Fig. 66E). Gular pores absent; gular region strigulate microsculptured. Antennomere XI elongate (Fig. 65J–L); antennomere proportions (n = 3) I 115/47 : II 106/52 : III 85/21 : IV 125/19 : V 138/21 : VI 115/22 : VII 150/36 : VIII 97/24 : IX 134/40 : X 130/37 : XI 155/39.

Prothorax (Fig. 66F–J). Pronotum strongly convex in lateral view (Fig. 65B); anterior bead (Fig. 66G) not visible in dorsal view (Fig. 66F) due to its curvature; shining; punctures moderately coarse and sparse; pubescence moderately sparse. Posterior angle trespassing hypomeron and not reaching anapleural line, in lateral view (Fig. 65G). Prosternal process spinose (Fig. 66H). Notosternal suture slightly curved (Fig. 66I). Profurca slightly curved and tapering towards apex (Fig. 66J).

Mesothorax (Fig. 67A–E). Scutellum not visible in dorsal view (Fig. 66F); mesonotum strongly sclerotized (Fig. 67A); tip rounded. Mesanepisternum with finely punctate; pubescence moderately dense (Fig. 67D). Mesoventral lines straight (Fig. 67B); secondary lines curved (Fig. 67D). Mesoventral process with an apical ridge curved downwards in lateral view (Fig. 67C).

Metathorax (Fig. 67B–H). Metaventrite shining, finely punctate, almost glabrous, and with coarse punctures near anapleural line (Fig. 67D) – sometimes absent (Fig. 67E); central region with imbricate microsculpture (Fig. 67D). Submesocoxal slightly sinuous, laterally, and connected at midline, forming a very acute angle; submesocoxal area with imbricate microsculpture; length: 0.07–0.09 mm (Fig. 67B, D). Metanepisternal suture impunctate, strongly marked, and straight; metanepisternum mostly covered by elytra (Fig. 67C–E). Metanotum with triangular and small alacrista; scutoscutellar suture laterally curved, trespassing apodeme (Fig. 67F). Stalk of metendosternite distinctly narrow anteriorly and widening towards arms (Fig. 67G).

Wings (Figs 65A–C, 67I–L). Elytra with punctures moderately coarse and denser than pronotum. Sutural striae shortened, extending from the apex to approximately 0.80 of the elytral sutural length (Fig. 66F). Lateral striae fine, impunctate, and curved near humeral region (Fig. 65B).

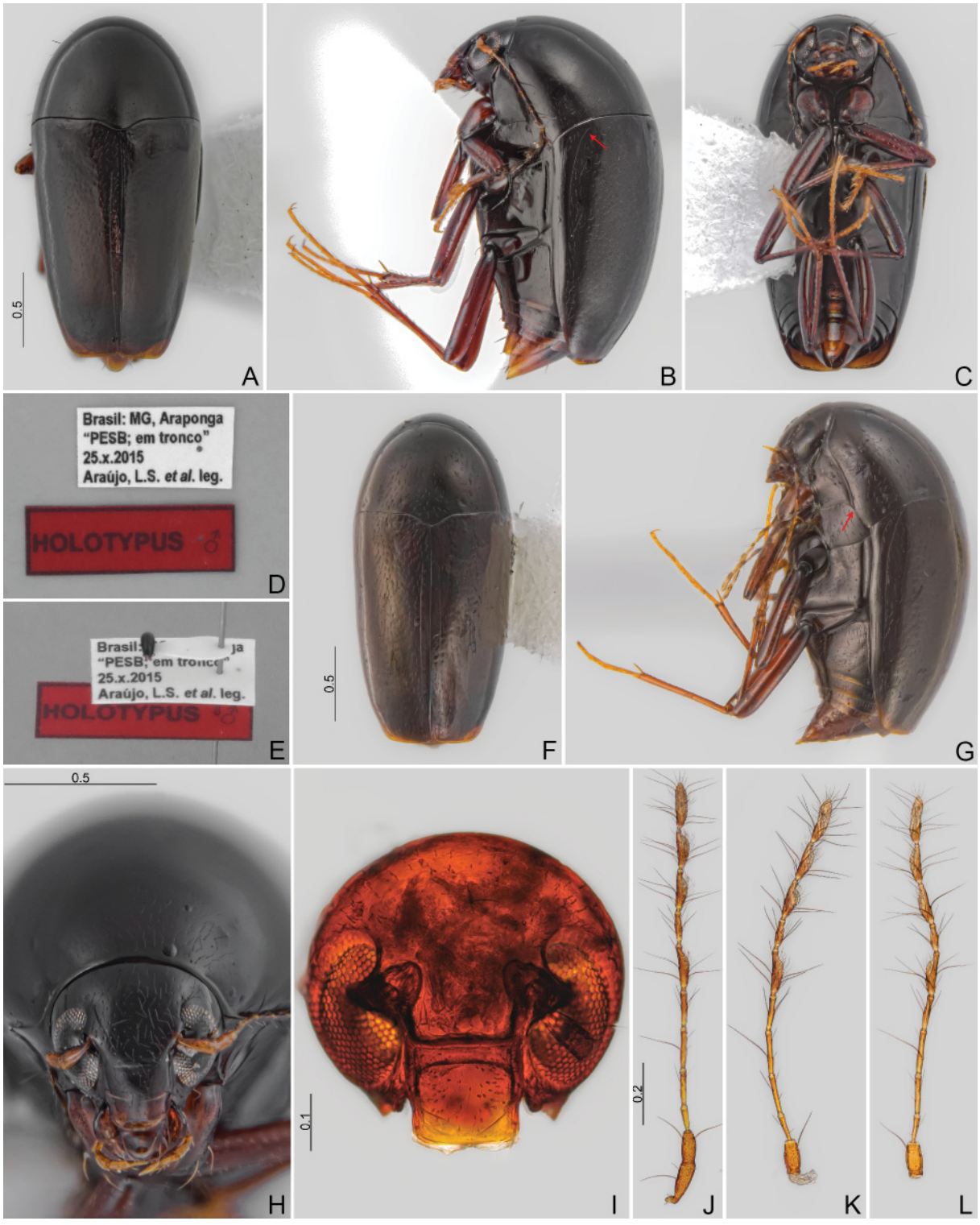

Fig. 65. *Toxidium brigadeirense* sp. nov. (CELC). **A–E**. Holotype, ♂. **A**. Dorsal view. **B**. Lateral view, arrow: curvature of lateral striae. **C**. ventral view. **D**. Labels. **E**. Pinned. **F–G**. Paratype, teneral (#09). **F**. Dorsal view. **G**. Lateral view, arrow: lateral carinae. **H–I**. Head, frontal view. **H**. Holotype, ♂. **I**. Paratype, ♂ (#12). **J–L**. Antennae. **J**. Paratype, ♂ (#12). **K**. Paratype, ♀ (#11). **L**. Paratype, ♂ (#09, Viçosa, MG). Scales in mm.

Legs (Fig. 68A–F). Meso- and metafemora and tibiae very elongate and slender; with imbricate microsculpture.

Abdomen. Ventral surface almost glabrous; posterior area of ventrite I, ventrites II–VI, with imbricate microsculpture (Fig. 67D–E). Pro- and pygidium with sparse pubescence and conspicuously microsculptured (Fig. 68H).

Males

Protarsomeres I–III widened, bearing tenent setae (Fig. 68D). Sternite VIII elongate, bearing a wide posterior projection (Fig. 68I). Tergite VIII narrow, with a small posterior projection (Fig. 68J). Tergite IX with ventral struts strongly curved (Fig. 68K). Sternite IX with laterals slightly curved (Fig. 68L). Tergite X triangular (Fig. 68M).

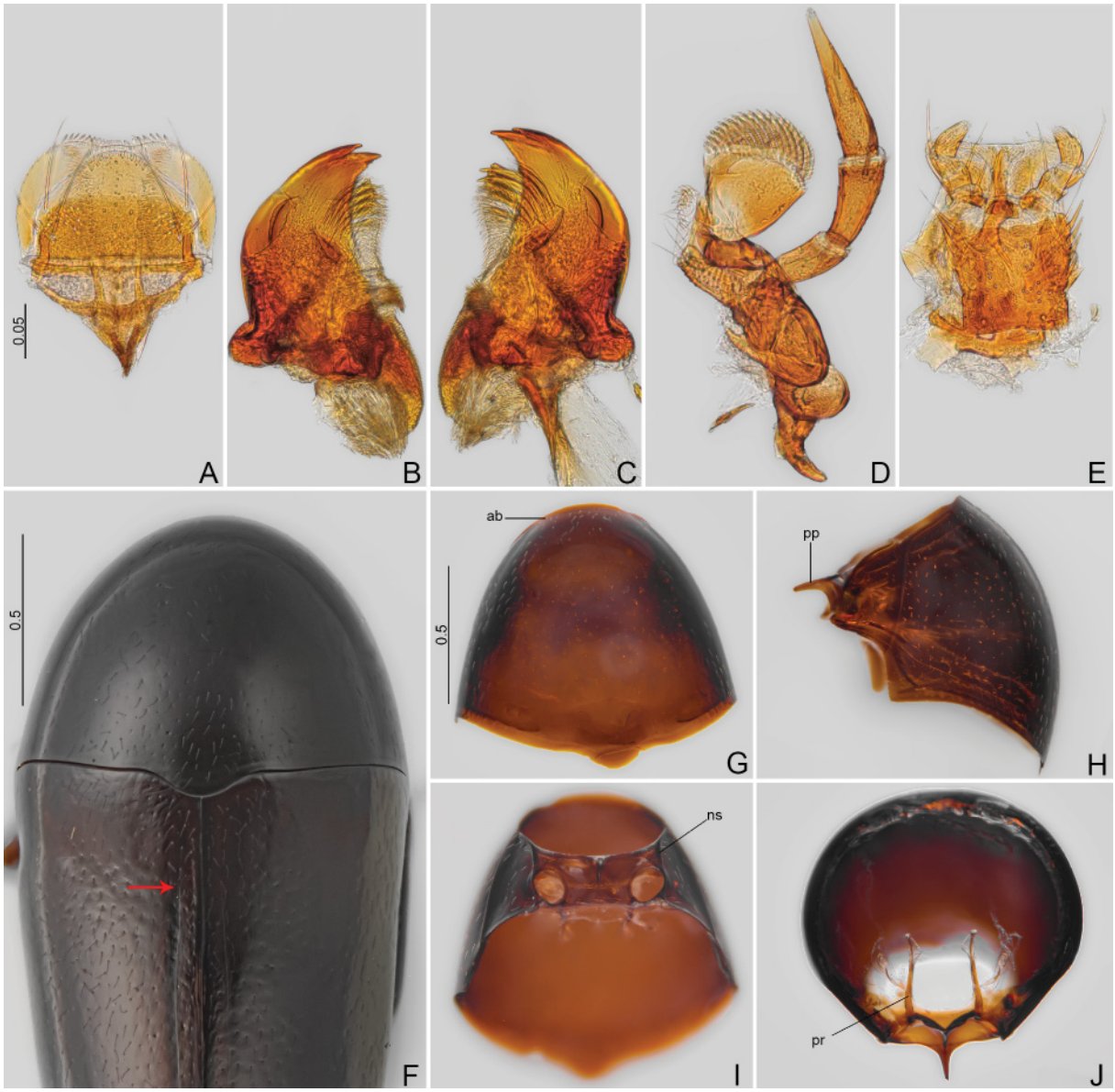

Fig. 66. *Toxidium brigadeirense* sp. nov. (CELC). **A–E**. Paratype, ♂ (#12). **A**. Labrum. **B–C**. Mandibles. **D**. Maxilla. **E**. Labium. **F**. Holotype, ♂, prothorax, dorsal view. **G–J**. Paratype, ♂ (#12), prothorax. **G**. Dorsal view. **H**. Lateral view. **I**. Ventral view. **J**. Inner view. Abbreviations: ab = anterior bead; ns = notosternal suture; pp = prosternal process; pr = profurca. Scales in mm.

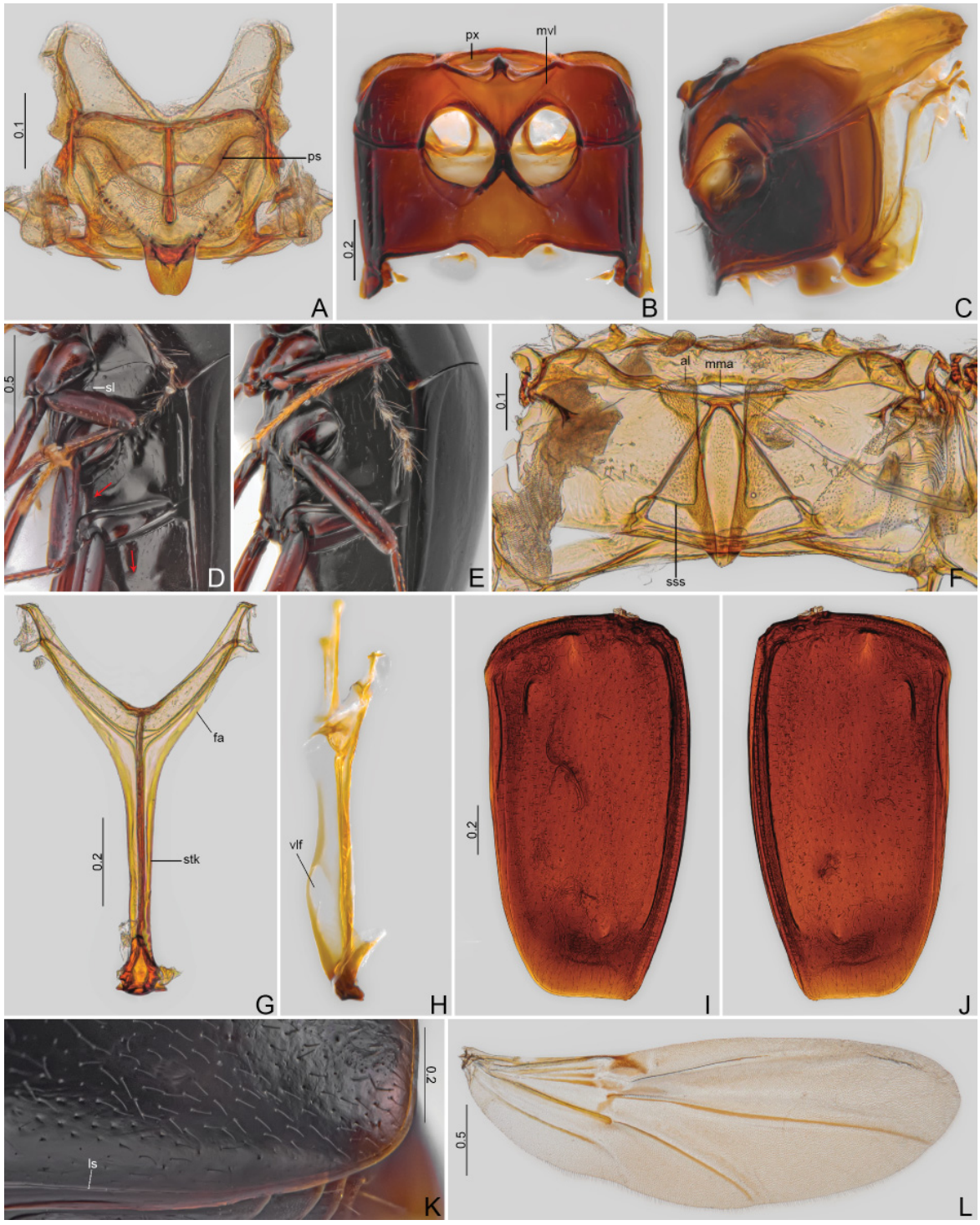

Fig. 67. *Toxidium brigadeirense* sp. nov. (CELC). **A–C**. Paratype, ♂ (#12). **A**. Scutellar shield. **B–E**. Meso- and metathorax. **B**. Ventral view. **C**. Lateral view. **D**. Holotype, ♂, oblique view, arrows: microsculptured areas. **E**. Paratype, ♀ (#11), oblique view. **F–J**. Paratype, ♂ (#12). **F**. Metanotum. **G–H**. Metendosternite. **G**. Dorsal view. **H**. Lateral view. **I–K**. Elytra. **I**. Left. **J**. Right. **K**. Holotype, ♂, lateral, apical area. **L**. Paratype, ♂ (#12), hind wing. Abbreviations: al = alacrista; fa = furcal arms; ls = lateral stria; mma = median membranous area; mvl = mesoventral line; ps = prescutellar line; px = procoxal rest; sl = sutural line; sss = scutoscutellar suture; stk = stalk; vlf = ventral longitudinal flange. Scales in mm.

Aedeagus (Fig. 69). Median lobe with basal bulb and apical lobe almost indistinct, just slightly curved in lateral view, and membranous. Apical lobe triangular, in frontal/dorsal view. Parameres bearing a curved and elongate posterior projection (Fig. 69C, G). Sclerite of internal sac J-shaped (Fig. 69D, H).

Measurements (n = 3, including holotype, unless otherwise specified; in mm; * = invariant). TL 2.18–2.33 (2.25 ± 0.08), SY 0.27–0.30 (0.28 ± 0.02), HW 0.86–0.89 (0.88 ± 0.02), IS 0.33–0.43 (0.39 ± 0.05),

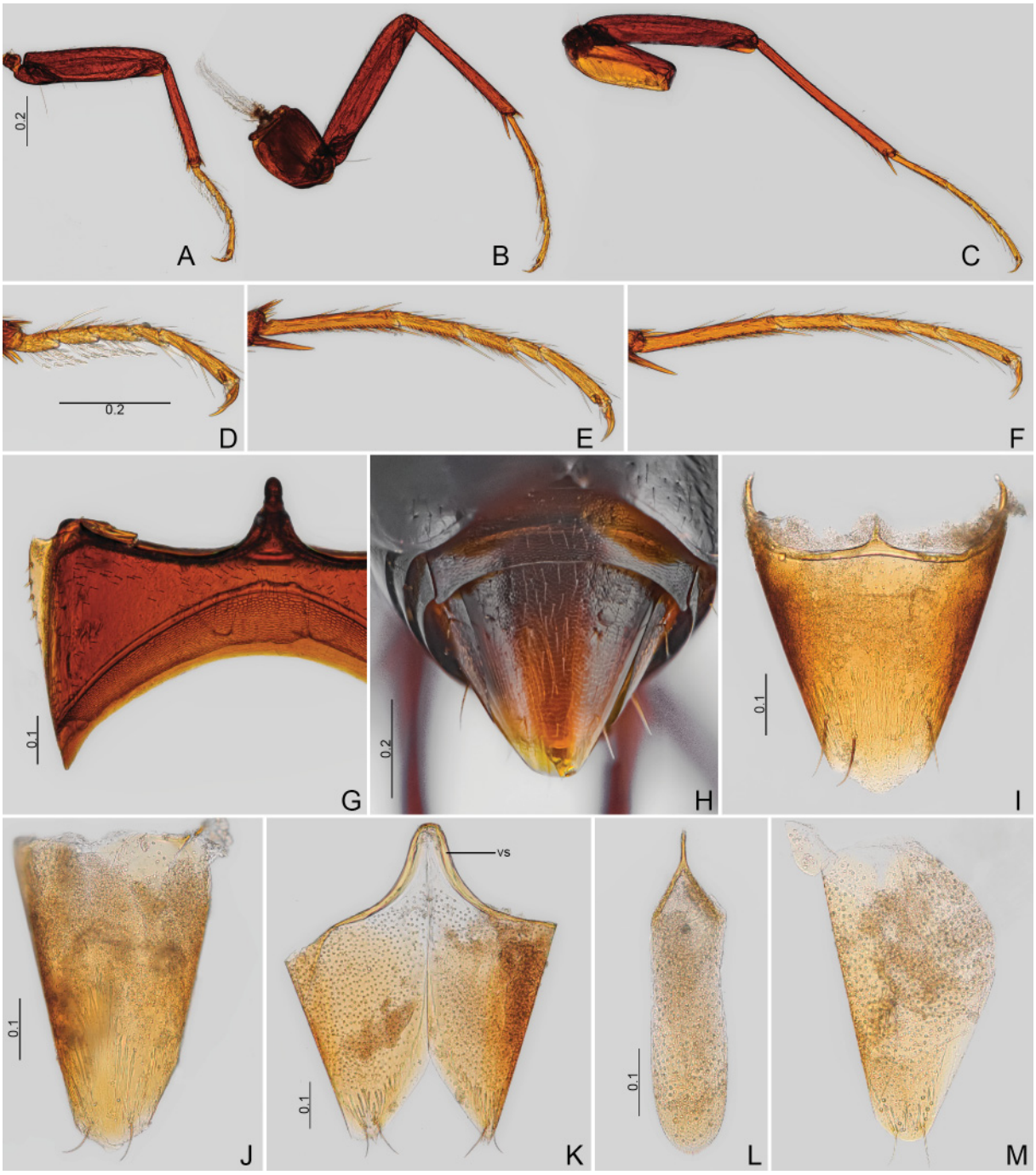

Fig. 68. *Toxidium brigadeirense* sp. nov. (CELC). **A–G**. Paratype, ♂ (#12). **A–C**. Legs. **A**. Fore. **B**. Middle. **C**. Hind. **D–F**. Tibiae. **D**. Pro. **E**. Meso. **F**. Meta. **G**. Ventrite I. **H**. Holotype, ♂, abdomen, dorsal view. **I–M**. Paratype, ♂ (#12). **I**. Sternite VIII. **J**. Tergite VIII. **K**. Tergite IX. **L**. Sternite IX. **M**. Tergite X. Abbreviation: vs = ventral strut. Scales in mm.

WA 0.22–0.25 (0.24±0.02), PL 0.84–1.00 (0.93±0.08), PA 0.59–0.61 (0.60±0.01), PB 1.02–1.20 (1.10±0.09), EI 1.48–1.52 (1.49±0.02), EL 1.58–1.68 (1.62±0.05), EW 0.53–0.55 (0.54±0.01), EH 0.70–0.78 (0.73±0.05), MB 0.12–0.15 (0.14±0.02), MC 0.11–0.16 (0.13±0.02), MeW (n=1) 0.35, ML 0.07–0.09 (0.08±0.01), VL 0.25–0.27 (0.26±0.01), VL2 0.43*, PrF 0.59–0.63 (0.61±0.02), PrT

Fig. 69. *Toxidium brigadeirense* sp. nov. (CELC). **A–H**. Aedeagus. **A–E**. Paratype, ♂ (#12). **A**. Frontal view. **B**. Lateral view. **C**. Dorsal view, arrow: posterior projection. **D–E**. Sclerite of internal sac. **D**. Lateral view. **E**. Frontal view. **F–H**. Paratype, ♂ (#09, Viçosa, MG). **F**. Frontal view. **G**. Lateral view, arrow: posterior projection. **H**. Sclerite of internal sac. Abbreviation: scl = sclerite of internal sac. Scales in mm.

(n = 2) 0.42–0.43 (0.43 ± 0.01), MsF 0.67–0.75 (0.70 ± 0.04), MsT 0.60–0.65 (0.62 ± 0.03), MtF 0.72–0.77 (0.75 ± 0.03), MtT 0.57–0.78 (0.68 ± 0.11).

Females (Fig. 70)

Ventrite VIII with a thin posterior projection (Fig. 70A). Tergite VIII with a small posterior projection (Fig. 70B). Distal gonocoxite very long, slightly tapering posteriorly; gonostylus elongate and slightly oblong (Fig. 70D–E).

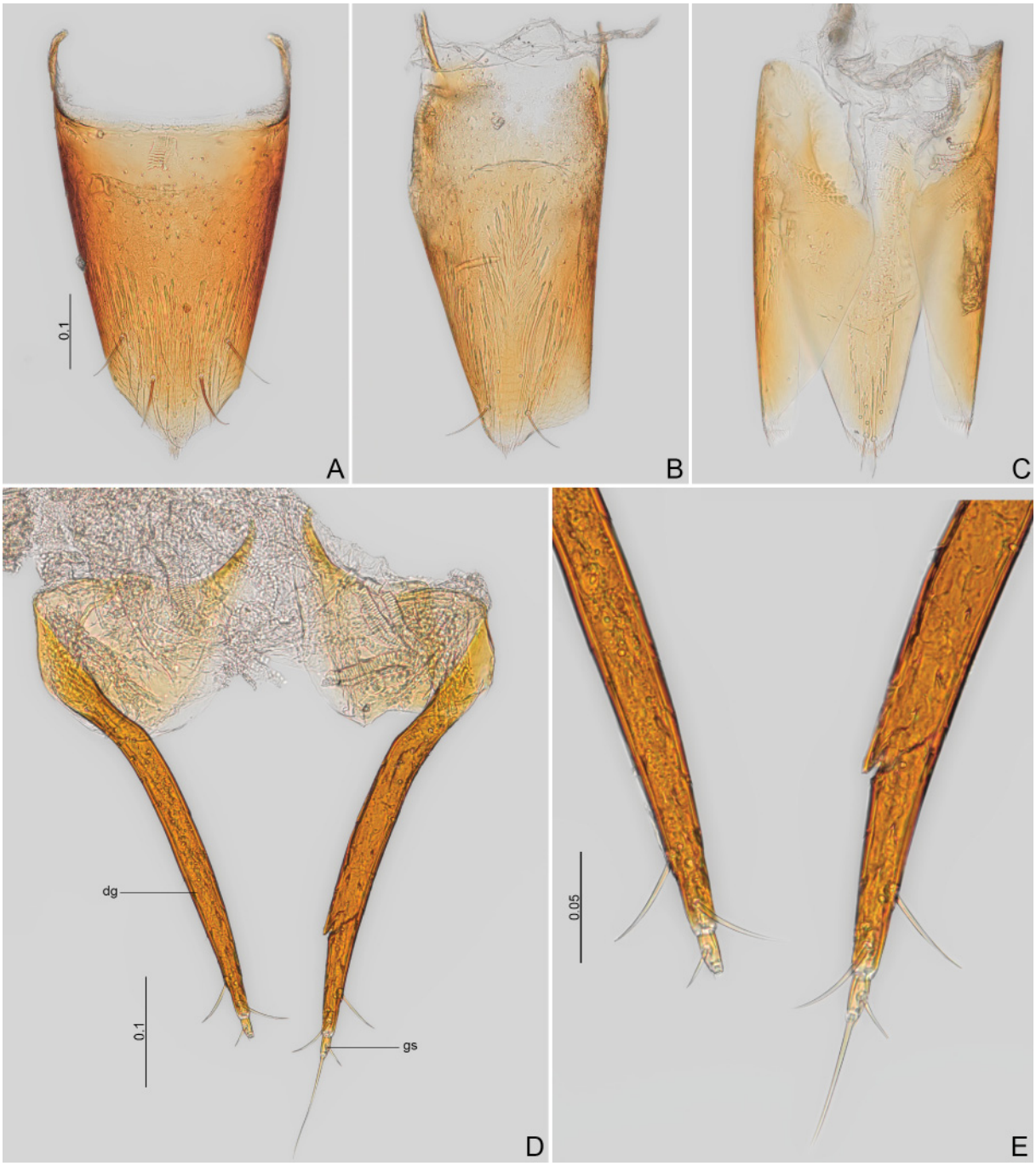

Fig. 70. *Toxidium brigadeirense* sp. nov., paratype, ♀ (#11) (CELC). **A**. Sternite VIII. **B**. Tergite VIII. **C**. Tergite IX. **D**. Genitalia. **E**. Ovipositor. Abbreviations: dg = distal gonocoxites; gs = gonostyli. Scales in mm.

Measurements (n = 1; in mm). TL 2.30, SY 0.30, HW 0.89, IS 0. 43, WA 0.25, PL 1.04, PA 0.63, PB 1.17, EI 1.56, EL 1.64, EW 0.52, EH 0.73, MB 0.14, MC 0.11, MeW 0.38, ML 0.07, VL 0.27, VL2 0.45, PrF 0.64, PrT 0.45, MsF 0.72, MsT 0.58, MtF 0.76, MtT 0.70.

Host

In Viçosa, collected from undetermined crust/resupinate fungi on logs.

Remarks

The sclerite of the internal sac is similar to the ones observed in *T. scalenum* sp. nov., *T. inusitatum* sp. nov., and *T. ultimum* sp. nov. However, this species can be easily distinguished by the following combination: the shortened hypomeron compared to pronotum, the strongly curved pronotum in lateral view, and the presence of posterior projections on the parameres.

Distribution

Mata do Paraíso, Universidade Federal de Viçosa, campus of Viçosa and from Araponga, state of Minas Gerais, Southeast Brazil (Fig. 1A–B).

Toxidium distortum sp. nov.
urn:lsid:zoobank.org:act:21F66F90-DE46-4DC0-8F72-71092A9F3DF4
Figs 1A–D, 71–73, 93E–F

Diagnosis

Body length: 1.88 mm. Brown. Ventral side almost glabrous. Sutural striae extending from apex to approximately 0.89 of the sutural length. Metaventrite I with few coarse punctures next to the submesocoxal lines. Metanepisternal suture sinuous. Abdominal ventrite I with micropunctures on the central region. Parameres of the aedeagus sinuous in lateral view; sclerite asymmetrical.

Etymology

The species epithet is a Latin word meaning ‘twisted’, due to the internal sac shape.

Material examined

Holotype

BRAZIL • ♂*; Minas Gerais, Viçosa, Mata da Biologia; 23 Nov. 2021; E. von Groll and G.L.N. Marins leg.; “/ Em Fungo branco ressupinado no tronco caído / Dissecado em 12.xi.2022 / HOLOTYPUS ♂”; CELC. (Fig. 71D–E)

Description

Colouration. Brown; mouthparts, antennae, and tibiae yellow; anterior part of femora dark ochreous; posterior tip of femora, tibiae, elytral apex, and apex of each abdominal ventrite, ochreous (Fig. 71A–C, F).

Head. Frons with punctures moderately sparse and coarse, and with some micropunctures; pubescence moderately dense (Fig. 71F). Antennomere XI elongate; antennomere proportions (Fig. 71H): I missing : II 107/41 : III 69/20 : IV 90/18 : V 104/18 : VI 100/16 : VII 121/36 : VIII 90/22 : IX 115/35 : X 115/36 : XI 157/42.

Prothorax. Smooth; punctures fine; pubescence moderately sparse (Fig. 71G). Hypomeron with punctures very fine and pubescence sparse (Fig. 71B). Posterior angle of pronotum somewhat acute, almost reaching anapleural line (Fig. 71B).

Mesothorax. Tip of scutellum just partially exposed (Fig. 71G). Mesanepisternum finely punctate; pubescence sparse (Fig. 71B). Mesoventral lines slightly sinuous; secondary straight (Figs 71B, 72A).

Metathorax. Metaventrite smooth, shining, with few lateral pubescence; punctures inconspicuous; few coarse punctures next to submesocoxal lines (Fig. 71B). Submesocoxal lines partially straight laterally, and connected at midline, forming an obtuse angle; submesocoxal area length: 0.09 mm (Fig. 71B). Metanepisternal suture sinuous (Fig. 72A).

Fig. 71. *Toxidium distortum* sp. nov., holotype, ♂ (CELC). **A**. Dorsal view. **B**. Lateral view. **C**. Ventral view. **D**. Labels. **E**. Pinned. **F**. Head, frontal view. **G**. Prothorax, dorsal view. **H**. Antenna. Scales in mm.

Wings (Figs 71A–C, 72B). Elytra moderately dense and coarse punctate – more than pronotum. Sutural striae just slightly shortened, extending from apex to approximately 0.89 of the elytral sutural length (Fig. 71A). Lateral striae impunctate, slightly curved at humeral region, and reaching elytral border (Fig. 71B).

Legs. With imbricate microsculpture (Fig. 72C–D).

Fig. 72. *Toxidium distortum* sp. nov., holotype, ♂ (CELC). **A**. Meso- and metathorax; oblique view. **B**. Elytra apex, dorsal view. **C–D**. Legs. **C**. Fore. **D**. Middle and hind. **E**. Abdomen, dorsal view. **F**. Ventrite VIII. **G**. Tergite VIII. **H**. Tergite IX. **I**. Sternite IX. **J**. Tergite X. Scales in mm.

Abdomen. Central region of ventrite I and propygidium micropunctured; ventral surface almost glabrous (Figs 71B, 72D). Pro- and pygidium with some coarse punctures, moderately pubescent, and micropunctured (Fig. 72E).

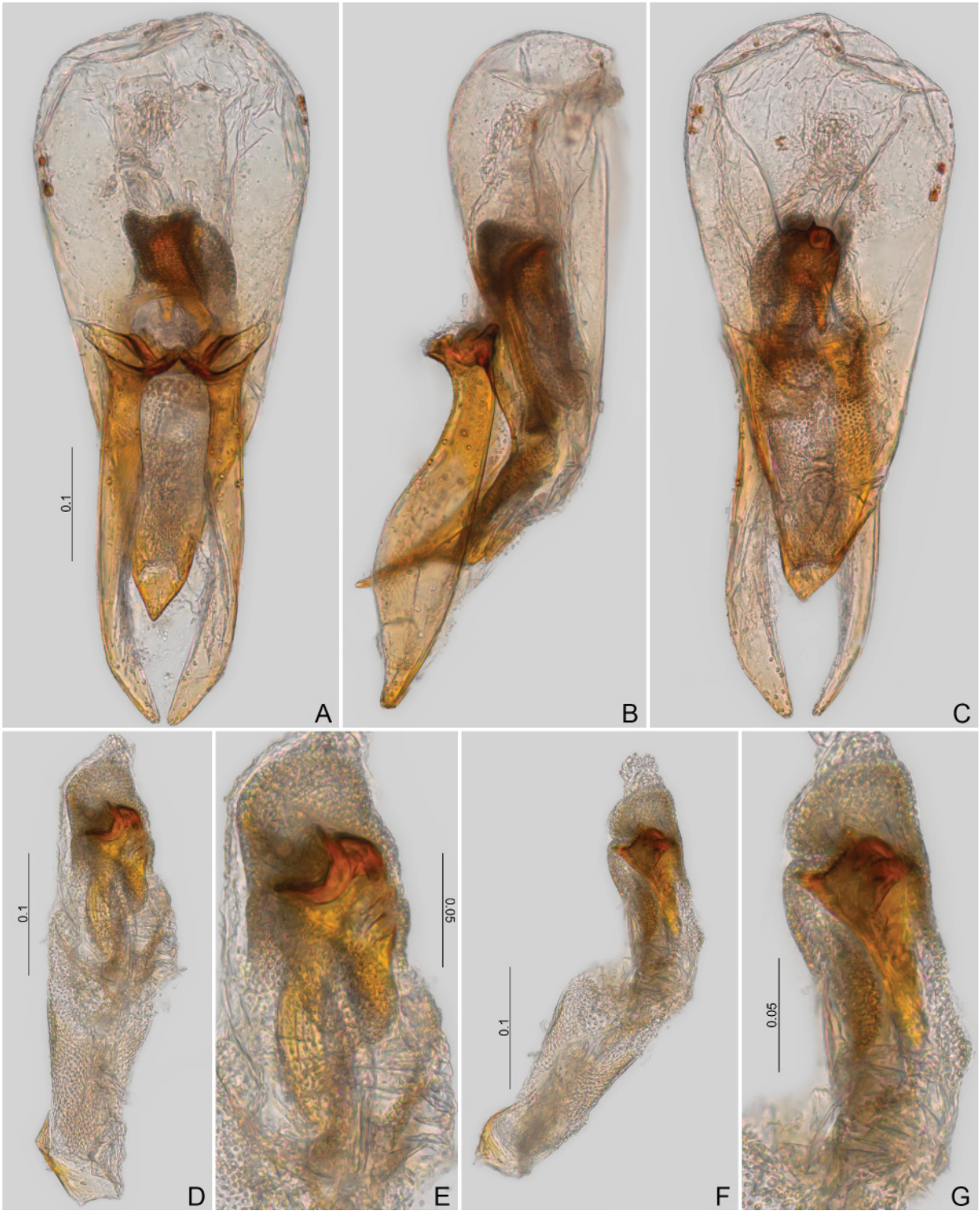

Fig. 73. *Toxidium distortum* sp. nov., holotype, ♂, aedeagi (CELC). **A**. Frontal view. **B**. Lateral view. **C**. Dorsal view. **D–G**. Sclerite of internal sac. **D–E**. Frontal views. **F–G**. Lateral views. Scales in mm.

Male

Protarsomeres I–III widened, bearing tenent setae (Fig. 72C). Sternite VIII shortened, bearing a triangular posterior projection (Fig. 72F). Tergite VIII with a wide posterior projection (Fig. 72G). Tergite IX with ventral struts almost straight (Fig. 72H). Sternite IX widened posteriorly (Fig. 72I). Tergite X triangular (Fig. 72J).

Aedeagus (Fig. 73). Basal bulb longer than apical lobe; apical lobe curved, just slightly sclerotized. Parameres sinuous and with strigulate microsculptures (Fig. 73B); sclerite of internal sac asymmetrical (Fig. 73D–G).

Measurements (n = 1, holotype; in mm). TL 1.88, SY 0.24, HW 0.78, IS 0.34, WA 0.17, PL 0.82, PA 0.53, PB 1.02, EI 1.22, EL 1.36, EW 0.55, EH 0.55, MB 0.24, MC 0.11, ML 0.09, PrF 0.49, PrT 0.34, MsF 0.59, MsT 0.44, MtF 0.60, MtT 0.54.

Host

Collected from an undetermined crust fungus (Fig. 93E–F).

Remarks

Similar to *T. ultimum* sp. nov. but differs by the shorter submesocoxal area, the absence of microsculpture on ventrite I, the dilatated parameres in lateral view, and by the asymmetrical sclerite of internal sac.

Distribution

Mata da Biologia, Universidade Federal de Viçosa, campus of Viçosa, state of Minas Gerais, Southeast Brazil (Fig. 1A–D).

Toxidium fleche sp. nov.
urn:lsid:zoobank.org:act:5B5CBA25-EFEF-41D5-9504-1D7B293BFCBA
Figs 1A–D, 74–76, 94E–F

Diagnosis

Body length: 1.90 mm. Dark brown. Dorsal surface pubescence very dense. Metaventrite coarsely punctate laterally. Metanepisternum triangular, wider next to the mesanepisternum. Aedeagus with parameres remarkably sinuous in lateral view. Sclerite of internal sac arrow-shaped.

Etymology

The species name is a French noun in apposition, meaning ‘arrow’, due to the arrow-shaped sclerite of the internal sac.

Material examined

Holotype

BRAZIL • ♂*; Minas Gerais, Viçosa, Mata da Biologia; 15 Oct. 2021; E. von Groll and A. Orsetti leg.; “Fungo 30 / Em Fungo branco ressupinado no tronco caído / Dissecado em 11.nov.2022 / HOLOTYPUS ♂”; CELC. (Fig. 74D–E)

Description

Colouration. Dark brown; clypeus, coxae, femora, and tibiae dark ochreous; antennae, mouthparts, tip of elytra, and apex of each abdominal ventrite yellow (Fig. 74).

Head. Frons with fine and dense punctures; pubescence dense; clypeus micropunctured. Antennomeres III–VI somewhat thicker, IX about 3.20 × as long as VIII, XI, oblong (Fig. 74H); proportions: I 115/38 : II 101/45 : III 58/18 : IV 76/16 : V 90/18 : VI 88/18 : VII 110/32 : VIII 70/21 : IX 110/33 : X 115/35 : XI 146/47.

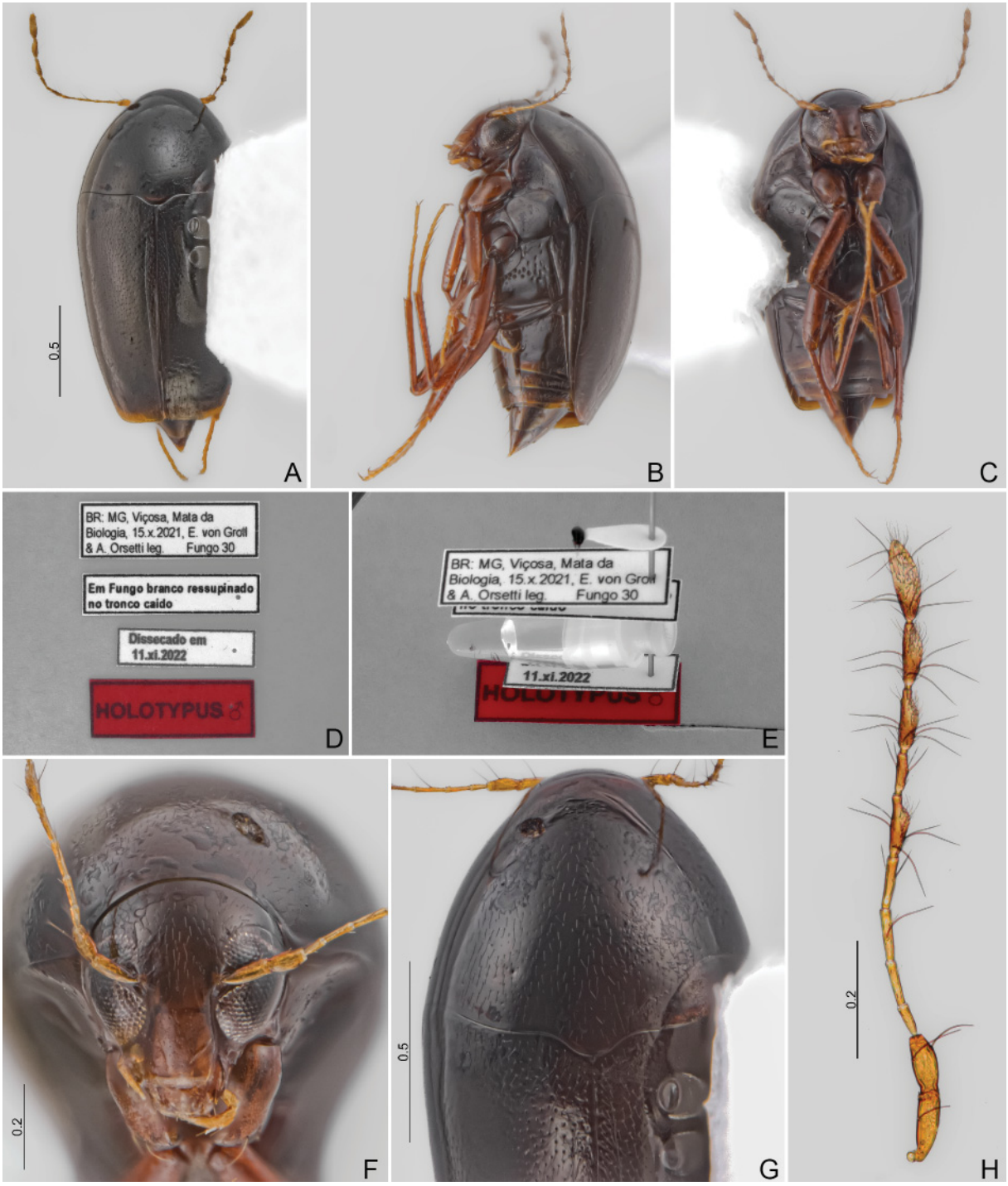

Fig. 74. *Toxidium fleche* sp. nov., holotype, ♂ (CELC). **A**. Dorsal view. **B**. Lateral view. **C**. Ventral view. **D**. Labels. **E**. Pinned. **F**. Head, frontal view. **G**. Prothorax, dorsal view. **H**. Antenna. Scales in mm.

Prothorax. Pronotum not strongly curved in lateral view; finely and densely punctate, pubescence dense (Fig. 74G). Posterior angles of pronotum slightly acute, reaching anapleural line (Fig. 74B).

Mesothorax. Tip of scutellum exposed (as long as wide) (Fig. 74G). Mesanepisternum with inconspicuous punctation, pubescence sparse (Fig. 74B). Secondary lines straight, not connected to mesocoxal cavities (Fig. 74B).

Fig. 75. *Toxidium fleche* sp. nov., holotype, ♂ (CELC). **A**. Meso- and metathorax; oblique view. **B**. Elytra apex, dorsal view. **C–D**. Legs. **C**. Fore. **D**. Middle and hind. **E**. Abdomen, dorsal view. **F**. Ventrite VIII. **G**. Tergite VIII. **H**. Tergite IX. **I**. Sternite IX. **J**. Tergite X. Scales in mm.

Fig. 76. *Toxidium fleche* sp. nov., holotype, ♂, aedeagi (CELC). **A**. Frontal view. **B**. Lateral view. **C**. Dorsal view. **D**. Parameres, lateral view. **E–F**. Sclerite of internal sac. **E**. Frontal view. **F**. Lateral view. Scales in mm.

Metathorax. Metaventrite with conspicuous coarse punctures between submesocoxal lines and metanepisternal suture; almost glabrous (Figs 74B, 75A). Submesocoxal lines not sinuous; submesocoxal area with imbricate microsculpture; length: 0.09 mm (Fig. 75A). Metanepisternal suture curved anteriorly; metanepisternum triangular, wider next to the mesanepisternum (Fig. 75A).

Wings. Elytra densely and coarsely punctate – coarser than pronotum; pubescence dense (Fig. 74A, G). Sutural striae not strongly shortened, extending from apex to approximately 0.82 of the elytral sutural length (Fig. 74A). Lateral striae impunctate, slightly curved at humeral region (Fig. 74B).

Legs (Fig. 75C–D). With imbricate microsculpture.

Abdomen. Ventral surface shining, almost glabrous (Fig. 74B). Ventrite I with micropuncture in middle. Propygidium micropunctured (Fig. 75E).

Male

Protarsomeres I–III widened, bearing tenent setae (Fig. 75C). Sternite VIII elongate, with a shallowt posterior projection (Fig. 75F). Tergite VIII straight posteriorly (Fig. 75G). Tergite IX with ventral struts thick and slightly curved (Fig. 75H). Sternite IX oblong (Fig. 75I). Tergite X triangular and rounded posteriorly (Fig. 75J).

Aedeagus (Fig. 76). Median lobe slightly sclerotized; basal bulb longer than apical lobe; apical lobe bent in lateral view (Fig. 76B). Parameres remarkably wide and sinuous in lateral view (Fig. 76D). Sclerite of internal sac arrow-shaped (Fig. 76E–F).

Measurements (n = 1, holotype; in mm). TL 1.88, SY 0.20, HW 0.75, WA 0.11, PL 0.88, PA 0.52, PB 0.95, EI 1.20, EL 1.32, EW 0.55, EH 0.55, MB 0.12, MC 0.14, MeW 0.30, ML 0.09, VL 0.23, VL2 0.35, PrF 0.50, PrT 0.35, MsF 0.57, MsT 0.42, MtF 0.54, MtT 0.53.

Host

Collected from undetermined crust/resupinate fungus (Fig. 94E–F).

Remarks

Similar to *T. robustum* Pic, 1930 due to the dilatated parameres and the not curved sclerite of the internal sac. Nonetheless, *T. fleche* sp. nov. can be easily distinguished by the longer sutural striae and by the absence of the basal ones.

Distribution

Mata da Biologia, Universidade Federal de Viçosa, campus of Viçosa, state of Minas Gerais, Southeast Brazil (Fig. 1A–D).

Toxidium inusitatum sp. nov.
urn:lsid:zoobank.org:act:EB24CEF0-5780-4B6F-A5D2-6119AE21702A
Figs 1A–B, 77–79

Diagnosis

Body length: 1.45 mm. Brown. Posterior angle of pronotum not acute and not trespassing anapleural line; lateral carina sinuous. Metaventrite with coarse and dense punctures under anapleural lines and next to metanepisternal suture. Metanepisternum entirely hidden beneath elytra. Submesocoxal area short = 0.04 mm. Parameres of aedeagus oar-shaped in lateral view; sclerite of internal sac strongly curved.

Etymology

The species epithet is a Latin word meaning ‘unusual’, due to the distinct aedeagus shape.

Material examined

Holotype

BRAZIL • ♂*; Minas Gerais, Viçosa, EPTEA Mata do Paraíso; 12 Nov. 2019; LabCol leg.; “Falcon 01 / Em tronco pequeno caído com hifa indet. / Dissecado em 12.xi.2022 / HOLOTYPUS ♂”; CELC. (Fig. 77D–E)

Fig. 77. *Toxidium inusitatum* sp. nov., holotype, ♂ (CELC). **A**. Dorsal view. **B**. Lateral view. **C**. Ventral view. **D**. Labels. **E**. Pinned. **F**. Head, frontal view. **G**. Prothorax, dorsal view. **H**. Antenna. Scales in mm.

Description

Colouration. Brown, ventral sclerites lighter near sutures; posterior half of clypeus, tip of elytra, coxae, femora, and tibiae ochreous; mouthparts, antennae, tarsi, and apex of each abdominal ventrite yellowish (Fig. 77A–C, F).

Fig. 78. *Toxidium inusitatum* sp. nov., holotype, ♂ (CELC). **A**. Meso- and metathorax; oblique view. **B**. Elytra apex, dorsal view. **C–D**. Legs. **C**. Fore and middle. **D**. Hind. **E**. Abdomen, dorsal view. **F**. Ventrite VIII. **G**. Tergite VIII. **H**. Tergite IX. **I**. Sternite IX. **J**. Tergite X. Scales in mm.

Head. Frons sparsely punctate and pubescent; punctation fine, with some punctures coarser and sparsely distributed. Antennomeres elongate (Fig. 77H); proportions: I 81/41 : II 86/42 : III 49/15 : IV 79/13 : V 93/14 : VI 87/16 : VII 113/24 : VIII 84/20 : IX 116/28 : X 108/33 : XI 137/42.

Prothorax. Pronotum with pubescence and punctures moderately dense (Fig. 77G). Hypomeron with punctures very fine and pubescence sparse (Fig. 77B). Prothoracic carina sinuous in lateral view (Fig. 77B). Posterior angles of pronotum not acute and not reaching anapleural lines (Fig. 77B).

Fig. 79. *Toxidium inusitatum* sp. nov., holotype, ♂, median aedeagi (CELC). **A**. Frontal view. **B**. Parameres, frontal view. **C**. Lateral view. **D**. Parameres, lateral view. **E–F**. Dorsal views. **G–H**. Sclerite of internal sac. **G**. Lateral view. **H**. Frontal view. Scales in mm.

Mesothorax. Tip of scutellum exposed (longer than wide). Mesanepisternum finely punctate, pubescence sparse. Secondary lines sinuous and connected to mesocoxal cavities (Fig. 77B).

Metathorax. Metaventrite lacking microsculpture, shining, almost glabrous; densely and coarsely punctate under anapleural lines and next to metanepisternal suture (Fig. 78A). Submesocoxal lines parallel to coxae; submesocoxal area micropunctured and short, length: 0.04 mm (Figs 77B, 78A). Metanepisternum completely hidden under elytra (Figs 77B, 78A).

Wings (Figs 77A–B, 78B). Elytra with coarse and moderately sparse punctures. Sutural striae shortened, extending from apex to about 0.80 of the elytral sutural length (Fig. 77A). Lateral striae impunctate, slightly curved at humeral region (Fig. 77B).

Legs (Fig. 78C–D). Meso- and metafemora slender, with imbricate microsculpture.

Abdomen. Ventral surface smooth, shining, almost glabrous (Fig. 77B). Propygidium micropunctured and sparsely pubescent (Fig. 78E).

Male

Protarsomeres I–III widened, bearing tenent setae (Fig. 78C). Sternite VIII with a shallow posterior projection (Fig. 78F). Tergite VIII convex posteriorly (Fig. 78G). Tergite IX with curved ventral struts (Fig. 78H). Sternite IX oblong (Fig. 78I). Tergite X rounded curved (Fig. 78J).

Aedeagus (Fig. 79). Membranous. Median lobe lacking obvious divisions between apical lobe and basal bulb; apical lobe curved backwards (Fig. 79C). Parameres without sclerotized anterior portion (that connects to median lobe) and oar-shaped in lateral view (Fig. 79C). Sclerite of internal sac strongly curved (Fig. 79C).

Measurements (n = 1, holotype; in mm). TL 1.46, SY 0.17, HW 0.44, WA 0.07, PL 0.61, PA 0.41, PB 0.74, EI 0.95, EL 0.99, EW 0.36, EH 0.46, MB 0.12, MC 0.04, ML 0.04, VL 0.17, PrF 0.35, PrT 0.29, MsF 0.42, MsT 0.33, MtF 0.52, MtT 0.43.

Host

Collected from a rotten small log, covered with undetermined hyphae.

Remarks

It is similar to *T. ultimum* sp. nov. but differs by the denser and coarser lateral punctures on the metaventrite and by the completely hidden metanepisternum. The aedeagus can be distinguished by the distinctly membranous median lobe, by the parameres shape, and the much longer sclerite of internal sac.

Distribution

Mata do Paraíso, Universidade Federal de Viçosa, campus of Viçosa, state of Minas Gerais, Southeast Brazil (Fig. 1A–B).

Toxidium scalenum sp. nov.
urn:lsid:zoobank.org:act:94F752A7-DBE6-490C-A3CF-2BEEC58756F0
Figs 1A–B, 80–82

Diagnosis

Body length: 1.90 mm. Reddish-brown; legs ochreous. Sutural striae extending from apex to approximately 0.74 of the elytral sutural length. Posterior angle of pronotum not reaching anapleural line.

Submesocoxal area and anterior area of metaventrite with strigulate microsculpture. Metanepisternum conspicuously wider next to the masanepisternum. Sclerite on internal sac of aedeagus J-shaped, long side 2.5 × as long as short side.

Etymology

The species epithet is the Latin adjective, meaning 'scalene', referring to the metanepisternum's scalene triangular shape.

Fig. 80. *Toxidium scalenum* sp. nov., holotype, ♂ (CELC). **A**. Dorsal view. **B**. Lateral view. **C**. Ventral view. **D**. Labels. **E**. Pinned. **F**. Head, frontal view. **G**. Prothorax, dorsal view. **H**. Antenna. Scales in mm.

Material examined

Holotype

BRAZIL • ♂*; Minas Gerais, Viçosa, EPTEA Mata do Paraíso; 17 Mar. 2022; E. von Groll *et al.* leg.; "Falcon 12 / Em Fungo branco ressupinado no tronco caído / Dissecado em 11.nov.2022 / HOLOTYPUS ♂"; CELC. (Fig. 80D–E)

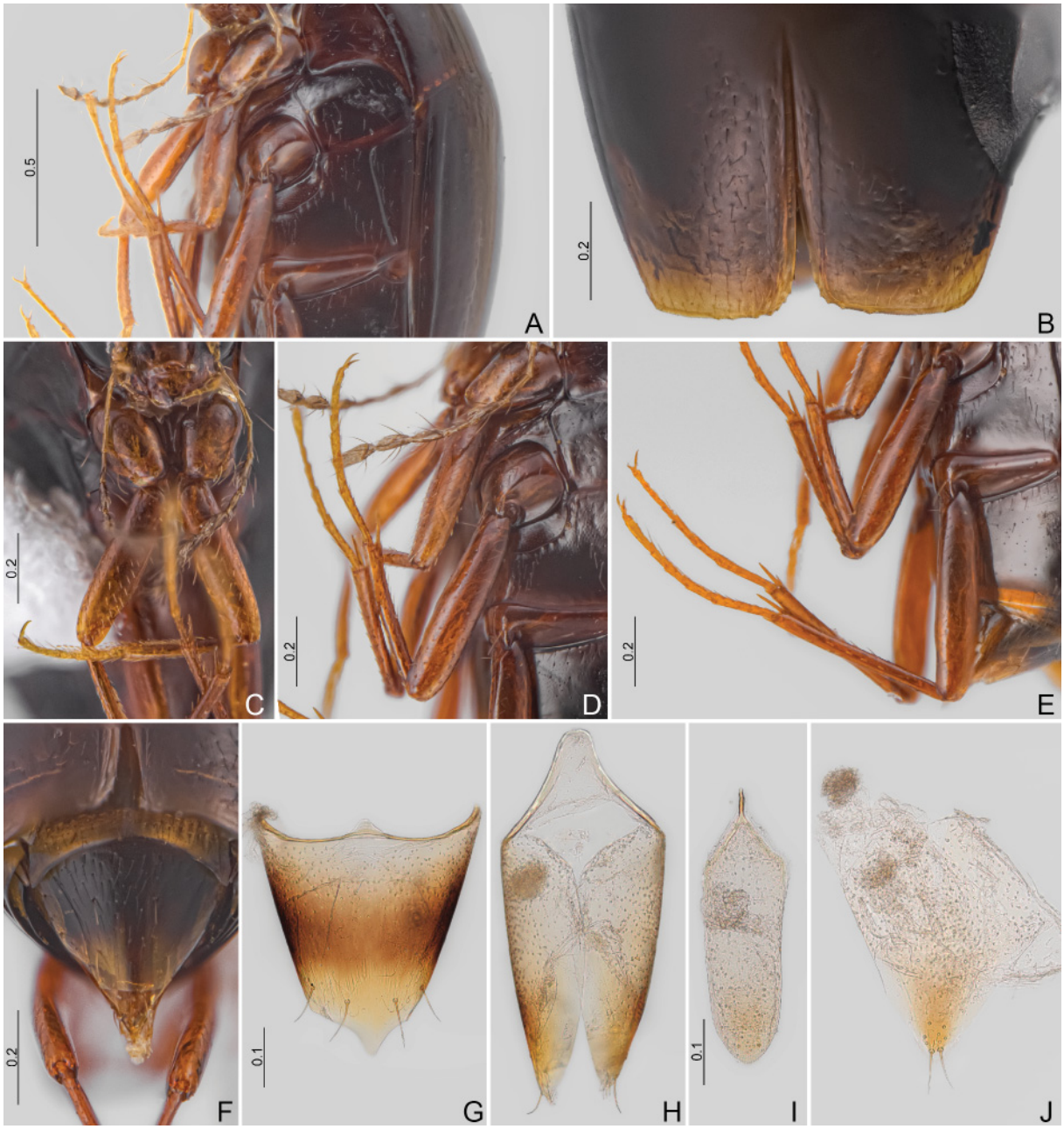

Fig. 81. *Toxidium scalenum* sp. nov., holotype, ♂ (CELC). **A**. Meso- and metathorax; oblique view. **B**. Elytra apex, dorsal view. **C–E**. Legs. **C**. Fore. **D**. Middle. **E**. Hind. **F**. Abdomen, dorsal view. **G**. Ventrite VIII. **H**. Tergite IX. **I**. Sternite IX. **J**. Tergite X. Scales in mm.

Description

Colouration. Reddish-brown, redder near sutures; shining; posterior area of clypeus, coxae, femora, and tibiae ochreous; antennae, mouthparts, tip of elytra, tarsi, and apex of abdominal ventrites yellow (Figs 80A–C, 81A–F).

Head. Frons with punctures dense and fine – few coarser punctures near frontoclypeal suture; pubescence dense (Fig. 80F). Antennomeres IV–VI distinctly slender (Fig. 80H), proportions: I 114/50 : II 106/50 : III 72/16 : IV 86/13 : V 103/11 : VI 98/13 : VII 117/27 : VIII 88/23 : IX 116/34 : X 114/38 : XI 143/46.

Prothorax (Fig. 80A–C, G). Somewhat elongate, smooth. Pronotum fine and moderately dense punctate. Lateral carinae dashed, visible in lateral view (Fig. 80B). Hypomeron with punctures very fine and poorly pubescent (Fig. 80B). Posterior angles of pronotum slightly acute, and not reaching anapleural line (Fig. 80B).

Mesothorax. Tip of scutellum exposed, slightly longer than wide (Fig. 80G). Mesanepisternum finely punctate; pubescence sparse (Fig. 80B). Mesoventral lines slightly curved, secondary lines straight (Fig. 81A).

Metathorax. Metaventrite with imbricate microsculpture between submesocoxal lines and metanepisternal suture; almost glabrous and impunctate (Fig. 81D). Submesocoxal lines punctate; submesocoxal area imbricate microsculptured; length: 0.10 mm (Fig. 81A). Metanepisternum triangular; conspicuously wider next to the mesanepisternum, pubescence denser near metanepisternal suture (Fig. 81A).

Wings. Elytra with coarse punctures – coarser than pronotum –, pubescence moderately dense (Fig. 80A). Sutural striae shortened, extending from apex up to approximately 0.74 of the sutural length (Fig. 80A). Lateral striae impunctate, just slightly curved at humeral region (Fig. 80B).

Legs (Fig. 81C–E). With imbricate microsculpture.

Abdomen. Shining. Ventrite I with micropuncture near submetacoxal bead (Fig. 81D). Propygidium micropunctured (Fig. 81F).

Fig. 82. *Toxidium scalenum* sp. nov., holotype, ♂, aedeagi (CELC). **A**. Frontal view. **B**. Parameres, frontal view. **C**. Lateral view. **D**. Dorsal view. **E**. Sclerite of internal sac, lateral view. Scales in mm.

Male

Protarsomeres I–III widened, bearing tenent setae (Fig. 81C). Sternite VIII with a posterior triangular projection (Fig. 81G). Tergite IX with ventral struts slightly curved (Fig. 81H). Sternite IX rounded posteriorly (Fig. 81I). Tergite X triangular, angulate posteriorly (Fig. 81J).

Aedeagus (Fig. 82). Poorly sclerotized. Basal bulb and apical lobe similar in length. Apical lobe triangular (Fig. 82). Parameres sinuous in lateral view (Fig. 82C). Sclerite of internal sac J-shaped, long side 2.5× as long as short side.

Measurements (n = 1, holotype; in mm). TL 1.90, SY 0.20, HW 0.81, IS 0.33, PL 0.84, PA 0.55, PB 0.98, EI 1.20, EL 1.26, EW 0.52, EH 0.58, MB 0.13, MC 0.16, MeW 0.30, ML 0.10, VL 0.25, VL2 0.37, PrF 0.50, PrT 0.35, MsF 0.56, MsT 0.46, MtF 0.59, MtT 0.55.

Host

Collected from an undetermined crust/resupinate fungus.

Remarks

Similar to *T. fleche* sp. nov. but differs mainly by the absence of coarse punctures on the metaventrite, the shallower elytral punctures, and by the bended sclerite of the internal sac.

Distribution

Mata do Paraíso, Universidade Federal de Viçosa, campus of Viçosa, state of Minas Gerais, Southeast Brazil (Fig. 1A–B).

Toxidium speratum sp. nov.
urn:lsid:zoobank.org:act:DB14D21D-F6B4-4B1F-AC1A-9578A88D43E0
Figs 1A–B, 83–88

Diagnosis

Body length: 2.08–2.25 mm. Dark reddish-brown. Posterior angle of pronotum slightly trespassing anapleural line. Metaventrite with some coarse punctures next to submesocoxal lines. Metanepisternal suture sinuous. Sutural striae shortened, extending from the apex to approximately 0.60 of the elytral sutural length. Elytra densely pubescent. Aedeagus with parameres constricted at posterior ⅔; sclerite of internal sac elongate and curved. Distal gonocoxite elongate, curved. Gonostylus tapering posteriorly.

Etymology

The species epithet is a Latin word meaning ‘hope’, because after collecting some specimens on one of the first field trips during my doctorate, I always returned to that same trunk hoping to collect more specimens, but never did.

Material examined

Holotype

BRAZIL • ♂; Minas Gerais, Viçosa, EPTEA Mata do Paraíso; 5 Nov. 2019; LabCol leg.; “Fungo 13 / Em *Hyphodontia* / HOLOTYPUS ♂”; CELC. (Fig. 83D–E)

Paratypes

BRAZIL • 2 ♂♂, 3 ♀♀ (1 ♂**, 1 ♀**); same collection data as for holotype; “Fungo 13 / Em *Hyphodontia*”; CELC • 2 ♀♀ (1 ♀*); same collection data as for holotype; 11 Feb. 2015; S. Aloquio, A. Orsetti, C. Lopes-Andrade and M. Bento leg.; CELC.

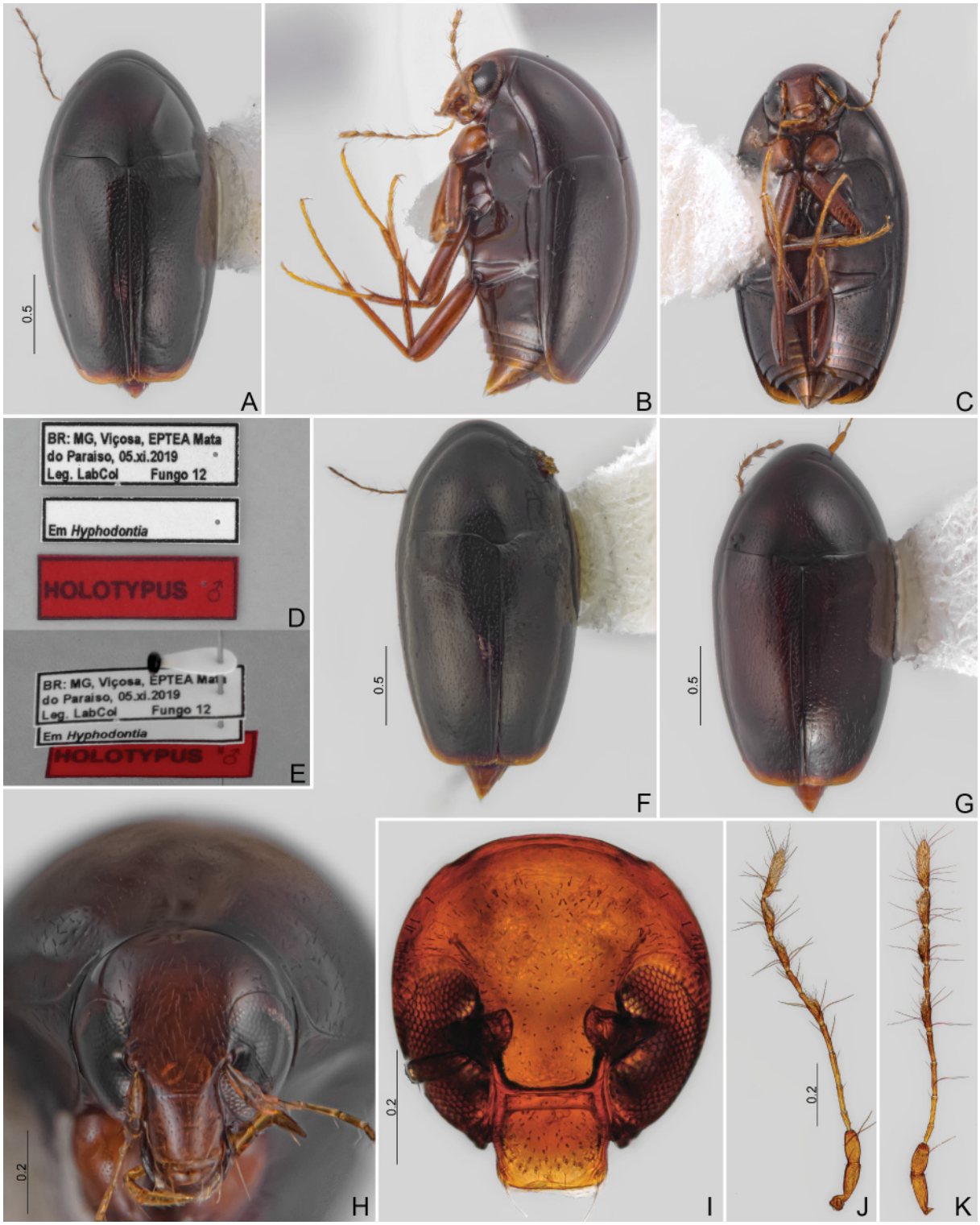

Fig. 83. *Toxidium speratum* sp. nov. (CELC). **A–E**. Holotype, ♂. **A**. Dorsal view. **B**. Lateral view. **C**. Ventral view. **D**. Labels. **E**. Pinned. **F**. Paratype, ♀ (#01), dorsal view. **G**. Paratype, ♂ (#05), dorsal view. **H–I**. Head, frontal view. **H**. Holotype, ♂. **I**. Paratype, ♀ (#05). **J–K**. Antennae. **J**. Paratype, ♂ (#04). **K**. Paratype, ♀ (#05). Scales in mm.

Description

Colouration. Dark reddish-brown; frons, femora, and tibiae dark ochreous; antennae, mouthparts, tarsi, apex of abdominal ventrites, and tip of elytra yellow (Fig. 83A–C). Variations: (1) reddish tonality less visible (Fig. 83F); (2) reddish tonality more visible (Fig. 83G).

Head (Figs 83H–K, 84A–E). Frons with punctation dense and fine – some punctures coarser near eyes. Clypeus squared, with coarse punctures (Fig. 83H–I). Labrum concave posteriorly; labral setae simple (Fig. 84A). Mandibles not strongly curved (Fig. 84B–C). Last maxillary palpomere about 3.90 × as long as wide; lacinia poorly pubescent (Fig. 84D). Last labial palpomere somewhat elongate and curved; mentum concave posteriorly (Fig. 84E). Gular pores absent; gular region with strigulate microsculpture (Fig. 84F). Antennomeres slender (Fig. 83J–K); antennomere proportions (n = 2): I 112/48 : II 104/52 : III 66/20 : IV 88/17 : V 110/18 : VI 95/20 : VII 126/39 : VIII 86/23 : IX 122/37 : X 124/40 : XI 168/41.

Prothorax (Figs 84G–K, 85D–E). Smooth, shining. Pronotum shining, punctures fine and moderately dense (Fig. 84G). Posterior angle acute, slightly trespassing anapleural line (Fig. 85D). Hypomeron finely punctate; pubescence moderately dense (Fig. 85D–E). Notosternal suture concave (Fig. 84J). Prosternal process strongly spinose (Fig. 84I). Profurca short and sinuous (Fig. 84K).

Mesothorax (Fig. 85A–E). Lacking microsculpture, shining (Fig. 85D–E). Scutellar plate strongly sclerotized and large; scutellum triangular, with sides slightly convex (Fig. 85A); just tip of scutellum exposed, longer than wide (Fig. 84G). Mesanepisternum with inconspicuous punctures, pubescence moderately dense (Fig. 85D–E). Mesoventral and secondary lines connected to mesocoxal cavity (Fig. 85B). Mesoventral process with a small ridge upwards in lateral view (Fig. 85C). Mesofurca sinuous (Fig. 85G).

Metathorax (Fig. 85B–J). Lacking microsculpture, shining. Metaventrite with inconspicuous punctures and pubescence sparsely pubescent (Fig. 85D–E); variation: some specimens with more or less coarse punctures next to submesocoxal lines (Fig. 85E). Submesocoxal area elongate; length: 0.10–0.15 mm (Fig. 85B). Metanepisternal suture convex, impunctate; metanepisternum wider at anterior part (Fig. 85D–E). Metanotum with triangular alacrista; scutoscutellar suture laterally acute, trespassing apodeme (Fig. 85F). Arms of metendosternite wider at stalk connection (Fig. 85H–J).

Wings (Figs 83A–C, F–G, 85K–M). Elytra with coarse and dense punctures – more than pronotum; pubescence dense. Sutural striae shortened, extending from apex to approximately 0.60 of the elytral sutural length (Fig. 83A). Lateral striae fine, impunctate, smoothly curved at humeral region (Fig. 83B).

Legs (Fig. 86A–F). With imbricate microsculpture. Femora and tibiae long and slender.

Abdomen. Smooth, shining. Each ventral segment with a row of apical setae (Fig. 83C). Tergites micropunctured (Figs 86G, 88A).

Males

Protarsomeres I–III widened, bearing tenent setae (Fig. 86D). Sternite VIII with a triangular posterior projection (Fig. 86J). Tergite VIII with a tiny posterior projection (Fig. 86K). Tergite IX with ventral struts somewhat curved (Fig. 86I, L). Sternite IX slightly acute posteriorly (Fig. 86M). Tergite X rounded posteriorly (Fig. 86N).

Aedeagus (Fig. 87). Median lobe strongly curved in lateral view; basal bulb longer than apical lobe (Fig. 87B). Parameres thick, with a small lobe, followed by a constriction at posterior ⅔ in frontal view (Fig. 87C). Sclerite of internal sac elongate and curved (Fig. 87E).

Measurements (n = 3, including holotype; in mm). TL 2.08–2.18 (2.12 ± 0.05), SY 0.22–0.25 (0.24 ± 0.02), HW 0.83–0.86 (0.85 ± 0.02), IS 0.30–0.35 (0.33 ± 0.03), WA 0.16–0.17 (0.17 ± 0.01), PL 0.82–0.92 (0.87 ± 0.05), PA 0.55–0.58 (0.56 ± 0.02), PB 1.11–1.16 (1.14 ± 0.02), EI 1.32–1.40 (1.37 ± 0.05), EL 1.44–1.50 (1.47 ± 0.03), EW 0.47–0.52 (0.50 ± 0.03), EH 0.56–0.69 (0.61 ± 0.07), MB 0.14–0.15 (0.14 ± 0.01), MC 0.16–0.19 (0.18 ± 0.02), MeW 0.32–0.34 (0.33 ± 0.01), ML 0.10–0.12 (0.11 ± 0.01), VL 0.31–0.33 (0.32 ± 0.01), VL2 0.42–0.47 (0.44 ± 0.03), PrF 0.52–0.57 (0.54 ± 0.03), PrT 0.33–0.43

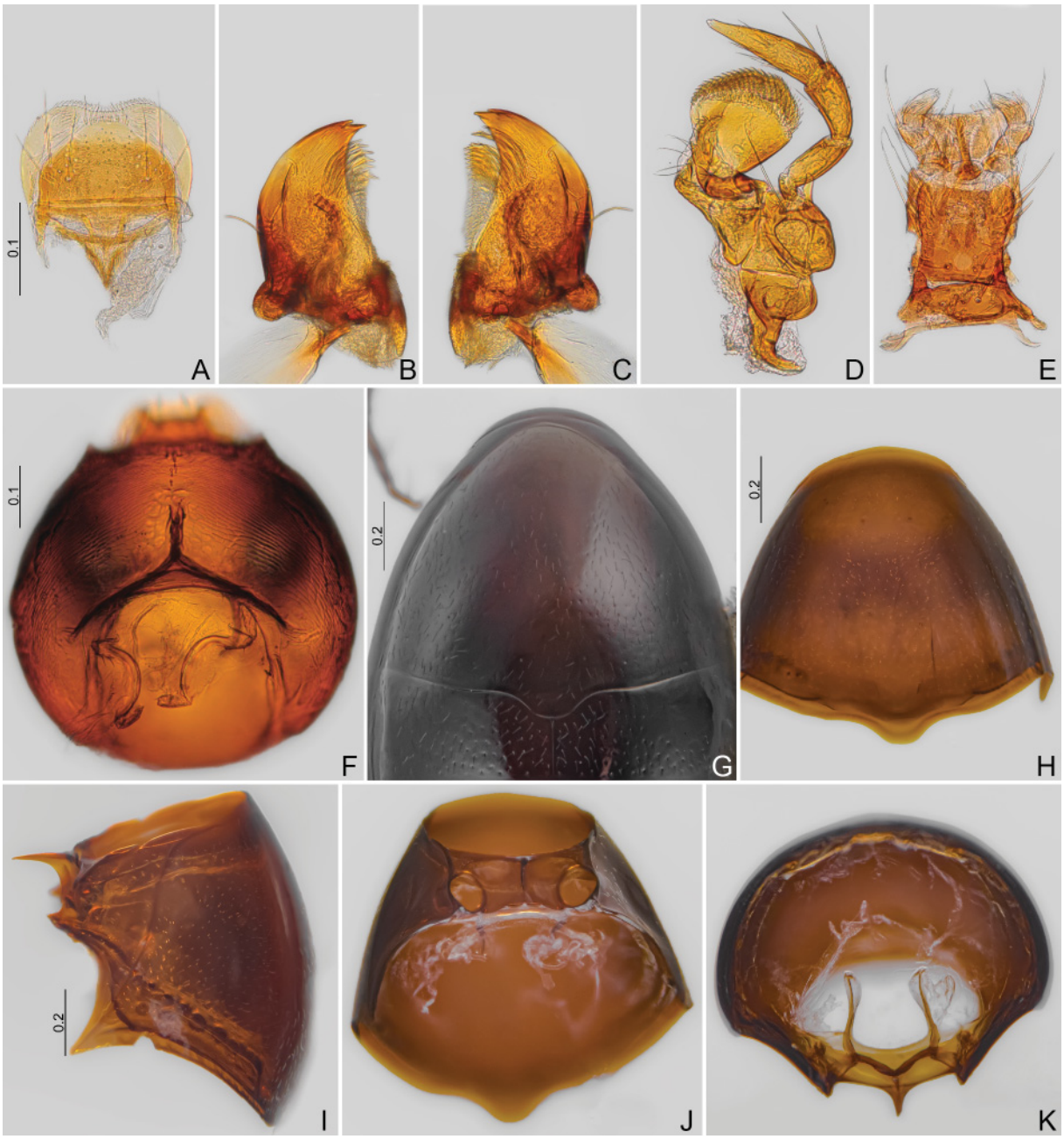

Fig. 84. *Toxidium speratum* sp. nov. (CELC). **A–E**. Paratype, ♂ (#04). **A**. Labrum. **B–C**. Mandibles. **D**. Maxilla. **E**. Labium. **F**. Paratype, ♀ (#05), head, ventral view. **G**. Holotype, ♂, prothorax, dorsal view. **H–K**. Paratype, ♂ (#04), prothorax. **H**. Dorsal view. **I**. Lateral view. **J**. Ventral view. **K**. Inner view. Scales in mm.

Fig. 85. *Toxidium speratum* sp. nov. (CELC). **A–C**. Paratype, ♂ (#04). **A**. Scutellar shield. **B–E**. Meso- and metathorax. **B**. Ventral view. **C**. Lateral view. **D**. Holotype, ♂, oblique view. **E**. Paratype, ♀ (#01), oblique view. **F–I**. Paratype, ♂ (#04). **F**. Metanotum. **G**. Mesothorax, internal view. **H–J**. Metendosternite. **H**. Dorsal view. **I**. Lateral view. **J**. Paratype, ♀ (#05), dorsal view. **K–M**. Paratype, ♂ (#04). **K–L**. Elytra. **M**. Hind wing. Abbreviations: mr = mesofurca; mvl = mesoventral line; px = procoxal rest; sl = secondary line. Scales in mm.

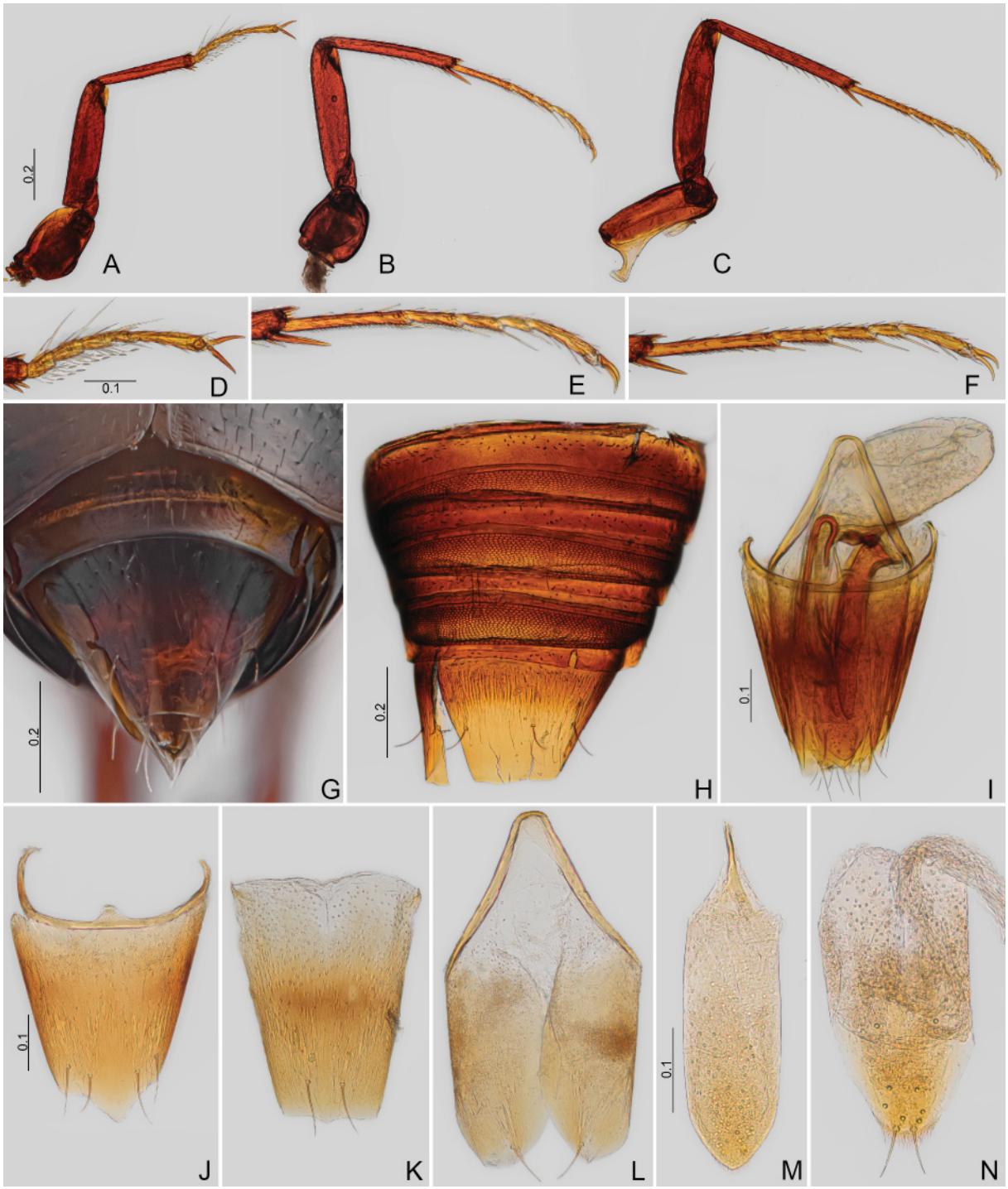

Fig. 86. *Toxidium speratum* sp. nov. (CELC). **A–F**. Paratype, ♂ (#04). **A–C**. Legs. **A**. Fore. **B**. Middle. **C**. Hind. **D–F**. Tibiae. **D**. Pro. **E**. Meso. **F**. Meta. **G**. Holotype, ♂, abdomen, dorsal view. **H–N**. Paratype, ♂ (#04). **H**. Abdomen, dissected, ventral view. **I**. Terminalia. **J**. Sternite VIII. **K**. Tergite VIII. **L**. Tergite IX. **M**. Sternite IX. **N**. Tergite X. Scales in mm.

(0.39±0.05), MsF 0.60–0.62 (0.61±0.01), MsT 0.49–0.53 (0.52±0.02), MtF 0.63–0.65 (0.64±0.01), MtT 0.60–0.65 (0.62±0.03).

Females (Fig. 88)

Sternite and tergite VIII with imbricate microsculpture. Sternite VIII with an acute posterior projection (Fig. 88B). Tergite VIII straight posteriorly (Fig. 88C). Spermatheca elongate and twisted posteriorly (Fig. 88D). Distal gonocoxite elongate, curved, gonostylus tapering posteriorly (Fig. 88E–H).

Fig. 87. *Toxidium speratum* sp. nov., paratype, ♂ (#04), aedeagi (CELC). **A**. Frontal view. **B**. Lateral view. **C**. Dorsal view. **D**. Parameres, ventral view. **E–F**. Sclerite of internal sac. **E**. Lateral view. **F**. Frontal view. Scales in mm.

Fig. 88. *Toxidium speratum* sp. nov. (CELC). **A**. Paratype, ♀ (#01), abdomen, dorsal view. **B–F**. Paratype, ♀ (#05). **B**. Sternite VIII. **C**. Tergite VIII. **D**. Terminalia. **E–F**. Ovipositor. **G–H**. Paratype, ♀ (#07), ovipositor. Scales in mm.

Measurements (n = 5; in mm). TL 2.18–2.25 (2.20 ± 0.04), SY 0.24–0.26 (0.25 ± 0.01), HW 0.83–0.88 (0.86 ± 0.02), IS 0.35–0.39 (0.37 ± 0.02), WA 0.15–0.18 (0.16 ± 0.01), PL 0.80–0.94 (0.86 ± 0.07), PA 0.58–0.63 (0.60 ± 0.02), PB 1.14–1.22 (1.18 ± 0.03), EI 1.34–1.50 (1.42 ± 0.08), EL 1.48–1.60 (1.52 ± 0.05), EW 0.47–0.53 (0.51 ± 0.03), EH 0.63–0.69 (0.66 ± 0.03), MB 0.13–0.19 (0.15 ± 0.02), MC 0.16–0.23 (0.18 ± 0.03), MeW 0.30–0.35 (0.33 ± 0.02), ML 0.10–0.15 (0.11 ± 0.02), VL 0.31–0.40 (0.34 ± 0.04), VL2 0.41–0.45 (0.43 ± 0.01), PrF 0.51–0.59 (0.55 ± 0.03), PrT 0.37–0.39 (0.38 ± 0.01), MsF 0.60–0.65 (0.62 ± 0.02), MsT 0.49–0.55 (0.51 ± 0.03), MtF 0.60–0.66 (0.64 ± 0.02), MtT 0.58–0.63 (0.61 ± 0.02).

Host

Collected from *Hyphodontia* sp. (Hymenochaetaceae).

Remarks

Similar to *T. scalenum* sp. nov. but differs mainly by the shorter sutural striae, the oblong metanepisternum, and by the presence of a constriction on the apical portion of the parameres. The sclerite of the internal sac is also distinctly rounded at the curvature when compared to all the other species of *Toxidium* described in this manuscript.

Distribution

Mata do Paraíso, Universidade Federal de Viçosa, campus of Viçosa, state of Minas Gerais, Southeast Brazil (Fig. 1A–B).

Toxidium ultimum sp. nov.
urn:lsid:zoobank.org:act:2B63D970-44EE-48E9-B41D-43F93E89373E
Figs 1A–B, E–F, 89–92, 94A–B

Diagnosis

Body length: 1.56–1.70 mm. Dark brown, elytra apex yellow-ochreous. Sutural striae extending from apex to approximately 0.84 of the elytral sutural length. Metaventrite I with few coarse punctures next to submesocoxal lines. Abdominal ventrite I with imbricate microsculpture. Parameres with poorly sclerotized lobe medially. Sclerite if internal sac D-shaped. Distal gonocoxite slightly fusiform. Gonostylus elongate.

Etymology

The species epithet is a Latin word meaning ‘the last one’, referring both to it being the last species described in this manuscript and the final specimen collected and dissected for this project.

Material examined

Holotype

BRAZIL • ♂*; Minas Gerais, Viçosa, UFV, Vila Gianetti; 3 Dec. 2022; E. von Groll leg.; “/ Em *Inonotus* sp. (Hymenochaetaceae) / Dissecado em 15.xii.2022 / HOLOTYPUS ♂”; CELC. (Fig. 89D–E)

Paratypes

BRAZIL • 1 ♂, 1 ♀ (1 ♂*, 1 ♀*); same collection data as for holotype; 3 Dec. 2022; E. von Groll leg.; “/ Em *Inonotus* sp. (Hymenochaetaceae)”; CELC.

Description

Colouration. Brown; antennae, clypeus, mouthparts, tarsi, apex of abdominal ventrites, and tip of elytra light ochreous; femora and tibiae ochreous (Fig. 89A).

Fig. 89. *Toxidium ultimum* sp. nov. (CELC). **A–E**. Holotype, ♂. **A**. Dorsal view. **B**. Lateral view. **C**. ventral view. **D**. Labels. **E**. Pinned. **F**. Paratype, ♂ (#02), dorsal view. **G–H**. Paratype, ♀ (#03). **G**. Dorsal view. **H**. Lateral view. **I**. Holotype, ♂, head, frontal view. **J–K**. Antennae. **J**. Holotype, ♂. **K**. Paratype, ♀ (#03). **L**. Holotype, ♂, prothorax, dorsal view. Scales in mm.

Head. Punctations moderately dense and coarse, some punctures coarser. Antennomeres elongate (Fig. 89J–K); proportions (n=3): I 89/42 : II 83/40 : III 60/17 : IV 76/16 : V 89/16 : VI 85/16 : VII 99/28 : VIII 71/19 : IX 95/30 : X 94/33 : XI 126/36.

Prothorax (Figs 89L, 90A–C). Pronotum elongate, slightly tapering towards to head, not strongly curved in lateral view (Fig. 89B); punctures moderately coarse; pubescence moderately sparse. Posterior angle of pronotum somewhat acute, and almost at same position as anapleural line (Fig. 90A–C).

Fig. 90. *Toxidium ultimum* sp. nov. (CELC). **A–C**. Meso- and metathorax, oblique view. **A**. Holotype, ♂. **B**. Paratype, ♂ (#02). **C**. Paratype, ♀ (#03). **D–L**. Holotype, ♂. **D**. Elytra apex, dorsal view. **E–F**. Legs. **E**. Fore. **F**. Middle and hind. **G**. Abdomen, dorsal view. **H**. Sternite VIII. **I**. Tergite VIII. **J**. Tergite IX. **K**. Sternite IX. **L**. Tergite X. Scales in mm.

Mesothorax (Fig. 90A–C). Tip of scutellum just partially exposed (longer than wide), hardly visible. Mesanepisternum finely punctate; pubescence sparse. Secondary lines connected to mesocoxal cavities.

Metathorax (Fig. 90A–C). Metaventrite lacking microsculpture, almost glabrous; with coarse punctures next to submesocoxal lines – density variable. Submesocoxal lines slightly truncate laterally; connected at midline, forming an acute angle (Fig. 90E); submesocoxal area: 0.07–0.08 mm. Metanepisternal suture almost straight or sinuous, impunctate; metanepisternum mostly covered by elytra.

Wings (Figs 89A–C, F–H, 90D). Elytra with moderately sparse punctures, some coarser than other, both coarser than on pronotum. Sutural striae not strongly shortened, extending from apex to approximately 0.84 of the elytral sutural length; variation: female with shorter striae: 0.47 of the sutural length. Lateral striae impunctate, slightly opening at humeral region (Fig. 89B).

Legs (Figs 90E–F, 92A–B). With imbricate microsculpture.

Abdomen. Sparsely pubescent. Anterior two-thirds of ventrite I (Figs 89B, 90A–C, 92C–D), and tergites (Fig. 90G) with imbricate microsculpture; remaining ventrites without microsculpture.

Males

Sternite VIII shortened, with acute posterior projection (Fig. 90H). Tergite VIII without posterior projection (Fig. 90I). Tergite IX with ventral struts short and almost straight (Fig. 90J). Sternite IX acute posteriorly (Fig. 90K). Tergite X triangular (Fig. 90L).

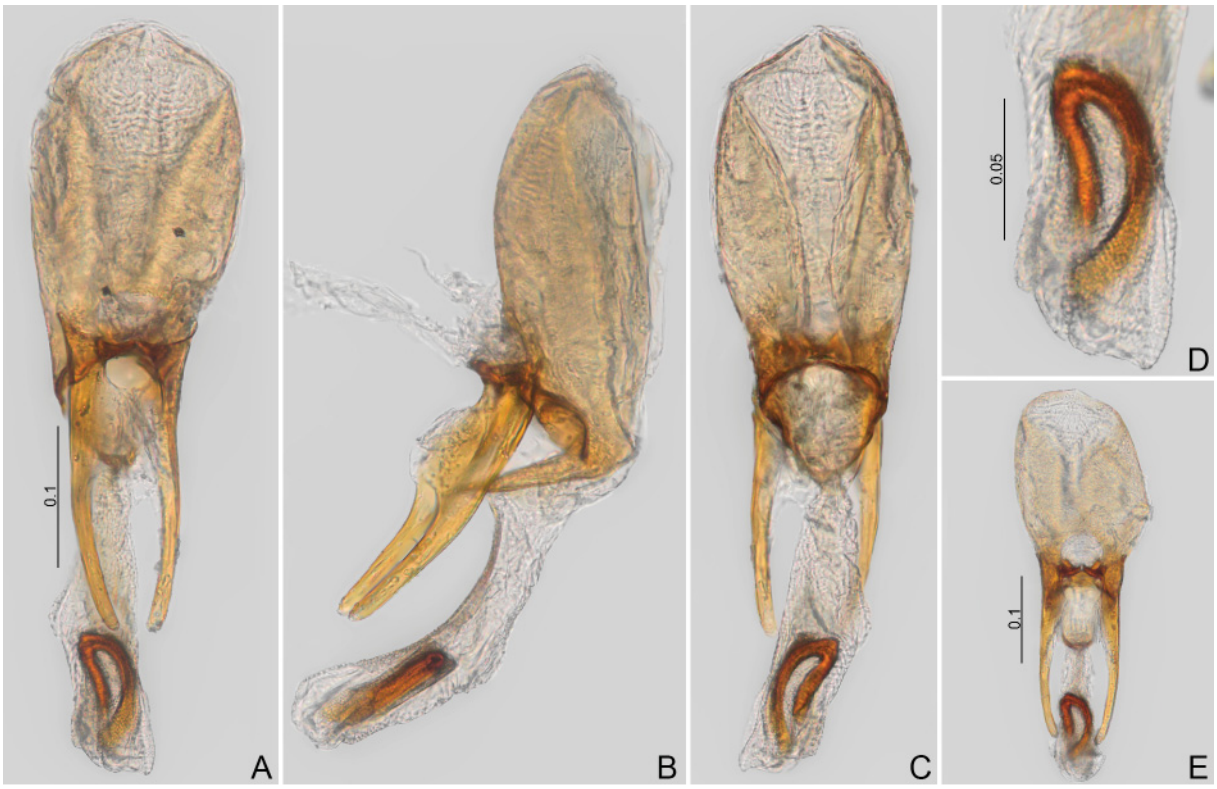

Fig. 91. *Toxidium ultimum* sp. nov., aedeagus (CELC). **A–D**. Holotype, ♂. **A**. Frontal view. **B**. Lateral view. **C**. Dorsal view. **D**. Sclerite of internal sac. **E**. Paratype, ♂ (#02), aedeagi, frontal view. Scales in mm.

Fig. 92. *Toxidium ultimum* sp. nov., paratype ♀ (#03) (CELC). **A–B**. Legs. **A**. Fore. **B**. Middle and hind. **C**. Ventrite I, detail, arrow: microsculpture. **D**. Abdomen, dorsal view. **E**. Sternite VIII. **F**. Tergite VIII. **G**. Genitalia. **H**. Ovipositor. Scales in mm.

Fig. 93. Hosts of Scaphidiinae Latreille, 1806 (Mata da Biologia, Viçosa, MG). **A–B**. Mushroom. **C**. Unknown fungus/myxomycete. **D**. *Ceratyomyxa fruticulosa* T.Macbr. **E–F**. Resupinate/crust fungi 1. **G–H**. Resupinate/crust fungi 2. **I–J**. Resupinate/crust fungi 3.

Aedeagus (Fig. 91). Basal bulb 2× as long as apical lobe; apical lobe bent (Fig. 91B). Parameres thin, bearing a poorly sclerotized lobe (Fig. 91B); sclerite of internal sac curved, D-shaped (Fig. 91D).

Measurements (n=2, including holotype; in mm; *= invariant). TL 1.56–1.60 (1.58±0.03), SY 0.19*, HW 0.42–0.43 (0.43±0.01), IS 0.14–0.15 (0.14±0.01), WA 0.26–0.27 (0.27±0.01), PL 0.64–0.65 (0.64±0.01), PA 0.40–0.41 (0.41±0.01), PB 0.76–0.79 (0.78±0.02), EI 1.03–1.06 (1.05±0.02), EL 1.11–1.14 (1.13±0.02), EW 0.41*, EH 0.40–0.41 (0.41±0.01), MB 0.10*, MC 0.29–0.33 (0.31±0.03), MeW 0.25*, ML 0.08*, VL 0.20–0.21 (0.21±0.01), VL2 0.32*, PrF 0.40–0.41 (0.41±0.01), PrT 0.31–0.33 (0.32±0.01), MsF 0.46*, MsT 0.36–0.37 (0.37±0.01), MtF 0.47–0.50 (0.49±0.02), MtT 0.45–0.49 (0.47±0.03).

Fig. 94. Hosts of Scaphidiinae Latreille, 1806 (Viçosa, MG). **A–D**. *Inonotus* sp. (Vila Gianetti) (Hymenochaetaceae). **C–D**. *Scaphisoma hilarum* sp. nov. 1 on *Inonotus* sp. **E**. Resupinate/crust fungi (Mata da Biologia). **F**. Resupinate/crust fungi (Mata da Biologia).

Female (Fig. 92)

Sternite and tergite VIII with imbricate microsculpture**.** Sternite VIII with an acute posterior projection (Fig. 92E). Tergite VIII lacking projections (Fig. 92F). Distal gonocoxite slightly fusiform, gonostylus elongate (Fig. 92G–H).

Measurements (n = 1; in mm). TL 1.70, SY 0.22, HW 0.46, IS 0.17, WA 0.30, PL 0.69, PA 0.44, PB 0.78, EI 1.13, EL 1.20, EW 0.43, EH 0.43, MB 0.12, MC 0.34, MeW 0.26, ML 0.07, VL 0.20, VL2 0.36, PrF 0.43, PrT 0.31, MsF 0.49; MsT 0.38, MtF 0.50, MtT 0.45.

Host

Collected from *Inonotus* sp., located on a tree in front of an avenue (Figs 1E–F, 94A–B).

Remarks

Similar to *T. distortum* sp. nov., differing mainly by the more elongate body, the longer submesocoxal area – reaching half of the metaventrite, by the presence of microsculpture on the ventrite I, the less sclerotized tergite IX, the shorter apex of the median lobe, the thinner parameres, and by the shape of the sclerite (D-shaped). Although the female has a larger size and a shorter sutural stria compared to the males, the specimen exhibits all other characteristics of the species. Therefore, these differences can be considered merely intraspecific variation.

Distribution

Universidade Federal de Viçosa, campus of Viçosa, state of Minas Gerais, Southeast Brazil (Fig. 1A–B, E–F).

Discussion

With the addition of these 20 new species, there are now 61 species of Scaphidiinae known from Brazil. Nonetheless, this number remains considerably lower than the country's potential. During my 22 collecting trips in Viçosa (MG), which resulted in the species described in this manuscript, I collected approximately 350 additional specimens requiring further study. Many of these likely represent new species.

Considering that collections from just three areas in one city yielded so many specimens, it is reasonable to assume that Brazil, a country with six biomes (Amazon, Caatinga, Cerrado, Pantanal, Atlantic Forest, and Pampa), 59% of which is covered by forests, and known for its megadiversity, harbors a far greater abundance and diversity of Scaphidiinae. Note that their scarcity in pinned collections reflects neither natural absence nor lack in museums, but rather: (1) collection challenges, (2) prioritization of other groups, and (3) declining taxonomist numbers (Löbl *et al.* 2023). For example, it is very common to find small beetles (of any family) still preserved in alcohol or entomological envelopes in most unsorted collections.

Although shining fungus beetles can be collected using intercept traps, Winkler extractors, and by sifting litter (Löbl & Leschen 2003b; Tang *et al.* 2014; Löbl *et al.*, 2021), specific and active collection methods are very important to collect these beetles (von Groll *et al.* 2021; von Groll & Lopes-Andrade 2021). While this approach may require more time and effort, yielding fewer results compared to intercept traps, it is the only way to establish host associations (Löbl & Leschen 2003b).

One finding regarding beetle × host interactions was that specimens of *Alexidia* showed a strong association with the myxomycete *Ceratiomyxa fruticulosa*. Also, the presence of a corbiculum (= setose pockets; = setose cavities (Newton 1984)) supports this relationship. The corbiculum has already been

hypothesized to function as mycangia or spore-retaining and aid in the dispersal of host spores (Newton 1984). This structure is also found in the genus *Baeocera*, which is well-known for feeding on slime mould bodies (Newton 1984).

Two additional peculiar morphological characteristics were observed. The first can be seen in *Scaphisoma peculiare* sp. nov. The genus *Scaphisoma* is characterized by a normal last maxillary palpomere ("tapering"; "typically as wide as the penultimate segment" Löbl & Leschen 2003b; Leschen & Löbl 2005). However, *S. peculiare* sp. nov. presents the last palpomere with a truncate apex, contrasting to the usual acute apex described for other *Scaphisoma* species. This species presents more atypical characteristics such as the absence of tenent setae on the male tarsomeres, a very short submetacoxal area, and distinct parameres, although these characteristics are not necessarily new to the genus.

The second peculiar characteristic is observed in *Toxidium brigadeirense* sp. nov., the most distinctive *Toxidium* species described here. Its hypomeron's posterior region is shorter than the pronotal angle's posterior end (best viewed laterally). This trait also occurs in undescribed *Toxidium* species and related genera (pers. obs.). It is noted that this groups of beetles require an urgent and extensive revision.

It is notable that this study provides more detailed descriptions than typically published. This more comprehensive morphological approach aimed to investigate additional diagnostic characters for species delimitation. Even similar species can be distinguished by subtle differences in the mouth parts, metendosternite, profurca, and other structures. Precise comparisons using these uncommon characteristics often require dissecting multiple specimens per species. This approach may be impractical compared to less invasive and more accurate methods, such as non-invasive genetic sampling techniques.

Nonetheless, the already known characteristics remain the most significant for identifications: antennomere length/width (Supp. file 2), shape and length of submesocoxal and submetacoxal lines, and aedeagus morphology. Additionally, the female terminalia (ventrites, tergites, and genitalia) also exhibited significative diagnostic characteristics. This comprehensive analysis not only helped distinguish similar species but also enabled association of females to their respective species – particularly important for closely related species sharing similar morphology and hosts.

One example of this situation can be observed in *Baeocera bottine* sp. nov., *B. colibri* sp. nov. and *B. pulga* sp. nov. These three syntopic species are remarkably similar, requiring comparison of males and female structures (metendosternite, mouthparts, and other less commonly used features), to determine female associations. *Baeocera ardua* sp. nov. was also analysed but females could not be confidently associated.

Despite the typically unrecognized importance of female terminalia, they can occasionally help define species groups (Ogawa & Sakai 2011; Ogawa & Löbl 2013). Here, the *ardua* species group is proposed based solely on male characteristics because the female of *B. ardua* sp. nov. remains unknown. However, it is highly probable that the female terminalia of *B. ardua* resemble those of other species in the group, given the strong similarity of the males. Supporting this, females with a comparable external morphology from the same collections were dissected and showed similar internal structures, though these were excluded due to identification uncertainties.

The two other species of *Baeocera* exhibit distinct morphologies and cannot be associated with the *ardua* species group or with each other. *Baeocera facilis* sp. nov. presents femora with a distinct microsculpture, sclerite of internal sac asymmetrical and undefined, and an elongate distal gonocoxite, while *B. inusitata* sp. nov. exhibits basal striae connected to the lateral and sutural ones, the sclerite of the internal sac as twisted plates, and a short distal gonocoxite lacking a gonostylus.

The female terminalia of *Alexidia* and *Toxidium* are described here for the first time. In *Alexidia*, the most significant differences occur in spermatheca and gonostylus shape. Females of *Toxidium* share a similar morphology but with variations (e.g., distal gonocoxite elongate but more curved in *T. speratum* sp. nov.; sternite VIII in *T. ultimum* sp. nov. short).

Male terminalia remain the best diagnostic feature, though technical challenges exist. For instance, comparing extracted versus non-extracted internal sacs (von Groll 2023) is difficult. Therefore, I suggest not removing the internal sac, to facilitate the observation of its position. Furthermore, it is a less destructive method.

Regarding the distribution, scaphidiine beetles were readily found and collected in both preserved and disturbed areas. Viçosa (MG) is a small city surrounded by remnants of Atlantic Forest, with a very favourable climate for insects (rainy summers), which might explain the ease of finding these beetles. However, it is unknown whether these beetles are distributed throughout the country. As a first step to address this question, I suggest visiting miscellaneous collections at universities and museums to investigate whether these beetles were collected using more comprehensive methods, such as Winkler extractors and FIT traps.

Checklist of the Brazilian species of Scaphidiinae *(* = described in this manuscript)*

1. *Cyparium achardi* von Groll & Lopes-Andrade, 2022. Brazil (Minas Gerais).
2. *Cyparium collare* Pic, 1920a. Brazil (Minas Gerais, Mato Grosso, Pernambuco).
3. *Cyparium ferrugineum* Pic, 1920a. Brazil (Piauí, Pernambuco, Mato Grosso).
4. *Cyparium fugitivum* sp. nov. Brazil (Minas Gerais)*.
5. *Cyparium grilloi* Pic, 1920b. Brazil (Paraná).
6. *Cyparium grouvellei* Pic, 1920a. Brazil.
7. *Cyparium lescheni* von Groll & Lopes-Andrade, 2022. Brazil (Minas Gerais).
8. *Cyparium loebli* von Groll & Lopes-Andrade, 2022. Brazil (Minas Gerais).
9. *Cyparium newtoni* von Groll & Lopes-Andrade, 2022. Brazil (Minas Gerais).
10. *Cyparium oberthueri* Pic, 1956 [*oberthüri* Pic, 1956]. Brazil (Mato Grosso, Minas Gerais).
11. *Cyparium pici* von Groll & Lopes-Andrade, 2022. Brazil (Mato Grosso).
12. *Cyparium pygidiale* Achard, 1922b. Brazil (Goias).
13. *Cyparium ruficolle* Achard, 1922b. Brazil (Mato Grosso).
14. *Cyparium rufohumerale* Pic, 1931. Brazil.
15. *Scaphidium bipunctatum* Redtenbacher, 1868. Brazil (Rio de Janeiro).
16. *Scaphidium bisbimaculatum* Pic, 1917. Brazil (Espirito Santo).
17. *Scaphidium castaneum* Perty, 1830. Brazil.
18. *Scaphidium cerasinum* Oberthür, 1883. Brazil (Tocantins, Amazonas).
19. *Scaphidium exclamans* Oberthür, 1883. Brazil (São Paulo); Paraguai.
20. *Scaphidium fasciatomaculatum* Oberthür, 1883. Brazil (Amazonas); Ecuador, Peru.
21. *Scaphidium fascipenne* Reitter, 1880. Brazil.
22. *Scaphidium gounellei* Pic, 1920a. Brazil.
23. *Scaphidium pantherinum* Oberthür, 1883. Brazil ("Rio Negro" Paraná).
24. *Scaphidium pardale pardale* Laporte, 1840. French Guiana, Brazil and *Scaphidium pardale nigripenne* Oberthür, 1883. Brazil.
25. *Scaphidium testaceum* Reitter, 1880. Brazil.
26. *Scaphidium undulatum* Pic, 1915c. Brazil.
27. *Alexidia convivalis* sp. nov. Brazil (Minas Gerais)*.
28. *Alexidia plaumanni* Löbl & Leschen, 2003a. Brazil (Santa Catarina).
29. *Alexidia solitaria* sp. nov. Brazil (Minas Gerais)*.
30. *Amalocera basipennis* Löbl, 1974. Brazil.

31. *Amalocera dentifera* Löbl, 1974. Brazil (Santa Catarina).
32. *Amalocera paulistana* Achard, 1922b. Brazil ("near São Paulo").
33. *Amalocera picta* Erichson, 1845. Brazil.
34. *Amalocera tibialis* Löbl, 1974. Brazil (Minas Gerais).
35. *Baeocera ardua* sp. nov. Brazil (Minas Gerais)*.
36. *Baeocera bottine* sp. nov. Brazil (Minas Gerais)*.
37. *Baeocera colibri* sp. nov. Brazil (Minas Gerais)*.
38. *Baeocera facilis* sp. nov. Brazil (Minas Gerais)*.
39. *Baeocera freudei* Löbl, 1967. Brazil (Amazonas).
40. *Baeocera inusitata* sp. nov. Brazil (Minas Gerais)*.
41. *Baeocera pulga* sp. nov. Brazil (Minas Gerais)*.
42. *Scaphisoma brunneipenne* Pic, 1916b. Brazil (Santa Catarina).
43. *Scaphisoma elongatum* Waterhouse, 1879. Brazil (Rio de Janeiro).
44. *Scaphisoma hilarum* sp. nov. Brazil (Minas Gerais)*.
45. *Scaphisoma infinitum* sp. nov. Brazil (Minas Gerais)*.
46. *Scaphisoma mutabile* sp. nov. Brazil (Minas Gerais)*.
47. *Scaphisoma nigrofasciatum* Pic, 1915b. Brazil (Minas Gerais). India, Mauritius, Nepal, La Réunion, Seychelles, Sri Lanka. (von Groll 2023).
48. *Scaphisoma pandemum* Groll & Lopes-Andrade, 2021. Brazil (Minas Gerais).
49. *Scaphisoma peculiare* sp. nov. Brazil (Minas Gerais)*.
50. *Scaphisoma phalacroide* Pic, 1920b. Brazil (São Paulo).
51. *Scaphisoma rubripes* Pic, 1920a. Brazil.
52. *Scaphisoma testaceiventre* Pic, 1928c. Brazil (São Paulo).
53. *Scaphisoma tropicum andreinii* Pic, 1920b. Brazil (São Paulo).
54. *Toxidium acuminatum* Pic, 1920c. Brazil.
55. *Toxidium brigadeirense* sp. nov. Brazil (Minas Gerais)*.
56. *Toxidium distortum* sp. nov. Brazil (Minas Gerais)*.
57. *Toxidium fleche* sp. nov. Brazil (Minas Gerais)*.
58. *Toxidium inusitatum* sp. nov. Brazil (Minas Gerais)*.
59. *Toxidium scalenum* sp. nov. Brazil (Minas Gerais)*.
60. *Toxidium speratum* sp. nov. Brazil (Minas Gerais)*.
61. *Toxidium ultimum* sp. nov. Brazil (Minas Gerais)*.

Conclusion

Brazil now has 61 described species of Scaphidiinae. While this may seem a modest contribution to the subfamily as a whole, it represents a significant progress for the country. Most specimens are meticulously illustrated, the morphological characteristics are described in detail, and collecting and dissecting methods are now widely known. I remain hopeful that studies of these small but fascinating beetles will continue to advance.

Acknowledgments

I would like to express my sincere thanks to Ivan Löbl (MHNG), Max Barclay (NHMUK) and Kristiaan Hoedemakers (EJT desk editor) for essential assistance. I am also grateful for valuable suggestions of the dissertation members committee: Gervasio S. Carvalho (retired professor), Jéssica Herzog Vianna (UEPA), Vinicius S. Ferreira (SDEI), and Gabriel Biffi (USP). I also thank the Department of Animal Biology (UFV) for allowing me to use the laboratory, equipment, and the specimens. Financial support was provided by CAPES (Coordenação de Aperfeiçoamento de Pessoal de Nível Superior - doctorate degree grant number 88882.437502/2019-01). I also acknowledge the financial support provided by Field Museum Visiting Scholarship (FMNH) and the Graduate Student Research Enhancement Awards

(GSREA, The Coleopterists Society), which enabled my visit to FMNH in the United States. This visit was instrumental in providing access to additional specimens which enriched the discussions and comparisons in this study.

References

Achard J. 1920. Notes sur les Scaphidiidae de la faune Indo-Malaise. *Annales de la Société entomologique de Belgique* 60: 123–136.

Achard J. 1922a. Essai de groupement des espèces du genre *Scaphidium* Ol. (Col. Scaphidiidae). *Fragments entomologiques*: 10–13.

Achard J. 1922b. Descriptions de scaphidides nouveaux (Col. Scaphidiidae). *Fragments entomologiques*: 35–45.

Achard J. 1923. Revision des Scaphidiidae de la faune japonaise. *Fragments entomologiques*: 94–120.

Achard J. 1924. Essai d'une subdivision nouvelle de la famille des Scaphidiidae. *Annales de la Société entomologique de Belgique* 65: 25–31.

Agassiz L. 1846. Nomenclatoris zoologici index universalis continens nomina systematica classium, ordinum, familiarum et generum animalium omnium, tam viventium quam fossilium, secundum ordinem alphabeticum unicum disposita, adjectis homonymiis plantarum, nec non variis adnotationibus et emendationibus. *In*: Agassiz L. (ed.) *Nomenclator Zoologicus, continens nomina systematica generum animalium tam viventium quam fossilium, secundum ordinem alphabeticum disposita, adjectis auctoribus, libris, in quibus reperiuntur, anno editionis, etymologia et familiis, ad quas pertinent, in singulis classibus*: fasc. 12, Jent and Gassmann, Solothurn. https://doi.org/10.5962/bhl.title.49761

Blackburn T. 1903. Further notes on Australian Coleoptera, with descriptions of new genera and species. *Transactions of the Royal Society of South Australia* 27: 91–182.

Casey T.L. 1893. Coleopterological notices V. Scaphidiidae. *Annals of the New York Academy of Sciences* 7: 510–533. https://doi.org/10.1111/j.1749-6632.1893.tb55411.x

Casey T.L. 1900. Review of the American Corylophidae, Cryptophagidae, Tritomidae and Dermestidae, with other studies. *Journal of the New York Entomological Society* 8: 51–172.

Cornell J.F. 1967. A taxonomic study of *Eubaeocera* new genus (Coleoptera: Scaphidiidae) in North America north of Mexico. *The Coleopterists Bulletin* 21: 1–17. https://doi.org/10.5962/p.372462

Crowson R.A. 1938. The metendosternite in Coleoptera: a comparative study. *Transactions of the Royal Entomological Society of London* 87 (17): 397–415. https://doi.org/10.1111/j.1365-2311.1938.tb00723.x

Erichson W.F. 1845. *Naturgeschichte der Insecten Deutschlands. Erste Abteilung. Coleoptera. Dritter Band. Lieferung 1*. Nicolaische Buchhandlung, Berlin. https://doi.org/10.5962/bhl.title.8270

Fairmaire L. 1898. Matériaux pour la faune coléoptérique de la région malgache, 5^{e} note. *Annales de la Société entomologique de Belgique* 42: 222–260.

Fierros-López H.E. 2005. Revisión del género *Scaphidium* Olivier, 1790 (Coleoptera, Staphylinidae) de México y Céntroamerica. *Dugesiana* 12: 1–152.

Friedrich F. & Beutel R.G. 2006. The pterothoracic skeletomuscular system of Scirtoidea (Coleoptera: Polyphaga) and its implications for the high-level phylogeny of beetles. *Journal of Zoological Systematics and Evolutionary Research* 44 (4): 290–315. https://doi.org/10.1111/j.1439-0469.2006.00369.x

Ganglbauer L. 1899. *Die Käfer von Mitteleuropa. Die Käfer der österreichisch-ungarischen Monarchie, Deutschlands, der Schweiz, sowie des französischen und italienischen Alpengebietes. Dritter Band. Staphylinoidea. Vol. 2: Scydmaenidae, Silphidae, Clambidae, Leptinidae, Platypsyllidae, Corylophidae,*

Sphaeriidae, Trichopterygidae, Hydroscaphidae, Scaphidiidae, Histeridae. Familienreihe Clavicornia. Sphaeritidae, Ostomidae, Byturidae, Nitidulidae, Cucujidae, Erotylidae, Phalacridae, Thoractidae, Lathridiidae, Mycetophagidae, Colydiidae, Endomychidae, Coccinellidae. Carl Gerold's Sohn, Vienna.

Gestro R. 1879. Note sopre alcuni coleotteri dell'Arcipelago Malese e specialmente delle isole della Sonda. *Annali del Museo civico di Storia naturale di Genova* [1879–1880] 15: 49–62.

Harris R.A. 1979. A glossary of surface sculpturing. *Occasional Papers in Entomology* 28: 1–31.

Hübler N. & Klass K.D. 2013. The morphology of the metendosternite and the anterior abdominal venter in Chrysomelinae (Insecta: Coleoptera: Chrysomelidae). *Arthropod Systematics & Phylogeny* 71 (1): 3–41. https://doi.org/10.3897/asp.71.e31762

Jałoszyński P. 2012. Taxonomy of '*Euconnus* complex'. Part I. Morphology of *Euconnus* s. str. and revision of *Euconnomorphus* Franz and *Venezolanoconnus* Franz (Coleoptera: Staphylinidae: Scydmaeninae). *Zootaxa* 3555 (1): 55–82. https://doi.org/10.11646/zootaxa.3555.1.3

Laporte F.L.N. de Caumont (Comte de Castelnau). 1840. *Histoire naturelle des insectes coléoptères; avec une introduction renfermant l'anatomie et la physiologie des animaux articulés, par M. Brullé; ouvrage accompagné de 155 planches gravées sur acier représentant plus de 800 sujets. Vol. 2*. P. Duménil, Paris. https://doi.org/10.5962/bhl.title.47104

Latreille P.A. 1802. *Histoire naturelle générale et particulière des crustacés et des insectes: ouvrage faisant suite aux Oeuvres de Leclerc de Buffon, et partie du Cours complet d'histoire naturelle rédigé par CS Sonnini*. *Vol. 73*. F. Dulart, Paris.

Latreille P.A. 1806. *Genera Crustaceorum et Insectorum, Secundem Ordinem Naturalem in Familias Dispositas, Iconibus Exemplisque Plurimus Explicata. Vol 2: [1807]*. Amand Koenig, Paris.

https://doi.org/10.5962/bhl.title.65741

Latreille P.A. 1810. *Considérations générales sur l'ordre naturel des animaux composant les classes des crustacés, des arachnides, et des insectes; avec un tableau méthodique de leurs genres, disposés en familles.* Schoell, Paris. https://doi.org/10.5962/bhl.title.39620

Lawrence J.F. & Newton Jr. A.F. 1980. Coleoptera associated with the fruiting bodies of slime moulds (Myxomycetes). *The Coleopterists Bulletin* 34: 129–143.

Lawrence J.F. & Ślipiński A. 2013. *Australian Beetles. Vol. 1. Morphology, Classification and Keys*. CSIRO Publishing, Collingwood. https://doi.org/10.1071/9780643097292

Lawrence J.F., Zhou Y.-L. Lemann C., Sinclair B. & Ślipiński A. 2021. The hind wing of Coleoptera (Insecta): morphology, nomenclature and phylogenetic significance. Part 1. General discussion and Archostemata–Elateroidea. *Annales Zoologici* 71 (3): 421–606.
https://doi.org/10.3161/00034541ANZ2021.71.3.001

Leach W.E. 1815. Entomology. *In*: Brewster D. (ed.) *Edingburg Encyclopaedia* 9: 57–172.

LeConte J.L. 1860. Synopsis of the Scaphidiidae of the United States. *Proceedings of the Academy of Natural Sciences of Philadelphia*: 321–324.

Leschen R.A.B. 1994. Retreat-building by larval Scaphidiinae (Staphylinidae). *Mola* 4: 3–5.

Leschen R.A.B. & Löbl I. 1995. Phylogeny of Scaphidiinae with redefinition of tribal and generic limits (Coleoptera: Staphylinidae). *Revue suisse de Zoologie* 102 (2): 425–474.
https://doi.org/10.5962/bhl.part.80472

Leschen R.A.B. & Löbl I. 2005. Phylogeny and classification of Scaphisomatini Staphylinidae: Scaphidiinae with notes on mycophagy, termitophily, and functional morphology. *Coleopterists Society Monographs* 3: 1–63. https://doi.org/10.1649/0010-065X(2005)059[0001:PACOSS]2.0.CO;2

Leschen R.A.B., Löbl I. & Stephen K. 1990. Review of the Ozark Highland *Scaphisoma* (Coleoptera: Scaphidiidae). *The Coleopterists Bulletin* 44: 274–294.

Lewis G. 1893. On some Japanese Scaphidiidae. *Annals and Magazine of Natural History* (6) 11: 288–294. https://doi.org/10.1080/00222939308677525

Linnaeus C. 1758. *Systema Naturae per Regna Tria Naturae Secundum Classes, Ordines, genera, Species, cum Characteribus, Differentiis, Synonymis, Locis. Tomus I. Editio decima, Reformata.* Laurentii Salvii, Holmiae. https://doi.org/10.5962/bhl.title.542

Löbl I. 1967. Beitrag zur Kenntnis der neotropischen Arten der Gattung *Baeocera* Er. *Opuscula zoologica* 97: 1–3.

Löbl I. 1970. Revision der paläarktischen Arten der Gattungen *Scaphisoma* Leach und *Caryoscapha* Ganglbauer der Tribus Scaphisomini (Col. Scaphidiidae). *Revue suisse de Zoologie* 77: 727–799. https://doi.org/10.5962/bhl.part.75925

Löbl I. 1971. Scaphidiidae von Ceylon (Coleoptera). *Revue suisse de Zoologie* 78: 937–1006. https://doi.org/10.5962/bhl.part.97084

Löbl I. 1974. New species of the genus *Amalocera* Erichson from Brazil (Coleoptera, Scaphidiidae). *Studies on the Neotropical Fauna* 9: 39–45. https://doi.org/10.1080/01650527409360468

Löbl I. 1975a. Beitrag zur Kenntnis der Scaphidiidae (Coleoptera) von Neuguinea. *Revue suisse de Zoologie* 82: 369–420. https://doi.org/10.5962/bhl.part.78265

Löbl I. 1975b. Beitrag zur Kenntnis der orientalischen Scaphisomini (Coleoptera, Scaphidiidae). *Mitteilungen der Schweizerischen entomologischen Gesellschaft* 48: 269–290.

Löbl I. 1984. Contribution à la connaissance des Baeocera du Japon (Coleoptera, Scaphidiidae). *Archives des Sciences* 37: 181–192.

Löbl I. 1992. The Scaphidiidae (Coleoptera) of the Nepal Himalaya. *Revue suisse de Zoologie* 99: 471–627. https://doi.org/10.5962/bhl.part.79841

Löbl I. 1997. *Catalogue of the Scaphidiinae (Coleoptera: Staphylinidae)*. Muséum d'Histoire naturelle, Genève. https://doi.org/10.1163/9789004375956_002

Löbl I. 2015. Staphylinidae: Scaphidiinae. *In*: Löbl I. & Löbl D. (eds) *Catalogue of Palaearctic Coleoptera. Vol 2: Revised and Updated Edition. Hydrophiloidea – Staphylinoidea*: 21. Brill, Leiden/ Boston.

Löbl I. 2018. *Coleoptera: Staphylinidae: Scaphidiinae*. Brill, Leiden. https://doi.org/10.1163/9789004375956

Löbl I. & Cosandey V. 2023. On the Cypariini (Coleoptera: Staphylinidae: Scaphidiinae) of Borneo. *Revue suisse de Zoologie* 130 (1): 1–9. https://doi.org/10.35929/RSZ.0084

Löbl I. & Leschen R.A.B. 2003a. Redescription and new species of *Alexidia* (Coleoptera: Staphylinidae: Scaphidiinae). *Revue suisse de Zoologie* 110: 315–324. https://doi.org/10.5962/bhl.part.80187

Löbl I. & Leschen R.A.B. 2003b. Scaphidiinae (Insecta: Coleoptera: Staphylinidae). *Fauna of New Zealand* 48: 1–94.

Löbl I. & Ogawa R. 2016. On the Scaphisomatini (Coleoptera, Staphylinidae, Scaphidiinae) of the Philippines, IV: the genera Sapitia Achard and Scaphisoma Leach. *Linzer biologische Beiträge* 48 (2): 1339–1492.

Löbl I., Leschen R.A.B & Warner W.B. 2021. Scaphisomatini of Arizona (Coleoptera, Staphylinidae, Scaphidiinae) collected by V-Flight Intercept traps. *Revue suisse de Zoologie* 128 (1): 173–185. https://doi.org/10.35929/RSZ.0043

Löbl I., Klausnitzer B., Hartmann M. & Krell F.-T. 2023. The silent extinction of species and taxonomists — an appeal to science policymakers and legislators. *Diversity* 15 (1053): 2–17. https://doi.org/10.3390/d15101053

Naomi S. 1988a. Comparative morphology of the Staphylinidae and the allied groups (Coleoptera, Staphylinoidea): III. Antennae, labrum and mandibles. *Japanese Journal of Entomology* 56 (1): 67–77.

Naomi S. 1988b. Comparative morphology of the Staphylinidae and the allied groups (Coleoptera, Staphylinoidea): IV. Maxillae and labium. *Japanese Journal of Entomology* 56 (2): 241–250.

Naomi S. 1989a. Comparative morphology of the Staphylinidae and the allied groups (Coleoptera, Staphylinoidea): VII. Metendosternite and wings. *Japanese Journal of Entomology* 57 (1): 82–90.

Naomi S. 1989b. Comparative morphology of the Staphylinidae and the allied groups (Coleoptera, Staphylinoidea): X. Eighth and 10th segments of abdomen. *Japanese Journal of Entomology* 57 (4): 720–733.

Naomi S. 1990. Comparative morphology of the Staphylinidae and the allied groups (Coleoptera, Staphylinoidea): XI. Abdominal glands, male genitalia and female spermatheca. *Japanese Journal of Entomology* 58 (1): 16–23.

Newton A.F. Jr. 1984. Mycophagy in Staphylinoidea (Coleoptera). *In*: Wheeler Q. & Blackwell M. (eds) *Fungus/Insect Relationships. Perspectives in Ecology and Evolution*: 302–353. Columbia University Press, New York.

Oberthür R. 1883. Scaphidiides nouveaux. *In*: *Coleopterorum Novitates. Recueil spécialement consacré à l'Étude des coléoptères*: 5–16.

Ogawa R. & Löbl I. 2013. A revision of the genus *Baeocera* in Japan, with a new genus of the tribe Scaphisomatini (Coleoptera, Staphylinidae, Scaphidiinae). *Zootaxa* 3652 (3): 301–326. https://doi.org/10.11646/zootaxa.3652.3.1

Ogawa R. & Löbl I. 2016. A review of the genus *Xotidium* Löbl, 1992 (Coleoptera, Staphylinidae, Scaphidiinae), with descriptions of five new species. *Deutsche entomologische Zeitschrift* 63 (1): 155–169. https://doi.org/10.3897/dez.63.8386

Ogawa R. & Sakai M. 2011. A review of the genus *Cyparium* Erichson (Coleoptera, Staphylinidae, Scaphidiinae) of Japan. *Japanese Journal of Systematic Entomology* 17: 129–136.

Olivier G.-A. 1790. *Entomologie, ou Histoire naturelle des Insectes, avec leurs Caracteres, génériques et spécifiques, leur Description, leur Synonymie, et leur Figure enluminée. Vol 2*: *Coléoptéres*. Baudouin, Paris. https://doi.org/10.5962/bhl.title.61905

Perty J.A.M. 1830. Insecta Brasiliensia. *In*: Perty J.A.M. (ed.) *Delectus animalium articulatorum, quae in itinere per Brasiliam annis MDCCCXVII-MDCCCXX jussu et auspiciis Maximiliani Josephi I. Bavariae regis augustissimi peracto collegerunt Dr. J.B. de Spix et Dr. C.F. Ph. de Martius*: 1–60. Munich, Impensis Editoris.

Pic M. 1915a. Nouvelles espèces de diverses familles. *Mélanges exotico-entomologiques* 15: 1–24.

Pic M. 1915b. Diagnoses de nouveaux genres et nouvelles espèces de Scaphidiides. *L'Echange, Revue linnéenne* 31: 30–32.

Pic M. 1915c. Diagnoses de nouveaux genres et nouvelles espèces de Scaphidiides. *L'Echange, Revue linnéenne* 31: 35–36.

Pic M. 1916a. Notes et descriptions abrégées diverses. *Mélanges exotico-entomologiques* 17: 2–8.

Pic M. 1916b. Diagnoses spécifiques. *Mélanges exotico-entomologiques* 17: 8–20.

Pic M. 1917. Descriptions abrégées diverses. *Mélanges exotico-entomologiques* 26: 2–24.

Pic M. 1920a. Nouveautés diverses. *Mélanges exotico-entomologiques* 32: 1–28.

Pic M. 1920b. Scaphidiides nouveaux de diverses origines. *Annali del Museo civico di Storia naturale di Genova* 9 (3): 93–97

Pic M. 1920c. Coléoptères exotiques en partie nouveaux. *L'Echange, Revue linnéenne* 36: 22–24.

Pic M. 1921. Nouveautés diverses. *Mélanges exotico-entomologiques* 33: 1–32.

Pic M. 1922. Nouveautés diverses. *Mélanges exotico-entomologiques* 36: 1–32.

Pic M. 1923. Nouveautés diverses. *Mélanges exotico-entomologiques* 38: 1–32.

Pic M. 1925. Notes sur les coléopteres scaphidiides. *Annales de la Société entomologique de Belgique* 64: 193–196.

Pic M. 1928a. Scaphidiidae du Congo Belge. *Revue de Zoologie et de Botanique africaines* 16: 33–44.

Pic M. 1928b. Nouveaux coléoptères de la République Argentine. *Revista de la Sociedad entomologica argentina* 2: 49–52.

Pic M. 1928c. Nové druhy koleopter z Brasilie. Nouveaux coléoptères du Brésil. *Sborník entomologického oddělení Národního musea v Praze* 6: 74–76.

Pic M. 1930. Coléoptères asiatiques nouveaux. *Sborník entomologického oddělení Národního musea v Praze* 8: 58–59.

Pic M. 1931. Nouveautés diverses. *Mélanges exotico-entomologiques* 57: 1–36.

Pic M. 1956. Nouveaux coléoptères exotiques. *Bulletin de la Société entomologique de France* 60: 173–175. https://doi.org/10.3406/bsef.1955.18803

Ramage T. & Löbl I. 2022. A new species of *Scaphisoma* Leach from the Society Islands with commentary on Staphylinidae of the French Polynesia (Coleoptera, Staphylinidae, Scaphidiinae). *Bulletin de la Société entomologique de France* 127 (1): 55–60. https://doi.org/10.32475/bsef_2224

Redtenbacher L. 1868. Coleopteren. *In*: Redtenbacher L., Sichel J., Mayr, G.L. & Brauer F. (eds) *Reise der Österreichischen Fregatte Novara um die Erde in den Jahren 1857, 1858, 1859 unter den Befehlen des Commodore B. von Wüllerstorf-Urbair. Zoologischer Theil. Zweiter Band*: I–249. Vienna.

Reitter E. 1880. Die Gattungen und Arten der Coleopteren-Familie: Scaphidiidae meiner Sammlung. *Verhandlungen des Naturforschenden Vereins in Brünn* 18 [1879]: 35–49.

Say T. 1823. Description of coleopterous insects collected in the late expedition to the Rocky Mountains, performed by order of Mr. Calhoun, Secretary of War, under the command of Major Long. *Journal of the Academy of Natural Sciences Philadelphia* 3 (1): 139–216.

Stephenson S.L., Wheeler Q.D., McHugh J.V. & Fraissinet P.R. 1994. North American associations of Coleoptera with Myxomycetes. *Journal of Natural History* 28 (4): 921–936. https://doi.org/10.1080/00222939400770491

Tang L., Li L.-Z. & He W.-J. 2014. The genus *Scaphidium* Olivier in East China (Coleoptera, Staphylinidae, Scaphidiinae). *ZooKeys* 403: 47–96. https://doi.org/10.3897/zookeys.403.7220

von Groll E. 2023. Rediscovery and redescription of *Scaphisoma nigrofasciatum* Pic (Coleoptera: Staphylinidae: Scaphidiinae): a remarkable new record from a distant continent. *Zootaxa* 5375 (4): 565–573. https://doi.org/10.11646/zootaxa.5375.4.7

von Groll E. & Lopes-Andrade C. 2021. *Scaphisoma pandemum* sp. nov. (Coleoptera: Staphylinidae: Scaphidiinae) from the Atlantic Forest of Southeast Brazil. *Zootaxa* 4999 (2): 143–156. https://doi.org/10.11646/zootaxa.4999.2.4

von Groll E. & Lopes-Andrade C. 2022. Contributions to the taxonomy of Neotropical *Cyparium* Erichson (Coleoptera: Staphylinidae: Scaphidiinae), with the description of five new species. *European Journal of Taxonomy* 835: 1–97. https://doi.org/10.5852/ejt.2022.835.1909

Waterhouse F.H. 1879. Descriptions of new Coleoptera of geographical interest, collected by Charles Darwin, Esq. *Journal of the Linnean Society, Zoology* 14: 530–534. https://doi.org/10.1111/j.1096-3642.1879.tb02449.x

Manuscript received: 20 March 2024
Manuscript accepted: 8 January 2025
Published on:19 May 2025
Topic editor: Tony Robillard
Section editor: Maxwell Barclay
Desk editor: Kristiaan Hoedemakers

Supplementary file 1. Material examined (with additional data).
https://doi.org/10.5852/ejt.2025.990.2903.13147

Supplementary file 2. Antennae of all species (same scale).
https://doi.org/10.5852/ejt.2025.990.2903.13149